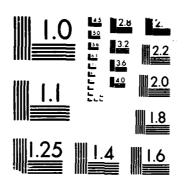
AD-A193 799 RLE (RESEARCH LABORATORY OF ELECTRONICS) PROGRESS
REPORT NUMBER 129(U) MASSACHUSETTS INST OF TECH
CAMBRIDGE RESEARCH LAB OF ELECTRON. J ALLEN ET AL.
JAN 87 ARO-23223 43-EL DARL03-86-K-0002 F/G 14/2 1/4 UNCLRSSIFIED



MASSACHUSETTS INSTITUTE OF TECHNOLOGY

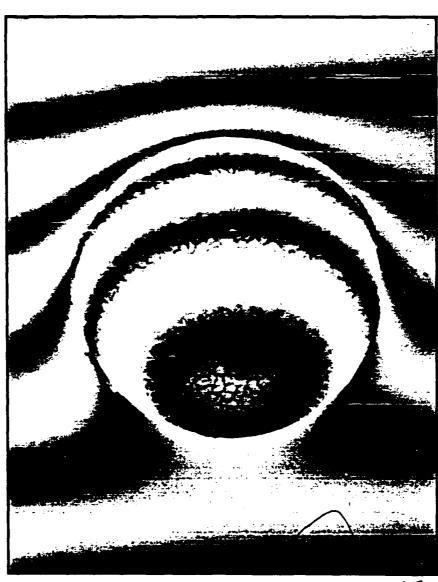


The RESEARCH LABORATORY of ELECTRONICS

799 AD-A193

PROGRESS REPORT

JANUARY 1987 NO. 129



113 88 4 11

SECURITY CLASSIFICATION OF THIS PAGE

<u>፞ዀዀዀዀዀዀዀዀዀዀዀዀዀዀዀዀዀዀዀዀዀዀዀዀዀዀዀዀዀዀዀዀዀዀዀዀ</u>	\$.44.46.46.46.46.46.46.46.46.46.46.	ner and the state of the state	Albert Crists of Safe	an and the test that	Bankarak da kankarak da kan
	•				
Unclassified					
ECURITY CLASSIFICATION OF THIS PAGE					
	REPORT DOCUM				
Unclassified		16. RESTRICTIVE	MARKINGS		
ZA SECURITY CLASSIFICATION AUTHORI	TY	3. DISTRIBUTION		-	
2b. DECLASSIFICATION/DOWNGRADING S	CHEDULE	Approved for distribution	•	•	
		discribation			
PERFORMING ORGANIZATION REPORT		5. MONITORING OF	GANIZATION RE	PORT NUMBER	\$)
RLE Progress Report No.				ARO 23	223.43-EL
Research Lab. of Electroni		7a. NAME OF MONI	TORING ORGANI	ZATION	
Mass. Inst. of Technology	.05				(
Sc. ADDRESS (City. State and ZIP Code)		76. ADDRESS (City.	State and ZIP Cod	e)	
77 Massachusetts Avenue Cambridge, MA 02139					1
			·		
Se. NAME OF FUNDING/SPONSORING ORGANIZATION	8b. OFFICE SYMBOL (If applicable)	9. PROCUREMENT	INSTRUMENT ID	ENTIFICATION N	IUMBER
U.S. Army Research Center		<u> </u>	DAAL03-86-	-K-0002	
Be. ADDRESS (City, State and ZIP Code) P.O. Box 12211		10. SOURCE OF FU		TASK	WORK UNIT
Research Triangle Park, NO	27709	PROGRAM ELEMENT NO.	PROJECT NO.	NO.	NO.
1. TITLE (Include Security Classification)		4			1 1
Progress Report No. 129					<u>. </u>
Jonathan Allen, Daniel R	Clennar				
134 TYPE OF REPORT 136 T	ME COVERED	14. DATE OF REPO			
progress report FRON	<u>1/86</u> то <u>12/86</u>	January	1987	283	pp.
IS. SUFFLEMENTANT NUTATION	•				1
					
FIELD GROUP SUB. GR.	Electronics,				
	signal process	sing, linguis	tics, speec	h communic	
9. ASSTRACT (Continue on reverse if necesse	radio astrono		gne <u>tic wave</u>	theory	
This is report No. 129 in			ssued by th	e Research	Laboratory
of Electronics at MIT. Th	ne report covers t	he period Jan	uary 1 thro	ugh Decemb	er 31, 1986
and contains a statement of	of research object	ives, summary	of research	h efforts	and lists
of funding sources and pro indexes of funding sources					
a listing of RLE personnel					
		`.			The state of the s
`					1
/ *	•				ŀ
20. DISTRIBUTION/AVAILABILITY OF ABS	TRACT	21. ABSTRACT SEC	URITY CLASSIFIE	CATION	
UNCLASSIFIED/UNLIMITED 🔀 SAME AS RPT. 🗆 DTIC USERS 🗆		Unclassified			
224. NAME OF RESPONSIBLE INDIVIDUAL		226. TELEPHONE N		22c. OFFICE SY	MBOL
Barbara Passero		(617) 253-2			į
		(617) 253-2	, סטכ		

DD FORM 1473, 83 APR

EDITION OF 1 JAN 73 IS OBSOLETE.

Unclassified

RLE Progress Report No. 129

January 1987

Submitted by:

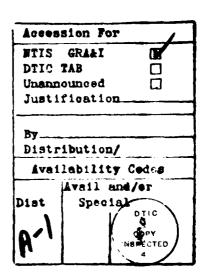
Prof. Jonathan Allen Prof. Daniel Kleppner

Research Laboratory of Electronics Massachusetts Institute of Technology Cambridge, MA 02139 USA Cover: X-ray lithography is an effective means of replicating submicron and nanometer structures. In order to apply this technology in the fabrication of deep submicron electronic devices and nanometer quantum-effect devices, distortion of the x-ray mask caused by stress in the absorber pattern must be eliminated. The figure shows interferograms, taken on a Linnik interferometer, out of the out-of-plane distortion of a membrane caused by extremely high tensile stress in a metal disk. Our research has demonstrated that such distortion can be eliminated by ion implanting into the metal to compensate the tensile stress. This work (reported in Chapter 1 of the Progress Report) is being done by graduate student Y.C. Ku under Prof. Henry I. Smith.

Prof. Smith is the inventor of x-ray lithography.

Photography by John F. Cook

© Massachusetts Institute of Technology, 1987 All Rights reserved.



PARADOSE POSSESSE PROCESSES PROPOSES PARASONS SERVING PROVINCE PARASONS SERVING PROVINCE PROPOSES IN

Table of Contents

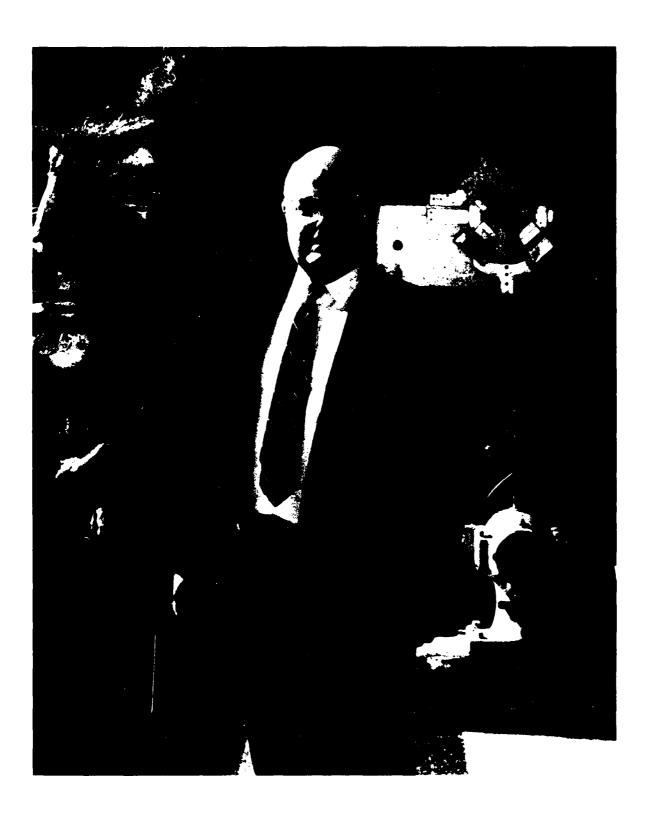
Intro	duction and Acknowledgements	IX
1.7 1.8 1.9 1.10	Submicron Structures Technology and Research Submicron Structures Laboratory Microfabrication at Linewidths of 0.1 µm and Below Improved Mask Technology for X-Ray Lithography Theoretical Analysis of the Lithography Process Studies of Electronic Conduction in One-Dimensional Semiconductor Devices Surface Superlattice Formation in Silicon Inversion Layers Using 0.2 µm Period Grating-Gate d-Effect Transistors Study of Surface Superlattice Formation in III-V Field-Effect Transistors Investigation of One-Dimensional Conductivity in Multiple, Parallel Inversion Lines Study of Electron Transport in MOSFETs in Si with Deep-Submicron Channel Lengths Application of the Shubnikov-de Haas Oscillations in Characterization of Si MOSFETs and GaAs DFETs Crystalline Films on Amorphous Substrates Ion-Beam-Enhanced Grain Growth in Thin Films Epitaxy via Surface-Energy-Driven Grain Growth	1 1 2 2 3 3 4 5 5 6 6 7
1.14 1.15 1.16	Submicrometer-Period Gold Transmission Gratings for X-Ray Spectroscopy High-Dispersion, High-Efficiency Transmission Gratings for Astrophysical X-Ray Spectroscopy Soft X-Ray Interferometer Gratings	8
2.0 2.1 2.2 2.3 2.4 2.5 2.6 2.7 2.8 2.9 2.10 2.11 2.12	Kinetic Phenomena in Thin Film Electronic Materials Normal and Secondary Grain Growth in Ultrathin (<1000 Å) Films of Silicon and Germanium Graphoepitaxy of Si, Ge and Model Materials Epitaxy via Surface-Energy-Driven Grain Growth Zone Melting Recrystallization of Silicon on Insulators Properties of Grain Boundaries with Controlled Orientations and Locations in Thin Silicon Films 1 Metastable Phase Formation in Lithographically Defined Particles of Semiconductors Kinetics of Silicide Formation at Refractory Metal-Silicon Contacts Grain Growth in Thin Films of Aluminum Thin and Narrow Metallic Interconnects Electromigration at Aluminum-Silicon Contacts in Integrated Circuits Computer Modeling of Microstructural Evolution in Thin Films Focussed Ion Beam Induced Deposition	13 14 14 15 16 16 17
3.0 3.1 3.2 3.3 3.4 3.5	Focused Ion Beam FabricationZFocused Ion Beam ProgramZFabrication of Graded Channel FETs in GaAs and SiZIon Induced DepositionZFocused Ion Beam Microsurgery for ElectronicsZMeasurement of Beam ProfileZ	21 21 22 22
4.0 4.1 4.2 4.3 4.4 4.5	Chemical Reaction Dynamics at Surfaces	25 25 26 27

5.0	Optics and Quantum Electronics	29
5.2 5.3	The Nonlinear Waveguide Interferometer Picosecond Optical Signal Sampling Surface Acoustic Wave Propagation in Gratings Solitons	30 31
5.5 5.6 5.7	Analysis and Characterization if III-V Guided Wave Optics Rib Waveguide Couplers Multiple Quantum Well Heterostructures and Diode Laser Arrays	33 34 35
5.8 5.9 5.10	Femtosecond Carrier Dynamics in GaAs	39
6.2	Optical Propagation and Communication Atmospheric Optical Communications in Local Area Networks Squeezed States of Light Laser Radar System Theory Fiber-Coupled External-Cavity Semiconductor High Power Laser	43 45 46
7.0 7.1 7.2 7.3 7.4 7.5	Infrared Nonlinear Optics Nonlinear Optics in HgTe Nonlinear Current-Voltage Characteristics in HgMnTe Free Carrier Spin-Induced Faraday Rotation in HgCdTe and HgMnTe Optical Nonlinearity Caused by Resonant Scattering Stress Tuned, Magnetic-Field-Induced Anticrossing in As-Doped Germanium	51 51 52 52
8.0 8.1 8.2	Phase Transitions in Chemisorbed Systems	55
9.0 9.1 9.2 9.3	X-Ray Diffuse Scattering	57 58
10.0 10.1 10.2 10.3	Semiconductor Surface Studies Surface Reconstruction Geometries Structural Phase Transitions Hydrogenation	63 64
11.0	Ultralow-Temperature Measurements of Submicron Devices	67
12.0 12.1	Quantum Transport in Low Dimensional Disordered Systems	69 69
13.0 13.1 13.2	Graphoepitaxy of Colloidal Crystals	71
14.0 14.1 Pho 14.2	Photon Correlation Spectroscopy and Applications	73
15.0 15.1 15.2 15.3 15.4 15.5 15.6	Custom Integrated Circuits Custom Integrated Circuits High Performance Circuit Design Extracting Masks from Optical Images of VLSI Chips Algorithmic Fault Tolerance on Digital Signal Processing Cellular Array for Image Processing Waveform Bounding for Fast Timing Analysis of Digital VLSI Circuits	77 80 80 81 82
16.0 16.1	Speech Communication	

Contract (Contract)	this the real text	1 Stop and Fricative Consonants 2 Vowel Perception 3 Analysis of a Female Voice 4 Alternative Analysis Procedures 5 Children's Speech Speech Recognition 1 Signal Representation for Acoustic Segmentation 2 Acoustic Evidence for the Syllable as a Phonological Unit Speech Synthesis Speech Planning 1 Error Studies 2 Prosody Studies 3 Cross-Language Studies Physiology of Speech Production 1 Articulatory Movement Transduction 2 Data Processing 3 Token-to-Token Variation of Tongue-Body Vowel Targets, Coarticulation Articulatory Co-Acoustic Relationships 4 Anticipatory Coarticulation: Studies of Lip Protrusion Linguistics Communication Biophysics Basic and Clinical Studies of the Auditory System External and Middle-Ear Transmission Cochlear Mechanisms Stimulus Coding in the Auditory Nerve Afferent and Efferent Systems in Mammalian Cochlea Middle-Ear Muscle Reflex Cochlear Implants Auditory Psychophysics and Aids for the Deaf Role of Anchors in Perception	VC
8			
{			
i			
1			
}			
g	16.1	1 Stop and Fricative Consonants	
1	16.1	2 Vowel Perception	
8	16.1	3 Analysis of a Female Voice	
	16.1	5 Children's Speech	
N	16.2	Speech Recognition	88
S	16.2	.1 Signal Representation for Acoustic Segmentation	89
3	16.2	.2 Acoustic Evidence for the Syllable as a Phonological Unit	90
N	16.3	Speech Synthesis	90
2	16.4	Speech Planning	
	16.4	.1 Error Studies	
<u> </u>	16.4	.3 Cross-Language Studies	92
<i>چ</i>	16.5	Physiology of Speech Production	92
Č Š	16.5	.1 Articulatory Movement Transduction	92
\{\delta}	16.5	.2 Data Processing	
2	16.5	.3 Token-to-Token Variation of Tongue-Body Vowel Targets, Coarticulation	
	and	\Articulatory-to-Acoustic Relationships	93
7	16.5	4 Anticipatory Coarticulation: Studies of Lip Protrusion	93
ZQ.	17.0	Linguistics	Q.F.
Ý.	17.0	Linguistics	33
3	18.0	Communication Biophysics	109
X	18.1	Basic and Clinical Studies of the Auditory System	109
Į.	18.1	.1 External and Middle-Ear Transmission 1	
	18.1	.2 Cochlear Mechanisms	110
-3 -3	18.1	.3 Stimulus Coding in the Auditory Nerve	110
	18.1	.4 Afferent and Efferent Systems in Mammalian Cochlea	111
į.	10.1	.6 Cochlear Efferent System	112
Č:	18.1	.7 Cochlear Implants	114
	18.2	Auditory Psychophysics and Aids for the Deaf	116
	18.3	Role of Anchors in Perception	116
	18.4	Hearing Aid Research	
	18.5	Additional Work	
	18.6	Multimicrophone Monaural Aids for the Hearing-Impaired	128
<u> </u>	19.0	Physiology 1	1 21
20	19.1	Strategies of Perception	
3	19.2	Image Sharpening in the Photoreceptor Layer of the Eye	
\gtrsim	19.3	Tectal Processing of Visual Information in a Frog	
\$			
ß	20.0	Molecular Physics	
[4	20.1	Molecule Microscopy	
	20.2	Electrical Neutrality of Molecules	13/
	21.0	Quantum Optics and Photonics	139
K	21.1	Investigation of Error Sources in a Laser Raman Clock	
	21.2	Physics of Stimulated Resonance Raman Effect	
ţ.	21.3	Observation of Raman-Ramsey Fringes in a Cesium Atomic Beam Using a Semiconductor	-
<u>.</u> -			140
<u>.</u>	21.4	Influence of Atomic Recoil on the Spectrum of Resonance Fluorescence From a Two-Level	
N.			141
Ŋ.	21.5 21.6	Studies in a Passive Resonator Gyroscope	
6	21.6	Investigation of Noise in a Fiber Interferometer Gyroscope	
N.	21.8	Sensitive Techniques for Detection of Residual Higher Order Modes in a Quasi-Single-Mode	, , ,
r.	Fiber		143
, 13	21.9	Investigation of Absolute Stability of Water-Vapor-Stabilized Semiconductor Laser	
兵	-		
<u>ದ</u>	22.0		145
(7)	22.1	Basic Atomic Physics	145

22.1.1 Rydberg Atoms in a Magnetic Field 22.2 Rydberg Atoms and Radiation 22.2.1 Inhibited Spontaneous Emission 22.2.2 Rydberg Atoms in Cavities 22.3 Experimental Study of Momentum Transfer to Atoms by Light 22.4 Atom-Molecule Collisions 22.5 Magnetic Trapping of Neutral Atoms 22.6 Precision Mass Spectroscopy of Ions	147 147 149 150 152 156
23.0 Plasma Dynamics 23.1 Relativistic Electron Beams 23.1.1 Nonlinear Characteristics of the Free Electron Laser 23.1.2 Effect of Electron Beam Temperature on FEL Operation 23.1.3 Optical Guiding Measurements 23.1.4 The Design of a New Type of Helical Wiggler 23.2 Plasma Wave Interactions - RF Heating and Current Generation 23.3 Coupled-Mode Propagation and Instability in Inhomogeneous Plasmas 23.4 Propagation, Mode-Conversion and Absorption in Ion-Cyclotron Heating 23.4.1 Transmission and Reflection of the Fast-Wave 23.4.2 Electron Absorption on the Mode-Converted Ion-Bernstein Wave 23.5 Relativistic Treatment of Lower Hybrid Current Drive with Wide Spectra 23.6 Absolute Instabilities from Cusp-Maps in the Complex Frequency Plane 23.7 Profile Consistency 23.7.2 Fishbones 23.7.3 Transport Simulation 23.7.4 Density Limit and Path to Ignition	161 162 162 162 166 166 169 170 173 174 175 177
24.0 Digital Signal Processing 24.1 Reconstruction of Two-Dimensional Signals From Distorted Zero Crossings 24.2 Digital Processing of Side Scan Sonar Data 24.3 Representation and Manipulation of Signal Processing Knowledge and Expressions 24.4 Iterative Algorithms for Parameter Estimation with Applications to Array Processing 24.5 A New Mixed-Excitation Speech Model and Its Application to Bit-Rate Reduction 24.6 Mixed Causuality IIR Filtering for Nonminimum Phase Channel Compensation 24.7 A 4.8 Kbps High Quality Speech Coding System 24.8 Multi-Representational Signal Matching 24.9 Detection of Narrowband Signals in Wideband Noise 24.10 Estimation of Coronary Artery Boundaries in Angiograms 24.11 Reconstruction of Multidimensional Signals from Multilevel Threshold Crossings 24.12 Knowledge-Based Pitch Detection 24.13 Reconstruction of a Two-Dimensional Signal from the Fourier Transform Magnitude 24.14 Model-Based Motion Estimation and its Application to Restoration and Interpolation of Motion Pictures 24.15 Signal Processing and Interpretation using Multilevel Signal Abstractions 24.16 Signal Representation for Symbolic and Numerical Processing 24.17 Reconstruction of Undersampled Periodic Signals 24.18 Silhouette-Slice Theorems 24.19 The Hilbert-Hankel Transform and Its Application to Shallow Water Ocean Acoustics 24.20 Speech Enhancement Using Adaptive Noise Cancellation	191 192 193 193 195 196 197 197 198 200 200 201
25.0 Cognitive Information Processing 25.1 Advanced Television Research Program 25.1.1 Goals 25.1.2 Background 25.1.3 Research Activities 25.2 Computer Graphics 25.2.1 Display Architecture for Interactive Graphics Programmable Frame Buffer Systems 25.2.2 Programmable Frame Buffer Systems 25.3 Computer Aided Fabrication System Structure	203 203 203 203 204 205 205 205 206
26.0 Electromagnetic Wave Theory and Applications	209

26.1 26.2 26.3 26.4 26.5 26.6 26.7 26.8 26.9 26.10 26.11 26.12	Electromagnetic Waves in Multilayer Media Remote Sensing with Electromagnetic Waves Remote Sensing of Earth Terrain Remote Sensing of Upper Atmosphere Microwave Emission and Scattering Active and Passive Remote Sensing of Ice Time Domain Wave Propoagation in Circuits Time Domain Electromagnetic Waves Wave Transmission and Coupling in Multilayered Media Radar Scene Generation for Tactical Decision Aids MMW Clutter Simulation Baseline Model Acoustic and Electromagnetic Wave Studies.	210 212 212 212 214 216 216 218 218
27.0 27.1 27.2 27.2 27.2 27.2 27.2 27.2	.2 Introduction	223 223 223 224 224 225
28.0 28.1 28.2 28.3 28.4 28.5 28.6 28.7	Radio Astronomy Galactic and Extragalactic Research Long-Baseline Astrometric Interferometers Tiros-N Satellite Microwave Sounder High-Resolution Passive Microwave Imaging of Atmospheric Structure Video Image Processing Nonthermal Radio Emission from the Jovian Planets Video Bandwidth Compression Techniques	229 229 231 231 232 233
29.0 29.1 29.2 29.3 29.4 29.5 29.6 29.7	Publications and Meetings Meeting Papers Presented Journal Papers Published Journal Papers Accepted for Publication Letters to the Editor Published Letters to the Editor Accepted for Publication Special Publications Reports Published	235 258 262 263 265 265
30.0	Current RLE Personnel	269
31.0	Research Support Index	275
32.0	Research Project Staff Index	279



Introduction and Acknowledgements

The Research Laboratory of Electronics (RLE) was established in 1946 as the Institute's first interdepartmental laboratory. Originally organized under the joint sponsorship of the Departments of Physics and Electrical Engineering, RLE currently maintains a broad interpretation of electronics by promoting a wide range of research.

The RLE environment provides both the freedom of action essential in an academic institution and the availability of large-scale laboratory facilities and services required by researchers. RLE's interdisciplinary setting offers many opportunities for creative and collaborative research. By fostering this powerful combination of research and education, RLE effectively penetrates beyond the horizon of new ideas and information.

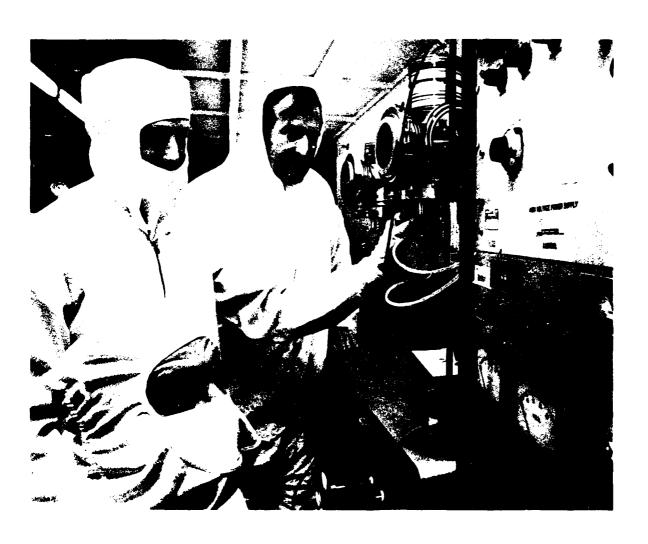
Progress Report No. 129 describes research programs at RLE for the period January 1 through December 31, 1986. This report contains both a statement of research objectives and a summary of research efforts for each of the research groups within RLE. Faculty, research staff and students who participated in these projects are identified at the beginning of each chapter, along with sources of funding.

We would like to highlight the following features of this report. Chapter 29 contains publications and papers presented by RLE staff during 1986, and reprints of articles may be obtained by contacting the authors directly. Chapter 30 is a roster of all current RLE staff. In addition, indexes of project personnel and sponsored research projects are located at the end of this report.

Progress Report No. 129 was produced by the RLE Communications Office. Further inquiries may be addressed to:

Barbara Passero
Communications Officer
Research Laboratory of Electronics
Building 36-412
Massachusetts Institute of Technology
Cambridge, Massachusetts 02139
(617) 253-2566

We thank the faculty, staff and students of RLE for their generous contributions. Our special thanks this year to Eric Watson for his effort and initiative and to Dave Foss for his technical advice.



1.0 Submicron Structures Technology and Research

Academic and Research Staff

Prof. H.I. Smith, Dr. M.L. Schattenburg¹, J.M. Carter

Graduate Students

S. Ajuria, E.H. Anderson, H.A. Atwater, P. Bagwell, J. Cho, S.Y. Chou, W. Chu, L. Clevenger, J. Floro, S.M. Garrison, J. Im, K. Ismail, H. Kahn, H.J. Kim, Y.C. Ku, J.C. Licini, U. Meirav, J.E. Palmer, S.L. Park, H.M. Quek, J. Scott-Thomas, G. Shahidi, M. Toth, C.C. Wong, A.T. Yen

Visiting Scientists

K. Komatsu, I. Plotnik, H. Tomita, I. Tanaka

1.1 Submicron Structures Laboratory

The Submicron Structures Laboratory at M.I.T. develops techniques for fabricating surface structures with feature sizes in the range from nanometers to micrometers, and uses these structures in a variety of research projects. The research projects of the Laboratory, which are described briefly below, fall into four major categories: development of submicron and nanometer fabrication technology; deep-submicron electronics and quantum-effect devices; crystalline films on amorphous substrates; and periodic structures for x-ray optics and spectroscopy.

1.2 Microfabrication at Linewidths of 0.1 μ m and Below

Joint Services Electronics Program (Contract DAAL03-86-K-0002)
National Science Foundation (Grant ECS 85-06565)
Lawrence Livermore Laboratory (Subcontract 9459005)

Erik H. Anderson, James M. Carter, William Chu, Kazu Komatsu, Hui M. Quek, Anthony Yen, Irving Plotnik, Mark L. Schattenburg, Henry I. Smith

A variety of techniques for fabricating structures with characteristic dimensions of 0.1 μ m and below are investigated. These include: x-ray nanolithography, holographic lithography, and reactive-ion etching. Development of such techniques is essential if we are to explore the rich field of research applications in the deep-submicron and nanometer domains. X-ray nanolithography is of special interest because it promises to provide high throughput and broad process latitude at linewidths of 0.1 μ m and below, something that cannot be achieved with scanning electron-beam lithography.

¹ M.I.T. Center for Space Research

We are developing a new generation of x-ray masks made from inorganic membranes (Si, Si_3N_4 , BN and possibly diamond) and are investigating means for precisely controlling mask-wafer gap, and achieving nanometer alignment. Phase shifting and transform x-ray masks (i.e., in-line x-ray holography) may permit us to achieve sub-50 nm linewidths at finite gaps. A new tri-level technique for making, by electron beam lithography, x-ray masks with linewidths of 50 nm was developed in collaboration with IBM.

Techniques for making x-ray masks from crystallographic templates are being improved. We hope to routinely achieve pattern replication in PMMA with nanometer scale line-edge smoothness.

Achromatic holographic configurations enable us to use deep UV excimer laser sources to produce gratings with finer periods (~ 100 nm) than are possible with conventional UV laser sources. Although such optical techniques can be used to prepare experimental samples, there are important advantages to using them only for preparing x-ray masks. These masks are then replicated using x-ray nanolithography. With C_k and Cu_L x-ray lithography high-aspect-ratio (almost 8:1) structures with linewidths less than 50 nm have been produced in PMMA.

1.3 Improved Mask Technology for X-Ray Lithography

Semiconductor Research Corporation (Contract 86-05-080)

Salmon Akhtar, Yao C. Ku, Markus Toth, Irving Plotnik, Mark Porter, Henry I. Smith

To utilize x-ray lithography in the fabrication of submicron integrated electronics, distortion in the x-ray mask must be eliminated. Distortion can arise from stress in the absorber, which is usually gold or tungsten. Tungsten is preferred because it is a closer match in thermal expansion to Si, and other materials used as mask membranes. However, W is usually under high stress when deposited by conventional means. We have demonstrated that stress in W can be compensated by ion implantation of Si. Strain-induced deflection of Si₃ N₄ membranes was measured in a Linnik interferometer. Stresses of $7x10^9$ dynes/cm² in W were reduced to zero by implantation of $1x10^{16}$ Si atoms/cm² at 25 keV.

1.4 Theoretical Analysis of the Lithography Process

Semiconductor Research Corporation (Contract 86-05-080)

Henry I. Smith

In an earlier theoretical analysis of lithography we studied the effects of statistical fluctuations on linewidth control, and compared the pixel transfer rates of the various lithographic techniques. This analysis has been expanded to include the effects of nonuniform illumination and other non-ideal factors. We have also derived a method for quantifying process-latitude in lithography, a critically important figure-of-merit in manufacturing. The normalized-process-latitude-parameter was evaluated, as a function of minimum linewidth for several UV and deep UV projection systems, and for an

x-ray system based on a laser-produced plasma source. As expected, the x-ray system showed a significantly larger process latitude in the important linewidth range between 0.1 and 1 μ m.

1.5 Studies of Electronic Conduction in One-Dimensional Semiconductor Devices

Joint Services Electronics Program (Contract DAAG-29-83-K-0003) National Science Foundation (Grant ECS 85-03443)

Dimitri A. Atoniadis, S. Field, Marc A. Kastner, Jerome C. Licini, Udi Meirav, Samuel L. Park, John Scott-Thomas, Henry I. Smith

At low temperatures, Si inversion layers of two-dimensional-electron-gas with widths less than 100 nm in Si, and less than 1 μ m in GaAs, become one dimensional. This happens when inelastic scattering is sufficiently reduced that the electronic wave functions have phase coherence over distances larger than the device width.

Three techniques are being employed to fabricate one-dimensional devices. In the first, field-effect transistors are fabricated in Si with widths as narrow as ~50 nm. The narrow gate of these MOSFETs is created by glancing-angle evaporation of tungsten onto a 50-nm high step etched in a 100-nm thick oxide on a Si (100) surface. The tungsten wires are more uniform than those fabricated previously of Al, presumably because of the smaller grain size. In a second technique under development, the inversion layer is created under a narrow slot in a wide metal gate by applying a potential to an upper metal gate separated from the first by a layer of SiO₂. The lower gate with the narrow slot is fabricated using x-ray lithography. To create one-dimensional devices in GaAs we are exploring the possibility of using p-implants to confine the two-dimensional electron gas created by modulation doping or by a gate.

Experiments are underway to characterize these devices at ultralow temperatures using a newly acquired dilution refrigerator.

1.6 Surface Superlattice Formation in Silicon Inversion Layers Using 0.2 μ m Period Grating-Gate Field-Effect Transistors

Joint Services Electronics Program (Contract DAAL03-86-K-0002)
U.S. Air Force - Office of Scientific Research (Contract AFOSR-85-0376)

Dimitri A. Antoniadis, Phillip Bagwell, William Chu, Khalid Ismail, Anthony Yen, Marc A. Kastner, Terry P. Orlando, Henry I. Smith

We have been investigating electronic conduction and distinctly quantum-mechanical effects in a surface superlattice (SSL) device. The device is a Si MOSFET with a dual stacked gate configuration. The lower gate is a tungsten grating of 200 nm period (100 nm nominal linewidth), and the upper gate is a uniform metal pad separated from the grating by 200 nm of deposited SiO_2 . We call these devices grating-gate-

field-effect transitors (GGFET's). The grating gate is fabricated using x-ray nanolithography and grating contact pads are made with deep-UV lithography. Drain to source current in the SSL device runs perpendicular to the grating wires. A distinguishing feature of our GGFET's is that the strength of the periodic modulation in the channel and the inversion-layer electron density can be independently controlled by external voltage supplies. At low temperatures we observe a modulation of the inversion layer conductance. The conductance variation with gate voltage ($\sim 10^{-5}\Omega^{-1}$) is about one hundred times larger than the universal fluctuations predicted by the theory of Lee and Stone. This is consistent with our suggestion that we are observing diffraction by the imposed periodic potential. We have proposed that the criterion for the observation of lateral surface superlattice effects is that the electronic wave functions be phase coherent over distances longer that the period of the grating. That is, that the inelastic diffusion length be larger than the period.

The first generation of devices had low fabrication yields due to poor gate contacts, adhesion problems, metallization problems and shorts to the substrate. Devices also had low mobility due to radiation damage. These problems have been resolved and a new processing sequence for the second generation devices has been developed.

1.7 Study of Surface Superlattice Formation in III-V Field-Effect Transistors

U.S. Air Force - Office of Scientific Research (Grant AFOSR-85-0376)

William Chu, Khalid Ismail, Dimitri A. Antoniadis, Marc A. Kastner, Terry P. Orlando, Henry I. Smith

In this project we are developing a surface superlattice (SSL) FET device based on the AlGaAs/GaAs heterostructure. This device will allow us to subject a high mobility two-dimensional-electron gas to a field-controlled SSL, similar to that in the silicon grating-gate MOSFET discussed in Section 1.6 of this report. The silicon GGFET device has exhibited reproducible "structure" in the drain current (and transconductance) vs. gate voltage curves at liquid helium temperatures. This structure was attributed to 'quasi-mini-gaps" in the energy band diagram caused by the periodic potential of the grating gate. Since their mobility in silicon is low, electrons do not travel much more than about 0.2 µm (which is comparable to the grating period) at a few degrees Kelvin before suffering an inelastic collision and thereby losing phase coherence. If an electron could travel several grating periods between inelastic scattering events, the surface superlattice effects should be much stronger. Such long inelastic lengths can be achieved in high electron mobility (HEMT) devices even at liquid nitrogen temperature. If the expected quantum effects are inherent to surface superlattice devices, then the effect observed in a Si GGFET at 1.2K should appear in the characteristics of a HEM-GGFET at 77 K and perhaps above, due to the substantially higher mobility of the latter device.

To get a better understanding of the HEMT, which is the basic block in building surface superlattices on III-V compound materials, our device structure has been simulated in the semiclassical limit. Many of the effects we anticipate from our HEM-GGFETs (e.g., Block oscillations, quantum tunneling, etc.) will need to be simulated in the quantum regime, which we are not yet able to do. Nevertheless, a semi-

March (Received Systems Systems) (National)

classical simulation of the HEMT based on the solution of Boltzmann's transport equation is very helpful to get the required thickness of layers and doping levels. At this time, devices are in fabrication using processes similar to those for the Si GGFET, appropriately modified for GaAs/GaAlAs heterostructures.

1.8 Investigation of One-Dimensional Conductivity in Multiple, Parallel Inversion Lines

Joint Services Electronics Program (Contract DAAL03-86-K-0002)

Phillip Bagwell, Anthony Yen, Dimitri A. Antoniadis, Marc A. Kastner, Terry P. Orlando, Henry I. Smith

To study one-dimensional conductivity without the statistical fluctuations normally associated with small systems, field-effect devices have been fabricated that use a submicron-period grating-gate structure to produce 250 narrow inversion lines in parallel. The device is fabricated on the same substrate and by the same procedures as the Si GGFET's discussed elsewhere in this report. In fact, the major difference is that the grating lines are now parallel to the electron flow. Others have reported a variety of devices which produce a single narrow "micro-channel," but the expected quasi-onedimensional density of states has been obscured by large random fluctuations inherent in small systems. Here, the parallel measurement of many such one-dimensional conductors results in an improved signal-to-noise ratio in the density-of-states sampling. This is due to the incoherence of random fluctutations in different micro-channels in the same device. Proper independent biasing of the two gate electrodes results in the formation of a parallel array of 50 to 100-nm-wide lines of inversion charge connecting the source and drain. Transconductance measurements demonstrate a weak, regular modulation that is consistent with the expected quasi-one-dimensional density-ofstates.

1.9 Study of Electron Transport in MOSFETs in Si with Deep-Submicron Channel Lengths

Joint Services Electronics Program (Contract DAAL03-86-K-0002)

Ghavam Shahidi, Dimitri A. Antoniadis, Henry I. Smith

Electron conduction in sub-100-nm channel length, Metal-Oxide-Semiconductor Field-Effect Transistors (MOSFETs) in Si is being studied. The devices were fabricated with a combination of x-ray and optical lithographies. The x-ray mask, which defined the minimum lithographic features, was fabricated with conventional photolithography, anisotropic etching, and oblique shadowing. The gate oxide thickness for these devices was 7.5 nm. Electron velocity overshoot, to values exceeding 10⁷ cm sec⁻¹ at room temperature and 1.5x10⁷ cm sec⁻¹ at liquid nitrogen temperature, was observed for the first time. Last year we reported electron velocity overshoot in MOSFETs with 95 nm channel length at liquid helium temperature. No evidence of overshoot at 77 K was found in those devices. Our present devices are similar to those in the earlier report, with the exception that the doping in the inversion layer is now about 10¹⁶ cm⁻³ instead

of $5x10^{17}$ cm⁻³. Control of punchthrough is achieved by a boron implant in the channel of $4x10^{12}$ cm⁻² at 50 keV. After oxidation at 900° C for 10 min in O_2 , to grow the gate oxide, the boron profile remains abrupt with a peak concentration of about $2.2x10^{17}$ cm⁻² at 0.19 μ m depth. The low-field mobility was estimated from long channel MOSFETs on the same substrate to be about 450 cm²/Vsec.

From our experiments we conclude that electron velocity overshoot must be taken into account when modeling electron transport at high electric fields in devices with relatively low doping concentration.

1.10 Application of the Shubnikov-de Haas Oscillations in Characterization of Si MOSFETs and GaAs MODFETs

Joint Services Electronics Program (Contract DAAL03-86-K-0002)

Stephen Y. Chou, Dimitri A. Antoniadis, and Henry I. Smith

The Shubnikov-de Haas magnetoconductance oscillations were used to measure directly the gate-to-channel capacitance of Si MOSFETs and GaAs MODFETs, detect the onset of parallel conduction in GaAs MODFETs and to provide an approximate measure of channel length in the sub-100-nm channel of Si MOSFETs. The measurements do not require knowledge of any device parameters, are immune to any gate parasitic capacitance, and are independent of source and drain series resistance. One needs to know only the magnetic field, the oscillation period (for gate-to-channel capacitance measurement), the gate voltage (for detection of the onset of parallel conduction), and the number of oscillation peaks (for the channel length charcterization). Experimental results have shown that the characterization methods are accurate, and can be applied to FETs with sub-100-nm channel length.

1.11 Crystalline Films on Amorphous Substrates

National Science Foundation (Grant ECS 85-06565)

Sergio Ajuria, Harry A. Atwater, Jerrold A. Floro, Stephen M. Garrison, Joyce E. Palmer, Hui M. Quek, Henry I. Smith, Carl V. Thompson

The development of methods for producing crystalline films on amorphous substrates is an important aspect of our program. This is motivated by the belief that the integration of future electronic and electrooptical systems will be facilitated by an ability to combine, on the same substrate, a broad range of materials (Si, III-V's, piezoelectrics, light guides, etc.). Zone melting recrystallization (ZMR) has been highly successful, but device-quality films are obtained only at the expense of high processing temperatures since the material of interest must be melted. ZMR has been an important testing ground for materials combination, and for a number of novel concepts based on the use of lithography to control in-plane orientation and the location of defects. In this year, an improved ZMR apparatus was built which permits the solidification front to be monitored with a video camera. Several distinct interface morphologies were observed

and a theory developed which explained the morphologies on the basis of dynamic balance between absorption of light by solid Si and reflection by molten Si.

The most promising approach in the long-term to crystalline films on amorphous substrates is, in our view, based on surface-energy-driven secondary grain growth (SEDSGG). In this approach, no melting or phase change occurs. Instead, we take advantage of the very large surface energies inherent in ultrathin (~20 nm) films to drive the growth of large secondary grains having specific crystallographic planes parallel to the surface. This phenomenon has been demonstrated, as has the use of very fine gratings (~100 nm linewidths) to control the in-plane orientation (i.e., graphoepitaxy in combination with SEDSGG). Currently, research is focused on basic studies of grain growth phenomena in ultra-thin films and means for promoting grain growth at temperatures many hundreds of degrees below the melting point. Theoretical models for surface-energy-driven secondary grain growth were developed and have, for the most part, been confirmed by experiments on Si, Ge and Au films. Both ion bombardment and intense optical irradiation enhance grain boundary mobility. In the case of Ge thin films, self implantation at 500°C with 30keV Ge ions achieves a grain growth that by thermal annealing would require 775°C. In thin films of gold, secondary grain growth occurs at room temperature as soon as the film becomes continuous (at ~18 nm). Low energy Ar ion bombardment enhances grain-boundary mobility in Au. In films of Ge 30 nm thick we achieved graphoepitaxial orientation by the purely solid-state, surfaceenergy-driven process. If our basic studies prove fruitful we may be able to develop a low temperature method, applicable to all crystalline film materials, for producing device-quality films on amorphous substrates. By means of lithography, defects in the films, such as dislocations and stacking faults, would be localized at predetermined positions out of the way of devices.

1.12 Ion-Beam-Enhanced Grain Growth in Thin Films

U.S. Air Force - Office of Scientific Research (Contract AFOSR-85-0154) National Science Foundation (Grant ECS 85-06565)

Harry A. Atwater, Jerrold A. Floro, Henry I. Smith, and Carl V. Thompson

We have been investigating the effect of ion bombardment on the motion of grain boundaries in normal and secondary grain growth, so called ion-beam-enhanced grain growth (IBEGG). The scientific objective is to better understand how grain boundaries move. The technological objective is to develop a low temperature process for obtaining crystalline films on amorphous substrates. IBEGG has been studied experimentally in thin (i.e., < 1000 Å) Ge, Au and Si films. Ion beams in the 40 100 keV range have been employed, resulting in an ion damage profile with a peak approximately in the center of the thin film. Concurrent with ion bombardment, samples were annealed at 500 - 1050°C for Ge and Si, and at room temperature for Au. The temperature is chosen so that ion damage is annealed dynamically. IBEGG has been characterized by varying the ion dose, ion energy, ion flux, ion species, termperature, and thin film deposition conditions. The effect of these parameters on grain size and microstructure has been analyzed both qualitatively and quantitatively using transmission electron microscopy (TEM). A transition state model has been developed to describe the motion of grain boundaries during ion bombardment. The model accounts for the dependence of IBEGG on experimental parameters. An atomistic picture of the jump rate at grain boundaries during IBEGG has been proposed. Monte-Carlo simulation of ion range and defect production was performed using the TRIM code and a modified Kinchin- Pease formula. The calculated defect yield per incident ion was correlated with enhanced grain growth and used to estimate the number of atomic jumps at the grain boundary per defect generated at the boundary for a given driving force, a quantity which is approximately constant for a given film material. The IBEGG and thermal growth rates have been related to their respective point defect population. That is, grain growth rate appears to depend only on the concentration of vacancies and interstitials, irrespective of whether they are created thermally or by ion bombardment.

1.13 Epitaxy via Surface-Energy-Driven Grain Growth

U.S. Air Force - Office of Scientific Research (Grant AFSOSR 85-0154) Exxon Foundation

Joyce E. Palmer, Carl V. Thompson, Henry I. Smith

Grain Growth in polycrystalline films on single-crystal substrates can lead to formation of low-defect-density or single-crystal films. We are investigating surface-enery-driven secondary grain growth in silicon films deposited on a variety of insulating single-crystal substrates including CaF_2 and Al_2O_3 . We are also further developing the theory of epitaxy by surface-energy-driven grain boundary motion.

1.14 Submicrometer-Period Gold Transmission Gratings for X-Ray Spectroscopy

Lawrence Livermore National Laboratory (Subcontract 9459005)

Erik H. Anderson, Mark L. Schattenburg,² Henry I. Smith

Gold transmission gratings with periods of 0.1 to 0.2 μ m, and thicknesses ranging from 0.5 to 1 μ m are fabricated using x-ray lithography and electroplating. The x-ray masks are made either with holographic lithography or scanning-electron-beam lithography. Transmission gratings are either supported on polyimide membranes or are made self-supporting by the addition of crossing struts. They are used for spectroscopy of the x-ray emission from plasmas produced by high-power lasers. Gratings fabricated in our lab by these techniques are used in key diagnostic instruments associated with the soft x-ray laser research at Lawrence Livermore National Laboratory.

1.15 High-Dispersion, High-Efficiency Transmission Gratings for Astrophysical X-Ray Spectroscopy

National Aeronautics and Space Administration (Grant NGL22-009-683)

² M.I.T. Center for Space Research

Eric H. Anderson, Mark L. Schattenburg, Claude R. Canizares³, Henry I. Smith

Gold gratings with spatial periods of 0.1 - 10 μ m make excellent dispersers for high resolution x-ray spectroscopy of astrophysical sources in the 100 eV to 10 KeV band. These gratings are planned for use in the Advanced X-ray Astrophysics Facility (AXAF) which will be launched in the mid 1990's. In the region above 3 KeV, the requirements of high dispersion and high efficiency dictate the use of the finest period gratings with aspect ratios approaching 10:1. To achieve this we first expose a grating pattern in 1.5 μ m thick PMMA over a gold plating base using Carbon-K x-ray nanolithography. To date, we have worked with gratings having periods of 0.3 or 0.2 μ m (linewidth 0.15 - 0.1 μ m). Gold is then electroplated into the spaces of the PMMA to a thickness of 1 μ m. Flight prototype gratings have been fabricated and are undergoing space worthiness tests. Efforts continue to increase the reliability and efficiency of the fabrication process.

1.16 Soft X-Ray Interferometer Gratings

Collaboration with KMS Fusion, Inc.

Erik H. Anderson, Henry I. Smith

In the soft x-ray region of the electromagnetic spectrum (1-10 nm) reliable optical constant data is scarce or non-existent. In order to fill this gap, an achromatic interferometer instrument is under construction at KMS Fusion, Inc. The critical optical components of this instrument are a set of matched, 200-nm-period transmission gratings which will be fabricated at M.I.T. Because these gratings will be used in an interferometer, the phase-front quality must be extremely good, and at the same time, the lines must be free-standing, i.e., have no support structure that would attenuate the x-rays. The fabrication process uses a thin membrane of silicon which is then etched to make free-standing lines. Gold lines were found to have too much distortion for this application.

Publications

Journal Articles

Canizares, C.R., H.V.D. Bradt, G.W. Clark, A.C. Fabian, P.C. Joss, A.M. Levine, W.H.G. Lewin, T.H. Market, W. Mayer, J.E. McClintock, S.A. Rappaport, G.R. Ricker, M.L. Schattenburg, H.I. Smith, and B.E. Woodgate, "The M.I.T. Spectroscopy Investigation on AXAF and the Study of Supernova Remnants," Astrophysics Lett. (to be published).

Chou, S.Y, H.I. Smith, and D.A. Antoniadis, "Sub-100nm Channel-Length Transistors Fabricated Using X-Ray Lithography," J. Vac. Sci. Tech. B 4, 253 (1986).

Chou, S.Y., D.A. Antoniadis, H.I. Smith, and M.A. Kastner, "Conductance Fluctuations in Ultra-Short-Channel Si MOSFETs," Solid State Communications 61, 571 (1987).

³ M.I.T. Center for Space Research

- Chou, S.Y., and D.A. Antoniadis, "Relationship between Measured and Intrinsic Transconductance of FETs," I.E.E.E. Trans. Electron Devices *ED-34*, 448 (1987).
- Chou, S.Y., D.A. Antoniadis, and H.I. Smith, "Application of the Shubnikov-de Haas Oscillations in Characterization of Si MOSFET's and GaAs MODFET's," I.E.E.E. Proc. Elec. Dev. *ED-34*, 883 (1987).
- Garrison, S.M., R.C. Cammarata, C.V. Thompson, and H.I. Smith, "Surface-Energy-Driven Grain Growth During Rapid Thermal Annealing (<10s) of Thin Silicon Films," J. Appl. Phys. 61, 1652 (1987).
- Geiss, M.W., H.I. Smith, and C.K. Chen, "Characterization and Entrainment of Subboundaries and Defect Trails in Zone-Melting-Recrystallized Si Films," J. Appl. Phys. 60, 1152 (1986).
- Kastner, M.A., R.F. Kwasnick, and J.C. Licini, "Conductance Fluctuations Near the Localized-to-Extended Transition in Narrow Si MOSFETs.", submitted to Phys. Rev.
- Kim, H.-J., and C.V. Thompson, "Compensation of Grain Growth Enhancement in Doped Silicon Films," Appl. Phys. Lett. 48 399, (1986).
- Palmer, J., C.V. Thompson, H.I. Smith, "Grain Growth and Grain Size Distribution in Thin Germanium Films on SiO₂," (to be published in J. Appl. Phys.).
- Smith, H.I., "A Review of Submicron Lithography," Superlattices and Microstructures 2, 129 (1986).
- Smith, H.I., "A Statistical Analysis of UV, X-Ray and Charged-Particle Lithographies," J. Vac. Sci. Tech. B 4, 148 (1986).
- Warren, A.C., D.A. Antoniadis, and H.I. Smith, "Semi-Classical Calculation of Charge Distributions in Ultra-Narrow Inversion Lines," I.E.E.E. Electron Devices Letters *EDL-7*, 413 (1986).
- Warren, A.C., I. Plotnik, E.H. Anderson, M.L. Schattenburg, D.A. Antoniadis, and H.I. Smith, "Fabrication of Sub-100 nm Linewidth Periodic Structures for Study of Quantum Effects from Interference and Confinement in Si Inversion Layers," J. Vac. Sci. Tech. B 4, 365 (1986).
- Warren, A.C., D.A. Antoniadis, and H.I. Smith, "Quasi One-Dimensional Conduction in Multiple, Parallel Inversion Lines," Phys. Rev. Lett. 56, 1858 (1986).
- Wong, C.C., H.I. Smith, and C.V. Thompson, "Surface-Energy-Driven Secondary Grain Growth in Thin Au Films," Appl. Phys. Lett. 48, 335 (1986).

Conference Proceedings

Atwater, H.A., H.I. Smith, and C.V. Thompson, "Ion Beam Enganced Grain Growth in Thin Films," to be published in *Beam-Solid Interactions and Transient Processes*, Mat. Res. Soc. Symp., (1986).

sky panama skiese kieske eskeese sekeen suuddi aluudaa auluda jäädist päääää jäädista jäädistä päääää

- Atwater, H.A., H.I. Smith, and C.V. Thompson, "Enhancement of Grain Growth in Ultra Thin Germanium Fioms by Ion Bombardment," Mat. Res. Soc. Symp. Proc. 51, 337 (1985).
- Chou, S.Y., C. Lam, D.A. Antoniadis, H.I. Smith, and C.G. Fonstad, "Characterization of Modulation-Doped FET's Using Shubnikov-De Haas Oscillations," 1986 International Symposium on Gallium Arsenide and Related Compounds (in press).
- Geis, M.W., C.K. Chen, H.I. Smith, P.M. Nitishin, B.-Y. Tsaur, and R.W. Mountain, "Elimination of Subboundaries from Zone-Melting-Recrystallized Silicon-on-Insulator Films," Mat. Res. Soc. Symp. Proc. 53, 39 (1986).
- Geis, M.W., C.K. Chen, and H.I. Smith, "Elimination of Subboundaries in 0. mm thick Si-on-insulator films produced by ZMR," to be published in Mat. Res. Soc. Symp. Proc., (1986).
- Im, J.S., C.V. Thompson and H. Tomita, "Solidification Morphologies in Zone-Melting Recrystallization," to be published in Mat. Res. Soc. Symp. Proc., (1986).
- Kim, H.J., and C.V. Thompson, "The Effects of Dopants on Surface-Energy-Driven Grain Growth in Ultrathin Si Films," Proceedings of the Fall Meeting of the Materials Research Society 51, Boston, MA, Dec. 2-6, 1985.
- Plotnik, I., M.E. Porter, M. Toth, S. Akhtar, and H.I. Smith, "Ion-Implant Compensation of Tensile Stress in Tungsten Absorber for Low Distortion X-Ray Masks," *Microcircuit Engineering* '86, Proceedings of the International Conference on Microlithography, 1986, Interlaken, Switzerland, edited by H.W. Lehmann and C. Bleiker, North-Holland, 1986, p. 51.
- Shahadi, S.I, D.A. Antoniadis, and H.I. Smith, "Electron Velocity Overshoot at 300K and 77K in Silicon MOSFETs With Submicron Channel Lengths," p. 824, 1986 I.E.E.E. International Electron Devices Meeting, Los Angeles, Calif., December 1986.
- Smith, H.I., "A Statistical Analysis of Microlithography," Extended Abstracts of the 1986 International Conference on Solid State Devices and Materials, Japan Society of Applied Physics, Business Center for Academic Societies, Japan, 1986, p. 13.
- Smith, H.I., M.W. Geis, C.K. Chen, and C.V. Thompson, "Crystalline Films on Amorphous Substrates by Zone Melting and Surface-Energy-Driven Grain Growth in Conjunction with Patterning," Mat. Res. Soc. Symp. Proc. 53, 3 (1986).
- Thompson, C.V., and H.I. Smith, "Secondary Grain Growth in Thin Films," Proceedings of the Materials Research Society 57, 449, Boston, Mass., Dec. 2-6 (1987).

Theses

Chou, S.Y., "Electronic Conduction in Ultra-Short Channel Si MOSFET's," Ph.D. Thesis, Dept. of Phys., M.I.T., Cambridge, Mass., 1986.

- Garrison, S.M., "The Kinetics of Secondary Grain Growth In Rapidly Thermal Annealed Thin Silicon Films," S.M. Thesis, Dept. of Mat. Sci. and Eng., M.I.T., Cambridge, Mass., 1986.
- Wong, G.G, "Fast Sub-100 nm Alignment For X-Ray Lithography: Fresnel Zone Plates and Reduced Scanning Field," Dept. of Electr. Eng. and Comp. Sci., M.I.T., Cambridge, Mass., 1986.
- Yonehara, T., "Low Temperature-Growth of Semiconductor Films Over Amorphous Insulating Substrates," Ph.D. Thesis, Waseda University, 1986.

THE PERSON NAMED IN THE PROPERTY OF THE PERSON NAMED IN THE PERSON

2.0 Kinetic Phenomena in Thin Film Electronic Materials

Academic and Research Staff

Prof. C.V. Thompson, Prof. H.I. Smith, Dr. R.C. Cammarata, Mr. H. Tomita, Prof. J. Melngailis

Graduate Students

S. Ajuria, H. Atwater, J. Cho, L. Clevenger, A.D. Dubner, J. Floro, S.M. Garrison, J. Im, E. Jiran, H. Kahn, H.-J. Kim, H. Longworth, C. Maiorino, J. Palmer, H.M. Quek, J. Ro, C.C. Wong

Undergraduate Student

H. Meng

Support Staff

M.L. Wilson, M. Porter

2.1 Normal and Secondary Grain Growth in Ultrathin (<1000 Å) Films of Silicon and Germanium

National Science Foundation (Grant ECS 85-06505)
U.S. Air Force - Office of Scientific Research (Contract AFOSR-85-0154)
Semiconductor Research Corporation (Contract 87-SP-080)

Hyoung-June Kim, Joyce E. Palmer, Harry A. Atwater, Stephen M. Garrison, Hui M. Quek, Sergio Ajuria, Jerrold A. Floro, Carl V. Thompson, Henry I. Smith

Polycrystalline semiconductor films are used in a wide variety of electronic applications including use as gates in MOS devices, base and emitter contacts in bipolar devices, diffusion sources, sensors, thin film transistors and solar cells. In thin films of semiconductors, normal grain growth is driven by the reduction of the total grain boundary energy and usually leads to grains with sizes roughly equal to film thickness. We have shown that in sufficiently thin films (<1000Å) of silicon and germanium, a secondary grain growth process leads to the continued growth of some grains to sizes much larger than the film thickness. These secondary grains often have near uniform crystallographic texture. We believe that surface-energy-anisotropy is responsible for the selective growth of these grains. That is, grains with orientations that minimize surface energy grow at the expense of other grains. We have shown that the rate of secondary grain growth increases with decreasing film thickness and increasing temperature. Unlike metals, addition of impurities (e.g., P and As in Si) can also lead to an increase in the secondary grain growth rate. We have recently shown that grain boundary mobility in silicon is directly related to the Fermi energy. We are developing

theoretical models for secondardy grain growth and grain boundary motion in semiconductors. We are also investigating the effects of rapid thermal annealing and ion bombardment on grain boundary motion.

2.2 Graphoepitaxy of Si, Ge and Model Materials

National Science Foundation (Grant ECS 85-06565)
U.S. Air Force - Office of Scientific Research (Contract AFOSR-85-0154)

C.C. Wong, Joyce Palmer, Stephen Garrison, Harry A. Atwater, Hui M. Quek, S. Ajuria, Jerrold A. Floro, Henry I. Smith, Carl V. Thompson

Graphoepitaxy is a process in which an overlayer film is crystallographically oriented by an artificial surface pattern. Graphoepitaxy can involve vapor to solid, liquid to solid and solid to solid transitions. In experiments on graphoepitaxy we use lithographically defined surface features with periodicities as low as 2000Å. Recent research has focused on the use of artificial surface features in controlling surface-energy-driven secondary grain growth (SEDSGG) in model materials. Periodic patterns with square-wave cross sections increase the driving force for SEDSGG by increasing the surface area. The driving force is increased for grains with specific in-plane orientations as well as texture. We have demonstrated graphoepitaxial alignment during surface-energy-driven secondary grain growth in gold and germanium films. Greater control of these solid state forms of graphoepitaxy may allow the development of low temperature processes for obtaining device quality semiconductor films on insulating substrates.

2.3 Epitaxy via Surface-Energy-Driven Grain Growth

U.S. Air Force - Office of Scientific Research (Contract AFOSR-85-0154)

Joyce Palmer, Carl V. Thompson, Henry I. Smith

Grain growth in polycrystalline films on single crystal substrates can lead to formation of low defect density or single crystal films. We are investigating surface-energy-driven secondary grain growth in films deposited on a variety of insulating single crystal substrates. We are also further developing the theory of epitaxy by surface-energy-driven grain boundary motion.

2.4 Zone Melting Recrystallization of Silicon on Insulators

International Business Machines, Inc. Sony International Business Machines, Inc.

James Im, Hisashi Tomita, Carl V. Thompson

Techniques for producing device-quality single-crystal films of semiconductors on insulators (SOI) are of interest for multilayer and multi-materials integrated circuits and

low-cost, high-efficiency solar cells. Such films can be obtained through directional solidification of confined thin films (zone melting crystallization, ZMR). While there are analogies to bulk crystal growth in ZMR, there are also phenomena and mechanisms unique to thin-film solidification of radiatively heated silicon. We are studying these phenomena in order to develop means of controlling crystal growth in ZMR. Direct observation of dynamic and static liquid-solid interface complements theoretical modeling of solidification.

2.5 Properties of Grain Boundaries with Controlled Orientations and Locations in Thin Silicon Films

International Business Machines, Inc.

Hyoung J. Kim, James S. Im, Carl V. Thompson, David A. Smith¹

We are using lithographic patterning of films in conjunction with zone melting recrystallization (ZMR) to produce isolated grain boundaries with controlled misorientations and locations. Preparation of these thin film "bicrystals" should allow study of grain boundary structure and composition via transmission electron microscopy. These will be correlated with electronic characterization. Motion of individual boundaries between grains with different textures will also be studied. The misorientation dependence of grain boundary structure, composition, atomic mobility and electronic properties will be studied.

2.6 Metastable Phase Formation in Lithographically Defined Particles of Semiconductors

National Science Foundation (Grant DMR 84-18718)

Eva Jiran, Carl V. Thompson

When divided into a large number of small particles, materials can undergo phase transformations at substantial departures from equilibrium. It has been shown, for example, that dispersions of small particles of liquid metals can be undercooled to 50-80% if their melting temperatures. These undercoolings are achieved due to the isolation of the heterogeneities that catalyze crystal nucleation into a minor fraction of the particles. At high undercoolings, metastable phases can result from configurational freezing (transformation from a liquid to an amorphous solid), through mestastable phase nucleation, or due to undercooling-induced rapid solidification. We are using advanced lithography techniques to create samples composed of large numbers of small (including submicron), identical particles of semiconductors for studies of nucleation and metastable phase formation.

International Business Machines, Inc.

2.7 Kinetics of Silicide Formation at Refractory Metal-Silicon Contacts

International Business Machines, Thomas J. Watson Research Center

Robert C. Cammarata, Lawrence Clevenger, Carl V. Thompson, K.-N. Tu²

There is considerable current interest in the use of refractory metals or refractory metal silicides as interconnects, as gate materials in MOS devices and as diffusion barriers at metal-silicon contacts in integrated circuits. One method of silicide formation is through reaction of metallic thin films with silicon substrates. This potential application raises fundamental questions about the rate and products of thin film metal-silicon reactions. There are four critical parameters in analysis and modeling of these reactions: interdiffusivities, free energy changes, surface energies and interface reaction constants. Of these, the first two parameters are fairly well understood and can be predicted. The purpose of this project is to develop a better understanding and predictive capability for the last two parameters. Surface energies are being determined through silicide precipitation experiments and interface reaction rate constants are being determined through analysis of interface limited reactions of thin films.

2.8 Grain Growth in Thin Films of Aluminum

Joint Services Electronics Program (Contract DAALO3-86-K-0002)

Cesar D. Maiorino, Hai Longworth, Carl V. Thompson

The thermal and electrical stability of metallic thin films and thin film lines are strongly affected by microstructure. Because grain boundary mobilities are high in metals, as compared to semiconductors, secondary grain growth can occur at relatively low homologous temperatures (T/Tm, Tm = the melting temperature), T/Tm = 0.5, and in relatively thick films ($\gtrsim 1 \mu m$). We have demonstrated that secondary grain growth in 0.75 μm films of A1-2%Cu-0.3%Cr can lead to grains with dimensions greater than 200 μm . Control of surface-energy-driven secondary grain growth in thin film lines with near unity aspect ratios may lead to total elimination of grain boundaries. Such lines would be highly resistant to thermally induced beading and electromigration. We are investigating the effects of deposition condictions, film composition and annealing conditions on secondary grain growth in A1 alloys. These alloys are widely used as interconnect materials in microelectronic devices and circuits.

2.9 Thin and Narrow Metallic Interconnects

Semiconductor Research Corporation (Contract 87-SP-080)

Joint Services Electronics Program (Contract DAALO3-86-K-0002)

Jaeshin Cho, Hai Longworth, Carl V. Thompson

International Business Machines, Inc.

Thin film lines of A1 and A1 alloys are used to interconnect devices in integrated circuits. Interconnects often fail due to damage resulting from current induced diffusion (electromigration), temperature-gradient-induced diffusion (thermomigration), and morphological changes driven by surface energy minimization (e.g., grain boundary grooving, void formation and/or beading). Reduced interconnect dimensions are sought in order to increase device densities and to improve device performance through reduction of parasitic capacitances. Decreased dimensions, however, can lead to increased rates of diffusion-induced failure. We are investigating the morphological and electrical stability of current-carrying submicrometer thick and wide metallic lines. Control of the microstructure of such lines should allow processing of interconnects with improved reliabilities.

2.10 Electromigration at Aluminum-Silicon Contacts in Integrated Circuits

Semiconductor Research Corporation (Contract 87-SP-080)

H. Kahn, Carl V. Thompson

Thin film lines of aluminum alloys are used to interconnect devices in integrated circuits. These interconnects must make contact with silicon through windows in silicon dioxide films. The properties of these contacts and their long term reliability greatly affect the functionality and utility of integrated circuits. Contacts fail via chemical-potential-driven or electromigration-induced interdiffusion. These failure mechanisms lead to leakage due to aluminum "spiking" through shallow junctions and/or due to increased contact resistance due to silicon precipitation. These problems are exacerbated by the shallow junctions, small area contacts, and reduced interconnect dimensions characteristic of very large scale integrated circuits. We have initiated a new program to investigate interdiffusion at aluminum-silicon contacts as well as contacts with diffusion barriers. We will correlate electronic characterization with microstructural features as revealed through electron microscopy. We anticipate development of new processing techniques for producing contacts with improved reliability for applications in very large scale integrated circuits.

2.11 Computer Modeling of Microstructural Evolution in Thin Films

National Science Foundation (Grant DMR 85-06030)

Carl V. Thompson, H.J. Frost³

In thin films final grain sizes and final grain shapes vary with crystal nucleation and growth rates during film formation. We have modeled two dimensional crystallization and have quantitatively shown that grain structures are easily topologically differntiable

³ Dartmouth College

when films form under conditions of nucleation site saturation or when constant nucleation rates persist. These results provide a post-formation means of analyzing the conditions under which polycrystalline thin films have been produced. We are also modeling two-dimensional grain growth in computer-generated initial grain structures. Capillarity effects due to surface energy as well as grain boundary energy are accounted for. This allows modeling of normal grain growth and secondary grain growth.

2.12 Focussed Ion Beam Induced Deposition

Charles Stark Draper Laboratory (Contract DL-H-261827) Nippon Telegraph and Telephone, Inc.

Andrew D. Dubner, Jaesang Ro, John Melngailis, Carl V. Thompson

It is now possible to produce ion beams with diameters as small as 500Å. This permits use of focussed ion beams for high spatial resolution implantation, sputtering and deposition. In principal, the latter can be used in integrated circuit mask repair or high resolution direct writing of interconnects. We are investigating the mechanisms of ion-beam-induced chemical vapor deposition from metal-bearing gases.

Publications

- Atwater, H.A., C.V. Thompson, and H.I. Smith, "Ion Beam Enhanced Grain Growth in Thin Films," In Proceedings of the Beam-Solid Interactions and Transient Processes Symposium of the Fall 1986 Materials Research Society Meeting.
- Atwater, H.A., H.I. Smith and C.V. Thompson, "Enhancement of Grain Growth in Ultra-Thin Germanium Films by Ion Bombardment," Proc. Mat. Res. Soc. Symp. 51 (1986), p. 337.
- Frost, H.J., J. Whang, and C.V. Thompson, "Modeling of Grain Growth in Thin Films," In *Annealing Processes-Recovery Recrystallization and Grain Growth*, 7th Riso International Symposium on Metallurgy and Materials Science, edited by N. Hanson, T. Lerrere and B. Ralph.
- Frost, H.J. and C.V. Thompson, "Modeling of Thin Film Grain Structures and Grain Growth," Proceedings of the Computer Based Microscipic Description of the Structure and Properties of Materials Symposium, Fall 1985 Meeting of the Materials Research Society.
- Frost, H.J. and C.V. Thompson, "The Effect of Nucleation Conditions on the Topology and Geometry of Two-Dimensional Grain Structures," to appear in Acta Metall.
- Garrison, S.M., R.C. Cammarata, C.V. Thompson and H.I. Smith. "Surface-Energy-Driven Grain Growth During Rapid Thermal Annealing (<10ns) of Thin Silicon Films," to appear in J. Appl. Phys.

- Kim, H.-J., and C.V. Thompson, "The Effects of Dopants on Surface-Energy-Driven Secondary Grain Growth in Ultrathin Si Films," In *Grain Boundary Structure and Related Phenomena*, Supp. to Trans. Jpn. Inst. Met. 27, 495 (1986).
- Kim, H.-J. and C.V. Thompson, "Compensation of Grain Growth Enhancement in Doped Silicon Films," Appl. Phys. Lett. 48, 399 (1986).
- Kim, H.-J., and C.V. Thompson, "The Effects of Dopants on Grain Boundary Mobility in Silicon," In *Grain Boundary Structure and Related Phenomena*, suppl. to Trans. Jpn. Inst. Metals 27, 495 (1986).
- Smith, H.I., M.W. Geis, C.V. Thompson and C.K. Chen. "Crystalline Films on Amorphous Substrate by Zone Melting and Surface-Energy-Driven Grain Growth in Conjunction with Patterning," Proceedings of the Beam Solid Interactions and Phase Transformations Symposium of the Fall 1985 Meeting of the Materials Research Society.
- Srolovitz, D.J. and C.V. Thompson, "Beading Instabilities in Thin Film Lines with Bamboo Microstructures," Thin Solid Films 139, 133 (1986).
- Thompson, C.V. and C.D. Maiorino, "Very Large Grained Aluminum Alloy Thin Films for Interconnects," Proceedings of the 18th International Conference on Solid State Devices and Materials, Tokyo, Japan, 1986, p. 491.
- Thompson, C.V. and H.I. Smith, "Secondary Grain Growth in Thin Films," Proc. Phase Transistions in Condensed Systems Symp., fall meeting of the Mat. Res. Soc. (1985).
- Thompson, C.V., H.J. Frost, and F. Spaepen, "The Relative Rates of Secondary and Normal Grain Growth," to appear in Acta Metall.
- Thompson, C.V. and J. Cho, "A New Electromigration Test Structure for Rapid Statistical Evaluation of Interconnect Technology," in I.E.E.E. Electron Dev. Lett., EDL-7, 667 (1986).
- Wong, C.C., H.I. Smith, and C.V. Thompson, "Room Temperature Grain Growth in Thin Au Films," in Grain Boundary Structure and Related Phenomena, suppl. to Trans. Jpn. Inst. Metals 27, 641 (1986).
- Wong, C.C., H.I. Smith and C.V. Thompson, "Surface-Energy-Driven Secondary Grain Growth in Thin Au Films," Appl. Phys. Lett. 48, 335 (1986).

Theses

- Garrison, S.M., "Kinetics of Secondary Grain Growth in Rapidly Thermal-Annealed Thin Silicon Films." M.S. Thesis., Dept. of Mat. Sci. and Eng., M.I.T., Cambridge, Mass., 1986.
- Maiorino, C.D., "The Effects of Composition and Layering of Secondary Grain Growth in Aluminum Alloy Thin Films." Thesis, Dept. of Mat. Sci. and Eng., M.I.T., Cambridge, Mass., 1986.

- Palmer, J.E. "Secondary Grain Growth in Ultrathin Films of Germanium on Silicon Dioxide," M.S. Thesis. Dept. of Electr. Eng. and Comp. Sci., M.I.T., Cambridge, Mass., 1985.
- Prevost, Lawrence N., II, "Secondary Grain Growth in Thin Aluminum Lines." S.B. Thesis, Dept. of Electr. Eng. and Comp. Sci., M.I.T., Cambridge, Mass., 1985.
- Wong, C.C., "Secondary Grain Growth and Graphoepitxy in Thin Au Films." Thesis, Dept. of Mat. Sci. and Eng., M.I.T., Cambridge, Mass., 1986.

COCCURS STREETS CONTRACT PROPERTY CONTRACTOR CONTRACTOR

3.0 Focused Ion Beam Fabrication

Academic and Research Staff

Prof. D.A. Antoniadis, Dr. J. Melngailis, Prof. C.V. Thompson

Collaborating Scientists

L. Mahoney¹, R.E. Lowther², J.L. Bartlett³, W.B. Thompson⁴

Graduate Students

A.D. Dubner, J.B. Jacobs, H. Lezec, C.R. Musil, G.M. Shedd, J. Ro

3.1 Focused Ion Beam Program

John Melngailis

A focused ion beam system capable of mass separation and accurate submicron beam writing on a wafer has been purchased from Ion Beam Systems Inc. as part of the Microsystems Technology Program. So far the system has demonstrated 150kV operation. It has exposed dots in PMMA of 0.1 μ m diameter and operated with the following ion species: Ga, Au, Si, Pd, B, As. The system will be delivered to M.I.T. in March 1987 and is scheduled to be in operation in May 1987. We had access to the machine and have carried out precision patterned doping of GaAs and Si.

In addition we have purchased a 50kV non-mass separated column which has a beam diameter of 0.05 μ m. This system is intended for ion milling and ion induced deposition and etching. A DOD/University Instrumentation Grant has been received for the construction of an ultrahigh vacuum chamber to be used with this column. In the meantime the system will be used with an ordinary vacuum chamber.

3.2 Fabrication of Graded Channel FETs in GaAs and Si

DARPA/Naval Electronic Systems Command (Contract MDA-903-85-C-0215)

Henri Lezec, Leonard Mahoney,⁵ Jarvis B. Jacobs, Rex E. Lowther, Christian R. Musil, Dimitri A. Antoniadis, and John Melngailis

¹ Lincoln Laboratory

² Visiting Scientist from Harris Semiconductor

³ Hughes Research Laboratory

⁴ IBS, Beverly, Mass.

⁵ Lincoln Laboratory

The goals of this program are to use the focused ion beam system to fabricated field effect transistors in GaAs and in Si with graded doping profiles and to model the behavior of these novel device structures. Graded doping profiles, where the implanted density varies linearly from source to drain, have been successfully implanted in GaAs. These implants were aligned to existing features, and, in addition, alignment marks were ion milled into the surface to align the gate electrodes with the ion implants. Preliminary results show an increase in transconductance in the graded devices as well as flatter I_D vs. V_D curves in the saturation region. Computer simulation of these structures are being carried out. In silicon, we have used a Pd/B/As liquid metal ion source to implant test structures. A mask has been designed for transistors which will have the channel region implanted by focused ion beams. In silicon, device models have been developed which include graded doping and the dependence of the mobility on the distance from the surface.

3.3 Ion Induced Deposition

THE PERSON STATES OF THE PROPERTY OF THE PROPE

rainings and something of the state of the states of the s

Charles Stark Draper Laboratory (Contract DL-H-261827) U.S. Navy - Office of Naval Research (Contract N00014-84-K-0073) Nippon Telephone and Telegraph

Gordon M. Shedd, Andrew D. Dubner, Henri Lezec, Carl V. Thompson, John Melngailis

A focused ion beam can be used to induce material deposition with submicron resolution if a local gas ambient is produced at the point of ion impact. The local gas ambient is produced by aiming a miniature gas nozzle at the surface in close proximity. We have, used WF₆ and deposited tungsten. However, because the deposition was carried out in a background vacuum of 10⁻⁶ to 10⁻⁷ torr, the film contains from 5 to 30% oxygen. We are building an ultrahigh vacuum chamber to eliminate the oxygen. In the meantime by choosing a less reactive material we have deposited gold from a gas of dimethyl gold hexafluoro acetylacetonate. The ions used were either 15kV Ga+ from a 0.5 µm diameter focused beam, unfocused 70 keV Si⁺ ions from an implanter, or 0.75 keV Ar⁺ from an ion miller. Deposition occurred in all cases with yields of between 5 to 16 atoms deposited/incident ion. Except for the expected Ga other contaminants such as C or O are at levels below 5%. The resistivity of the film was measured to vary between 20 and 500 $\mu\Omega$ cm (bulk gold is 2.5 $\mu\Omega$ cm) depending on the deposition conditions. This is comparable to or better than polysilicon which is used as an IC interconnect material. With the focused ion beam lines of 0.5 μ m width (equal to the beam diameter) were deposited. Thus this is a promising technique for integrated circuit rewiring, repair, or prototyping, and for repair of x-ray lithography masks.

3.4 Focused Ion Beam Microsurgery for Electronics

Charles Stark Draper Laboratory (Contract DL-H-261827)

C.R. Musil, J.L. Barrett, and John Melngailis

⁶ Hughes Research Laboratory

The modification of selected areas of an integrated circuit to alter its electrical function has many potential applications. The simplest such application is the breaking or making of electrical connnections, which can lead to circuit diagnostics and debugging, to customization, and to defect avoidance. At present lasers are used in large integrated circuit memories to cut conductors and excise faulty circuit elements and wire in redundant spares. However, lasers typically blast away the conductors leaving craters 5-10 μ m in diameter. The focused ion beam can perform such cutting in a much more controlled fashion with submicron resolution.

We have demonstrated the cutting of conductors and also developed methods for electrically connecting two overlapping conductors initially separated by oxide. The cost of the increased resolution is the time taken to cut conductors. This can extend to minutes if a fine beam is simply scanned over an area to mill an opening in the conductor. To make connections we have developed a method which consists of milling two concentric square sided pits through a conductor-insulator-conductor sandwich. Deliberate redeposition on vertical sidewalls makes an electrical connection. The pits ranged in size from $3x3~\mu m$ to 0.5~x0.5 μm . For the smallest pits a 4 to 8 Ω connection can be made in 7 seconds. In addition, in many cases the breaking or making of connections can be verified by using the focused ion beam in the scanning ion microscope mode. Depending on the electrical connections parts of a circuit will charge up to different voltages limiting the secondary electron emission and showing up on the screen with different contrast. As circuit dimensions shrink and their complexity grows focused ion beam circuit restructuring, because of the increased control and precision, will become an increasingly useful technique.

3.5 Measurement of Beam Profile

Hitachi Central Research Laboratory

John Melngailis and W.B. Thompson⁷

The focused ion beam profile is expected to be Gaussian. We have measured the profile over five orders of magnitude in intensity and found that from about two orders of magnitude below the peak, the profile has shoulders which make the beam broader. We also plan to investigate the relation between resolution in the imaging mode and beam diameter, and the relation between beam diameter and the resolution of the dopant pattern implanted.

Publications

Lowther, R.E., J.B. Jacobs, and D.A. Antoniadis, "Simulation of Implantation and Diffusion of Profiles Made with a Focused Ion-Beam Implanter," I.E.E.E. Trans. Electron Dev., *ED-33*, 1251 (1986).

Melngailis, J., D.J. Ehrlich, S.W. Pang, J.N. Randal, "Cermet as an Inorganic Resist for Ion Lithography," J. Vac. Sci. Tech. B 5, 379 (1987).

⁷ IBS, Beverly, Mass

- Melngailis, J., "Focused Ion Beam Technology and Applications," a review, J. Vac. Sci. Tech., 469 (1987).
- Melngailis, J., G.J. Dunn, and W.B. Thompson, "Focused Ion Beam Induced Deposition," Techical Proceedings of SEMICON/EAST 1986, Boston, Mass., 1986, pp. 53-61.
- Melngailis, J., C.R. Musil, E.H. Stevens, M. Utlaut, E.M. Kellogg, R.J. Post, M. Geis, and R.W. Mountain, "The Focused Ion Beam as an Integrated Circuit Restructuring Tool," J. Vac. Sci. Tech. *B4*, 176 (1986).
- Melngailis, J., "Focused-Ion-Beam Technology," I.E.E.E. Electrotech. Rev. (1986), p. 58.
- Musil, C.R., J.L. Bartlett, and J. Melngailis, "Focused-Ion-Beam Microsurgery for Electronics," I.E.E.E. Electron Devices Lett., *EDL-7*, 285 (1986).
- Musil, C.R., J.L. Bartlett, and J. Melngailis, "Focused Ion Beam Microsurgery for Integrated Circuit Customization and Repair," Proceedings of the I.E.E.E. 1986 Custom Integrated Circuits Conference, p. 591.
- Shedd, G.M., H. Lezec, A.D. Dubner, and J. Melngailis, "Focused Ion Beam Induced Deposition of Gold," Appl. Phys. Lett. 49, 1584 (1986).

Thesis

THE REPORT OF THE PROPERTY OF

Shedd, G.M., "Ion Assisted Deposition of Gold," M.S. Thesis, Dept. Nucl. Eng., M.I.T., Cambridge, Mass., 1986.

4.0 Chemical Reaction Dynamics at Surfaces

Academic and Research Staff

Prof. S.T. Ceyer

Visiting Scientist

J.R. Wang

Graduate Students

J.D. Beckerle, D.J. Gladstone, A.D. Johnson, M.B. Lee, M. McGonigal, M. Schulberg, R.J. Simonson, Q.Y. Yang

4.1 Lack of Translational Energy Activation of the Dissociative Chemisorption of CO on Ni(111)

National Science Foundation (Grants CHE 85-08734 and DMR 81-19295)
Research Corporation
Camille and Henry Dreyfus Foundation
Joint Services Electronics Program (Contract DAAL03-86-K-0002)

Sylvia T. Ceyer, John D. Beckerle, Myung B. Lee, Sau Lan Tang

The activation of the dissociative chemisorption of CO on Ni(111) by translational and vibrational energy is probed. Molecular beam techniques produce CO molecules with high kinetic energies and with some vibrational excitation. Thermal desorption and high resolution electron energy loss spectroscopy detect the product of the chemisorption event. The maximum translational and vibrational energies attainable in these experiments, 45 kcal/mole and 18 kcal/mole, respectively, are observed not to activate the dissociative chemisorption of CO. These experiments are sensitive to dissociation probabilities as small as 2 x 10⁻⁶ and 9 x 10⁻⁴ at the maximum values of translational and vibrational energy, respectively. It is concluded that translational energies greater than 45 kcal/mole do not contribute to the CO dissociation rate at high pressures. Rather, the potential energy surface of the CO-Ni(111) interaction likely requires vibrational excitation greater than the amount that can be achieved in this experiment for activation of the C≡0 bond.

4.2 Dynamics of the Activated Dissociative Adsorption of CH₄ on Ni(111)

M.I.T. Energy Laboratory, Synthetic Fuels Center National Science Foundation (Grant CHE 85-08734) Research Corporation Camille and Henry Dreyfus Foundation

Sylvia T. Ceyer, Andrew Johnson, Myung B. Lee, Qingyun Yang

The dynamics of the activated dissociative chemisorption of CH₄ on Ni(111) are studied by molecular beam techniques coupled with high resolution electron energy loss spectroscopy. The probability of the dissociative chemisorption of CH₄ increases exponentially with the normal component of the incident molecule's translational energy and with vibrational excitation. The dissociative chemisorption probability of CD₄ exhibits the same trends with a large kinetic isotope effect. High resolution electron energy loss spectroscopy identifies the nascent products of the dissociative chemisorption event as an adsorbed methyl ardical and a hydrogen atom. These results, which have shown that there is a barrier to the dissociative chemisorption, are interpreted in terms of a deformation model for the role of translational and vibrational energy in promoting dissociative chemisorption. The barrier likely arises largely from the energy required to deform the molecule sufficiently to allow a strong attractive interaction between the carbon and the Ni surface atoms. Tunneling is suggested as the final process in the C-H bond cleavage. The presence of this barrier to dissociative chemisorption presents a plausible explanation for the pressure gap in heterogeneous catalysis.

4.3 Chemical Reaction Dynamics on Semiconductor Surfaces

Joint Services Electronics Program (Contract DAAL-03-86-K-0002)

Sylvia T. Ceyer, David J. Gladstone, Marianne McGonigal, Michelle Schulberg

The etching of semiconductor materials in halocarbon plasma environments is a complex chemical process. The purpose of the plasma is the production of radical species that are highly reactive with the semiconductor surface. Since many different species, including neutral dissociation products of the halocarbon to atomic halogens and halocarbon radicals and ions and fragment ions produced by electron bombardment, are produced in the plasma, the chemistry is difficult to probe in this environment. Our program is aimed at systematically probing with molecular beam reactive scattering techniques the role of the neutral radical species in the etching process.

In this experimental arrangement, a beam of reactant atoms is aimed at a semiconductor surface and the volatile product molecules are detected after desorption from the surface by a quadrupole mass spectrometer. Since the molecular beam allows the production of a single reactive neutral species, the chemistry of the reactive species can be studied in a controlled fashion. The product molecule is unperturbed by collisions before detection allowing the reaction probabilities and the nascent product distribution to be determined unambiguously. We are planning to determine the reaction probabilities of F, C1, O and H atoms, common neutral radical species present in plasma environments, with silicon and to determine the identities of their reaction products and the dynamics of the chemical reaction. Test experiments are underway.

4.4 Spectroscopic Study of the Adsorption of C₂H₄ and C₂H₂ on Gd(0001)

Joint Services Electronics Program (Contract DAAL -03-86-K-0002)
National Science Foundation (Grant DMR 81-19295)

Sylvia T. Ceyer, Robert J. Simonson, Jun Rong Wang

The adsorption of ethylene and acetylene on a rare earth metal surface, Gd(0001), has been studied primarily by ultraviolet photoemission and Auger electron spectroscopy. Both species adsorb dissociatively on the clean Gd(0001) surface at 165 K. Sticking probabilities for both species are estimated to be in the range 0.18 - 0.42. Carbon-carbon bond scission occurs with unit probability. Carbon-hydrogen bond scission is also observed. Molecular adsorption occurs at 165 K after passivation of the Gd(0001) surface with adsorbed C and CH_{χ} species. As the substrate temperature is increased above 300 K, these molecularly adsorbed species dissociate rather than desorb. Gadolinium carbide is formed at higher temperatures.

4.5 Stabilization of the CO Precursor Molecule to Molecular Chemisorption

National Science Foundation (Grant CHE 85-08734)

Sylvia T. Ceyer, John D. Beckerle, Qingyun Yang, Andrew D. Johnson

We have recently found that there are two pathways through which CO chemisorbs on Ni(111): a pathway through which the CO molecule is initially adsorbed as a precursor to molecular chemisorption and a pathway through which adsorption into the molecular chemisorption state occurs directly from the gas phase. These conclusions result from initial adsorption probabilities, saturation coverages and CO mobilities measured in an apparatus combining molecular beam techniques with ultrahigh vacuum surface spectroscopies. We are pursuing this work in an attempt to trap the CO precursor molecule and to identify it spectroscopically. We have built a liquid helium cryostat that is capable of cooling the crystal to 8 K. This temperature should be sufficiently low to prevent the precursor from converting into a chemisorbed molecule. We will identify the precursor molecule by high resolution electron energy loss spectroscopy.

Publications

- Ceyer, S.T., J.D. Beckerle, M.B. Lee, S.L. Tang, Q.Y. Yang, and M.A. Hines, "Effect of Translational and Vibrational Energy on Adsorption: The Dynamics of Molecular and Dissociative Chemisorption," J. Vac. Sci. Tech. A 5, 501 (1987).
- Lee, M.B., Q.Y. Yang, S.L. Tang, and S.T. Ceyer, "Activated Dissociative Chemisorption of CH₄ on Ni(111): Observation of a Methyl Radical and Implications for the Pressure Gap in Catalysis," J. Chem. Phys. 85, 1693 (1986).

- Lee, M.B., J.D. Beckerle, S.L. Tang, and S.T. Ceyer, "Lack of Translational Energy Activation of the Dissociative Chemisorption of CO on Ni(111)," J. Chem. Phys. 87, 723 (1987).
- Lee, M.B., Q.Y. Yang, and S.T. Ceyer, "Dynamics of the Activated Dissociative Chemisorption of CH₄ and Implication for the Pressure Gap in Catalysis: A Molecular Beam-High Resolution Electron Energy Loss Study," J. Chem. Phys. 87, 2724 (1987).
- Simonson, R.J., J.R. Wang, and S.T. Ceyer, "Spectroscopic Study of the Adsorption of C_2H_2 and C_2H_4 on a Rare Earth Single Crystal. I. Metallic Gd(0001)," J. Chem. Phys. *91*, 500 (1987).
- Tang, S.L., M.B. Lee, Q.Y. Yang, J.D. Beckerle, and S.T. Ceyer, "Bridge/Atop Site Conversion of CO on Ni(111): Determination of the Binding Energy Difference," J. Chem. Phys. 84, 1876 (1986).
- Tang, S.L., J.D. Beckerle, M.B. Lee, and S.T. Ceyer, "Effects of Translational Energy on the Molecular Chemisorption of CO on Ni(111): Implications for the Dynamics of the Chemisorption Process," J. Chem. Phys. 84, 6488 (1986).
- Tang, S.L., Q.Y. Yang, M.B. Lee, J.D. Beckerle, and S.T. Ceyer, "Site Conversion of CO on Ni(111): Difference in Binding Energy between Bridge and Atop Sites," J. Vac. Sci. Tech. A 4, 1429 (1986).

AND ANDRES PROPERTY WISHING RESISSION REPORTS TO THE

5.0 Optics and Quantum Electronics

Academic and Research Staff

Prof. H.A. Haus, Prof. E.P. Ippen, Prof. C.G. Fonstad, Jr., Prof. J.G. Fujimoto

Visiting Scientists

Dr. R. Seif, M. Shirasaki, S. Oho, W.Z. Line, P. Mataloni, R. Birngruner

Graduate Students

N. Whitaker, D.L. Wong, L. Molter-Orr, W.P. Huang, L.Y. Liu, M.R. Phillips, K.K. Anderson, R.W. Schoenlein, S.D. Brorson, N. Dagli, E. Towe

5.1 The Nonlinear Waveguide Interferometer

Joint Services Electronics Program (Contract DAAL03-86-K-0002)
National Science Foundation (Grants ECS 83-05448 and Grant ECS 83-10718)

Hermann A. Haus, Shigeru Oho, Randa Seif, Masataka Shirasaki, Norman A. Whitaker, Dilys L. Wong

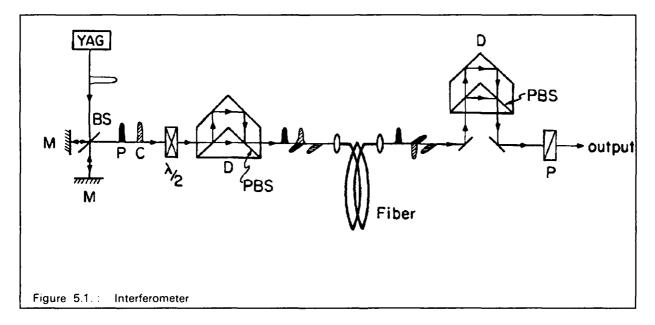
The nonlinear optical interferometer transforms a phase modulation into an amplitude modulation. With a continuous stream of optical pulses as the "bias", control pulses can affect the passage of individual pulses. In this way one may realize any logic gate operation. The throughput rate of the interferometer is determined solely by the material relaxation time and thus can be extremely high (>100 Gbit). The travel time of the pulses through the interferometer determines the delay time.

A nonlinear waveguide interferometer was built by N. A. Whitaker in GaAs, with access waveguides as originally realized in LiNbO₃ by Lattes et al.¹ The doped substrate provided the lower index for the guiding layer of undoped GaAs, and the lateral confinement was achieved with etched ridges. This interferometer was tested as an electrooptic device with a voltage applied to electrodes mounted for this purpose. Better than 13 db extinction ratio was realized. The nonlinear response was limited by the damage threshold at the input waveguide-interface.² It was found that for input intensities exceeding several Mw/cm² the cleaved facet exhibited damage. This was attributed to the free carrier absorption of the substrate, and could be eliminated in principle by replacing the substrate with undoped GaAlAs. Because of the findings described below, we decided to take a different approach.

An investigation by C. Gabriel on the operation of a nonlinear interferometer formed of a GaAs/AlGaAs heterostructure ridge waveguide with cleaved endfaces revealed the importance of thermal effects in determining a limit to the rate of throughput through the interferometer.⁵ The (small) free-carrier absorption of the nominally undoped sample was sufficient to account for most of the nonlinear phase shift at a 100MHz repetition rate of the 1.06 micron pulse-stream. The estimated absorption coefficient was 2x10⁻⁴ cm⁻¹. In view of this finding we questioned the use of the bulk nonlinearity in

GaAs as a means for high-rate all-optical switching. Similar difficulties do not arise in silica fibers, and thus we decided to use fibers for all-optical nonlinear interferometers.

A particularly promising realization of the nonlinear fiber interferometer has been carried out by M. Shirasaki, a visiting researcher from Fujitsu Laboratories, and D. L. Wong, a graduate student.⁴ The interferometer utilizes one single fiber in which two mutually orthogonal polarized versions of the same pulse, delayed with respect to each other, interfere under control of a cotraveling pulse (see Fig. 5.1). A probe pulse (P) is separated in a pulse divider (D) into two mutually orthogonally polarized pulses with the same power that are delayed with respect to each other and are injected into a fiber. At the fiber output they are recombined by an analogous pulse combiner arrangement. Because the two pulses travel through the fiber with subnanosecond time separations, their relative phase is insensitive to slow fluctuations of the effective index of the fiber. A control pulse (C) advanced by a time corresponding to the path difference in the pulse divider is similarly separated into two orthogonally polarized pulses, the second of which travels synchronously with the front probe-pulse, changing the index seen by this part of the probe pulse. As a result, the polarization of the probe pulse is changed after recombination.



In the experiment a fiber length of 400 m was used and the pulses were generated from a modelocked Nd:YAG laser operating at 1.06 microns at 100 MHz repetition rate. The interferometer was found to be extremely stable, with no feedback stabilization required. Of course, the repetition rate could be much higher, because the fiber nonlinearity is still instantaneous on a subpicosecond time scale. Because of the success of the preliminary experiments on this interferometer, we plan to explore its potentialities further in the coming year.

5.2 Picosecond Optical Signal Sampling

Joint Services Electronics Program (Contract DAAL03-86-K-0002) National Science Foundation (Grant ECS 83-10718)

Hermann A. Haus, Lynn Molter-Orr, Weiping Huang

The work on nonlinear waveguide sampling devices⁵ has led into the reexamination of the theory of modecoupling and into the study of waveguide dispersion characteristics, with particular attention devoted to the single-mode nature of the guides.

The conventional theory of mode coupling was challenged by Hardy and Streifer.⁶ For strong coupling these authors showed by means of an expansion in terms of normal modes that modifications are necessary in the coupling coefficients and propagation constants. We showed that such modifications are already contained in the derivation of the coupled mode theory from a variational principle for the guide-propagation constant set up for the study of traveling wave tubes in 1958.^{7,8} A more subtle consequence of the revised coupled mode theory is the appearance of crosstalk in switches that is not predicted by the conventional theory. We have shown that proper modification of the coupling structure can prevent crosstalk.^{8,9} In order to test the predictions of the revised coupled mode theory, they were compared with the exact analysis on a simple coupler structure. It was found that the agreement is excellent, even in the limit of rather strong coupling.¹⁰

Another issue in the design of nonlinear waveguides is the determination of the mode profile, and the design criteria for the "single-modedness" of a waveguide. Many analyses have appeared in the past; the approximate analyses are unsatisfactory near mode cutoff, the more accurate analyses are computation intensive. We have developed a reliable method for the evaluation of propagation constants based on a variational principle. The method requires much less computation than previous methods and will be extended to provide coupling constants for two-guide couplers.

5.3 Surface Acoustic Wave Propagation in Gratings

National Science Foundation (Grant ECS 82-11650)

Hermann A. Haus, Weiping Huang

We have begun to study higher order effects in metal-strip SAW gratings. The purpose is to develop theoretical expressions for the quadratic dependence of the frequency shift upon η/λ , where η is the thickness of the grating fingers and λ is the wavelength. This dependence is observed experimentally over and above the linear dependence and is matched with empirical coefficients. The SAW research group at the Siemens Research Laboratory in Munich is sharing with us their experimental results in an effort to arrive at a reliable theory for SAW grating resonator design.

5.4 Solitons

Joint Services Electronics Program (Contract DAAL03-86-K-0002) National Science Foundation (ECS 83-10718)

Hermann A. Haus, Ling-Yi Liu, Mary R. Phillips, Kristin K. Anderson

The nonlinear fiber interferometer developed for optical switching and described in the section on the Nonlinear Waveguide Interferometer will require the use of solitons when very high throughput rates are the objective. Hence we are continuing the study of soliton propagation that was initiated with the study of the soliton laser¹¹ developed by Stolen and Mollenauer at AT&T Bell Laboratories. Dr. Islam is now a member of the Bell Laboratories group and the exchange of information is continuing. With Dr. Nakazawa, who was a visiting scientist from NTT, Japan, we developed the theory of the Fiber Raman Soliton Laser (FRASL) which was demonstrated by Drs. Islam and Mollenauer.¹² The theory¹³ establishes limits on the obtainable pulse-width.

The nonlinear fiber interferometer uses the interaction of two orthogonally polarized fields. This effect is described by two coupled nonlinear Schrodinger equations, a phenomenon that has not been studied extensively since the first publication of the application of the inverse scattering theory to this problem.¹⁴ We have determined the phase shift produced by two orthogonally polarized solitons passing through each other on a birefringent fiber by a perturbation analysis.¹⁵ The full theory of soliton interactions will be the subject of continued research.

References

- ¹ A. Lattes, H.A. Haus, F.J. Leonberger, and E.P. Ippen, "An Ultrafast All-Optical Gate," I.E.E.E., J. Quant. Electron. *QE-19*, 1718, (1983).
- ² N.A. Whitaker, "All-Optical Signal Processing in Semiconductor Waveguides," Ph.D. Thesis, Dept. Electr. Eng. and Comp. Sci., M.I.T., Cambridge, Mass., 1986.
- ³ M.C. Gabriel, H.A. Haus, and E.P. Ippen, "Thermal Index Changes by Optical Absorption in Group III-V Semiconductor Waveguides," J. Lightwave Tech. *LT-4*, 1482, (1986).
- ⁴ H.A. Haus, M. Shirasaki, and D. Liu Wong, "A Nonlinear Fiber Interferometer and Logic Gate," to be presented at CLEO '87, Baltimore, Maryland, April 27, 1987.
- ⁵ L.A. Molter-Orr, H.A. Haus, and F.J. Leonberger, "20 GHz Optical Waveguide Sampler," I.E.E.E., J. Quant. Electron. *QE-19*, 1877 (1983).
- ⁶ A. Hardy and W. Streifer, "Coupled Mode Theory of Parallel Waveguides," J. Lightwave Tech. *LT-3*, 1135 (1985).
- ⁷ H.A. Haus, "Electron Beam Waves in Microwave Tubes," Proceedings of the Symposium on Electronic Waveguides, Polytechnic Institute of Brooklyn, April 1958.
- ⁸ H.A. Haus, W.P. Huang, S. Kawakami, and N.A. Whitaker, "Coupled-Mode-Theory of Optical Waveguides," J. Lightwave Tech. *LT-5*, 17, (1987).
- ⁹ H.A. Haus, "Coupled-Mode Theory Revisited," S.P.I.E. Conference on Fiber Optics, Optoelectronics and Laser Applications in Science and Eng., Cambridge, Mass., September 1986, Paper no. 70417.
- ¹⁰ J.P. Donnelly, H.A. Haus, and L.A. Molter, "Cross Power and Cross Talk in Waveguide Couplers," submitted for publication to J. Lightwave Tech.

- ¹¹ L.F. Mollenauer and R.H. Stolen, "The Soliton Laser," Opt. Lett. 9, 13, (1984).
- ¹² M.N. Islam and L.F. Mollenauer, "Fiber Raman Amplification Soliton Laser," 14th International Quantum Electronics Conference, San Francisco, Calif., June 1986.
- ¹³ H.A. Haus and M. Nakazawa, "Theory of the Fiber Raman Soliton Laser," J. Opt. Soc. Am. B (accepted for publication).
- 14 S.V. Manakov, "On the Theory of Two-Dimensional Stationary Self-Focusing of Electromagnetic Waves," Sov. Phys. JETP 38, 248, (1974).
- ¹⁵ H.A. Haus, "Collisions of Orthogonally Polarized Solitons," Quantum Electronics and Femtosecond Optics, M.I.T., R.L.E. Memo No. 9, Cambridge, Mass., 1987.

5.5 Analysis and Characterization if III-V Guided Wave Optics Rib Waveguide Couplers

National Science Foundation (Grant ECS 84-13178)

Nadir Dagli, Clifton G. Fonstad, Jr., Hermann A. Haus

Rectangular waveguides and couplers are being analyzed as part of a program to make efficient multiple waveguide optical switches and modulators capable of operating at very high data rates. In these studies III-V compound semiconductors were used and the fabrication, characterization and modeling of waveguide devices were undertaken. In this context a new technique was developed to model open guided wave structures. The technique is basically a mode-matching technique which results in a microwave equivalent circuit for the geometry under consideration. In order to accurately describe open guided wave structures, contributions from the continuum spectra as well as the guided spectra should be taken into account. This is difficult, however, because in the model expansions, the continuum set is represented as integrals and such integral terms are not suitable for an equivalent circuit representation. Usually these terms are converted into summations by artificially bounding the structure with conducting boundaries. In our work these terms are discretized by converting integrals into summations using suitable basis function expansions. This results in a transmission line representation for all regions, even those where there are no guided modes. Therefore, it is possible to analyze structures where there are no guided modes in the outer regions, situations which cannot be analyzed with simple approximate techniques such as the effective dielectric constant method. The resulting model is modular, and, consequently, the method can be used to analyze a wide variety of rectangular dielectric waveguides. Because of modularity, it is possible to divide a complex structure into a cascade of dielectric steps and uniform regions. Steps are modeled as a transformer network and uniform regions as uniform transmission lines.

A general computer program was developed to analyze open guided wave structures. The structure under consideration can be a single guide or multiple coupled waveguides with nonidentical widths and spacings. The geometry of the waveguides can be either ideal with vertical sidewalls or more complex with non-ideal sidewalls like the sloped sidewalls produced with chemical etching techniques. Results indicate that conver-

gence of propagation constant values is very fast as the number of discretized continuum modes is increased. Results of this method were compared with the results of other mode matching techniques for rectangular fibers, rib guides, strip guides and channel guides. Agreement is excellent and the required computational effort is less than that of the other techniques. Using this technique universal design curves were generated and plotted for the design of rib guides. Results demonstrate that when there are well guided modes in the slabs, the contribution from the continuous spectra is very small even for structures with large discontinuities.

Once the equivalent circuit parameters for a waveguide are developed the extension of the analysis to couplers is very easy and requires very little additional computation. Both directional couplers and three guide couplers have been analyzed. Propagation constant values of the supermodes of the structure were calculated and using these values, transfer lengths were determined. The results of these theoretical predictions were experimentally verified by measurements on rib waveguides and multiple coupled guides in GaAs. These devices are produced with chemical etching techniques, and hence have sloped sidewalls. Furthermore, they are very tightly coupled. Experimentally determined transfer lengths on directional couplers and three guide couplers of various dimensions are in excellent agreement with the theoretical predictions. Other approximate techniques either cannot analyze such devices at all or are not accurate enough. Such an accurate technique is very important in the design of integrated optical switches, modulators, power dividers and combiners.

5.6 Multiple Quantum Well Heterostructures and Diode Laser Arrays

National Science Foundation (Grant ECS 84-13178)

Joint Services Electronics Program (Contract DAAL-03-86-K-002)

Elias Towe, Clifton G. Fonstad, Jr.

Our program on (Al,Ga)As/GaAa quantum well heterostructures has progressed to the point where we can now routinely grow very high quality single and multiple quantum well structures. We have been able to achieve the high optical optical layers we need for laser structures by a careful attention to the growth conditions. A feature that we have found to be instrumental in obtaining high luminscent efficiency from our layers was the incorporation of a superlattice buffer layer before growing the device structures.

Broad area lasers with the typical dimensions of 400 μ m \times 210 μ m \times 100 μ m fabricated from our best multiple quantum well laser structure exhibited measured threshold current densities of around 220 A/cm². This value is comparable to those reported in the literature for state-of-the-art devices of similar structures grown by molecular beam epitaxy.

We have also recently developed a novel type of diffraction-coupled phase-locked laser array, the mixed-mode phase-locked (M²PL) laser. This new device has the usual parallel-element array of lasers but it incorporates a section in the middle of the device where the modes are unguided. This middle section forms the mode-mixing region and allows the modes in the individual elements to couple and mix by diffraction, thus es-

tablishing a common phase for all the elements. Stable, single-lobe far-field patterns are routinely obtained from these devices. For a seven-element array, patterns as narrow as 2° have been measured and up to 60 m W has been obtained in a single peak.

For the M²PL lasers which have been studied thus far, the mode-mixing region has been 75 μ m long and the guiding regions on either side of it have been approximately 100 μ m long. The individual array element ridge guides and the mode-mixing region are photolithographically defined and wet chemically etched. The guides are aligned so that the etched regions between them are v-shaped; the top metallization forms Schottky contacts on the lightly-doped AlGaAs regions between the guides and ohmic contacts to the ridges themselves. Each guide is 3.0 μ m wide and the center-to-center spacing is 7.0 μ m.

At the present time analytical models for the new device are being developed so that design curves for the optimal mode-mixing region length can be determined and the device performance can be optimized.

Publications

- Dagli, N. and C.G. Fonstad, "Microwave Equivalent Circuit Representation of Rectangular Dielectric Waveguides," Appl. Phy. Lett. 49, 308 (1986).
- Dagli, N. and C.G. Fonstad, "A New Method of Analyzing and Modeling Integrated Optoelectronic Components," Digest of the 1987 I.E.E.E. Microwave and Millimeter-Wave Monolithic Circuits Symposium, in press.
- Towe, E. and C.G. Fonstad, "Mixed-Mode Phase-Locked Quantum Well Laser Arrays," Technical Digest of the I.E.E.E. International Devices Meeting, 1986, p. 626.

5.7 Femtosecond Laser Systems and Pulse Generation

Joint Services Electronics Program (Contract DAAL03-86-K-0002) National Science Foundation (Grant ECS 85-52701)

James G. Fujimoto, Erich P. Ippen

During the past year we have focused on two principle areas of ultrashort pulse generation: the development of a high repetition rate femtosecond laser source and amplifier and the development of a wavelength tunable femtosecond laser system. These new systems provide capabilities for the measurement of ultrafast phenomena in a wider variety of physical systems with greater sensitivity than previously possible.

Our high repetition rate femtosecond laser amplifier consists of a colliding pulse modelocked (CPM) ring laser with a copper vapor laser pumped amplifier. The CPM laser uses passive modelocking with an intercavity dispersion compensating prism arrangment similar to that demonstrated by Fork et al. at AT&T Bell Laboratories.¹ The laser operates at 625 nm and can produce pulse durations as short as 35 fs. The laser output consists of a train of .1 nJ pulses at a 100 MHz repetition rate. The high repe-

tition and short pulse duration of this system make it ideal for time resolved studies requiring extremely high temporal resolution and sensitivity.

For many experiments, however, it is desirable to generate pulses of higher intensity. For these applications the output of the CPM laser can be amplified in a high repetition rate amplifier.² Our system uses a copper vapor laser operating at an 8 kHz repetition rate as the pump source for a dye amplifier. Using a 6 pass configuration in a thin gain jet, we have obtained gains of greater than 104 corresponding to single pulse energies of 2 $2\mu J$ with output pulse durations as short as 50 fs. The peak intensities are greater than 10⁸ W, sufficient for most nonlinear optical experiments involving pump-probe or transient four wave mixing techniques. In addition, these amplified pulses can be used to generate a broadband femtosecond continuum via self-phase-modulation. continuum provides a broadband wavelength probe suitable for the measurement of transient absorption or reflectivity lineshape on a femtosecond time scale. The high repetition rate of this system permits the use of lock-in detection techniques and single averaging so that very high sensitivity measurements are possible. Changes in optical properties as small as 1 part in 10⁵ - 10⁶ are detectable.

Our second major topic of research in ultrashort pulse generation involves the development of a tunable femtosecond laser system for wavelengths in the visible and near IR. This system is based on a Nd dye laser. The Nd μ m at a repetition rate of 80 MHz. These pulses are compressed by using self-phase-modulation in a single mode optical fiber followed by a diffraction grating dispersive delay line. Pulse durations as short as 5-10 ps may be obtained with CW average powers as high as 3 W. Using a nonlinear second harmonic crystal (KTP), output powers of ~ 1 W are generated at 532 nm with pulse durations of less than 5 ps. This source is then used to pump a synchronously modelocked tunable dye laser. Since no passive modelocking dyes are used the wavelength of the dye laser may be tuned over the bandwidth of the dye. Using rhodamine 6G we have generated pulses as short as 300 fs tunable over a range of λ = 580 to 625 nm. Further wavelength tunability may be accomplished by changing the dye and laser mirrors. Tuning of the laser output between 580 and 850 nm should be possible.

Shorter pulse durations may be generated by cavity dumping the synchronously pumped dye laser and using an addition stage of optical fiber pulse compression. Pulse durations of less than 50 fs have been demonstrated using this technique in the visible.³ Tunable femtosecond sources are extremely important since they allow the investigation of transient processes associated with different energy level or resonance behavior in materials. The visible and near IR wavelength region is especially important for studies in electronic and optoelectronic semiconductors such as GaAs.

References

- ¹ J.A. Valdmanis, R.L. Fork, and J.P. Gordon, "Generation of Optical Pulses as Short as 27 Femtoseconds Directly from a Laser Balancing Self-Phase Modulation, Group-Velocity Dispersion, Saturable Absorption, and Saturable Gain," Opt. Lett. 10, 131 (1985).
- W.H. Knox, M.C. Downer, R.L. Fork, and C.V. Shank, "Amplified Femtosescond Optical Pulses and Continuum Generation at 5-kHz Repetition Rate," Opt. Lett. 9, 552 (1984).

³ J.D. Kafka and T. Baer, "Generation of Tunable Femtosecond Pulses," Technical Digest of the Conference on Lasers and Electro-Optics, Baltimore, Maryland, May 1985, Paper ThZZ5-1.

5.8 Femtosecond Carrier Dynamics in GaAs

US Air Force - Office of Scientific Research (Contract AFOSR-85-0213) National Science Foundation (Grant ECS 85-52701)

Erich P. Ippen, James G. Fujimoto

The investigation of transient behavior of excited carriers in GaAs is relevant to electronic and optoelectronic devices which will require high speed nonequilibrium carrier phenomena. The recent advent of new and more versatile femtosecond laser generation techniques provide opportunities for the investigation of transient scattering relaxation and transport processes which occur on the femtosecond time scale.

The scattering mechanisms of optically excited carriers in GaAs and AlGaAs were investigated using pump and probe measurement of transient absorption saturation. 1-5 Pulses as short as 35 fs at 625 nm (2 eV) were generated by our CPM dye laser and used to excite carriers and investigate their subsequent scattering out of their initial optically excited states. A two component relaxation process was observed with an initial relaxation occurring on a time scale comparable to the pulse duration and a slower ~1 ps relaxation corresponding to a cooling of the excited carrier distribution to the lattice temperature. New measurement techniques using varying pulse duration, chirp and polarization were developed to investigate the dynamics of the initial femtosecond relaxation process. Measurements performed in GaAs at carrier densities ranging from 10¹⁷ to 10¹⁸ cm⁻³ indicated the presence of an initial relaxation process with a 30 to 13 fs relaxation time. These measurements are significant because they suggest the presence of an extremely rapid carrier density dependent relaxation mechanism for highly excited carrier in the GaAs. In addition, these results demonstrate the measurement of transient processes on a time scale as short as 10 femtoseconds, comparable to or less than the incident laser pulse duration.

Additional measurements of carrier relaxation have been performed in Al, Ga₁, As with varying mole fraction compositions of Al. Changing the semiconductor composition produces changes in the energy band gaps and allows an investigation of the effects of excited carriers with different excess energies in the conduction and valance bands. As the mole fraction of Al is increased the direct energy band gap at the Ga point increases as well as the indirect gaps to the X and L valleys. As the band gap is increased, a dramatic decrease in the rate of carrier scattering out of the initial optically excited states is observed. Scattering times of 13 fs, 20 fs, 80 fs, 130 fs, and 300 fs are observed for mole fractions χ = 0, \, 0.1, \, 0.2, \, 0.3, and 0.4, respectively. The observed change in carrier scattering rate may be attributed to a number of possible factors including the generation of carriers with less excess energy and decreased effective temperature, changes in allowable scattering states, changes in screening effects, as well as possible changes in intervalley scattering rates.

While these measurements permit the investigation of extremely rapid scattering processes, in order to describe more fully the relaxation of the excited carriers it is necessary to perform measurements at multiple excitation and probe wavelengths. These investigations have only recently been made possible through the development of high sensitivity, high repetition rate, femtosecond amplified pulse sources. We have extended our preliminary investigations in GaAs and AlGaAs using femtosecond pump and continuum probe absorption saturation measurements.⁵ Our preliminary experimental results provide evidence for transient nonthermal carrier distributions occuring on a time scale of several tens of femtoseconds. These processes are observed as transient spectral hole burning and correspond to the excited electrons and holes before they reach a quasi-thermal distribution. In addition to transient, continuum probe measurements demonstrate that carriers excited high into the band in GaAs are scattered to energies several hundred MeV away within a time scale of several tens of femtoseconds. The scattering dynamics of highly excited carriers and the possibility of anisotropic excitation in k space or ballistic transport are relevant to high speed devices fabricated in these materials systems.

Additional experiments are planned using our tunable femtosecond dye laser source to investigate processes such as intervalley scattering in GaAs and GaAlAs. The role of $\Gamma-X$ and $\Gamma-L$ scattering is particularly important since it produced the negative differential resistivity observed in these materials. In addition, we are currently investigating techniques for the measurement of real space transport phenomena and tunneling in these systems. The use of quantum wells for the generation and detection of excited transient carriers is being studied as a possible technique for investigating transport phenomena on the submicron scale.

References

- ¹ R.W. Schoenlein, W.Z. Lin, J.G. Fujimoto, and G.L. Eesley, "Femtosecond Studies of Nonequlibrium Electronic Processes in Metals," in *Ultrafast Phenomena V*, edited by G. R. Fleming and A. E. Siegman. New York: Springer-Verlag, 1986.
- ² W.Z. Lin, J.G. Fujimoto, E.P. Ippen, and R.A. Logan, "Femtosecond Carrier Dynamics in GaAs," Appl Phys. Lett. *50*, 124, (1987).
- ³ W.Z. Lin, J.G. Fujimoto, E.P. Ippen, and R.A. Logan, "Femtosecond Studies of Absorption Saturation Dynamics in GaAs," Technical Digest of the 14th International Conference on Quantum Electronics, San Francisco, Calif., 1986, p. 50.
- ⁴ W.Z. Lin, J.G. Fujimoto, E.P. Ippen, and R.A. Logan, "Femtosecond Carrier Dynamics in GaAs and Al₂Ga₁₋₂As" presented at Lasers '86, Orlando, Florida, November 1986.
- ⁵ W.Z. Lin, R.W. Schoenlein, S.D. Brorson, J.G. Fujimoto, and E.P. Ippen, "Femtosecond Carrier Thermalization in GaAs and AlGaAs," 15th International Conference on Quantum Electronics, Baltimore, Maryland, April 1987, paper TuJJ2.

5.9 Femtosecond Spectroscopy of Electronic and Optical Materials

Joint Services Electronics Program (Contract DAAL03-86-K-0002)
US Air Force - Office of Scientific Research (Contract AFOSR-85-0213)
National Science Foundation (Grant ECS 85-52701)

James G. Fujimoto, Erich P. Ippen

Complementing our research in the area of ultrashort pulse generation, we are investigating femtosecond time resolved spectroscopic techniques and measurements in a variety of materials and systems which are relevant to electronic, optoelectronic, and all-optical signal processing.

In addition to studies of semiconductors, we are also investigating transient processes in metals. Because of their inherent high densities, many of the transient processes occuring in these systems are extremely rapid, occuring on a femtosecond time scale. In contrast to semiconductors, changes in optical properties associated with metallic systems can be extremely small. Thus, transient spectroscopy on metals has been only recently possible through the development of high sensitivity techniques. Using transient reflectivity and photoemission, it is possible to generate and investigate nonequilibrium electron heating. If the incident pulse duration is shorter than or comparable to the electron-phonon energy transfer time, electron temperatures far in excess of lattice temperature may be generated. Experiments in noble metals allow measurements of the transient electron temperature through optical transitions from the d bands. Our experiments demonstrate the generation of nonequilibrium temperatures in the electron gas which relax to the lattice temperature on a time scale of $\sim 1 \text{ ps.}^{1-3}$ In addition, we have performed pump-probe time-of-flight measurements to investigate electronic heat transport phenomena in thin gold films of varying thickness.1-3 Subpicosecond thermal transport times are observed in 1000-2000Å thick samples demonstrating the presence of nonequilibrium electronic heat transport with a velocity of ~108 cm/sec. These measurements of the first observations are nonequilibrium electronic transport phenomena in metals. Extensions of these techniques to semiconductor-metal interfaces will be of potential importance in investigating transport phenomena in electronic materials and devices. In addition, the generation of transient high temperature electrons in metals without the presence of lattice melting is relevant to transient high current devices as well as transient high current photoemission and electron beam sources.

Organic polymers are another potentially interesting material system for time resolved spectroscopy. In particular, the polydiacetylenes are a potentially important material for applications in all-optical signal processing because of their high nonlinear susceptibilites $X^{(3)} > 10^{-9}\ esu$ and rapid response speeds. We have performed pump-probe measurements of transient excited state dynamics in these systems and observed relaxation times as short as $\sim 100 {\rm fs.}^4$ In addition to exhibiting high nonlinear susceptibility, the polydiacetylenes also provide an important model to test the role of electron localization to quasi-one-dimensional systems. Investigations of transient dynamics associated with the excited states of these systems should provide important information on the nature of the elementry excitations in polydiacetylene as well as the limitations of these materials for high speed optical signal processing.

References

- ¹ R.W. Schoenlein, W.Z. Lin, J.G. Fujimoto, and G.L. Eesley, "Femtosecond Studies of Nonequilibrium Electronic Processes in Metals," In *Ultrafast Phenomena V*, edited by G.R. Fleming and A.E. Siegman. New York: Springer-Verlag, 1986, p. 260.
- ² S.D. Brorson, J.G. Fujimoto, and E.P. Ippen, "Femtosecond Nonequilibrium Electronic Heat Transport in Thin Gold Films," Technical Digest of the Picosecond Electronics and Optoelectronics Conference, Incline Village, Nevada, January 1987, p. 136.
- ³ R.W. Schoenlein, W.Z. Lin, S.D. Brorson, E.P. Ippen, and J.G. Fujimoto, "Femtosecond Transient Electron Heating in Metals," 15th International Quantum Electronics Conference, Baltimore, Maryland, April 1987, paper TuDD4.
- ⁴ J.M. Huxley, J.G. Fujimoto, E.P. Ippen, G.M. Carter, and P. Mataloni, "Femtosecond Absorption Saturation Dynamics in Polydiacetylene," Conference on Lasers and Electro-Optics, Baltimore, Maryland, April 1987, paper ThF2.

5.10 Short and Ultrashort Pulse Laser Medicine

National Institutes of Health (Contract 5-R01-GM35459) U.S. Navy - Office of Naval Research (Contract N00014-86-K-0117)

James G. Fujimoto, Erich P. Ippen

Two years ago we initiated a new program to investigate the applications of short and ultrashort pulsed lasers to laser medicine. This research is being conducted in collaboration with investigators at the Massachusetts Eye and Ear Infirmary and the Wellman Laboratory of the Massachusetts General Hospital. The objectives of our program are to develop and apply new time resolved spectroscopic and diagnostic techniques for the study of physical processes relevant to laser medicine as well as to investigate laser tissue interaction produced by pulsed radiation.

One area of interest has been the study of laser induced optical breakdown produced by a pulsed nanosecond or picosecond laser sources. This type of laser-tissue interaction is an important therapeutic technique in ophthalmic laser surgery for the surgical incision of interocular structures which are nominally transparent to the laser wavelength. We have investigated the transient processes associated with optical breakdown using pump and probe techniques. These processes include plasma formation, acoustic shock wave generation and propagation, and cavititation. These types of phenomena are also present in pulsed laser interaction with pigmented structures and are relevant to the therapeutic process of pulsed laser surgery. Additional investigations are aimed at determining laser parameters including intensity, pulsed duration, and pulse profile which can better channel the laser radiation into the desired physical process.

As an example to demonstrate the control of laser parameters to produce a desired effect, we have performed investigations of thermal diffusion in retinal damage using a

novel interferometric exposure technique.² A Michaelson interferometer was used to generate a sinusoidal fringe exposure pattern on the retina and exposures were made for differing laser intensity and exposure time. Exposures at durations comparable to the thermal relaxation time produced spatially confined lesions following the periodicity of the exposure pattern, while those at much longer durations resulting in significant diffusion of the thermal damage beyond the primary targeted regions. This exposure technique is interesting because the sinusoidal exposure pattern is itself an eigenfunction of thermal diffusion equation. In addition, the role of thermal diffusion can be assessed directly from the opthalmascopic and histologic appearances of the lesions. This technique can thus be used to study thermal diffusion and other transport phenomena occurring in laser-tissue interactions.

The use of laser pulses for medical diagnostics has also been under investigation. We have demonstrated the first application of femtosecond optical ranging in biological systems. This technique is analogous to radar or ultrasound except that short pulses of light are used instead of radio or acoustic waves. Using pulsed durations of 70 fs, we have performed measurements of corneal thickness in rabbit eyes in vivo as well as epidermal structure in human skin in vitro.³ We are currently investigating the application of these techniques to study the cornea profile alterations produced by UV excimer laser ablation as well as processes which produce changes in scattering structure in the cornea such as cataract formation.

Finally, we are investigating the biological aspects of laser-tissue interaction in the femtosecond regime. We have performed the first study of retinal damage thresholds and mechanisms produced by exposure to high intensity femtosecond laser pulses. This research was conducted in collaboration with Dr. R. Birngruber of the University of Munich. Retinal damage thresholds were evaluated using 80 fs pulses at 625 nm in chinchilla gray rabbits. ED₅₀ injury thresholds of 0.75 mJ and 4.5 mJ were measured using fluorescein-angiographic and opthalmoscopic visibility criteria. Ultra-structural studies including light and electron microscopy were performed on selected lesions. Results suggest that the primary deposition of energy in the retinal occur in melanin even for pulses of this short duration. However, in contrast to laser injury produced by longer pulses, exposures of up to 20 χ threshold in the 50-100 μ J range did not produce significantly more severe lesions or hemorrhage. This suggests the presence of a non-linear damaging limiting mechanism.

References

- ¹ J.G. Fujimoto, W.Z. Lin, E.P. Ippen, C.A. Puliafito, and R.F. Steinert, "Time-Resolved Studies of Nd:YAG Laser Induced Breakdown: Plasma Formation, Acoustic Wave Generation, and Cavitation," Invest. Ophthal. Vis. Sci. 26, 1171, (1985).
- ² J.M. Krauss, C.A. Puliafito, W.Z. Lin, and J.G. Fujimoto, "Interferometric Technique for Investigation of Laser Thermal Retinal Damage," Invest. Ophthal. Vis. Sci. (in press).
- ³ J.G. Fujimoto, S. DeSilvestri, E.P. Ippen, C.A. Puliafito, R. Margolis, and A. Oseroff, "Femtosecond Optical Ranging in Biological Systems," Opt. Lett. 11, 150 (1986).

- ⁴ R. Birngruber, C.A. Puliafito, A. Gawande, W.Z. Lin, R.W. Schoenlein, and J.G. Fujimoto, "Femtosecond Retinal Injury Damage Studies," Invest. Ophthal. Vis. Sci., Suppl. 27, p. 314 (1986).
- ⁵ R. Birngruber, C.A. Puliafito, A. Gawande, W.Z. Lin, R.W. Schoenlein, and J.G. Fujimoto, "Femtosecond Retinal Injury Study," Technical Digest of the Conference on Lasers and Electro-Optics, San Francisco, Calif., June 1986, p. 152.

THE PERSON REPORTED BELLEVIEW SERVING SERVING

6.0 Optical Propagation and Communication

Academic and Research Staff

Prof. J.H. Shapiro, Dr. P. Kumar, Dr. R.H. Rediker, Dr. N.C. Wong

Graduate Students

K.K. Anderson, B.T. Binder, D.E. Bossi, J.K. Bounds, C.J. Corcoran, R.H. Enders, S.M. Hannon, S.-T. Ho, R.K. John, D.R. Lane, K.-W Leong, S.K. Liew, M.W. Maeda, M.B. Mark, D. Park, G. Saplakoglu, R.K. Shu, N.E. Silman, P.T. Yu

The central theme of our programs has been to advance the understanding of optical and quasi-optical communication, radar, and sensing systems. Broadly speaking, this has entailed: 1) developing system-analytic models for important optical propagation, detection, and communication scenarios; 2) using these models to derive the fundamental limits on system performance; and 3) identifying and establishing through experimentation the feasibility of, techniques and devices which can be used to approach these performance limits.

6.1 Atmospheric Optical Communications in Local Area Networks

National Science Foundation (Grant ECS 85-09143)

Jeffrey H. Shapiro, Bradley T. Binder, Jeffrey K. Bounds, Daniel R. Lane, Peter T. Yu

A local area network is prototypically a high-bandwidth (1-10 Mb/s) geographically compact (0.1 - 5 km diameter) packet-switched network that employes twisted pair, coaxial cable, or fiber optics as its transmission medium. These networks interconnect computers within a single company, often within a single building. They are distinguished from wide-area packet networks in that the high-bandwidth, short delay, low-cost transmission media employed in local area networks permit the use of simplified protocols and control strategies.

Atmospheric optical communication links are a natural choice for certain high-bandwidth short-haul terrestrial transmission applications in which cable rights-of-way are unobtainable, or in which frequent link and network reconfiguration is necessary. The utility of these links will be limited primarily by the occasional outages they experience due to local adverse weather conditions.

The natural advantages of atmospheric optical links make them attractive candidates for such local area network (LAN) applications as bridges between buildings containing cable subnetworks, and temporary quick-connects for new outlying hosts for which cable runs are initially unavailable. In this program, we have undertaken a combined analytical and experimental study of the use of atmospheric optical communications in local area networks. A brief summary of recent accomplishments follows.

Experiment

The purpose of the experimental research has been to establish an atmospheric optical communication/LAN test bed for probing the utility of such hybrid networks in actual user environments. Under earlier NSF funding, two through-the-air optical transceivers were constructed, using continuous-wave GaAlAs laser diodes and Silicon APD/preamplifier modules.\(^1\) The initial links were employed for packet transmission over a 150 m outdoor path between buildings on the M.I.T., Cambridge, Mass. campus. They were later modified for direct substitution into the PROTEON proNET cable ring network,² which is a 10 Mb/s token passing ring structure in use at M.I.T., Cambridge, Mass. that admits to extensive interconnection through what are called wire centers. During the past year, link hardware has been improved through the addition of automatic gain control to the receivers and feedback temperature compensation to the transmitters.3 In addition, the hardware4 and software3 needed to accumulate internal transceiver status information while network operation is proceeding has been developed and installed. With these advances, remote computation experiments are now proceeding with two IBM-PC computers connected as a 2-node through-the-air laser communication ring network.3

Theory

Because future developments in LANs will likely occur in the area of very high speed (100 Mb/s - 1 Gb/s) systems based on single-mode optical fiber, our theoretical work has been aimed primarily at the use of atmospheric optical communications in such networks. Here the impact of atmospheric propagation on network performance is expected to be more severe than in our earlier analysis of 1-10 Mb/s systems.⁵ We have explored⁶ the viability of placing an atmospheric optical link into some of the proposed very high speed fiber-optic LANs, such as FASNET.⁷ In bad weather, the network must cope with optical link outages that will force it to divide into subnetworks. Moreover, in clear weather, the fading due to atmospheric turbulence, which was not a severe problem for Mb/s systems owing to their greater power margin, will affect atmospheric link performance in a way that requires protocol modification. In another problem area, we have made a systematic study⁸ of various fiber-optic alternatives for providing very high speed bus communications within a computer. This study has established the trade-offs between serial (bit by bit) and parallel (byte by byte) implementations.

References

- ¹ K. Wong, "A Variable-Rate Atmospheric Optical Link for Local Area Networks," S.M. Thesis, Dept. of Electr. Eng. and Comp. Sci., M.I.T., Cambridge, Mass., 1984.
- ² D.R. Lane, "A Modified Atmospheric Optical Link for Local Area Networks," S.B. Thesis, Dept. of Electr. Eng. and Comp. Sci., M.I.T., Cambridge, Mass., 1985.
- ³ B.T. Binder, "Remote Computation with an Atmospheric Optical Ring Network," S.M. Thesis, Dept. of Electr. Eng. and Comp. Sci., M.I.T., Cambridge, Mass., 1986.
- ⁴ A. De Rozairo, "A Data Acquisition System for Atmospheric Optical Links," S.B. Thesis, Dept. of Electr. Eng. and Comp. Sci., M.I.T., Cambridge, Mass., 1986.

- ⁵ T.T. Nguyen, "Atmospheric Optical Communications in Local Area Networks," Ph.D. Diss., Dept. of Electr. Eng. and Comp. Sci., M.I.T., Cambridge, Mass., 1985.
- ⁶ J.K. Bounds, "Atmospheric Optical Communications in Very Fast Local Area Networks," S.M. Thesis, Dept. of Electr. Eng. and Comp. Sci., M.I.T., Cambridge, Mass., 1986.
- ⁷ J.O. Limb and C. Flores, "Description of Fasnet A Unidirectional Local-Area Communications Network," Bell Syst. Tech. J. *61*, 1413 (1982).
- ⁸ D.R. Lane, "Fiber Optic Alternatives for Fast Bus Communications," S.M. Thesis, Dept. of Electr. Eng. and Comp. Sci., M.I.T., Cambridge, Mass., 1986.

6.2 Squeezed States of Light

Maryland Procurement Office (Contract MDA 904-84-C-6037) National Science Foundation (Grant ECS 84-15580)

Jeffrey H. Shapiro, Prem Kumar, Ngai C. Wong, Mari W. Maeda, Seng-Tiong Ho, Kin-Wai Leong, Roy K. John, Gurhan Saplakoglu, Roberto K. Shu

Recent work has highlighted the potential applications of squeezed states, also known as two-photon coherent states (TCS), in optical communications and precision measurements. These states have an asymmetric noise division between their quadrature components, with the low-noise quadrature exhibiting lower fluctuation strength than that of a coherent state. We are engaged in a program to generate and verify the quantum noise behavior of squeezed state light and analyze the physics and applications of such light. Our recent progress is summarized below.

Experiments

Our first successful squeezed-state generation experiment produced 0.2 dB of noise reduction below the vacuum-state level in homodyne detection of light that had undergone nearly-degenerate forward four wave mixing in sodium vapor.\(^1\) Following this success, we had to shut down experimental work while our laboratory underwent an extensive renovation. This renovation, completed in September 1986, gave us additional high quality laboratory space for use in future experiments. Since then we have begun work on an improved atomic-vapor squeezed-state experiment using ytterbium. We have also pursued preliminary experiments in the areas of self-phase modulation squeezed-state generation, and squeezed-state generation via feedback photodetection around an optical nonlinearity. These areas represent a radical departure form atomic vapor work, but appear to hold great potential for future applications.

Theory

As a foundation for the preceding experiments, we have continued to work on the theoretical underpinnings of squeezed-state generation. In support of the atomic vapor experiments, we have developed a vector-wave quantum theory for squeezed-state generation via degenerate four-wave mixing,² and a scalar-wave quantum theory for

squeezed-state generation via non-degenerate four wave mixing.³ The latter work includes important advances in treating quantum field propagation in material media. In the area of self-phase modulation, we have developed a multimode treatment for the classical and quantum noise transformations produced by this interaction.⁴ This analysis transcends the simple coupled-mode theory regime. Finally, we have developed the semiclassical and quantum theories for closed-loop photodetection,^{5,6} with the latter including a potential scheme for quasi-state synthesis.

References

- ¹ M.W. Maeda, P. Kumar, and J.H. Shapiro, "Observation of Squeezed Noise Produced by Forward Four-Wave Mixing in Sodium Vapor," Opt. Lett. 12, 161 (1987).
- ² S.-T. Ho, P. Kumar, and J.H. Shapiro, "Vector-Field Quantum Model of Degenerate Four-Wave Mixing," Phys. Rev. A *34*, 293 (1986)
- ³ S.-T. Ho, P. Kumar, and J.H. Shapiro, "Quantum Theory of Nondegenerate Multiwave Mixing," Phys. Rev. A *35*, 3982 (1987).
- ⁴ R.K. John, J.H. Shapiro, and P. Kumar, "Classical and Quatum Noise Transformations Produced by Self-Phase Modulation," presented at *IQEC '87* Baltimore, Maryland, April 1987.
- ⁵ J.H. Shapiro, M.C. Teich, B.E.A. Saleh, P. Kumar, and G. Saplakoglu, "Semiclassical Theory of Light Detection in the Presence of Feedback," Phys. Rev. Lett *56*, 1136 (1986).
- ⁶ J.H. Shapiro, G. Sapakoglu, S.-T. Ho, P. Kumar, B.E.A. Saleh, and M.C. Teich, "Theory of Light Detection in the Presence of Feedback," J. Opt. Soc. Am. B in press.

6.3 Laser Radar System Theory

U.S. Army Research Office - Durham (Contract DAAG29-84-K-0095)

Jeffrey H. Shapiro, Martin B. Mark, Dongwook Park, Robert H. Enders, Stephen M. Hannon, Naomi E. Silman, Donald E. Bossi

Coherent laser radars represent a true translation to the optical frequency band of conventional microwave radar concepts. This program is aimed at developing a system theory for the emerging technology of multifunction coherent CO₂ laser radars. It includes a collaboration arrangement with the Opto-Radar Systems Group of M.I.T., Cambridge, Mass. Lincoln Laboratory whereby the experimental portions of the research are carried out with measurements from their CO₂ laser radar test beds. Our recent work is summarized below.

Multipixel Detection Theory

We have derived quasi-optimum range-only and intensity-only processors for the detection of an extended speckle target located at unknown range, azimuth, and elevation, within a speckle (ground) background of known terrain profile. The receiver

operating characteristics for these processors have also been obtained, and used to quantify a variety of resolution/performance trade-offs for these systems. Two of the key assumptions in the preceding analysis are being relaxed in a follow-up study,² experimental confirmation of the processor performance theory will be sought in future measurements using the M.I.T., Cambridge, Mass. Lincoln Laboratory 2-D pulsed imager laser radar test bed.

Unconventional Laser Radars

We have begun a theoretical study of the combined effects of target speckle, local-oscillator shot noise, and laser frequency instability on a variety of unconventional laser radars, i.e., radars which use range and/or Doppler measurements to perform imaging with spatial resolution beyond the diffraction-limit of the radar optics.³ Thus far we have completed spatial resolution, carrier-to-noise ratio (CNR), and signal-to-noise ratio (SNR) assessments for 2-D and 3-D synthetic aperture systems. Additional work is underway on range-Doppler imaging and inverse Fourier transform imaging.

References

- ¹ M.B. Mark, "Multipixel Multidimensional Laser Radar System Performance," Ph.D. Diss., Dept. of Electr. Eng. and Comp. Sci., M.I.T., Cambridge, Mass., 1986.
- ³ S.M. Hannon, "Analysis of Quasi-Optimal Multipixel Laser Radar System Processors," S.M. Thesis proposal, Dept. of Electr. Eng. and Comp. Sci., M.I.T., Cambridge, Mass., 1986.
- ³ D. Park, "Unconventional Laser Radars," Ph.D. Diss. proposal, Dept. of Electr. Eng. and Comp. Sci., M.I.T., Cambridge, Mass., 1986.

6.4 Fiber-Coupled External-Cavity Semiconductor High Power Laser

U.S. Navy - Office of Naval Research (Contract N00014-80-C-0941)

Robert H. Rediker, Kristin K. Anderson, So Kuen Liew, Christopher J. Corcoran

Last year's annual report described the high spectral purity of the output from an ensemble of five discrete diode lasers when operated cw. The linewidth of the cw output of this external-cavity-controlled ensemble of diode lasers was shown to be less than 7.5 MHz (\sim 2 x 10⁻⁸ of the center frequency). Also reported last year was high-spectral-purity pulsed output from this external cavity controlled laser. In 1986 the pulsed operation of this laser was investigated in detail both experimentally and theoretically.

Figure 6.1 is a schematic of the external-cavity arrangement. Linewidths of the order of the 7.5-MHz instrument resolution have been obtained. To achieve this high spectral purity in a pulse mode of operation, three alternate gain elements (elements number one, three, and five in Fig. 6.1) are operated cw and the intermediate two elements are pulsed. For a coherent ensemble of only three alternate gain elements, the spacing between the major intensity maxima in the Fourier plane (the filter plane) is decreased

by a factor of 2 relative to the spacing with all five elements operating coherently. As a result, the lasing threshold for the three-element ensemble is much higher because significant radiation hits the opaque areas of the filter. A calculation of the single-pass filter transmission for this case yields a value of 0.48 as compared to the transmission of 0.92 when all five elements are running.

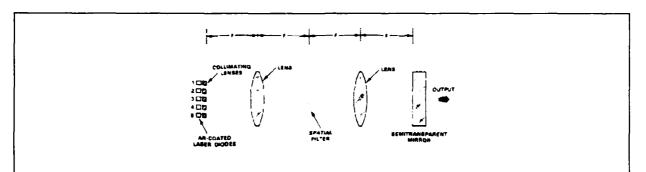


Figure 6.1.: Schematic of multiple-element external-cavity arrangement showing the placement of the five antireflection-coated diode lasers, the associated collimating optics, the two lenses, spatial filter, and end mirror. As indicated on the figure, the elements are seperated by the focal length of the lenses so the light undergoes a Fourier transform four times during one round trip through the cavity.

The spectral output of the ensemble when operated with current pulses applied to elements number two and four and cw excitation to the other three was measured for two different cases. First, the dc biases on the two pulsed elements were set so the laser ensemble was just above threshold when the pulse was off. In this case, the spectrum for the pulse output remains at the value set by the low-level cw output of the external cavity. The linewidth in this case is within the 7.5-MHz instrument resolution. It should be pointed out that if any of the five external-cavity lasers operating independently without the spatial filter are pulsed from below threshold, there is a 1-Å (\approx 40 GHz) output frequency shift (chirp) during the pulse, and there is still a chirp larger than 1.5 GHz if all five elements of the coherent ensemble with the spatial filter are pulsed simultaneously from above the ensemble threshold. For the second case, the dc biases on the two pulsed elements were reduced to a point where the ensemble was well below threshold with the pulse off. The measured linewidth is 9 MHz.

The narrow linewidth pulses can be explained by a compensation effect. Refractive index and gain in pulsed elements two and four are changing because of increased temperatures and carriers caused by the increased current. In the other three elements, however, changes occur in the opposite direction because of decreased temperatures and carriers and the simultaneous decrease in carrier lifetime.

A third case which has implications for an all-optical repeater is to operate elements one, three and five at a high enough level so this ensemble of alternate elements is just below threshold. A very small pulse output from elements two and four brings the entire ensemble above threshold with an output pulse well over a factor of 100 (20 dB) larger than the input pulse. The practical implementation of this all optical repeater would surely be different from the sketch of Fig. 6.1, but would use the same principle of obtaining gain by changing the spatial configuration of the electromagnetic field in the Fourier plane.

THE PARTY OF THE PROPERTY OF THE PARTY OF TH

Publications

- ¹ K.K. Anderson, R.H. Rediker, and L.J. Van Ruyven, "Pulsed Operation of an Array of Diode Lasers with Feedback in the Fourier Plane and a Chirp Less Than 7.5 MHz Measurement Resolution," Technical Digest of 6th Topical Meeting on Intergrated and Guided Wave Optics (IGWO), Atlanta, Georgia, February 1986, p. 30.
- ² K.K. Anderson and R.H. Rediker, "High Spectral Purity cw and Pulsed Output from an Ensemble of Discrete Diode Lasers," Appl. Phys. Lett. *50*, 1 (1987).



7.0 Infrared Nonlinear Optics

Academic and Research Staff

Prof. P.A. Wolff, Dr. R.L. Aggarwal, Dr. P. Becla, Prof. L.R. Ram-Mohan, Dr. S.Y.C. Yuen

Graduate Students

E. Isaacs, C. McIntyre, J. Stark, S. Wong

7.1 Nonlinear Optics in HgTe

U.S. Air Force - Office of Scientific Research (Grant AFOSR-85-0269)

Peter A. Wolff, Sunny Y.C. Yuen

HgTe has been shown¹ to have the largest known third order optical nonlinearity with response time in the picosecond range. At T = 300K, we find $\chi^{(3)} = 2 \times 10^{-4} \text{esu}$ and $\tau = 5 \text{psec}$. The nonlinear susceptibility was measured with four wave mixing experiments performed with a pair of Q-switched CO₂ lasers. The sample was a HgTe epilayer 3μ thick, MBE-grown on a CdTe substrate.

The nonlinear signal varied as $P_3 \sim P_2$ P_2 to the highest laser intensities, $P_1 = P_2 = 500 \text{kw/cm}^2$ used in these experiments. The absence of saturation is striking; most strong nonlinear processes in semiconductors saturate at lower pump intensities. In the HgTe case, the dielectric constant of the epilayer was modulated by more than 10% when $P_1 = P_2 = 500 \text{kw/cm}^2$. This result implies an oscillating plasma density exceeding 10^{17} carriers/ $_{cc}$. Calculations suggest that this oscillating plasma could be an efficient source of FIR radiation.

The optical nonlinearity of HgTe is attributed to interband population modulation, caused by carrier excitation from the heavy mass Γ_8 valence band to the light mass Γ_8 conduction band. The theory predicts values of $\chi^{(3)}$ in agreement with those observed. Further enhancement of the nonlinearity of HgTe may be achieved with doping, or by alloying with Cd.

7.2 Nonlinear Current-Voltage Characteristics in HgMnTe

Defense Advanced Research Projects Agency (Contract N00014-83-K-0454)

Stephen Wong, Piotr Becla, Peter A. Wolff

S-type nonlinear I-V characteristics have been demonstrated² in bulk p-type HgMnTe samples with bandgaps from 50 to 250 meV at T = 4.2K and 1.6K. At zero magnetic field, regions of strong negative differential resistivity and composition dependent

breakdown, have been observed using electric fields up to 1000V/cm and current densities to $2A/cm^2$. The nonlinearity is twice as large at 1.6K as at 4.2K. When a modest magnetic field is applied (B \simeq 3 tesla), the zero-bias resistivity drastically decreases, and the region of negative differential resistivity ($dV/dI \simeq -100\Omega cm$) disappears. this is the first observation of nonlinear I-V characteristics in narrow gap diluted magnetic semi-conductors, and may have applications in both nonlinear electrical and optical devices.

7.3 Free Carrier Spin-Induced Faraday Rotation in HgCdTe and HgMnTe

U.S. Air Force - Office of Scientific Research (Grant AFOSR-85-0269)

Sunny Y.C. Yuen, Peter A. Wolff

Free carrier, spin-induced Faraday rotation has been studied³ in n-type HgCdTe and HgMnTe as a function of laser intensity and wavelength in the 10μ region. When the photon energy is close to the semiconductor bandgap, E_G , the Verdet constant of the spin-induced process is considerably larger than that of the interband or free-carrier plasma Faraday effects.

In a HgCdTe sample with $E_G = 130$ meV, the Faraday rotation saturates for B > 4kG, which is the magnetic field required to fully align the electron spins. Below saturation, the Verdet constant is V = 0.19 degrees/cm - G. The theoretical value, estimated from the spin flip cross section, is V = 0.12 degrees/cm - G. The figure of merit, $V/_x$, for HgCdTe is comparable to that of pure InSb.

At low laser intensities, the n-HgMnTe samples have behavior similar to the HgCdTe samples. At higher intensities, the Faraday rotation decreased substantially. This effect is attributed to spin heating, resulting from electron — Mn²⁺ spin flip processes.

7.4 Optical Nonlinearity Caused by Resonant Scattering

U.S. Air Force - Office of Scientific Research (Grant AFOSR-85-0269)

Sunny Y.C. Yuen, Peter A. Wolff

In $Hg_{0.7}$ $Cd_{0.3}$ S: Fe crystals, the Fe⁺³ level lies near the conduction band of this small gap semiconductor. The Fe atoms act as donors, and also cause a sharp scattering resonance, with width $\Delta = 10\text{-}20$ meV, near the band edge. Kaw had previously predicted a large nonlinear optic susceptibility under these conditions. Four wave mixing experiments⁴ demonstrate a 30-fold enhancement of $\chi^{(3)}$, compared to comparable crystals without Fe impurities. An extension of the Kaw Theory predicts linear absorption and nonlinear susceptibility in agreement with those measured. Further enhancement of $\chi^{(3)}$ is expected in alloys with optimized composition.

7.5 Stress Tuned, Magnetic-Field-Induced Anticrossing in As-Doped Germanium

U.S. Air Force - Office of Scientific Research (Grant AFOSR-85-0269)

Eric R. Youngdale, Roshan L. Aggarwal

In n-Ge, magnetic fields induce an anticrossing between two states of the 1s(T₂) donor manifold. The field at which the anticrossing occurs can be tuned with uniaxial stress along the [110] direction in Ge:As. We have used CO₂ laser four-wave mixing spectroscopy to determine the energy levels as a function of stress. The behavior of the anticrossing is consistent with the theory of People and Wolff, and shows that the effect is due to anistropy of the g-tensor for conduction band electrons. Uniaxial stress is also shown to alter the g-factors, and the strength of the anticrossing.

References

- ¹ P.A. Wolff, S.Y. Yuen, K.A. Harris, J.W. Cook, Jr., and J.F. Schetzina, "Optical Nonlinearity in HgTe," Appl. Phys. Lett., in press.
- ² S. Wong, P. Becla, and P.A. Wolff, "Magnetic Field Dependent Nonlinear Current-Voltage Characteristics in HgMnTe," Bull. Am. Phys. Soc. *32*, 491 (1987), Abstract CT12.
- ³ S.Y. Yuen, P.A. Wolff, and P. Becla, "Free Carrier Spin-Induced Faraday Rotation in HgCdTe and HgMnTe," J. Vac. Sci. Tech., in press.
- ⁴ S.Y. Yuen, P.A. Wolff, and A. Mycielski, "Nonlinear Optical Susceptibility Caused by Scattering Resonances in HgCdSe:Fe," to be published.
- ⁵ E.R. Youngdale, and R.L. Aggarwal, "Observation of Stress Tuned, Magnetic-Field Induced Anticrossing in As-doped Germanium," Phys. Rev. B., in press.



8.0 Phase Transitions in Chemisorbed Systems

Academic and Research Staff

Prof. A.N. Berker

Graduate Students

K. Hui, S.R. McKay

8.1 Phase Transitions under Random Fields

Joint Services Electronics Program (Contract DAAL03-86-K-0002)

A. Nihat Berker, Susan R. McKay

Substrate imperfections locally differentiate between chemisorption sublattices, thereby creating a random-field situation for epitaxial ordering. We have solved the three-dimensional random-field Ising model by pursuing the global renormalizationgroup trajectories of the full, coupled probability distribution of local fields and bonds.2 The underlying local transformations are effected by the Migdal-Kadanoff approximation applied to bonds and fields with distinct values. The phase diagram and critical properties, as well as magnetization and specific heat curves, are calculated. A novel "hybridorder" phase transition is discovered: the boundary between the ferromagnetic and paramegnetic phases has a discontinuous magnetization, as in a first-order transtion, and a power-law specific-heat singularity, as in a second-order transition. This boundary is controlled by an unstable strong-coupling fixed distribution, justifying our previously derived modified hyperscaling relation. Analogous calculations are performed for several other values of dimensionality, showing a lower-critical dimension $d_i = 2$, below which the random-field ferromagnetic phase has disappeared, and suggesting a novel medium-critical dimension $d_m > 3$, above which the fixed distribution moves away from strong coupling, which implies a singularity in the critical properties as a function of dimension. This new result could conciliate previous conflicting works.

8.2 Phase Transitions in Systems with Competing Interactions

Joint Services Electronics Program (Contract DAAL03-86-K-0002)

Kenneth Hui, A. Nihat Berker

An extended mean-field method is developed to study a partially frustrated stacked triangular system, in which planes of Ising spins with antiferromagnetic nearest-neighbor and ferromagnetic next-nearest-neighbor interactions are connected in the vertical direction by ferromagnetic bonds. For weak next-nearest-neighbor couplings, the system undergoes three successive second-order phase transitions as the temperature is lowered. This is consistent with the experimental results on CsCoCl₃ and CsCoBr₃. In another study, an "anti-metamagnet" is constructed by reversing the signs

of all interactions in a metamagnet. This anti-metamagnet is studied by our extended mean-field method. We find that the system displays a reentrant phase transition behavior for a narrow window in magnetic-field strengths.³

References

- ¹ A.N. Berker and S.R. McKay, Phys. Rev. B 33, 4712 (1986).
- ² S.R. McKay and A.N. Berker, preprint (1987).
- ³ K. Hui, preprint (1987).

9.0 X-Ray Diffuse Scattering

Academic and Research Staff

Prof. R.J. Birgeneau, Prof. A. Aharony, Dr. J.W. Chung, Dr. C.J. Peters

Graduate Students

K. Evans-Lutterodt, H. Hong, B. Keimer, A. Mak, D.Y. Noh, E. Specht, T. Thurston

Joint Services Electronics Program (Contract DAAL03-86-K-0002)

Robert J. Birgeneau

In this research program, modern x-ray scattering techniques are used to study the structures and phase transistions in novel states of condensed matter. We have two principal experimental facilities. At M.I.T. we have four high-resolution computer-controlled x-ray spectrometers using high intensity rotating anode x-ray generators. The angular resolution can be made as fine as 1.8 seconds of arc; this enables one to probe the development of order from distances of the order of the x-ray wavelength, $\sim 1 \text{Å}$, up to 30,000Å. The sample temperature may be varied between 2K and 500K with a relative accuracy of $2 \times 10^{-3} \text{K}$. We also have, in collaboration with IBM, a two spectrometer system at the National Synchrotron Light Source at Brookhaven National Laboratory. A third beam line designed to operate at short wave lengths is currently under development. These make possible high resolution scattering experiments with a flux more than three orders of magnitude larger than that from a rotating anode x-ray generator; this, in turn, has opened up a new generation of experiments.

As part of the JSEP program we have built an x-ray compatible high vacuum single crystal apparatus. This enables us to use synchrotron radiation to study the structure and transitions occuring at a single surface; the first generation of such experiments has now been performed. Our current experiments in this program are concentrated in three areas: 1) the phases and phase transitions of metal and semiconductor surfaces and surface overlayers; 2) the structure and phase transitions of smectic liquid crystals; and 3) the growth, structure and phase transitions of intercalant materials.

9.1 Single Crystal Surface Studies

As noted above, x-ray synchrotron sources provide sufficient flux that it is possible to carry out high resolution diffraction studies of a single monolayer. In the past year we have studied three different systems: 1) monolayer xenon on graphite; 2) tungsten (100) with either oxygen or hydrogen adsorbed on the surface; and 3) pristine silver (110) as a function of temperature.

The xenon-on-graphite experiments represented a considerable technical advance on previous surface overlayer experiments. We used a single crystal of graphite with a mosaicity of 0.01° full-width-at-half-maximum (FWHM). This corresponds to a real space resolution of ~2 microns. The xenon coverage was accurately controlled using

a vermicular graphite ballast adjacent to the single crystal sample. We find that for a broad range of coverages, ~ 9 to 1.2 monolayers, with decreasing temperature the xenon exhibits the sequence of structures: aligned hexagonal incommensurate \rightarrow rotated hexagonal incommensurate \rightarrow aligned hexagonal incommensurate \rightarrow 3 \times 3 R30° commensurate. The first and third transitions are first order while the second is continuous. The incommensurate-commensurate transition is similar to that exhibited by monolayer kyrpton on graphite with a 1/3 power-law behavior; however, for xenon this power law is pre-empted by a first order transition at 1% incommensurability. From the data it is possible to deduce precise information about the surface potential and thereby to assess first principle's theoretical predictions for this model surface system.

From low energy electron diffraction studies it is known that tungsten (100) exhibits a variety of interesting surface phases when either oxygen or hydrogen is adsorbed onto the surface. We have used high resolution synchrotron radiation to study the surface oxygenation and hydrogenation processes. Because of the extreme reactivity of the tungsten surface, these experiments are technically quite difficult. We have, nevertheless, managed to observe both the saturated oxygen overlayer structure, which has a simple 2 x 2 symmetry, and various other chemisorbed phases. These data are still being analyzed. Quite fascinating results are obtained with the absorption of hydrogen. For about 0.2 monolayers of hydrogen, a centered 2 x 2 structure forms; we observe intense x-ray diffraction from this phase at room temperature. This necessitates that there is considerable movement of the tungsten surface atoms in the formation of the 2 x 2 structure. With increasing hydrogen coverage a commensurate-incommensurate transition occurs. These data are currently being analyzed.

Surface roughening is a novel phenomenon which has been extensively investigated theoretically and by computer simulation. However, there have been only limited experimental investigations in real materials. Recent atom beam scattering experiments have suggested that low index metal surfaces may show a reversible roughening transition. We have carried out a detailed study of the Ag (110) surface. We find that at about 400°C the Ag (110) surface indeed becomes rough and by ~600° the surface is sufficiently disordered that it no longer gives a clear diffraction signal. Remarkably, as the sample is cooled, the surface reforms reversibly recovering its original form at room temperature. The data from this experiment are currently being analyzed.

9.2 Structure and Phase Transitions of Smectic Liquid Crystals

The mechanism by which crystalline order is established as a fluid freezes is still an unsolved problems. In liquid crystal materials, the freezing process may occur in several steps. Each step may be thought of as the freezing out of some particular type of random motion or disorder as the system cools. Choosing the orientation in space of the axes of the crystalline lattice is one of the crucial steps necessary for the establishment of crystalline order. In most physical systems, this choice of orientation occurs simultaneously with the establishment of a true spatially periodic crystal lattice. However, there is no reason why the two processes must occur simultaneously. The logical possibility that a phase of matter might have a well defined orientation for the crystal axes without having actually established the lattice has been recognized for 50 years. These strange phases of matter are called Bond Orientationally (BO) ordered to indicate that

it is the orientation of the bonds between nearest neighbors, not the distance between nearest neighbors, which is becoming fixed.

The suggestion that several of the unusual liquid crystal phases might be physical realizations of BO ordered phases was made several years ago. However, samples of high enough quality and x-ray scattering equipment with high enough intensity at high resolution were not readily available. The sample problems were solved by the development of freely suspended film techniques of liquid crystal at Harvard, Bell Labs and MIT. The development of high resolution x-ray scattering apparatus on synchrotron x-ray sources has solved the latter obstacle.

The signature of a BO ordered phase in an x-ray scattering experiment is a periodic variation in the scattered intensity while rotating the lattice. We therefore performed a series of such angular scans as the sample was cooled through the putative hexatic phase transition. At high temperatures the scan is flat to within our counting statistics. As the sample is cooled, a measurable modulation develops. Further cooling causes the slight modulation to grow into definite peaks, one every 60°.

Taking advantage of this extremely high quality data taken at NSLS, we performed a detailed line-shape analysis. The analysis led to the empirical discovery of mathematical scaling relations describing the growth of the BO order. Motivated by this discovery, a theoretical model was developed which explains the growth of BO order based only on the underlying symmetry of the physical system. Since the model applies to any physical system with the appropriate symmetry, it is applicable to a wide variety of theoretical and experimental systems. Using our model we can describe exactly how the orientation of the crystal lattice develops with temperature without any knowledge of the details of the system other than its symmetry.

9.3 Intercalation Compound Structures and Transitions

Intercalation compounds represent a family of materials in which a foreign species (e.g., Br_2) is inserted between the layers of a lamellar material such as graphite. If the intercalant enters every nth layer then the resultant material is referred to as a stage-n intercalation compound. In this program we study both the intercalation process itself and the structure and transitions of the intercalation compound as a function of temperature, concentration, and stage index. Our current work is concentrated on the system bromine-intercalated graphite $C_{7n}Br_2$.

Bromine-intercalated graphite has turned out to be an interesting model two dimensional system. Above 69.3°C the bromine has a novel structure in which it is inregistry with the graphite in one direction and out of registry or incommensurate in the other. This is referred to as a <u>stripe-domain</u> structure. One of the unusual features of such a structure, which we have characterized thoroughly, is that in a diffraction pattern there are no true Bragg peaks. Rather, the diffraction is characterized by power law singularities, $(Q - Q_n)^{-2+\nu_n}$, where the exponent ν_n depends on the order (n) of the harmonic. Here the ν_n are predicted exactly by theory. One of the interesting questions which had not been addressed quantitativley to date is how such a solid melts. Qualitatively, it is expected that one could have a continuous melting transition in which the bromine melts while the graphite stays crystalline. Further, on universality grounds it is expected that such a transition, if continuous, would be isomorphous to

the superfluid transition in two-dimensional helium which is well-described by a theory due to Kosterlitz and Thouless - a dramatic theoretical prediction. We have used high resolution x-ray synchrotron techniques to study this melting transition. A high quality single crystal of stage-8 bromine intercalated graphite was grown "in situ" on the x-ray spectrometer.

Our results show a number of striking features: (1) the transistion is indeed continuous, at least for length scales varying from several thousand Angstroms to fifty Angstroms; (2) higher harmonics of the mass density wave vanish successively as the temperature is raised. Thus, even though from the peak positions we know that the domain walls remain microscopically sharp, the order parameter acquires a sine-wave character; (3) the transition is very rapid, with the primary evolution in the structure factor occurring within 1°C; (4) the aspect ratio of the scattering changes through the transition; and (5) the detailed nature of the correlations is unusual in that a power-law description of $S(\bar{Q})$ works throughout the temperature range studied; that is, the anticipated crossover from algebraic to exponential decay of the positional correlations at $\eta_1 = 1/4$ does not seem to occur.

We have also carried out a combined electron and x-ray diffraction of SbCl₅ Of particular interest is the unusual commensurate intercalated graphite. $(\sqrt{7} \times \sqrt{7})$ R19.1° to glass "phase change" (C-G) in the intercalate layer that has been observed to take place on cooling below ~ 180K using TEM, where the lowtemperature phase is the glass phase. The C-G phase change is not observed in x-ray diffraction experiments. It was first suggested that the C-G phase change reported for stages 1-4 occured only in dilute samples, and that further the intercalate layer was dilute in the thin samples needed for TEM, but not in the thick samples used in x-ray diffraction. In order to determine whether the discrepancy between the x-ray and TEM results was due to differences in sample composition or to differences in the experimental techniques, we performed x-ray diffraction and electron microscopy studies at low temperatures using stage-2 SbCl5-ClG samples of common origin for both types of experiments. We investigated the dependence of the C-G phase change on host material, host crystallite size and experimental technique. We find from x-ray and electron diffraction experiments performed on stage-2 SbCl₅ -GIC samples that the crystalline to glass-phase change results from electron-beam damage. Two competing annealing processes are observed with two different activation energies. crystalline-glass phase change is the result of damage attributed to atomic displacements indirectly induced by electron beam irradiation. We have devised a model for the damage process that induces the C-G phase change. The model is supported by a computer image simulation of the commensurate ($\sqrt{7}$ × $\sqrt{7}$) R19.1° phase.

Publications

Birgeneau, R.J., and P.M. Horn, Science 232, 329 (1986).

Brock, J.D., A. Aharony, R.J. Birgeneau, K.W. Evans-Lutterodt, J.D. Litster, P.M. Horn, G.B. Stephenson, and A.R. Tajbakhish, Phys. Rev. Lett. 57, 98 (1986).

Mochrie, S.G.J., A.R. Kortan, P.M. Horn, and R.J. Birgeneau, Phys. Rev. Lett. 58, 690 (1987).

Ocko, B.M., R.J. Birgeneau, and J.D. Litster, Z. Phys. B 62, 487 (1986).

Salamanca-Riba, L., G. Roth, J.M. Gibson, A.R. Kortan, G. Dresselhaus, and R.J. Birgeneau, Phys. Rev. B *33*, 2738, (1986).



10.0 Semiconductor Surface Studies

Academic and Research Staff

Prof. J.D. Joannopoulos, Dr. Y. Bar-Yam, Dr. G. Gomez-Santos

Graduate Students

K. Rabe, E. Kaxiras, M. Needles

Joint Services Electronics Program (Contract DAAG29-83-K-0003)

John D. Joannopoulos

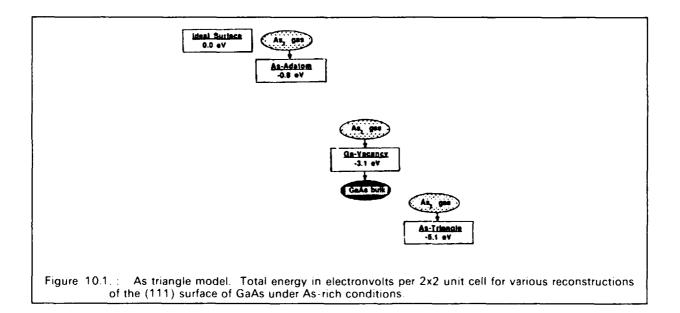
Understanding the properties of surfaces of solids and the interactions of atoms and molecules with surfaces has been of extreme importance both from technological and academic points of view. The recent advent of ultrahigh vacuum technology has made microscopic studies of well-characterized surface systems possible. The way atoms move to reduce the energy of the surface, the number of layers of atoms involved in this reduction, the electronic and vibrational states that result from this movement, and the final symmetry of the surface layer are all of utmost importance in arriving at a fundamental and microscopic understanding of the nature of clean surfaces, chemisorption processes, and the initial stages of interface formation. Actually, one of the most difficult and fundamental problems in surface studies, both from the experimental and theoretical points of view is simply the determination of the precise positions of the atoms on a surface. Currently, there are many surface geometries, even for elemental surfaces, that remain extremely controversial.

The theoretical problems associated with these systems are quite complex. We are, however, currently in the forefront of being able to solve for the properties of real surface systems (rather than simple mathematical models). In particular, we are continuing our goal of calculating the total ground-state energy of a surface system form the "first principles" so that we may be able to provide accurate theoretical predictions of surface geometries. Our efforts in this program have concentrated in the areas of surface growth reaction pathways, surface reconstruction geometries, structural phase transitions, and hyrdogenation.

10.1 Surface Reconstruction Geometries

Using "first principles" total energy calculations, it is possible to determine on a microscopic scale how atoms behave when they are on the surface of a solid. This is a fundamental problem that has plagued both theorists and experimtalists for decades. The difficulty lies with the very strong interactions that may exist between the surface atoms and the host atoms constituting the rest of the solid. These interactions can strongly disturb the original idealized atomic arrangement at the surface changing the nature of the bonding and even the original stoichiometry.

In recent years there has been considerable activity focused on determining the exact equilibrium geometry of the [111] surfaces of the III-V compounds. One of the most popular and intriguing models is the Ga/vacancy geometry where the removal of one out of four Ga atoms on the surface was believed to proceed exothermically and result in the lowest energy structure. For binary compound surface systems, however, it becomes meaningless to simply ask "What is the lowest energy surface geometry?" It is crucial to know the preparation conditions and the nature of the Ga and As reservoirs during the growth process. The relevant atomic reservoirs for the GaAs (111) surface are Ga-gas, As₂ -gas, Ga-metal droplets and the GaAs-bulk. In Fig. 10.1 we illustrate the energies of several possible (2x2) recontruction geometries we have studied, along with the corresponding reservoirs, relative to the ideal surface. We note that under As-rich conditions the lowest energy (2x2) reconstruction is a new model, the Astriangle geometry. This is shown in Fig. 10.2 and consists of three As adatoms bonded through As-As bonds which effectively compensate for the energy required to dissociate As₂ molecules which are the source of excess As atoms. Moreover, the triangle results in a nearly perfect geometric coordination of the remaining surface As and Ga atoms.



Finally, under Ga-rich conditions, we find that the Ga-vacancy geometry is indeed most favorable. Our results predict, then, that by varying the relative chemical potential of As and Ga, a phase transition should occur between the As-triangle and Ga-vacancy geometries. There are indirect experimental observations that appear to be consistent with this prediction.

10.2 Structural Phase Transitions

All the calculations described in the previous section were at zero temperature. It is now becoming possible, however, to begin studying the statistical mechanics and temperature phase transitions of surfaces of solids. This is a completely new and unex-

64

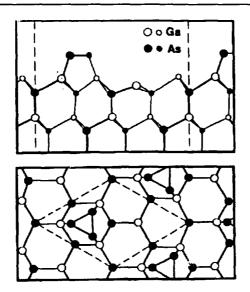


Figure 10.2.: As triangle model. Upper panel: side view [(100)plane] of the GaAs(111)2x2 surface As triangle model. Larger size atoms are in the plane of the paper. Smaller size atoms are in a parallel plane. Lower panel: top view of the As-Triangle model. Dashed lines indicate a 2x2 cell unit.

plored area. As an example, the myriad of surface reconstructions that may exist on clean semiconductor surfaces at different temperatures is an extremely interesting and fundamental problem that needs to be investigated. Modern studies of phase transitions utilize a powerful theoretical tool which is the renormalization group scheme. The scheme is based on scaling ideas, and has as input simple spin Hamiltonians which model the degrees of freedom of the system. Until now there has been no way of calculating what these Hamiltonian parameters should be for real surfaces of solids. The total energy calculations described above, however, should provide precisely the kind of information needed. The exciting possibility then arises of coupling the results of microscopic studies of surface systems (at zero temperature) with simple spin Hamiltonians and the renormalization group approach to study phase transitions at finite temperatures from "first principles."

Using a simple semi-empirical total energy approach we succeeded in developing such a scheme and have applied it to the Si(100) surface, resolving important questions regarding the structure of the Si(100) surface. For example, we show that the (2x1) reconstruction geometry is not the ground state of the Si(100) surface and that higher order reconstructions can exist on the surface. In fact, it is found that two distinct families of reconstructed geometries (the "2x1" family and the "c(2x2)" family) can exist on the surface, with independent phase transitions occurring within each. Two critical transition temperatures are predicted representing order-disorder transitions. We are presently investigating the possible phase transitions that may occur on the Ge(100) surface. This system, however, cannot be described accurately by a semi-empirical approach so that we are forced to use the more powerful and much more complex ab-initio total energy method discussed in section 10.1.

To perform these studies we have been developing a new scheme for relaxing a system with many degrees of freedom to its lowest energy configuration. The scheme

is based on a molecular dynamics approach to calculating quantum mechanical total energies and resembles a simulated quench. Our calculations of the Ge(100) surface are currently underway.

10.3 Hydrogenation

The interaction of atomic hydrogen with cleaned semiconductor surfaces has been extensively studied for over a decade. Hydrogen atoms appear to saturate surface dangling bonds resulting in a nearly ideal, bulk-terminated plane of exposed surface atoms. It is interesting that in cases where the surface does not have the geometry and periodicity of the bulk-terminated plane, the interaction of hydrogen with surface atoms is strong enough to unreconstruct the complicated reconstruction patterns. This process takes place for example on the (2x1) Si(111) surface, which exhibits a low-energy π -bonded-chain reconstruction. Upon hydrogenation this chain of Si atoms with (2x1) periodicity reverts to the (1x1) pattern of the bulk-terminated plane. Similar phenomema have been observed on the Ge(111) surface. Theoretically, this process is not very well understood and a realistic, first-principles study with adequated accuracy to define precise low energy positions of atoms, corresponding total energies, and vibrational excitations above the ground state is completely lacking. Such a study is currently underway. Preliminary results, using ab-initio quantum mechanical total energy calculations, indicate that the atomic positions of the hydrogenated Si and Ge(111) surfaces differ significantly from those of an ideal bulk-terminated plane.

11.0 Ultralow-Temperature Measurements of Submicron Devices

Academic and Research Staff

Prof. M.A. Kastner, S. Field, C. Licini, D. Face

Graduate Students

U. Meirav, J. Scott-Thomas, S. Park

Joint Services Electronics Program (Contract DAAL03-86-K-0002)

Resulting in a large part from the work of Prof. P.A. Lee, a unified theory has emerged to explain the fluctuations of the conductance in very small conductors. In our collaborative research with Professors H.I. Smith and D.A. Antoniadis, we have used Si MOSFET's to explore these fluctuation phenomena experimentally.

The theory predicts that for long, narrow disordered conductors at zero temperature, there will be exponentially large fluctutations of conductance from one sample to another, one value of the Fermi energy to another or one value of applied magnetic field to another. If one could make the samples arbitrarily short, the theory predicts that the fluctuations would become smaller when the sample length L becomes smaller than the localization length. When this happens, that is, when the electronic states are extended over the entire sample, the fluctuations are predicted to have magnitude e²/ h independent of sample size or geometry.

In addition to these zero-temperature predictions, a theoretical description of the behavior at finite temperatures has been developed based on the experimental studies of narrow Si MOSFET's by groups at MIT, IBM and AT&T Bell Labs. The MIT experiments provided the first clear evidence that, in the exponentially-large-fluctuation regime, the fluctuations result from the limitation of the current by a single localized state in the one-dimensional MOSFET. This led Lee to propose his model of one-dimensional photon-assisted hopping. The MIT experiments also provided the first observation of the universal (e²/h) fluctuations in one-dimensional MOSFET's. Chu, Antoniadis, Smith and Kastner reported the first observation of such fluctuations in short wide MOSFET's.

A wide variety of quantum-effect devices are being fabricated by students of Antoniadis, Smith, Orlando and Kastner using Si MOSFET's as well as GaAs two-dimensional electron gas structures. The experience of IBM and AT&T as well as the MIT group is that the understanding of the electronic phenomena in submicron devices requires experiments at ultralow temperature. Kastner's JSEP program is therefore devoted to the development of the capability of characterizing submicron electronic devices at temperatures as low as 20 mK. A dilution refrigerator furnished with a 10 T superconducting magnet has been delivered and installation should be complete near the beginning of February 1987. The refrigerator is isolated from radio-frequency interference by a shielded enclosure. All information will be transferred into and out of the enclosure by a fiber-optic IEEE extender, to eliminate r.f. from the computer used

to control experiments and acquire data. These precautions are necessary because below $\sim 0.1 \, \text{K}$, the electrons in submicron devices have poor thermal contact with the lattice. Any electrical noise then raises the electron temperature.

As temperature is increased from T=0, it is predicted that the decrease of the inelastic diffusion length will have the same effect as shortening the sample. That is, there will be a transition from localized states with exponentially large fluctuations to extended states with e²/h fluctuations when the inelastic diffusion length becomes as short as the localization length. The first experiments with our dilution refrigerator will be a study of this transition. There are clear predictions of how the fluctuations will vary with the inelastic diffusion length and both depend on gate voltage in a MOSFET.

12.0 Quantum Transport in Low Dimensional Disordered Systems

Academic and Research Staff

Prof. P.A. Lee

Graduate Students

R.A. Serota, W. Xue

12.1 Effect of a Magnetic Field on Hopping Conduction in Quasi-One-Dimensional MOSFET's

Joint Services Electronics Program (Contract DAAG29-83-K-0003)

Patrick A. Lee

Electronic transport measurements in 1D metal-oxide semiconductor field-effect transistors (MOSFET's) reveal unusually large fluctuations in conductance with variations in gate voltage. According to our recent work,1 this random structure is a manifestation of Mott's variable-range hopping conduction. The original motivation for this explanation was that MOSFET wires are typically 30-70 times the localization length. Since a Mott hop covers several localization lengths, only a few hops are required to traverse the entire sample. In the hopping model, each hop is exponentially activated and the resistance of the sample is determined by a critical hop at the percolation threshold. Since the resistors have a log-normal distribution, variations of chemical potential can change the sample resistance by orders of magnitude. A recent study of resistance fluctuations as a function of sample size2 reveals that the average of the logarithm of the resistance increases as $(\ln 2\alpha L)^{1/2}$ while the relative magnitude of the fluctuations decreases as $(\ln 2\alpha L)^{-1/2}$ where α is the inverse localization length and L the sample size. The resistance fluctuations are therefore inherent in the hopping model and not just due to finite-size effects. The similarity between resistance fluctuations in the hopping model and those observed experimentally suggests that the experiments are probing something fundamental, namely, a critical hop between a pair of localized states. This presents the exciting possibility of investigating the effect of magnetic field on an individual hop between a pair of localized states. The investigation of the effects of a magnetic field on hopping conduction is the subject of our recent work.3

The influence of magnetic field on variable-range hopping conduction enters through the Zeeman shift and changes in wave functions of localized states. With an increased magnetic field, we find that the Zeeman effect rigidly moves conductance fluctuations to lower or higher values of chemical potential; on the other hand, the orbital effect does not cause any systematic shifts in the fluctuation spectrum. Rigid shifts due to the Zeeman effect reflect the nature of the dominant hopping process which, in turn, is related to the relative population of singly and doubly occupied sites in the system. Together with density-of-states measurements, this information can be used to estimate the value of the intrasite Coulomb repulsion in 1D MOSFET's.

The experimental implications of our results are as follows. Orbital and Zeeman effects can be experimentally separated by the orientation of the magnetic field. If the field is parallel to the sample, we predict that the fluctuations in conductance arise because of hopping from either (a) singly occupied sites to unoccupied sites, or (b) doubly occupied sites to singly occupied sites. With an increase in magnetic field, the fluctuations associated with weak links of type (a) shift to lower while those corresponding to process (b) shift to higher gate voltages. If the magnetic field is perpendicular to the sample, both the orbital effect and the Zeeman shift influence conductance fluctuations. But systematic shifts in the conductance-fluctuation spectrum can be solely attributed to Zeeman shifts of occupied sites. Recent experiments by Webb, Wainer and Fowler at IBM are in good agreement with our predictions.

References

- ¹ P.A. Lee, Phys. Rev. Lett. *52*, 1641 (1984).
- ² R.A. Serota, R.K. Kalia and P.A. Lee, Phys. Rev. B 33, 8441 (1986).
- ³ R.K. Kalia, W. Xue and P.A. Lee, Phys. Rev. Lett. 57, 1615 (1986).

13.0 Graphoepitaxy of Colloidal Crystals

Academic and Research Staff

Prof. J.D. Litster

Graduate Students

R. Francis, B. McClain

13.1 Growth of Colloidal Crystals

Joint Services Electronics Program (Contract DAAL03-86-K-0002)

R. Francis, J. David Litster

The goal of this project is to use colloidal crystals of polystyrene latex spheres as models to study epitaxial growth on patterned substrates. Using lithographic techniques, it is possible to control the texture and patterns of the substrate precisely on the "atomic" scale of the model systems - which is about 0.1 μ m. Thus light scattering may be used to study ordering in these materials in a way analogous to the use of x-rays to study ordinary crystals, with the added advantage that dynamic information can be obtained.

A thin cell in which the ionic strength of the colloid can be reduced to the point where crystallization occurs has been constructed. Preliminary light scattering experiments of the freezing with smooth substrates are in progress. For analysis of the intensity of scattered light, we have developed computer codes based on the theory of interacting charged spheres; the code has been tested on data obtained by neutron scattering from micellar solutions and found to work well. It will be interesting to see how well this theory works near the "freezing" transition of the colloidal crystals.

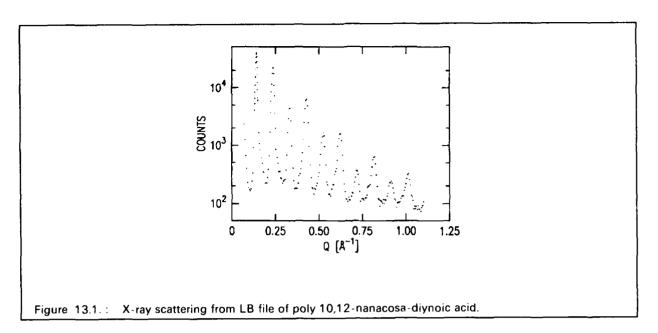
13.2 Structure of Langmuir-Blodgett Films

Joint Services Electronics Program (Contract DAAL03-86-K-0002)

B. McClain, J. David Litster

This project aims to use surface sensitive x-ray scattering to study the surface of Langmuir-Blodgett films pulled in the standard way from monolayers on the surface of water. These films have potential for device applications and are also model systems for studying the structure of two-dimensional materials.

Initial experiments have been carried out on a Langmuir-Blodgett sample with 192 multilayers polymerized with a poly-diacetylene linkage. The layers were pulled from monomers of the cadmium salt of 10,12-nanacosa-diynoic acid dispersed on a substrate containing 10⁻² M of CdCl₂. Polymerization was done by ultraviolet irradiation after the films were pulled. X-ray scattering data for this film that were taken at our beam line



at the Brookhaven National Synchrotron Light Source are shown in the accompanying figure; the momentum transfer was normal to the film and shows many harmonics with an interesting alternating intensity of the peaks. No structure could be detected in the plane of the film.

14.0 Photon Correlation Spectroscopy and Applications

Academic and Research Staff

Prof. S.-H. Chen, Dr. M.A. Ricci¹

Graduate Students

T.L. Lin, E.Y. Sheu, C.F. Wu, B. Carvahlo, X.B. Wei, K.Y. Wang

14.1 Structure and Dynamics of Colloidal Solutions Studied by Small Angle Neutron Scattering and Photon Correlation Spectroscopy

National Science Foundation (Grant DMR-84-18718)

Sow-Hsin Chen, M.A. Ricci, E.Y. Sheu, C.F. Wu, B. Carvahlo

Small angle neutron scattering technique has been used to study systematically the structure and interaction of ionic and zwiterionic micelles formed from ionic and polar surfactants in aqueous solutions. A recently developed theory of highly asymmetic ionic liquids has been shown to apply to dense micellar solutions where the charge density on the micellar surface is very high. Combination of the structural studies and the theoretical evaluation of the inter-micellar correlations allow an unambiguous analysis of neutron scattering data to obtain: 1) micellar aggregation number; 2) renormalized micellar charge; and 3) micellar shape, size and hydration as functions of the surfactant and salt concentrations. Thus, the micellar growth and polydisperity can be simultaneously studied.

zweiterionic micelles formed from short chain lecithins series of (dihexanoylphosphatidylcholine, diheptanoylphophatidylcholine, etc.) studied. In contrast to the long-chain lecithins (C₁₄ and longer) which form bilayers and therefore are important for studies of artificial membranes, the short-chain lecithins form globular micelles. However, the conformational features of the head groups are expected to be the same in the two cases. We have analyzed the SANS data using a thermodynamic model, called ladder model, which is expected to be valid for cylindrical micelles. This model contains three parameters, namely, the minimum size micelle N_o, the free energy advantage of inserting No monomers in the straight section of the cylinder as compared to that in the end caps, $(\Delta - N_o) / \kappa_B T$, and the free energy of inserting a monomer, $\delta/\kappa_{\rm B}T$, once the minimum micelle is formed. This model is capable of explaining the phenomenon of critical micelle concentration and the growth and polydispersity of the micellar system as functions of concentration and temperature. SANS data was shown to yield all three basic parameters of the theory and to provide the size and size distribution of the cylinders.

¹ Visiting Scientist

A high resolution spectroscopic technique based on analyses of scattered light intensity fluctuations has been in use for some time. Our method is based on the digital time-domain pulse correlation technique using a 256-channel clipped correlator developed in the laboratory. The correlator-multichannel memory system is controlled by a PDP 11/MINC computer system which is capable of high-speed data acquisition and analysis necessary for the study of time-varying phenomena.

We have applied this photon correlation technique to study the Brownian dynamics of strongly interacting colloidal systems. Interesting results on the variation of mutual diffusion coefficient of the micellar solutions with addition of salts and alcohol have been observed.

Publications

ASSA CONTROL RESPONDE RESOLUTION DECERTION (NOTES DE L'EXPLICATION DE PORTE DE PRÉSENTAINE DE PRÈSE DE L'EXPLICATION DE L'EXP

- Bratko, D., H.L. Friedman, S.-H. Chen, and L. Blum, "Intrepretation of the Intermicellar Structure Factors in the Hypernetted-chain Percus-Yevick Approximation," Phys. Rev. A 34, 2215 (1986).
- Chao, Y.S., E.Y. Sheu, and S.-H. Chen, "Experimental Test of a Theory Dressed Micelles," J. Phys. Chem. 89, 4862 (1985).
- Chao, Y.S., E.Y. Sheu, and S.-H. Chen, "Intermicellar Interactions in Lithium Dodecyl Sulfate Solutions, Effects of Divalent Ions," J. Phys. Chem. 89, 4395 (1985).
- Chen, S.-H., "Interactions and Phase Transitions in Micellar and Microemulsion Systems Studied by SANS," Physica 137B, 183 (1986).
- Chen, S.-H., "Small Angle Neutron Scattery Studies of the Structure and Interaction in Micellar and Microemulsion Systems," Ann. Rev. Phys. Chem. 37, 351 (1986).
- Chen, S.-H. and J.S. Huang, "Dynamic Slowing-down and Nonexponential Decay of Density Correlation Functions in Dense Microemulsions," Phys. Rev. Lett. 55, 1888 (1985).
- Sheu, E.Y., C.F. Wu, S.-H. Chen, and L. Blum, "Application of a Rescaled Mean Apherical Approximation to Strongly Interacting Ionic Micellar Solutions," Phys. Rev. A 32, 3807 (1985).
- Sheu, E.Y., C.F. Wu, and S.-H. Chen, "Effects of Ion Sizes on the Aggregation and Surface Change of Ionic Micelles in 1:1 Electrolytes," J. Phys. Chem. 90, 4179 (1986).

14.2 Basic Studies of Laser-Cell Interactions

Wan-Yuan Company, Beijing, Peoples Republic of China Contract

Sow-Hsin Chen, X.B. Wei, X.Y. Wang

An instrument consisting of a copper vapor laser coupled to an optical fiber/chemical injector catheter for the treatment of occluded arteries has been constructed and tested.

The combined application of three steps: the pre-irradiation injection of a light absorbing dye, HPD, brief copper laser irradiation (at 578 nm), and a urokinase infusion after the irradiation, produced the striking effect of liquification and resolution of thrombus. The histological examination of the arteries after the treatment showed no apparent damage of the arterial wall.

Publication

Wei, X.B., X.Y. Wang, and S.-H. Chen, "A Copper Vapor Laser and Optical Fiber Catheter System for Liquification and Removal of Thrombus in Occluded Arteries." Sent to Lasers in Surgery and Medicine. "Method and Apparatus for Laser Angiosurgery," to be published in 1987.



15.0 Custom Integrated Circuits

Academic and Research Staff

Prof. J. Allen, Prof. L. Glasser, Prof. B.R. Musicus, Prof. P. Penfield, Jr., Prof. J.L. Wyatt, Jr.

Graduate Students

R.C. Armstrong, D.G. Baltus, C. Bamji, L.M. Brocco, C. Hauck, H. Jeong, S.L. Lin, S.P. McCormick, K. Nabors, A. Malamy, P. O'Brien, C. Selridge, D. Standley, B. Thompson, H. Wright

15.1 Custom Integrated Circuits

U.S. Air Force - Office of Scientific Research (Grant AFOSR-86-0164)

Robert C. Armstrong, Donald G. Baltus, Cyrus Bamji, Lynne M. Brocco, Charles Hauck, Shing Lih Lin, Steven P. McCormick

The research goal of this project is to devise CAD techniques for the performance-directed synthesis of digital VLSI circuits, focused on digital signal processing applications. The main goal is to develop expert system techniques that are designed to yield optimal performance in these signal processing systems through a fundamental approach to the design task. An overall design involves the specification of multiple constraint domains corresponding to various levels of representation. These facets include the function, architecture, logic, circuit, layout, and device levels. They must be coherently related so that each is a consistent and correct projection of the complete design onto a single facet or type of representation. This viewpoint has led to three major concerns:

- 1. Appropriate representations and constraint mechanisms for each design level must be discovered and built. This task is particularly difficult for those levels that are far from the physical reality of the circuit itself.
- 2. Expert systems must be constructed to achieve optimal design. This approach depends on and affects the representational issues mentioned above.
- 3 Performance optimization must apply both within and across representational domains. Hence, it must provide both local and global optimization.

The intent in performance-directed synthesis is to avoid long synthesis phases followed by comprehensive analysis. Instead, this research aims to drastically shorten the synthesis-analysis loop, providing for both rapid generation of designs at the various levels, as well as their fast and accurate assessment by new, optimized analysis tools. The design techniques developed under this grant can be viewed as components of an overall expert system for high-performance design. Effective algorithms are combined within heuristic frameworks to capture, and even exceed, the capability of experienced and talented designers.

A major goal of high-performance design is to squeeze the corresponding layout into the smallest possible area. Under this grant, Lin and Allen¹ developed a constraint graph-based compactor that minimizes total area on each of the layout levels, subject to a designer-specified weighting factor. In addition, Reichelt² developed the necessary data representations for hierarchical compaction. A parameter specified in this representation allows the designer to compact designs hierarchically with direct control over the amount of overlap between adjacent cells. As a result, hierarchical designs can be compacted with only abbutting cells, or with overlapping cells, to the extent permitted by the design rules. This new representation is now being exploited to build a high-performance hierarchical compactor that utilizes both symbolic and direct geometric input of layouts. In this way, the compacter can be used for technology tracking and direct realization of high-performance layouts from a symbolic design representation.

The next level above symbolic layout is the circuit level of representation. Baltus³ has built a new expert system for the conversion of a circuit's net representation to an optimized layout. This strategy allows the user to deal selectively with varying aspect ratios, constraints due to input/output pins, constraints imposed by different circuit styles, and the difficulties introduced when widely varying device sizes (due to speed optimizations) are utilized. High-quality layouts have already been obtained in both NMOS and CMOS for many different circuit macros, and effective packing is obtained by introducing groups of transistors according to similar sizes rather than their structural affinity in the original design. This new level of representation has proven very useful, and serves as an appropriate interface to the symbolic compactor mentioned above to yield final layout.

The creation of an effective floor plan, or global placement of modules in a minimal area that allows optimal interconnect in terms of both length and time delay, has been achieved by S. Weiner.⁴ This program dynamically chooses and switches between several floor planning strategies using problem-specific facts as a guide. This has been an exceedingly good area for expert systems, since no single strategy is uniformly optimal, and since it is possible to characterize the floor plan problem at a representational level that can be effectively exploited to choose the best strategy.

In order to complement the Regular Structure Generator⁵ previously developed under this grant, L. Brocco⁶ has developed a new program for the estimation of delay through circuit blocks in a VLSI design. This program achieves accuracy within 5% of SPICE for generalized inverter-type structures in CMOS. Using abstract, functionally based macro models that permit the introduction of nonlinearities (which are essential for high-accuracy modeling), transmission gate circuits have been analyzed effectively with errors well below 10% of the corresponding SPICE results. This is the first time that transmission gate circuits (which are characterized by two distinct time constants) have been adequately modelled for delay purposes in a unified manner with inverter-like circuits. Not only are the delays obtained accurately, but the computational time is approximately 0.001 of the magnitude of SPICE runs for circuits as complex as array multipliers. This program permits the rapid assessment and exploration of design alternatives, and, hence, makes performance-directed synthesis a viable design option for a wide class of high-performance applications.

In a major new development, formal grammars have been introduced to permit the formal unification of several different levels of design representation. For example, context-free grammars are used for circuit-level representations, and regular grammars

are used for layout. A context-free grammar has been demonstrated that readily generates and accepts all classical CMOS circuits. C. Bamji has developed a new technique to elaborate all legitimate designs, subject to a user-specified set of input constraints, which can be examined in a design exploration phase. The individual grammars for each level of design representation are unified by a coupling grammar which pulls together the separate grammars. It is important to note that these grammars can generate all legitimate representational couplings, and can be used with a parser to analyze conjoined representational descriptions of designs for correctness.

Formal grammars can also be utilized as the fundamental data objects for design editing, in order to maintain "alignment" between the various levels of representation. When a designer edits one level of representation (e. g., layout), changes must be automatically propagated to the corresponding effects at other levels of representation (e. g., circuit or logic). Since the formal grammars for these levels of representation can be coupled as previously mentioned, R. Amstrong has developed a new mechanism that provides a strong linguistic base for all design editing, regardless of the "design facet" being changed. The two projects cited that utilize formal grammars provide a new basis for design representation and manipulation which can be used as an extendable kernel, around which the various performance-directed algorithms can be attached.

All of these CAD programs are being developed in the context of high-performance 68020-based workstations with high-resolution color displays, a minimum of 8 megabytes of memory, local area network connections, a minimum of a 130 megabytes of disk storage, utilization of the UNIX operating system, and the provision of the x-windows display system. This computational environment, coupled with the performance-directed synthesis tools described here, leads to higher levels of capability in the correct, quick, and economical generation of high-performance VLSI designs.

References

- ¹ S. Lin and J. Allen, "MINPLEX -- A Compactor that Minimizes the Bounding Rectangle and the Individual Rectangles in a Layout," Proceedings of the 23rd Design Automation Conference, July 1986, p. 123.
- ² M. Reichelt and W. Wolf, "An Improved Cell Model for Hierarchical Constraint-Graph Compaction." Proceedings of the International Conference on Computer-Aided Design, November 1986, p. 482.
- ³ D.G. Baltus, "Generating Efficient Layouts from Optimized MOS Circuit Schematics." M.S. Thesis, Dept. of Electr. Eng. and Comp. Sci., M.I.T., Cambridge, Mass., 1987.
- ⁴ S.S. Weiner, "APRICOT: A Priority-Conscious Tool for VLSI Floorplanning," M.S. thesis, Dept. of Electr. Eng. and Comp. Sci., M.I.T., Cambridge, Mass., 1987.
- ⁵ C.S. Bamji, C.E. Hauck, and J. Allen, "A Design-by-Example Regular Structure Generator," Proceedings of the 22nd Design Automation Conference, June 1985, p. 16.
- ⁶ L.M. Brocco, "Macromodelling CMOS Circuits for Timing Simulation," M.S. Thesis, Dept. of Electr. Eng. and Comp. Sci., M.I.T., Cambridge, Mass., 1987, R.L.E. Tech. Report No. 529.

15.2 High Performance Circuit Design

Lance A. Glasser, A. Malamy, C. Selridge, B. Thompson

This year significant progress was made in the three complementary areas of theory, experiment, and computer-aided design (CAD).

Theoretical progress was made in the classical area of linear circuit analysis. Tight bounds on the highest natural frequency of oscillation of circuits composed of linear devices have been derived. A catalog analogy best describes the work. Given a linear model of each type of element in a catalog, we can predict exactly the highest frequency of oscillation of any network built of any number of these elements, taken in any multiplicity (one can order as many parts from the catalog as one wants), impedance scaled by any positive real number (if the catalog has a 10 Ohm resistor one can order 100 and 2 Ohm resistors), and connected together with ideal wire and ideal transformers. This work has application to device and circuit design.

In the experimental area, we have successfully demonstrated the transmission of power to integrated circuits without pins. We have used magnetic coupling and on-chip inductors and rectifiers to couple several hundred microwatts of power at several volts--enough power to drive low power CMOS circuits. This work has potential application to smart credit cards and biomedical implants.

In the CAD area, progress has been made on two programs. We have a working program to discover the maximum frequency of oscillation of complex linear circuits, as discussed above. This program is written in LISP. We have also continued our work on RELIC, a unique reliability simulator for integrated circuits. This program enables the simultaneous simulation of several different reliability mechanism for VLSI circuits.

15.3 Extracting Masks from Optical Images of VLSI Chips

Bruce R. Musicus, Hong Jeong, Rosalind Wright

One of the chief dificulties in studying image modeling and image understanding is that it is difficult to find useful models to aid in interpreting unconstrained images. In order to better understand the role of image modelling, we are therefore concentrating on the particular problem of "reverse-engineering" a VLSI chip given a microphotograph of the chip. An enormous amount of information is available concerning the design of VLSI chips; they are deposited in layers of known composition and optical appearance, the images are formed from strips of material delineated by clear, though ragged, boundaries, the strips must form electrical circuits with known characteristics. Given all this a priori information, including knowledge of minimum line and feature widths as well as rules about the composition of layers making up the chip, our goal is to build an efficient analysis system for reconstructing the masks that were used to manufacture the chip.

Our initial work in this area focused on low level image processing issues, such as compensating for improper focusing, imbalanced lighting, and texture, while trying to accurately segment the image into line strips. It was found that "local" analysis meth-

the personal resolution felicities sections describes

ods, analyzing small windows to decide if they contained an edge or not, worked reasonably well and were relatively insensitive to lighting and texture fluctuations.

Our latest work is to address the back end of the analysis system. Given a clean line drawing representing a section of the VLSI chip, how do we piece together the various strips into the masks that formed the chip? At present we are developing various algorithms which deduce all possible legal interpretations of a given line drawing using only information about the edges. Using a database of rules of VLSI design, the programs start with edges and vertices, piece together "paths" marking the edges of strip in some mask, assign the paths to layers, and label the layers. The most difficult part is to correctly infer where mask strips cross over each other, and to properly interpret "accidental edges," where several strip edges coincide in the image.

Publications

Jeong, H., Ph.D. Diss., M.I.T., Cambridge, Mass., expected 1987.

Jeong, H. and B. Musicus, "Mask Extraction from Optical Images of VLSI Circuits," I.E.E.E. International Conference on Acoustics, Speech, and Signal Processing, Dallas, Texas, April 1987.

Wright, R., "Highly Distributed Image Understanding Algorithms Applied to Segmentation of VLSI Images," S.M. Thesis, M.I.T., Cambridge, Mass., 1986.

15.4 Algorithmic Fault Tolerance on Digital Signal Processing

Bruce R. Musicus, William Song

Information theory suggests a specific strategy for communicating information reliably across a noisy channel. Using a model of the noise process in the channel, a coder spreads the information in the signal across the channel bandwidth in such a way that a noise spike may destroy part of many bits, but not an entire bit. The decoder at the receiving end uses redundant information transmitted down the channel to reconstruct the entire message without error. Careful coding allows systems to achieve nearly 100% correct information transfer with only modest overhead for the coding.

Unfortunately, coding ideas do not always translate well into fault-tolerant computer architectures. Some computer modules, such as memory, buses, or networks, are easily protected against transient or permanent part failures by error-coding techniques. These applications, however, are restricted to modules which do not modify the data. Computational modules are not easily protected by error-coding techniques. Instead, conventional approaches for building fault-tolerant processors rely on duplicating, triplicating, or quadruplicating all computational resources, and voting on information transferred across module boundaries in order to discard bad results.

In this project, we are developing a new approach to fault tolerance, in which we can protect certain types of linear computation against processor failure. The basic strategy can be applied when the same computation is applied to many different data items, and when an error coding computation can be found which commutes with the

processing computation. The "coder" distributes data to various independent processors, and also computes various functions of the input data to form inputs for some redundant processors. The "decoder" verifies that the output of the redundant processors is consistent with the output of the other processors; if not, it then isolates which processor (s) have failed, and corrects them (if possible).

One application of this idea uses a bank of analog-to-digital converters operating in round-robin fashion to achieve an overall sampling rate somewhat above the Nyquist rate for the signal. A dither system and digital low-pass filter combine to reduce quantization errors in the front end. This same low-pass, however, can be used to detect and interpolate over temporary or permanent errors in any of the converters, without substantially increasing the total amount of computation. The system is able to trade off additional hardware for greater accuracy and higher levels of fault protection. As converters fail, all that happens is that the effective quantization error increases.

Another application is to the FFT processor system used in range and velocity doppler sonar processing. Here we use a set of processors to process multiple scans of sonar data from a phased-array antenna. Each processor does the same linear FFT processing, but on different sets of range cells. Adding extra processors working on linear combinations of the inputs to the other processors allows simple fault detection and correction. Regardless of the number of processors in the system, detecting K simultaneous failures requires only extra processors; detecting and correcting K simultaneous failures requires only 2K extra processors. When conventional truncation or rounding arithmetic is used, however, then the error checking can only be approximate. In this case, adding more processors improves the accuracy of the fault checking and correction. We are presently working with Draper Labs on the design of a sonar system incorporating these concepts.

15.5 Cellular Array for Image Processing

Bruce R. Musicus, G.N. Srinivassa Prasanna, Hong Jeong, Andrew Fraley, Mitchell Oslick, Edward Schembor, John Deroo, Kevin O'Connor

Low level image processing operations, such as contrast stretching, compensation for lighting variation, noise suppression, or edge enhancement, often rely on highly repetitive processing of the pixels in the image. In conventional image processing architectures, this characteristic is exploited by pipelining the image data through a computational pipeline which repeatedly executes the same instruction on all the data flowing through it. An alternative approach, which we are exploring, is to build a large number of small processors, and use these processors in parallel to execute the same instructions on different parts of the image. The Connection Machine is the best known commercial implementation of this architectural idea. Our goal is to explore much simpler and cheaper implementations, which may be carefully matched to the algorithmic domain in order to achieve high performance at low cost.

To explore hardware, software, and algorithmic issues involved in this approach, we are building a small 16 by 16 array of 256 single-bit processors, packaged on 2 VME boards with data memory, a horizontally microcoded sequencer, and a host interface. Combined with a frame grabber and a 68000 controller card, we will have a very high performance machine capable of extremely high speed computation for a particular

class of signal processing problems. The array is built from four AAP chips from OKI Semiconductor, and operates at a 6.5 MHz rate, performing 256 bit-operations on every clock tick. Both bit-serial and bit-parallel arithmetic are supported. Data memory is specially designed to supply overlapping frames of bit-serial or bit parallel data to the processor array. The machine is programmed with a micro-assembler with high-level control constructs and expression evaluation. Various algorithms for low level image processing and matrix arithmetic are under development.

15.6 Waveform Bounding for Fast Timing Analysis of Digital VLSI Circuits

U.S. Navy - Office of Nava! Research (Contract N00014-80-C-0622) National Science Foundation (Grant ECS-83-10941)

John L. Wyatt, Jr., Paul Penfield, Jr., Lance A. Glasser, Keith Nabors, David Standley, Peter O'Brien, Desmond Kirkpatrick

Our work over the last year has been concentrated on reworking the waveform bounding results of Penfield, et al., originally created for timing analysis of MOS chips, into a form useful for delay estimation in ECL circuits. A smaller effort has also been devoted to the circuit design and layout of a parallel analog MOS VLSI chip for early vision applications.

Peter O'Brien has continued to work on ECL delay estimation for his S.M. thesis, in cooperation with Digital Equipment Corporation. The final product we envision is a timing analyzer, written in C, for use on ECL standard cell designs. The goal remains: accurate estimation of signal propagation delay without resorting to computationally intensive numerical solution of the network equations. In apparent contrast to the earlier MOS-related work, the largest technical problem we've encountered is not estimating signal delay in interconnect, but rather accurately modeling the electrical behavior of the gates themselves. The ECL gates we've studied act like voltage sources with internal resistance when pulling a line high, but like almost ideal current sources when pulling it low. The latter case does not fit easily into the framework of the Penfield approach, which is tailored to voltage-source drives.

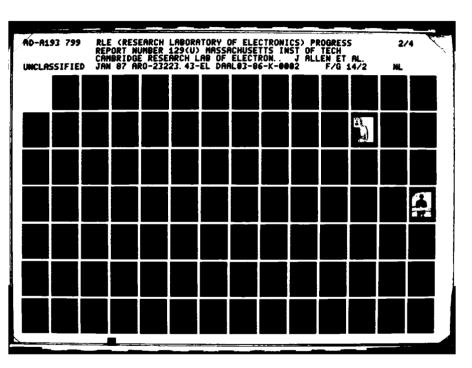
Our modeling progress to date consists of a reasonably simple macromodel for the gates themselves, and an approximation to the driving-point impedance of loaded, branched metal interconnect lines that lets us translate a current- source drive into an approximate resulting voltage waveform at the output of the driving gate. This combined procedure gives delay results that agree with detailed SPICE simulations to around 4%, with a savings of about three orders of magnitude in computer time. The only fundamental hurdle remaining is to find a simple but accurate way of approximating the voltage waveform at the input of any driven gate by a simplified waveform, such as a saturated ramp, that permits closed-form calculation of the gate macromodel's response.

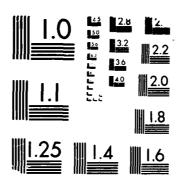
Our other project, design of the analog depth-interpolation chip, has progressed to the point that we expect to send the first test chip to MOSIS in November. This design contains a 4x4 pixel array that is directly accessible from the pins, and test structures

with each of the subcircuits needed for the final system, e.g., A/D and D/A converters and differential amplifiers. We'll tell you how it worked in the next progress report.

Publications

- Kirkpatrick, D., "Numerical Solution of the RC Mesh," S.B. Thesis, Dept. of Electr. Eng. and Comp. Sci., M.I.T., Cambridge, Mass., 1986.
- O'Brien, P.R. and J.L. Wyatt, Jr., "Signal Delay in ECL Interconnect," in Proceedings of the 1986 International Symposium on Circuits and Systems, Santa Clara, Calif., May 1986, p. 755; (M.I.T. VLSI Memo No. 86-296).
- Standley, D. and J.L. Wyatt, Jr., "Improved Signal Delay Bounds for RC Tree Networks," M.I.T. VLSI Memo No. 86-317, May 1986.
- Wyatt, J.L., Jr., C.A. Zukowski and P. Penfield, Jr., "Step Response Bounds for Large-Scale Linear Systems Described by M-Matrices, with VLSI Application," SIAM Conference on Linear Algebra in Signals, Systems and Control, Boston, Mass., 1986; abstract appeared on p. A35 of Conference program.
- Zippel, R.E., P. Penfield, Jr., L.A. Glasser, C.A. Leiserson, J.L. Wyatt, Jr., F. T. Leighton, and J. Allen, "Recent Results in VLSI CAD at M.I.T.," to appear in Proceedings of the Fall Joint Computer Conference, Dallas, Texas, November 1986; M.I.T. VLSI Memo No. 86-341.





16.0 Speech Communication

Academic and Research Staff

Graduate Students

A. Alwan, M. Anderson, C. Bickley, N. Daly, S. Dubois, C. Espy-Wilson, J. Glass, C. Huang, R. Kassel, L. Lamel, H. Leung, L. Pastel, J. Pitrelli, M. Randolph, T. Wilson

C.J. Lebel Fellowship

National Institutes of Health (Grants 5 T32 NS07040 and 5 R01 NS04332)

National Science Foundation (Grant 1ST 80-17599)

U.S. Navy - Naval Electronic Systems Command Contracts (N00039-85-C-0254, N00039-85-C-0341, N00039-85-C-0290)

16.1 Studies of the Acoustics and Perception of Speech Sounds

16.1.1 Stop and Fricative Consonants

Several studies of the production, acoustics, and perception of stop and fricative consonants are in progress. The aim of these studies is to specify the articulatory and

Staff Member, Kurtzweil Applied Intelligence

² Visiting Scientist

³ Assistant Professor, Department of Speech Disorders, Boston University

⁴ Research Scientist, Department of Speech Disorders, Boston University

⁵ Staff Member, Voice Processing Corporation

⁶ Staff Member Kurtzweil Applied Intelligence

⁷ Director, Neurolinguistics Laboratory, Massachusetts General Hospital, Institute of Health Professions

⁸ Professor of Special Education, Boston University

⁹ Associate Professor, Department of Psychology, Northeastern University

¹⁰ Visiting Scientist

¹¹ Staff Member, Bolt, Beranek and Newman, Inc.

¹² Visiting Scientist

acoustic correlates of the features that distinguish between aspirated and unaspirated consonants, between consonants produced with different places of articulation along the vocal tract, and between voiced and voiceless cognates of these consonants. These consonants have the common property that their production involves the generation of turbulence noise at some region along the vocal tract. The sound that is radiated from the lips is dependent on the properties of the turbulence noise source in the vicinity of the constriction and on the filtering imposed on this source by the vocal-tract shape.

In one set of experiments we are examining the mechanism of production of sound when turbulence is generated in the airflow through a constriction in a tube. The dimensions of this mechanical model are selected to simulate some aspects of the vocal tract during the production of fricative consonants. We are extending the results of previous experiments by investigating a variety of configurations and orientations of the constriction and of an obstacle downstream from the constriction in order to be able to predict more precisely the location, amplitude, and spectrum of the turbulence noise source for different vocal-tract configurations. One outcome of these experiments is that the source is often distributed through a region that extends several centimeters along the vocal tract, and that there are variations in the spectrum for the components of the source located at different places within the region.

Another set of experiments consists of acoustic and perceptual studies of aspiration, i.e., the sound produced in the vicinity of the glottis when the glottis is spread. One finding is that the onset of voicing following an interval of aspiration shows an enhancement of the low-frequency spectrum amplitude, similar to that for breathy vowels. Preliminary perceptual experiments indicate that this characteristic of the onset of voicing influences listener judgements of the distinction between aspirated and unaspirated consonants in English.

In other experiments we have been looking at the acoustic and perceptual attributes that distinguish velar consonants from alveolars and labials. In terms of distinctive feature theory, we are examining the acoustic and perceptual correlates of the feature of compactness, or, equivalently, the feature of anteriority as commonly used in phonology. The findings indicate that compact consonants require a spectral prominence in the midfrequency range that matches approximately in frequency and amplitude to the prominence formed by the second or third formant in an adjacent vowel.

Finally, we are carrying out theoretical and experimental studies to determine the acoustic correlates of voicing for stop and fricative consonants. The theoretical analysis suggests that the initiation of voicing in these consonants requires careful coordination and control of articulatory and laryngeal movements, and that simultaneous generation of voicing and strong turbulence noise for stops and fricatives is somewhat incompatible. We are beginning the collection of acoustic data that we will attempt to interpret in terms of the theoretical model.

16.1.2 Vowel Perception

We are carrying out several experiments that are attempting to elucidate the mechanisms whereby human listeners process vowel sounds. Some current experiments are investigating: 1) the perceptual interpretation of spectral details in the vicinity of the

CANCERD - TOTAL STATES AND ACCORDED TO CONTRACT

first formant; 2) the perceptual interpretation of two closely-spaced spectral prominences.

The perceptual interpretation of spectral details in the vicinity of the first formant (F1) remains an important unresolved research topic. Aspects of the spectrum below 1000 Hz are thought to signal: 1) tongue height, as implied by the location of the first formant frequency; 2) the distinction between oral and nasalized sounds; and 3) the contrast between normal and breathy phonation. Confounding the disentanglement of these factors is: 1) variation in the fundamental frequency of the voice (a high fundamental frequency implies that relatively few harmonic samples are available as cues to deduce the shape of the vocal-tract transfer function); 2) variation in the source spectrum due to changes in glottal state (the relative amplitudes of harmonics are affected by the rapidity of glottal closure and other details of the vibration pattern); 3) presence of tracheal resonances when the glottis is sufficiently open; and 4) source-tract interactions such as an increase in first formant bandwidth during the open phase of a period for low vowels. Research on these issues has focused on the perceptual location of the first formant frequency as fundamental frequency varies. Using carefully designed synthetic speech stimuli, it has been shown that the listener is able to recover the "true" location of F1 in spite of harmonic/formant interactions that are such as to fool linear prediction and other energy-based methods of formant estimation. It is not easy to explain this behavior in terms of peripheral mechanisms of audition because individual harmonics are resolved under the stimulus conditions studied. Accounting for the perceptual data in terms of simple processing strategies is not yet possible, but if the central auditory system is provided with the frequencies and amplitudes of harmonics near (F1), a moderately complex calculation could yield (F1) with minimal error.

The experiments concerned with the perceptual interpretation of closely spaced spectral prominences involve the matching of single-formant synthetic vowels against multiformant vowels with various formant locations. The results are in general agreement with previous work, which shows the match of a single formant to a vowel with two closely spaced formants tends to be located at an effective "center of gravity" of the two formants, but the conditions under which this behavior occurs are somewhat different from earlier findings. For example, for high back vowels, matching tends to be to the first formant frequency, whereas for nonhigh back vowels, the matching is intermediate between the first and second formant frequencies. The data also suggest that there is a rather abrupt shift in matching behavior as the formant pattern for the target vowel crosses a boundary between back and front vowels.

16.1.3 Analysis of a Female Voice

Waveforms and spectra of a set of speech materials collected from a single female speaker have been studied. This pilot effort, an attempt to determine some of the acoustic characteristics that differentiate male and female voices, may lead to improved synthesis of female voices.

Data have been examined on breathy onsets, breathy offsets, glottalized onsets, glottalized offsets, and vowel spectra over extended intervals involving large changes to fundamental frequency. Harmonic spectra reveal a significant breathy (noise) component in the mid and high-frequency region of the spectrum. Locations of spectral zeros are consistent with inferences that the open quotient remains at about 50% over

much of the data, but decreases for glottalized sounds and increases in the vicinity of a voiceless consonant or breathy offset. Turbulence spectra for [h], measured with a long-duration window to minimize statistical variation, indicate the presence of extra poles and zeros at relatively fixed locations across vowels. These probably reflect acoustic coupling to tracheal resonances. Glottal attacks are often accompanied by a brief interval of turbulence noise - presumably a manifestation of pharyngeal frication.

16.1.4 Alternative Analysis Procedures

Theoretical and experimental studies of the acoustic properties at the release of stop and nasal consonants show that rapid spectral changes occurring over time intervals of a few milliseconds can carry information about some of the features of these consonants. Conventional spectral analysis tools are often unable to resolve some of the details of these rapid changes. We have been exploring whether application of the Wigner distribution to these signals can provide insight into acoustic attributes at the consonant release that are not well represented by conventional methods. Procedures for calculating and displaying the Wigner distribution have been implemented, and comparisons between this representation and other spectrographic representations for a variety of speech and speechlike sounds are being made.

16.1.5 Children's Speech

Studies of the properties of the speech of children in the age range of one to three years old show substantial differences from the speech of adults. Some of these differences can be attributed to differences in dimensions and configurations of airways and mechanical structures of the larynx and vocal tract, and to differences in motor control capabilities. We are examining how these differences impose constraints on the sounds produced by children. Among the topics being studied through theoretical analysis and through acoustic measurements are: 1) the influence of the reduced dimensions of the airways on the spectral characteristics of children's utterances; 2) the effect of the substantial differences in dimensions of the laryngeal structures on vocal-fold vibration; and 3) the constraints imposed on temporal properties of children's speech by their reduced respiratory dimensions and ranges and their ability to control and coordinate rapid movements of articulatory and other structures.

16.2 Speech Recognition

The overall objectives of our research in machine recognition of speech are:

- to carry out research aimed at collecting, quantifying, and organizing acoustic-phonetic knowledge, and;
- 2. to develop techniques for incorporating such knowledge, as well as other relevant linguistic knowledge, into speech recognition systems.

During the past year, progress has been made on several projects related to these broad objectives.

16.2.1 Signal Representation for Acoustic Segmentation

The task of phonetic recognition can be stated broadly as the determination of the mapping of the acoustic signal to a set of phonological units (e.g., distinctive feature bundles, phonemes, or syllables) used to represent the lexicon. In order to perform such a mapping, it is often desirable to first transform the *continuous* speech signal into a *discrete* set of acoustic segments. During the past year, we have explored a number of alternative acoustic segmentation algorithms, and have compared the results based on several signal representations.

The objective of the segmentation algorithm is to establish stable acoustic regions for further phonetic analysis. One of the more promising segmentation algorithms adopts the strategy of measuring the similarity of a given spectral frame to its immediate neighbors. The algorithm moves on a frame-by-frame basis, from left to right, and attempts to associate a given frame with its immediate past or future, subject to a similarity measure. Acoustic boundaries are marked whenever the spectral vector changes affiliation from past to future. The algorithm makes use of the fact that certain acoustic changes are more significant than others and that the criteria for boundary detection often change as a function of context. It can self-adapt to capture short regions that are acoustically distinct. In addition, the algorithm's *sensitivity* to acoustic changes can also be controlled so that the resulting acoustic description can be as broad or as detailed as is desired.

Using this acoustic segmentation algorithm, we performed a set of experiments exploring the relative merits of five different spectral representations for acoustic segmentation. The five spectral representations are as follows:

- 1. Wideband: The spectral vector is obtained by applying a 6.7-ms Hamming window to the speech waveform.
- 2. **Smoothed narrowband**: The spectral vector is obtained by applying a 25.6-ms Hamming window to the speech waveform, followed by smoothing with a 3-ms window in the cepstral domain.
- 3. **LPC**: The spectral vector is obtained from a 19th-order LPC analysis on a 25.6-ms segment of speech.
- 4. Critical band: The spectral vector is obtained from the first stage of an auditory model and represents the outputs of a bank of critical-band filters.
- 5. Hair cell: The spectral vector is obtained from intermediate outputs of the same auditory model and represents the outputs of the hair-cell/synapse transduction stage. The envelope response of the filter outputs corresponds to the mean-rate response of neural firing.

For each spectral representation, a 39-dimensional spectral vector is computed once every 5 ms. The array of spectral vectors is the only information used for acoustic segmentation. To evaluate the effectiveness of the spectral representations for acoustic segmentation, the sentences are transcribed phonetically and the transcriptions are time-aligned with acoustic landmarks. For each experiment, the output of the acoustic segmentation is compared with the hand transcription, and the numbers of extra and missed boundaries (insertions and deletions) are tabulated. By adjusting the sensitivity

parameters, one can bias the algorithm to favor segment insertion or deletion. Using a database of 1,000 sentences spoken by 100 talkers, we tested each spectral representation in more than 24 experiments covering a wide range of insertion and deletion errors. The "best" result for each spectral representation was defined to be the one that minimizes the *sum* of the number of inserted and deleted segments. A comparison of the results shows that the hair-cell spectral representation is superior (with the lowest total insertion and deletion rate - 25%), followed closely by the critical-band and LPC representations. These representations were consistently better than the discrete Fourier transform representations, by 3% to 4% on average. We view the results as lending support to the speculation that signal representation based on auditory modeling can potentially benefit phonetic recognition.

16.2.2 Acoustic Evidence for the Syllable as a Phonological Unit

Phonetic recognition is difficult partly because the contextual variations of the acoustic properties of speech sounds are still poorly understood. Traditionally, such systematic variations have been described in the form of context-sensitive rules. More recently, it has been suggested that rules that make reference only to the local phonemic environment may be inadequate for describing allophonic variations. Instead, one may have to utilize larger phonological units such as the syllable in order to describe such regularities. While evidence in support of the syllable as a relevant unit in the formulation of acoustic-phonetic rules has come from diverse sources, direct acoustic evidence of its existence has been scarce. During the past year, we have conducted a durational study of stop consonants, with the goal of determining the possible role of syllable structure on their realizations.

Our database consisted of some 5,200 stops collected from 1,000 sentences. Phonemic transcriptions, including lexical stress and syllable markers, were provided and aligned with the speech waveforms. The stops were categorized according to their position within syllables (e.g., syllable-initial-singleton, syllable-final-affix, etc.) and marked according to their local phonemic context. Segment durations were measured and the stops were classified as released, unreleased, or deleted on the basis of their duration and voice onset time (VOT). In the analysis of these data, including the examination of VOT and other durational measurements, we found substantial effects due to syllable structure. For example, the probability of a stop being released, unreleased, or deleted is largely determined by its position in a syllable template. Even if released, the distributions of the VOT differ substantially depending again on the position of the stop within a syllable.

Our plans are to continue these experiments by completing our investigation of the stop consonants and expanding to other classes of sounds. Eventually we would like to develop a computational framework that incorporates contextual knowledge in phonemic decoding.

16.3 Speech Synthesis

An extensive manuscript reviewing text-to-speech conversion for English has been submitted and accepted for publication in the Journal of the Acoustical Society of America. The paper traces the history of research, the nature of the scientific problems,

some solutions developed for the Klattalk system (a text-to-speech system developed at MIT several years ago), and areas where future research is needed. A companion tape recording provides examples of 30 milestones in the development of synthesis capabilities.

16.4 Speech Planning

We have continued our study of the phonological planning process for speech production using speech error analysis as a tool, and have expanded the scope of this investigation to include the analysis of acoustic phonetic correlates of lexical and phrasal stress or prominence.

16.4.1 Error Studies

Earlier work has shown that when single-consonant speech errors occur, they are more strongly influenced by shared word position than by shared stress or syllable position. Word-onset consonants are particularly susceptible to interaction errors, as in "sissle theeds" for "thistle seeds." Patterns of errors elicited by tongue twisters like "parade fad foot parole" and "repair fad foot repeat" confirm this finding, for both word-list and phrasal stimuli. We are currently extending the elicitation experiments to determine: 1) whether an earlier finding that phrasal stimuli protect word-final consonants against errors is due to the syntactic or prosodic structure of the phrases, or to some interaction between these two effects; 2) whether the similarity of adjacent vowels influences the probability that two consonants will interact (i.e., will there be more /t/-/k/ errors for "tan cats" than for "ten kits"); and 3) whether different types of single-segment errors are governed by different constraints and therefore can be presumed to occur at different points during the planning process (e.g., exchanges like "boting vooths" for "voting booths" appear to be more sharply limited to word-onset positions than do anticipatory substitutions like "boting booths."

16.4.2 Prosody Studies

The phenomenon of Stress Shift has been described as the leftward movement of lexical stress near the end of a polysyllabic word, to prevent stress clash with the following word. For example, missisSIPpi become MISsissippi MUD, for some speakers, and siaMESE becomes Slamese CATS. In the early stages of a study designed to determine what proportion of speakers shift their stress, when they do so, and what the acoustic correlates are, it has become clear that the data suggest quite different hypotheses about the nature of this apparent shift. While the study is still in progress, we can state these hypotheses as follows: 1) the large pitch change that has sometimes been associated with lexical stress in the literature is in fact associated with phrasal prominence instead; 2) Stress Shift is what occurs when phrasal prominence is not placed on a content word, and reflects the lack of a large pitch change on the lexically-stressed syllable (rather than an actual shift in the location of that pitch change to an earlier syllable, as sometimes claimed); and 3) failure to place the phrasal pitch change on the lexically stressed syllable of a word occurs in environments where there is NO stressed word following, for many speakers. (For example, the syllable "-ra-" may have no substantial pitch rise in "TRANSport operations"; similarly, there may be no substantial pitch rise on any of the syllables in "mississippi mud" in the utterance "But

I HATE mississippi mud.") These observations cast some doubt on the hypothesis that Stress Shift occurs to prevent stress clash with a following syllable.

Taken together, these initial formulations suggest that the survey of acoustic-phonetic correlates of lexical and phrasal prominence now under way may reveal distinctions between these two kinds of prosodic phenomena. These distinctions will be useful in evaluating models of the production planning process.

16.4.3 Cross-Language Studies

For both the speech error and prosody studies, we are beginning to extend our investigations into other languages, in a series of collaborative studies.

16.5 Physiology of Speech Production

16.5.1 Articulatory Movement Transduction

Work has been completed on an alternating magnetic field system for transducing midsagittal-plane movements of the tongue, lips, mandible and velum. consists of two transmitter coils mounted in an assembly that fits on the head and a number of bi-axial transducer-receiver coils that are mounted on articulatory structures, with fine lead wires that connect to receiver electronics. Output voltages from each receiver are digitized and converted to Cartesian coordinates using algorithms implemented with the MITSYN signal processing languages. The system was tested extensively and was found to meet design specifications. It tracks as many as 9 points (2 fixed---for a maxillary frame of reference-and 7 movable) with a resolution of better than .5 mm at a bandwidth from DC to 100 Hz. This performance is maintained: in the presence of dental fillings, up to 30 degrees of transducer tilt, several degrees of transducer "twist" and with off-midsagittal plane transducer placements of up to .5 cm. Three experiments have been run with human subjects, demonstrating that the system can be used to gather extensive data on articulatory movements. This work is reported in R.L.E. Technical Report No. 512.

The system does have several disadvantages which make it cumbersome to use; therefore, before embarking on an extensive series of experiments, we are exploring an alternative, theoretically advantageous three-transmitter design. Prior testing of a three-transmitter system had shown it to be less accurate than the-two transmitter system, most likely because of asymmetries in the magnetic fields generated by the transmitters. The field geometry of the original transmitters has now been explored in detail, documenting its asymmetrical nature. A computer simulation of the three-transmitter system has been implemented, allowing us to optimize the system design. The behavior of the simulation suggests that with symmetrical fields, the three-transmitter system would equal the performance of the two-transmitter system, with much greater ease of A transmitter which should generate symmetrical fields has been designed and use. is under construction. A modest amount of further testing will enable us to choose between the two systems, allowing us to begin extensive data gathering in the near future.

16.5.2 Data Processing

Two Digital Equipment Corporation VAX Station engineering workstations have been acquired for physiological data processing and analysis. Peripherals are being acquired for multichannel A/D and D/A conversion, data storage and graphical hard copy. An updated version of the MITSYN signal processing languages is being implemented (under subcontract) for the VMS operating system, and software for graphical and statistical analysis of data is on order. This new facility will make it possible to efficiently digitize and analyze the large number of channels of data generated by the alternating magnetic field movement transducer system.

16.5.3 Token-to-Token Variation of Tongue-Body Vowel Targets, Coarticulation and Articulatory-to-Acoustic Relationships

Using the new alternating magnetic field movement transducer system, we have examined token-to-token variation of vowel targets for a midsagittal point on the tongue body of a single speaker of American English. The subject pronounced multiple repetitions of nonsense utterances of the form /bV1CV2b /, in which V = /i/, u/, /a/ and C = /b/, /h/, with stress on the second syllable. For each vowel (V1 and V2) in each environment, a scatter plot of articulatory "target" locations (at the time of minimum tangential velocity) in the midsagittal plane was generated from all tokens having the same context. In general, the vowel-target distribution for multiple repetitions of the same utterance is elongated. When V1 and V2 are different from one another, the long axis of the distribution for one vowel in the utterance points toward the location of the target for the other vowel, providing a "statistically-based" demonstration of context-dependence of articulatory targets. When V1 = V2 the long axis is approximately parallel to the vocal tract midline at the place of maximum constriction for the vowel, suggesting that movement to the vowel target location is sensitive to the differential effects on vowel acoustics of change in degree of constriction vs. change in constriction location.

16.5.4 Anticipatory Coarticulation: Studies of Lip Protrusion

Work has continued on testing a "hybrid model of anticipatory coarticulation" in which gesture onset times and spatial characteristics are context-dependent, and there is "co-production", i.e., overlapping and summation of multiple influences on articulatory trajectories (see R.L.E. Progress Report No. 128). Lip protrusion movements and the acoustic signal for the vowel /u/ (embedded in carrier phrases) have been recorded from four speakers of American English, and plots have been generated in which movement events for multiple individual tokens can be examined in relation to interactively-determined times of acoustic events (sound segment boundaries). Initial qualitative examination of trajectories indicates a considerable amount of token-totoken variation in lip protrusion movements for most utterances. Movement event times and durations of various articulatory and acoustic intervals are currently being analyzed statistically to test the hybrid model.

SYNDYN REFERE SSSSY BESTER RESSSY FRE

17.0 Linguistics

Academic and Research Staff

Prof. M. Halle, Prof. N.A. Chomsky

The work of the Linguistics group is directed towards obtaining a better grasp of the mental capacities of human beings through the study of the nature, acquisition and use of language. Language is a uniquely human faculty in that only humans appear to be capable of learning and using a language and that every normal human acquires knowledge of one or more languages during his/her lifetime. This knowledge is represented somehow in the speaker's mind, which is a special organ located in the human brain. Viewed from this vantage point, the central issues of linguistics research are:

- 1. What is the nature of this knowledge? What do speakers of a particular language Lattvian, Spanish or Walpiri know, and how does knowledge of one language differ from and resemble that of some other language?
- 2. How do speakers acquire this knowledge?
- 3. How do speakers put this knowledge to use in producing and understanding utterances?
- 4. What are the physiological mechanisms that provide the material basis for the storage, acquisition and utilization of linguistic knowledge?

There are considerable differences in our ability to answer these questions. It would seem that at resent we have advanced more with regard to question 1 and least with question 4. These differences are also reflected in the research conducted by the group. At this time, it is most heavily concentrated on issues concerned with the nature of the knowledge that characterizes fluent speakers of various languages. Yet the other three questions have not been overlooked, and significant efforts are being devoted to their solution.

The study of these topics is being carried out along a number of parallel lines. On the one hand, linguists have investigated the principles by means of which words are concantenated to form meaningful sentences. These principles have been the primary domain of inquiry of the disciplines of syntax and semantics. Phonology studies the sound structure of words while morphology examines the manner in which different languages combine different meaning-bearing units (specifically, stems, prefixes, suffixes and infixes) to form words. The latter topic has attracted increasing interest in recent years and is likely to become more prominent in the future.

Chains and Anaphoric Dependence: On Reconstruction and Its Implications

Andrew Barss

Submitted to the Department of Linguistics and Philosophy in partial fulfillment of the requirements for the degree of Doctor of Philosophy in Linguistics

Abstract

This thesis is concerned with developing an account within the Government and Binding (GB) theory of the grammaticality of such structures as (1), and exploring the implications of this account for the theory of empty categories, chains, and scope. The hallmark characteristic of such grammatical S-Structure representations as (1) is that the anaphor is outside the c-command domain of its understood antecedent. The basic anaphoric effect is termed connectivity.

1) [which of each other's friends] [did the men see t]?

Chapter 1 is a brief overview of the necessary definitions presumed in the thesis, and an outline of the subsequent chapters. Chapter 2 introduces a large body of data which must be treated on a par with (1), and reviews and criticizes several existing proposals which have been made to account for (1). The chapter argues that the binding theory must apply to structures having the essential form of (1). We demonstrate that no treatment which involves lowering the anaphor into the c-command domain of the antecendent via "reconstruction" operations, or involves applying the Binding Theory at a level at which WH movement is not represented, can be maintained. Chapter 3 develops a revision of the binding theory, focusing on Condition A, which is capable of treating all the connectivity data in a unified way. The major formal construct proposed in the chapter is the chain accessibility sequence, essentially a path of nodes through which the potential antecedents for an expression are accessed. The revised binding theory is defined in terms of such sequences; as the name implies, the notion chain plays a prominent role. This approach to connectivity is developed in the spirit of the Path theory of Kayne (1983) and Pesetsky (1982). We also discuss the properties of structures of the form of (1), but where the constituent containing the anaphor is predicative in nature. We shall see that the predicative nature of the constituent significantly constrains the possibilities of assigning the anaphor an antecedent. This chapter adopts, and argues in favor of, the Linking theory of binding introduced by Higgenbotham (1983).

Chapter 4 focuses on the theory of empty categories, arguing that it is desirable to construct the theory so that no empty categories bear binding features (the features [+/-] anaphoric] and [+/-] pronominal] are thus restricted to over categories). This proposal, which I term the No Features Hypothesis, departs from the characteristic treatment of ECs in GB theory. The chapter adopts Brody's (1985) proposals concerning the distribution of PRO and NP-trace. We adopt, and later extend, the Local Binding Condition (LBC) on A chains, argued by Rizzi (1982) to constrain the well-formedness of A chains. We reformulate it in terms of Linking theory, as the Chain Obviation Condition (COC), and argue that it holds of all chain types. This is shown

to be a principle with considerable generality, subsuming the LBC, Condition C of the binding theory, and the anti-c-command condition on linking. Adopting the COC, along with the NFH, allows the elimination of the class R-expression from the inventory of binding types. It will be shown that the anti-c-command condition on parasitic gaps derives directly from the COC, with no stipulations. The chapter concludes with a defense of the proposal that the theory of anaphora must recognize anaphoric dependences and obviation as separate relations as argued by Lasnick (1976, 1981), and Higgenbotham (1985).

Chapter 5 discusses constraints on the interpretation of sentences in which a quantificational NP is the antecedent of an NP-trace which it does not c-command. These considerations lead us to formulate a constraint on movement operations. The chapter also argues that the operations of WH-movement and QR are strictly ordered in the LF component.

A Case for Movement

Kyle Brian Johnson

Submitted to the Department of Linguistics and Philosophy in partial fulfillment of the requirements for the degree of Doctor of Philosophy in Linguistics

Abstract

This thesis defends the position that the syntactic level of D-structure has an existence autonomous from S-structure. It does this by showing that Movement, a relation between D- and S-structure, is constrained at intermediate levels. Two constraints on Movement are investigated. One subagency is argued to make reference to the syntax of thematic role assignment. The second, the Empty Category Principle, is held to make reference to the syntax of the Case assignment. The first holds at intermediate levels in the Syntax; the second at S-structure and Logical Form. Subajacency is shown to constrain rightward movement as well as leftward movement. The Empty Category Principle is factored into independent principles, one holding of chains, the other holding of empty categories. The assymetrical boundedness of leftward and rightward movement is argued to stem from this version of the Empty Category Principle. A short account of ps1 predicates is included.

A Theory of Category Projection and Its Applications

Naoki Fukui

Submitted to the Department of Linguistics and Philosophy in partial fulfillment of the requirements of the Degree of Doctor of Philosophy in Linquistics

Abstract

This thesis proposes a new system of category projection where Lexical categories and Nonlexical (or "Functional") categories project in different ways, which is crucially different from the standard views in which all categories project in the same fashion.

In Chapter 1, I introduce some of the basic notions of Government-Binding theory within which all of the discussion in this thesis takes place. The aim of Chapter 2 is to show the fundamental difference between Lexical categories and Functional categories. That is, Lexical categories have Lexical Conceptual Structures (LCS) in the sense of Hale and Keyser (1985), whereas Functional categories do not have Lexical Conceptual Structures comparable to the ones Lexical categories have, and the latter type of categories only have the function of "connecting" two syntatic units via some sort of "binding" and "agreement." Based on this fundamental difference, a new projection system is introduced, in which Lexical categories project up to a single-bar level, allowing free recursion at that level, while Functional categories can project up to a double-bar level, taking a unique complement.

Chapter 3 explores various consequences of the projection system introduced in Chapter 2. One important consequence is that the proposed projection system, combined with "bottom-up" θ -marking mechanism, predicts that the so-called "external argument" appears within the projection of a Lexical head at D-structure, receiving the external θ -role in that position, and then moves outside the Lexical projection to its S-structure position, for Case reasons. This move makes possible the explicit syntactic representation of what has been called the "implicit argument" both in noun phrases and in clauses (in the case of passives).

In Chapter 4, I proceed to focus on Japanese and propose a new phrase structural configuration for this language in the light of the projection system introduced in Chapter 2. It is argued that Japanese lacks the Functional categories DET and COMP, and has a very defective INFL which contains no agreement features. From this, it immediately follows that Japanese has no specifiers, which close off the category projection. I argue there that this is indeed the case, i.e., that Japanese has no specifiers and every phrase in this language is always "open." Other consequences of my proposal, including the derivability of overt wh movement in Japanese, are also discussed in this chapter.

The Syntax of Operators

Isabelle Haik

Submitted to the Department of Linguistics and Philosophy in partial fulfillment of the requirements for the degree of Doctor of Philosophy

Abstract

S. Mariera Seeder Statement Seeder Mariera

The aim of this thesis is to explore the implications that the existence of Logical Form has, both for the derivation of sentences and for the interaction of subtheories of Universal Grammar. Given that the behavior of lexical anaphors can be reduced to that of NP traces, as in Chomsky (1985a), it will be shown that principles A and B of the Binding theory can be derived from Theta theory. Arguments will be represented abstractly as chains, whose formation is governed by Principle A and the Empty Category Principle, as formulated by Kayne (1981a). In addition to argument movement certain predicates are shown to move at LF, to permit th-marking of their arguments. This movement will be similarly constrained.

A major claim of this thesis is that a bound prenominal confers operator status on the category which contains it, and hence must be assigned scope. This claim receives independent support insofar as it explains an apparent counter example to the hypothesis above, that Principle A must hold between links of a chain. Furthermore, this property of bound pronouns will play a central role in the availability of certain readings in sentences involving sloppy identity, and certain structures involving VP-deletion and parasitic gaps. In these structures, it is just the assignment of scope to the category containing the bound pronoun which gives rise to the appropriate logical forms.

In addition to standard types of LF movement, i.e., movement to COMP (as in wh-movement in Chinese), and adjunction (as in Quantifier Raising), it will be argued that a third type exists. This involves the identification of the moved category with its target, yielding a structure in which subtrees are represented on distinct planes, which meet at the merged (i.e., identified) node. The creation of such coordinates structures will account for the properties of parasitic gaps, which become across-the-board gaps at LF. Moreover, sloppy identity obtains only in coordinate structures, thus making it unnecessary to appeal to λ -abstraction to account for it.

In addition to permitting movement, LF licenses the insertion of material missing at S-structure. This enables various 'deletion' constructions to be properly interpreted.

Subject and Object in Turkish

Laura Ellen Knecht

Submitted to the Department of Linguistics and Philosophy in partial fulfillment of the requirements for the degree of Doctor of Philosophy in Linguistics.

Abstract

PERSONAL RECEIPT SECURITY SECURITY PERSONAL RESERVE WITHOUT PROVINCE PROVINCE PROVINCE PROVINCE PROVINCE

This dissertation is a study of rules in Turkish which change grammatical relations or are sensitive to them. It addresses issues of interest to descriptive Turkish grammar and to general linguistic theory. Two chapters are devoted to questions about intransitive clauses. Chapter 2 examines the claim that impersonal passivization, like personal, impassivization, involves the advancement of a direct object to subject. Evidence is presented that this is not the case in Turkish. Chapter 4 is an investigation of the Unaccusative Hypothesis, the proposal that some intransitive clauses have an initial direct object but no initial subject. It has been argued that there is one construction in Turkish which provides evidence for the Unaccusative Hypothesis. The control rule that operates in this construction is shown to be sensitive to thematic roles rather than toinitial grammatical relations; it cannot, therefore, serve as a diagnostic for initial unaccusativity.

The topic of Chapter 3 is non-referential direct objects and subjects. Evidence is presented that a subset of such nominals, i.e., those that occur without the indefinite article, undergo incorporation with the verb, which accounts in part for the observation that sentences with non-referential subjects behave as if they were subjectless and that those with non-referential direct objects behave as if they were intransitive. I propose that incorporees are not final chomeurs, as have been claimed, but instead bear the final-stratum relation INC(orporated). Furthermore, I argue that sentences with incorporated subjects lack a final subject and, consequently, that the Final 1 Law is too strong.

The causative construction is the subject of the final chapter, and the central question addressed is whether causative formation in Turkish is a lexical process which derives one verb from another or a syntactic process which collapses clauses together (Clause Union). While the lexical account explains a class of rule interaction phenomena, I present evidence that causatives must be analyzed as underlying complex. A general condition is proposed which blocks syntactic rules of a particular kind from applying on the imbedded clause prior to Clause Union. The discussion of causatives includes an analysis of quirky casemarking in Turkish.

Adjunctions and Projections in Syntax

Margaret Jean Speas

Submitted to the Department of Linguistics and Philospohy in partial fulfillment of the requirements for the degree of Doctor of Philosophy in Linguistics

Abstract

This dissertation presents a theory of projection of syntactic configuration from the lexicon. The first chapter outlines a theory of the D-structure level of representation in which all well-formedness conditions on underlying structures are deductable from other independent principles of the Grammar. This theory extends the work of Stowell, who argued that linear precedence relations could be derived from independent principles. I propose that domination relations may likewise be derived from independent This proposal is based on the theory of lexical representations of Higgenbotham (1985, 1986), in which words of all lexical categories (N, V, A, P) are thought to have a "theta grid" as part of their lexical entry. It is argued that the relations which hold among these grids are sufficient to give all the information that we need to deduce the domination relations which result when these lexical entries are projected from the lexicon. These structures which are so projected, which I call Thematic Structures, are universal abstract relational structures. They encode domination relations, which are derived from thematic relations, but do not encode precedence nor do they encode adjacency. It is further proposed that non-lexical or "Functional" categories are heads at D-Structure, but that the way that they project differs in significant ways from the way that lexical categories project. The first chaper concludes with a discussion of the properties of adjunction constructions, pointing out that the claims of May (1985) about domination relations in LF adjunction structures lead to the conclusion that such structures are always three-dimensional.

The second chapter has to do with the two related issues which have come to be associated with the term "Configurationality." The first is the question of whether all languages distinguish structurally between subject and object. The diverse data which have been adduced as evidence for variation in configurationality are brought together in order to clarify the issue. While it is often assumed that "nonconfigurational" languages are those with 'flat' structures, the data actually seem to call for some sort of dual representation.

The second issue is then shown to be related to, but independent of, the issue of underlying domination relations. It is claimed that the proposal of Jelinek (1984) that the Configurationality parameter should be stated in terms of the status of overt nominals as adjuncts and of pronominal clitics as arguments is on the right track, but it makes the wrong prediction in certain cases, and it could allow violations of the Projection Principle.

The language used as a case study is Navajo. It has been proposed that Navajo overt nominals are actually adjuncts, and that pronominals clitics are the 'real' arguments. There are two problems with this. First, by standard syntactic tests, overt nominals do not behave like adjuncts, they behave like arguments. Second, the pronominal clitics

are embedded within an apparently unstructured string of prefixes, and it is not obvious that they are accessible to syntax at all, let alone in argument positions.

Chapter 3 considers in detail the status of the Navajo prefixes which mark subject and object agreement. Arguments are given that these agreement prefixes must be infixes, that is, that they must be inserted into a discontinuous lexical item.

If this infixation model for Navajo is correct, then the problem of the accessibility of the pronominal agreement clitics in the syntax is not so serious; in fact, it might be proposed that they are in argument positions at D-Structure and S-Structure, and simply infix at PF. However, such a proposal would contradict the syntactic evidence that overt nominals are in argument, not adjoined, positions. As a solution to this problem, an extension of the definition of an allowable syntactic CHAIN is suggested, whereby the tail of a CHAIN may be in a non-theta position only if it is a subpart of a word.

The syntactic facts which have led previous researchers to consider Navajo to be nonconfigurational are considered in Chapter 4. These facts involve some curious restrictions on the interpretation of null pronominals, which seem to violate binding conditions. It is claimed that the data reveal a parallelismrestriction on the assignment of Grammatical Relations, which is best handled if we treat the relevant constructions as Across-the-Board (ATB) constructions. This explanation is designed to capture and explain the original insight of those who proposed that Navajo has a parsing strategy, while showing that the differences between Navajo and more familiar languages are a matter of variation in independently available grammatical principles.

After an ATB account of the Navajo facts is presented in general terms, the question of the status of these representations in grammatical theory is addressed. It turns out that all of the constructions for which an ATB account has been proposed share the configurational properties of adjunction constructions. As was pointed out in Chapter 1, what is currently known about adjunction structures in general leads us to expect parallelism effects in just these constructions.

CARLOR PROPERTY TO THE PROPERTY OF THE PROPERT

Operations on Lexical Forms: Unaccusative Rules in Germanic Languages.

Lorraine S. Levin

Submitted to the Department of Linguistics and Philosophy in partial fulfillment of the requirements for the degree of Doctor of Philosophy

Abstract

This thesis describes a theory of relation changing rules in LFG, concentrating on rules which distinguish between unaccusative and unergative verbs. I call these rules Unaccusative Rules (URs). In order to handle URs I introduce a mechanism which I call Argument Classification (AR) which mediates between thematic roles and grammatical functions. AC puts thematic arguments into one of four argument classes: unexpressed, semantically restricted, subjective unrestricted, and general unrestricted. Then, grammatical functions are assigned to these classified arguments instead of being assigned to unprocessed thematic argument slots. The theory of relation changing rules specifies allowable argument classifications and allowable assignments of functions to classified arguments. In order to illustrate the theory, I formulate a number of rules in English and Dutch.

Chapter 1 provides background information about grammatical relations and relation changing rules in LFG. Chapter 2 summarizes properties of relation changing rules which a theory should account for: semantic conditioning, syntactic productivity, ability to distinguish between subjects of unaccusative verbs and subjects of unergative verbs, and apparent directionality of subject-to-object relation changes. Chapter 3 describes a new theory of relation changing rules based on the notion of argument classification and the distinction between semantically unrestrictedgrammatical functions. Chapter 4 applies the theory to several constructions in English and raises three additional issues: the status of Burzio's Generalization, the treatment of double object verbs, and the treatment of oblique subjects and dummy subjects. The theory yields particularly good insights on the latter two points. Chapter 5 illustrates the theory further using three Dutch URs. This chapter continues the discussion of non-nominative subjects and also discusses the problem of rule mismatches. Rule mismatches arise when a given predicate acts as if it were unaccusative in one construction and acts as if it were unergative in another. I discuss possible resolutions of the mismatches and their implications for the status of AC as a level of representation.

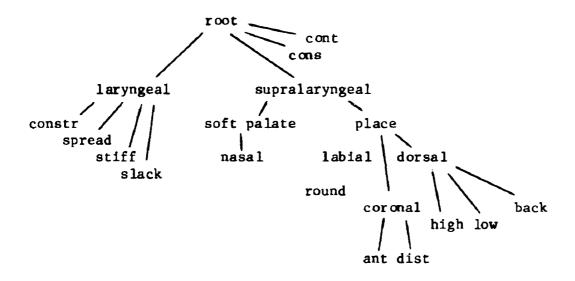
The Representation of Features and Relations in Non-Linear Phonology

Elizabeth Caroline Sagey

Submitted to the Department of Linguistics and Philosophy in partial fulfillment of the requirements for the degree of Doctor of Philosophy in Linguistics

Abstract

In this thesis, I propose the following hierarchical representation for the distinctive features of phonology.



This hierarchy is based on phonetics: features are grouped according to articulator in the vocal tract that they are executed by. Articulators are grouped according to their acoustic effects on the formant structure. The hierarchy, which is proposed to be universal, provides a straightforward explanation for the complex phenomena that surround multiply-articulated segments, such as labiovelars, labiocoronals, coronovelars (e.g., clicks), and labialized, palatalized, or velarized consonants. This type of segment, with unordered or simultaneous multiple articulations, I refer to as a complex segment. The theory of representation I propose makes it possible to represent all the complex segments that occur, and provides an explanation of why those complex segments that occur are possible in language, as well as of why those that do not occur are impossible. Furthermore, it makes possible an account of the derivation of complex segments, where they are derived, and of their behavior with respect to phonological processes. In addition, the proposed theory of representation is shown to account for unrelated phenomena in languages without complex segments, which provides independent

support and shows that the representation is universal, rather than particular to complex segment languages.

In Chapters 1 and 2, I argue for the hierarchical feature groupings shown above. (The root, laryngeal, supralaryngeal, and place constituents were proposed by Mohanan (1983) and Clements (1985). I demonstrate that the only complex segments that occur are those combining two or more of the hierarchical constituents: labial, coronal, dorsal. I argue, based on timing, syllabification, reduplication, compensatory lengthening, prenasalization, and nasal assimilation, that complex segments occupy single x-slots, and, furthermore, that the multiple articulations in complex segments must be represented within a single place node. Complex segments are contrasted with contour segments, in that the latter involve sequences of articulation within a single segment - a distinction which determines phonological rules. Furthermore, I show that the structure within the place node required by complex segments finds independent support in languages without complex segments. For example, the structure allows us to account for patterns of blocking and transparency in harmony systems. Thus, the structure within the place mode is a universal property of the representation of distinctive features, rather than just a peculiarity of complex-segment languages.

In Chapter 3, I propose a mechanism for assigning the degree of closure features [continuant, consonantal] to the articulators that execute them. This representation of degree of closure features is necessary in order to account for the behavior of complex segments to be represented identically to that in simple segments. The modifications of the feature representation that are necessary to represent and account for the behavior of complex segments lead to a concise characterization of the possible complex segments in human language.

In Chapter 4, I redefine the distinctive features (i.e., the terminal nodes in the hierarchy) in light of the proposals made in Chapters 1, 2, and 3, and I define the non-terminal nodes in the hierarchy.

Chapter 5 contains a further demonstration of the possibility of explaining phonology in terms of external factors. I demonstrate that the association lines among features and x-slots that connect all the tiers in the hierarchy must represent the relation of overlap in time, and I show that when they are correctly defined as representing overlap, the ill-formedness of crossing association lines follows from the relations represented in a phonological representation, together with knowledge of the world, and need not be stipulated as a well-formedness condition in UG.

Finally, in Chapter 6, I discuss two aspects of phonetic representation that are made possible by the view of phonological representations taken in Chapters 1 through 5 degrees of closure of individual articulators and subsegmental timing.

Event Logic and the Interpretation of Plurals

Barry Schein

Submitted to the Department of Linguistics and Philosophy in partial fulfillment of the requirements for the degree of Doctor of Philosophy in Linguistics.

Abstract

Simple sentences with plurals have interpretations that cannot be reduced to predications about individual objects. Such an interpretation for a sentence with \underline{n} plurals cannot be represented by a logical form containing quanifiers over individuals that bind into an atomic \underline{n} -adic predicate:

- (i) NP $_{1}(x_{1}).....,NP(x_{n})V(x_{1}-x_{n})$
- (ii) Ten boys ate ten pies.

Chapter 1 introduces the classes of interpretations that cannot be so represented. An example is that interpretation of (ii) which is true in a situation where there are ten boys and ten pies, the boys eat the pies and no one boy eats more than part of any one of the pies. No individual boy ate any individual pie.

Chapter 2 on set-denotative logic presents the standard view according to which the non-reducibility of plurals is taken to show that the \underline{n} plurals in (i) are quantifiers over sets of individuals that bind into an atomic \underline{n} -adic predicate expressing a relation among sets of individuals.

Chapter 3 proposes event logic as an account of plural interpretations. Adding an argument position for events, it assumes a Davidsonian (1967) decomposition of the predicate into constituents expressing the role of each NP in an event of V-ing:

(iii) e's eaters are ten boys & eat(e) & e's eaten are ten pies

Quantifying over events in general replaces quantifying over sets. There are no atomic predicates expressing relations among sets of individuals.

An important feature of the event logic's syntax exploits the predicate's decomposition into constituents. It allows for restricted qualification, "[Q:A]", in which one of the constituents occurring in, say, A is separated from the remaining constituents and from the verb itself which are in B. Note that the set-denotative logic's <u>atomic</u> predicate does not allow a NP's semantic role to be separated from it. It appears with its full valence, providing a place for every argument in the relation it expresses.

Chapter 4 shows that a domain of quantification in the set-denotative logic cannot include all subsets of individual objects. If there is to be quantification over sets, it is restricted by a relationship to events.

Chapter 5 considers the extension of set-denotative logic that admits in the predicate a place for events while retaining the view that plurals are quantifiers over sets of indi-

viduals binding into atomic $\underline{n}+1$ -adic predicates. The event logic, by quantifying over events, quantifies indirectly and in a restricted way over sets containing their participants. Chapter 5 shows that the extended set-denotative logic must be constrained to recover the relationship between sets and events derived in the event logic. A predicate in the extended set-denotative logic must not denote a set unless it is all the participants of an event, and the predicate must be about the set's activity only with a single event.

Chapter 6 argues for the syntax of event logic, showing that the constituents of the predicate's decomposition must sometimes be divided between the restriction and the matrix on which a quantifier operates.



18.0 Communication Biophysics

Academic and Research Staff

Prof. L.D. Braida, Prof. L.S. Frishkopf, Prof. N.Y.S. Kiang, Prof. W.T. Peake, Prof. W.M. Siebert, Prof. T.F. Weiss, Prof. V.W. Zue, Dr. M.C. Brown, Dr. D.K. Bustamante, Dr. H.S. Colburn, Dr. B. Delgutte, Dr. R.A. Eatock, Dr. L.A. Delhorne, Dr. N.I. Durlach, Dr. D.K. Eddington, Dr. J.J. Guinan, Jr., Dr. D.R. Ketten, Dr. J.B. Kobler, Dr. W.M. Rabinowitz, Dr. J.J. Rosowski, Dr. P.M. Zurek, I.A. Boardman, R.M. Brown, M.L. Curby, J.A. Frisbie, K.W. Grant, J.D. Koehnke, N.A. Macmillan, E.M. Luongo, K. Payton, C.M. Reed, B. Schneider, F.J. Stefanov-Wagner, D.A. Steffens

Graduate Students

C.A. Bickley, C.R. Corbett, S. Dynes, D.M. Freeman, D.A. Frost, G. Girzon, R.P. Goldberg, Y. Ito, R.C. Kidd, G. Kline, D.F. Leotta, M.E. Machado, J.R. Melcher, X-D Pang, C. Passero, S.L. Phillips, M.H. Power, P.M. Peterson, L. Stephens, R.M Uchanski

18.1 Basic and Clinical Studies of the Auditory System

National Institutes of Health (Grants 5 PO1 NS13126, 5 RO1 NS18682, 5 RO1 NS20322, 5 RO1 NS20269, and 5 T32NS 07047)
Symbion, Inc.

Lawrence S. Frishkopf, Nelson Y.S. Kiang, William T. Peake, William M. Siebert, Thomas F. Weiss, M. Christian Brown, Bertrand Delgutte, Ruth A. Eatock, Donald K. Eddington, John J. Guinan, Jr., Darlene R. Ketten, J.B. Kobler, William M. Rabinowitz, John J. Rosowski, Ian A. Boardman, Robert M. Brown, Mark L. Curby, Frank J. Stefanov-Wagner, D.A. Steffens, Scott B.C. Dynes, Dennis M. Freeman, Gary Girzon, R.C. Kidd, J.R. Melcher, Xiao-Dong Pang, Susan L. Phillips

Investigations of signal transmission in the auditory system are being carried out in cooperation with the Eaton-Peabody Laboratory for Auditory Physiology at the Massachusetts Eye and Ear Infirmary. The long-term objective is to determine the anatomical structures and physiological mechanisms that underlie vertebrate hearing and to apply that knowledge to clinical problems. Studies of cochlear implants in humans continue in the Cochlear Implant Laboratory in a joint program with the Massachusetts Eye and Ear Infirmary. The ultimate goal of these devices is to provide speech communication for the deaf by using electric stimulation of intracochlear electrodes to elicit patterns of auditory nerve fiber activity that the brain can learn to interpret.

18.1.1 External and Middle-Ear Transmission

Darleen R. Ketten, Xiao-Dong Pang, William T. Peake, Susan L. Phillips, John J. Rosowski

To determine the interaction between the transformations of acoustic signals performed by the external ear and by the middle ear, it is important to know not only the input impedance of the middle ear but also the output (or radiation) impedance of the

external ear. We measured the radiation impedance of the external ear of cat and evaluted the ear's performance as a coupler of acoustic power.¹ The results are important to our understanding of middle-ear function in that they allow us to calculate the impedance matching capabilities of the middle ear and also allow computations of power flow through the external and middle ears. Our measurements suggest that the pinna-flange acts to damp high-frequency resonances in the radiation impedance; the low-frequency impedance is primarily determined by the concha and external canal. Whereas the cat external and middle ear act as a nearly perfect (i.e., matched) acoustic-power coupler at 4 kHz, they are far from perfect at other frequencies in the audible range. The measure of acoustic performance that can be determined from these measurements, diffuse-field pressure ratio and diffuse-field absorption cross-section, will be important in comparing the performance of the ears of different species. For instance, it may be that some species have evolved highly directional external ears with decreased ability to absorb acoustic power.

Two earlier studies have been published.^{2.3}

18.1.2 Cochlear Mechanisms

Ruth A. Eatock, Dennis M. Freeman, R.C. Kidd, Thomas F. Weiss, Lawrence S. Frishkopf

A theoretical study of the hydrodynamic stimulation of the hair bundles of hair cells has been completed⁴ and some of the results have been published⁵ and presented at scientific meetings.⁶

A theoretical study of the signal processing properties of calcium channels was completed. Models of calcium channel gating and calcium ion accumulation were investigated. It was found that these two mechanisms can contribute substantially to the loss of synchronized responses of cochlear nerve fibers in the ear. Thus there are three important lowpass filter mechanisms in the cochlea. They result from the membrane capacitance of the hair cell, the kinetics of gating of calcium channels, and the kinetics of intracellular accumulation of calcium channels.

18.1.3 Stimulus Coding in the Auditory Nerve

Bertrand Delgutte

A fundamental problem in auditory theory is to reconcile the wide range of stimulus level over which listeners make fine spectral discriminations with the relatively narrow dynamic range of auditory-nerve fibers. That is, the discharge rate of auditory-nerve fibers grows with stimulus level only over a 30-dB range between threshold and saturation. It has been suggested that such saturation might limit psychophysical performance at high sound levels, and that certain important features for discrimination might be encoded in temporal patterns of auditory-nerve activity ("phase-locking"). In the past year, ^{8 o} we used a detection theoretic approach to examine quantitatively how much information for intensity discrimination is available in the discharge patterns of auditory-nerve fibers. This line of research is based on the principle that the stochastic behavior of auditory neurons imposes fundamental limitations on the performance that is achievable in any detection or discrimination task (Siebert, Kybernetic 2, 206-215, 1965). Specifically, we measured intensity difference limens (DL's) of single

auditory-nerve fibers for both tone and noise stimuli using paradigms and detectability measures that explicitly mimic those of psychophysics. These physiological data were then incorporated into a model that combines intensity information from many auditory-nerve fibers. This model is the first to include both a physiologically realistic distribution of fiber thresholds and multiple, frequency-selective channels.

Responses of auditory-nerve fibers to pairs of tone or broadband noise stimuli with different levels were recorded in anesthetized cats. Intensity DL's of single fibers were measured by adjusting the level of difference until the most intense stimulus evoked more spikes than the weakest stimulus for about 75% of the presentations. For both tones and noise, variations in physiological DL's with intensity had basically a U shape, with a minimum (meaning best performance) in the range where discharge rate grows rapidly with level. Minimum DL's ranged between 1 and 7 dB, implying that a small number of fibers could account for psychophysical performance (about 1 dB). However, this good correspondence between physiological and psychophysical DL's occurs only over a narrow (20-40 dB) range of levels, so that, in order to account for psychophysical performance over a broad range of levels, information from fibers with different thresholds must be combined.

Our model for combining intensity information from an array of 30,000 fibers was based on the optimum combination rule of signal-detection theory, under the assumption that the spike counts of different fibers are statistically independent Gaussian random variables. For both tones and noise, model predictions well exceeded psychophysical performance in intensity discrimination over at least a 90-dB range of stimulus levels. This implies that psychophysical performance is not limited by saturation of auditory-nerve fibers, but by the efficiency with which the central auditory system processes the information available at the level of the auditory nerve.

This conclusion is reinforced by the result that the dependence of model predictions on intensity clearly differed from that of psychophysical DL's; model predictions show a degradation at high stimulus levels, whereas psychophysical performance is either constant (for broadband noise) or improves with level (for tones). More realistic level dependence of predicted DL's was obtained by assuming that the central processor gives more "weight" to information from high-threshold fibers than to that from low-threshold fibers. This modified model also provided a robust representation of the spectra of speech sounds with respect to variations in stimulus level.

18.1.4 Afferent and Efferent Systems in Mammalian Cochlea

M. Christian Brown

CONTRACTOR CONTRACT RESPONDE ASSOCIATION

Our goal has been to understand the functional significance of the several types of afferent and efferent innervations of the mammalian cochlea. We have used techniques involving horseradish peroxidase labeling of neurons to resolve several anatomical issues which have functional significance. 10.11.12 One specific goal is to determine the central projections of type-II spiral ganglion cells. Peripherally in the cochlea, these ganglion cells provide the afferent innervation of the outer hair cells. In material from the guinea pig cochlea, central axons of labeled type-II ganglion cells could be traced from the spiral ganglion, through the auditory nerve, and into the cochlea nucleus, which is the first auditory nucleus in the central nervous system. Although these axons

followed the course taken by the thick, myelinated axons from type-I ganglion cells, the type-II axons were much thinner (about 0.5 μ m diameter) and appeared to be unmyelinated. Conduction times which were computed on the basis of these diameters indicate that information from afferent terminals on hair cells arrives at the cochlear nucleus in 0.3 msec (type-I) or 6.1 msec (type-II). The functional significance of these observations is that the type-II neurons play a role in auditory processes which involve slow time courses. Ongoing studies in mice and gerbils indicate that the central projections of type-I and type-II ganglion cells are topographically similar, although some type-II central axons do not innervate the dorsal cochlear nucleus.

We have used similar techniques to reconstruct the cochlear projects of olivocochlear efferent neurons. For efferents, the unmyelinated fibers innervate near the inner hair cells whereas the myelinated fibers innervate the outer hair cells, which is the converse of the afferent innervation pattern. Unmyelinated efferent fibers innervating near inner hair cells have been shown to fall into two categories: those with very discrete terminations which might influence discrete regions of afferent fibers, and those with very broad terminations which presumably can influence afferent fibers conveying information from a large range of frequency regions.¹¹ Myelinated efferents innervating outer hair cells have also been reconstructed but it has not yet been possible to establish categories based on the terminal patterns of these fibers. Ongoing labeling studies of these myelinated fibers at the single-unit level in cat¹² and guinea pig may succeed in establishing categories for their peripheral innervation patterns.

18.1.5 Middle-Ear Muscle Reflex

John J. Guinan, Jr., James B. Kobler, Xiao-Dong Pang, Michael P. McCue

We aim to determine the structural and functional bases of middle-ear reflexes. We have continued our work recording from individual stapedius motoneurons in Ketamine-anesthetized or decerebrate cats. We have now distinguished five groups of motoneurons. In addition to the four groups previously distinguished on the basis of the laterality of their responses to sound, we have now distinguished a fifth category, motoneurons with spontaneous activity. These neurons typically respond to sound in either ear and have axons with conduction velocities that are approximately half as large as all of the other groups (based on the spike latency from electrical stimulation in the floor of the fourth ventricle). Manuscripts describing this work and related work are in preparation.

The cell bodies of stapedius motoneurons are located in four loose groups around the facial nucleus and near the descending facial nerve. We have attempted to find correlations between these four anatomical groups and our five physiological groups by injecting single, physiologically characterized stapedius motoneurons with HRP and indentifying their cells of origin in the brain. To date, over twenty stapedius motoneurons have been characterized and identified. Motoneurons in all classes, except spontaneously active motoneurons, have been labeled. Stapedius motoneurons which responded only to sound in the contralateral ear were found only in the ventromedial perifacial nucleus and no other type was found there. The other neuron types were located throughout the remaining stapedius motoneuron cell groups with no strong pattern emerging. These results are consistent with, and greatly extend, our earlier results based on gross lesions.

We have recently begun two projects, one aimed at determining the amplitudes and time courses of the middle-ear transmission changes produced by individual stapedius motor units and muscle fibers, and the second aimed at determining the effects of stapedius-muscle contractions on the responses of single auditory-nerve fibers. During the past year we completed a manuscript on the asymmetries in the acoustic reflexes of the cat stapedius muscle.¹³ Based on measurements of electromyographic activity (EMG), we found that the crossed stapedius reflex had a maximum amplitude which was about 1/3 of the maximum amplitude of the uncrossed reflex. This indicates that the crossed reflex probably produces correspondingly smaller changes in middle-ear sound transmission than the uncrossed reflex. Since most measurements of the effects of middle-ear reflexes have used only crossed sound, it seems likely that the effects of middle-ear reflexes due to uncrossed or binaural sound have been underestimated.

18.1.6 Cochlear Efferent System

John J. Guinan, Jr.

ACCOUNT BOSSON SONDAY COCCOS BODDON

Our aim is to understand the physiological effects produced by medial olivocochlear (MOC) efferents which terminate on outer hair cells. To do this we have measured the sound pressure in the ear canal generated by a sound source, with and without electrical activation of MOC fibers by an electrode in the fourth ventricle (OCB stimulation). The efferent-induced change in the ear-canal sound pressure, P_{oc} , can be thought of as a change in a sound of cochlear origin. Measurements of P_{oc} are of interest because P_{oc} gives a measure (albeit indirect) of the MOC-induced change in cochlear mechanics. Using continuous tones, we found that: (1) the phase delay of P_{oc} was approximately a monotonic increasing function of sound frequency¹⁴ and (2) group delays calculated from P_{ac} phase vs. sound frequency were generally longer at lower frequencies. During the past year we have implemented a paradigm in which similar experiments are done using short tone 'pips' instead of continuous tones. These experiments show that for low frequencies, the sound in the ear canal outlasts by a few ms the sound produced by the sound source (i.e., there appears to be a 'cochlear echo') when there is no OCB stimulation. With OCB stimulation, however, this 'cochlear echo' is greatly reduced. Thus, OCB stimulation appears to suppress cochlear echoes. These data provide the interpretation that P_{oc} measured with continuous tones is the suppression of a cochlear echo.

During the past year we have analyzed and prepared for publication work done with M.L. Gifford. A paper has been submitted on the effects of electrical stimulation of efferent neurons with an electrode either at the origin of the MOC efferents (MOC stimulation) or at the floor of the fourth ventricle (OCB stimulation). Our results indicate that the effects produced by both kinds of stimulation are attributable only to MOC efferents and not to lateral olivocochlear (LOC) efferents. Furthermore, OCB stimulation in the cat probably stimulates both crossed and uncrossed MOC efferents. These experiments provide a new interpretation of the neural elements responsible for the empirical findings reported in previous experiments in which auditory efferents were electrically stimulated.

During the past year, two previously submitted papers were published. The anatomy and organization of the auditory efferents was reviewed in a joint paper with W.B. Warr and J.S. White of Boys Town National Institute.¹⁶ In a joint paper with other researchers

in the Eaton-Peabody Laboratory, data from changes induced in the firing patterns of auditory-nerve fibers were used to consider the interrelationships among the effects produced by the efferent system, acoustic trauma, ototoxic lesions, and pharmacological manipulation of endocochlear potential.¹⁷

18.1.7 Cochlear Implants

Donald K. Eddington, Gary Girzon

This year work centered in three areas: 1) electrical modeling of the human cochlea; 2) electrical and psychophysical measures in human subjects with implants; and 3) preparation of a program project grant that was submitted to and funded by the NIH.

The goal of work in the first area is to construct a software model of the cochlea that predicts the patterns of current flow due to the stimulation of arbitrarily placed intracochlear electrodes. Human temporal bone sections were digitized and resistivites assigned to the major cochlear elements (e.g., bone, nerve, perilymph, endolymph). Finite element techniques were used to convert the anatomical and resistivity data to a set of equations representing a three-dimensional mesh of 512 by 512 by 46 nodes. Current sources were defined at nodes representing positions of intracochlear electrodes in implanted subjects and the equations solved. Maps of nodal potentials located along the length of the spiraling scala tympani displayed a monotonic reduction of potential from the stimulating electrode toward the base and a potential plateau toward the apex. For basal stimulating electrodes, "bumps" in the potential plateaus between 15 and 20 mm from the base indicated current pathways between turns in addition to the pathway along the length of the cochlea.

Measurements of potentials at unstimulated electrodes made in five human subjects implanted with intracochlear electrodes demonstrated the asymmetric potential distributions predicted by the model. The "bumps" predicted by the model were also present in the potential distributions measured during the stimulation of the most basal of the implanted electrodes in all five subjects. Psychophysical measures are continuing to determine if these asymmetric potential distributions are also reflected in aspects of the subject's perception.

September marked the beginning of an NIH Program Project Grant that supports individuals from Harvard and M.I.T. who investigate a wide range of issues related to cochlear implants.

References

A DESCRIPTION SECRETARIES FOR STATEMENT FOR THE FOR THE SECRETARIES SECRETARIES FOR SECRETARIAN AND PARTICULAR AND PARTICULAR

- ¹ J. Rosowski, L.H. Carney, and W.T. Peake, "The Radiation Impedance of the External Ear of Cat: Measurements and Applications," submitted to J. Acoust. Soc. Am.
- ² J. Rosowski, J.H. Carney, T.J. Lynch, III, and W.T. Peake, "The Effectiveness of External and Middle Ears in Coupling Acoustic Power into the Cochlea," *Peripheral Auditory Mechanisms*, edited by J.B. Allen, J.L. Hall, A. Hubbard, S.T. Neely, and A. Tubis, New York: Springer-Verlag, 1986, pp. 3-12.

- ³ X-D. Pang and W.T. Peake, "How do Contractions of the Stapedius Muscle Alter the Acoustic Properties of the Ear?," *Peripheral Auditory Mechanisms*, edited by J.B. Allen, J.L. Hall, A. Hubbard, S.T. Neely, and A. Tubis, New York: Springer-Verlag, 1986, pp. 36-43.
- ⁴ D.M. Freeman, "Hydrodynamic Study of Stereociliary Tuft Motion in Hair Cell Organs," Ph.D. Thesis, Dept. of Electr. Eng. and Comp. Sci., M.I.T., Cambridge, Mass., 1986.
- ⁵ D.M. Freeman and T.F. Weiss, "On the Role of Fluid Inertia and Viscosity in Stereociliary Tuft Motion: Analysis of Isolated Bodies of Regular Geometry," *Peripheral Auditory Mechanisms*, edited by J.B. Allen, J.L. Hall, A. Hubbard, S.T. Neely, and A. Tubis, New York: Springer-Verlag, 1986, pp. 147-154.
- ⁶ D.M. Freeman and T.F. Weiss, "Hydrodynamic Study of Stereociliary Tuft Motion," The IUPS Satellite Symposium on Hearing, San Francisco, California, July, 1986,
- ⁷ R.C. Kidd, "A Theoretical Study of the Signal Processing Properties of Calcium Channel Kinetics in the Peripheral Auditory System," S.M. Thesis, Dept. of Electr. Eng. and Comp. Sci., M.I.T., Cambridge, Mass., 1986.
- ⁸ B. Delgutte, "Intensity Discrimination: Relation of Auditory-Nerve Activity to Psychophysical Performance," J. Acoust. Soc. Am. 80, S48 (1986).
- ⁹ B. Delgutte, "Peripheral Auditory Processing of Speech Information: Implications from a Physiological Study of Intensity Discrimination," *In The Psychophysics of Speech Perception*, edited by B. Schouten (in press).
- ¹⁰ M.C. Brown, "Morphology of Labeled Efferent Fibers in the Guinea Pig Cochlea," J. Comp. Neurol. (in press).
- ¹¹ M.C. Brown, "Morphology of Labeled Efferent Fibers in the Guinea Pig Cochlea," J. Comp. Neurol. (in press).
- ¹² M.C. Liberman and M.C. Brown, "Physiology and Anatomy of Single Olivocochlear Neurons in the Cat," Hear. Res. 24, 17 (1986).
- ¹³ J.J. Guinan, Jr. and M.P. McCue, "Asymmetries in the Acoustic Reflexes of the Cat Stapedius Muscle," Hear. Res. (in press).
- ¹⁴ J.J. Guinan, Jr., "Effect of Efferent Neural Activity on Cochlear Mechanics." Scand. Audiol. Suppl. *25*, 53 (1986).
- ¹⁵ M.L. Gifford and J.J. Guinan, Jr., "Effects of Electrical Stimulation of Medial Olivocochlear Neurons on Ipsilateral and Contralateral Cochlear Responses," submitted to Hear. Res.
- ¹⁶ W.B. Warr, J.J. Guinan, Jr., and J.S. White, "Organization of the Efferent Fibers: The Lateral and Medial Olivocochlear Systems." *Neurobiology of Hearing: The Cochlea*, edited by R.A. Altschuler, D.W. Hoffman, and R.P. Bobbin. New York: Raven Press, 1986, pp. 333-348.

¹⁷ N.Y.S. Kiang, M.C. Liberman, W.F. Sewell, and J.J. Guinan, Jr., "Single-Unit Clues to Cochlear Mechanisms." Hear. Res. *22*, 171 (1986).

18.2 Auditory Psychophysics and Aids for the Deaf

Academic and Research Staff

L.D. Braida, D.K. Bustamante, H.S. Colburn, L.A. Delhorne, N.I. Durlach, J.A. Frisbie, K.W. Grant, J.D. Koehnke, N.A. Macmillan, E.M. Luongo, K. Payton, W.M. Rabinowitz, C.M. Reed, B. Schneider, V.W. Zue, P.M. Zurek

Students

C.A. Bickley, C.R. Corbett, D.A. Frost, R.F. Goldberg, Y. Ito, G. Kline, D.F. Leotta, M.E. Machado, C. Passaro, M.H. Power, P.M. Peterson, L. Stephens, R.M. Uchanski

18.3 Role of Anchors in Perception

National Science Foundation (Grants BNS 83-19874 and BNS 83-19887)

Louis D. Braida, Nathaniel I. Durlach, Neil A. Macmillan, L. Stephens

This research seeks to provide a unified theory for identification and discrimination of stimuli which are perceptually one-dimensional (e.g., sounds differing only in intensity, Braida and Durlach, 1986). During this period, we examined the identification and (fixed-level) discrimination of synthetic consonant-vowel syllables differing in VOT or in place of articulation.

Stimuli were constructed using Klatt's (1979) software synthesizer. The VOT stimuli consisted of an 85-msec bilabial stop with a VOT ranging from 0 to 36 msec, followed by a 273-msec vowel, /a/. There were nine stimuli; step size was 6 msec, except for the stimuli with a VOT between 12 and 24 msec, where it was 3 msec. The place continuum was created by varying the linear transitions of the first three formants over the first 40 msec. All stimuli in this set were 400 msec in duration.

In the VOT experiments, sensitivity reached a peak in mid-range in all tasks. The peak in fixed discrimination implies a region of high basic sensitivity near 15 msec, since labeling, phonemic or otherwise, plays only a minor role in that task. Similar results were obtained in the place-of-articulation experiments: two peaks appear in the fixed data, one between each phonemic category, and sensitivity follows the same qualitative pattern in all tasks.

The relative size of context-coding noise can be estimated by comparing sensitivity in identification and fixed discrimination tasks. For VOT, context-coding variance is roughly 2/3 the size of sensory variance; for place of articulation the variances are roughly equal. Thus the ability to identify these consonants could not be much better, given the inevitable sensory limitations.

For VOT, sensitivity in identification tasks is best for the extreme /ba/ and /pa/. For place, sensitivity is best near the center of a phonemic category. The best remembered consonants on these continua appear to be the "best" exemplars; other syllables are identified with reference to those prototypes.

It is interesting to compare the present results with those from the vowel studies, and also with our laboratory's experiments of the tone-intensity continuum. First, of the three continua, only consonants exhibit peaks in the basic (sensory) sensitivity function: peaks are observed on vowel and intensity continua only when memory limitations are significant. Second, the range (in inds) of consonant continua is not necessarily less than that of vowel continua. Ades (1977) speculated that some processing differences between consonants and vowels might arise from differences in this range. But the total number of inds between /ba/ and /pa/ is about the same as between /i/ and /l/. Third, context variance is greater for vowels than for consonants; that is, it is easier to label consonants than vowels. Notice that this is true even for two-category continua, where the jnd range is the same. An intensity range of 6 JND's has a context variance roughly 1.5 times the sensory variance, while a range of 15 JND's has a context variance roughly 4 times the sensory variance. For comparable ranges, vowels are more similar to intensity than are consonants with respect to the growth of context variance. Fourth, the stimuli with regard to which identification judgments are made, are different for all three continua. For consonants, they are prototypes; for vowels, stimuli near category boundaries are remembered best; and for intensity, stimuli at the edges that serve as anchors.

The experimental work has required two types of analysis: decision-theoretic (to separate measures of sensitivity from measures of response bias) and statistical (to estimate the reliability of differences in measures of sensitivity and bias. We (Macmillan and Kaplan, 1986) have been developing a technique, based on log-linear models, which integrates these two analyses. In simple detection paradigms log-linear parameters measure the sensitivity and bias parameters of Choice Theory. In experiments with multiple conditions or observers, comparison of different log-linear models permits statistical testing of hypotheses.

References

- ¹ L.D. Braida and N.I. Durlach, "Peripheral and Central Factors in Intensity Perception," in *Functions of the Auditory System*, edited by G.M. Edelman, W.E. Gall and W.M. Cohen. New York: Wiley, 1986.
- ² D.H. Klatt, "Software for a Cascade-Parallel Formant Synthesizer," J. Acoust. Soc. Am. 77, Supp. 1, S7 (1985).
- ³ A.E. Ades, "Vowels, Consonants, Speech and Nonspeech," Psych. Rev. 84, 524 (1977).
- ⁴ N.A. Macmillan and H.L. Kaplan, Log-Linear Models Provide Answers to Signal-Detection Questions. New Orleans, Lousiana: Psychonomic Society, 1986.

Publications

- Goldberg, R.F., "Perpetual Anchors in Vowel and Consonant Continua," M.S. Thesis, Dept. of Electr. Eng. and Comp. Sci., M.I.T., Cambridge, Mass., 1986.
- Goldberg, R.F., N.A. Macmillan and L.D. Braida, "A Perpetual-Anchor Interpretation of Categorical Phenomena on a Vowel Continuum (abstract)," J. Acoust. Soc. Am. 77, Supp. 1, S7 (1985).
- Macmillan, N.A., L.D. Braida and R.F. Goldberg, In *Psychophysics of Speech Perception*, edited by M.E.H. Schouten (Martinus Nijhoff, in press).
- Rosner, B.S., "Perception of Voice-Onset Time: a Signal-Detection Analysis," J. Acoust. Soc. Am. (1984).
- Sachs, R.M. and K.W. Grant, "Stimulus Correlates in the Perception of Voice-Onset Time (VOT): II. Discrimination of Speech with High and Low Stimulus Uncertainty (abstract)," J. Acoust. Soc. Am. 60, S91 (1976).
- Watson, C.S., D. Kewley-Port and D.C. Foyle, "Temporal Acuity for Speech and NonSpeech Sounds: the Role of Stimulus Uncertainty (abstract)," J. Acoust. Soc. Am. 77, Supp. 1, S27 (1985).

18.4 Hearing Aid Research

National Institutes of Health (Grant 6 R01 NS 12846)

Louis D. Braida, Diane K. Bustamante, Lorraine A. Delhorne, Nathaniel I. Durlach, Matthew H. Power, Charlotte M. Reed, Rosalie M. Uchanski, Victor W. Zue, Patrick M. Zurek

This research is directed toward improving hearing aids for persons with sensorineural hearing impairments. We intend to develop improved aids and to obtain fundamental understanding of the limitations on such aids. The work includes studies of 1) effects of noise on intelligibility; 2) amplitude compression; 3) frequency lowering; and 4) clear speech.

Effects of Noise on Intelligibility

We have completed a study (Zurek and Delhorne, 1986) to determine the extent to which the difficulty experienced by impaired listeners in understanding noisy speech can be explained merely on the basis of elevated detection thresholds. Twenty impaired ears of fourteen subjects (age 50 years or younger), spanning a variety of audiometric configurations with average hearing losses to 75 dB, were tested for reception of consonants in a speech-spectrum noise. Speech level, noise level, and frequency-gain characteristic were varied to generate a range of listening conditions. Results with impaired listeners were compared to those of normal-hearing listeners tested under the same conditions but with masking noise added to simulate approximately the impaired listeners' elevated thresholds. Each group of impaired listeners with similar audiograms was simulated with a group of normal-hearing listeners. In addition to this direct com-

parison, results were also compared by computing articulation indices for the various listening conditions, treating hearing loss as resulting from an internal additive noise. The articulation index takes into account the minor differences between actual and simulated thresholds.

The results indicate that masking noise is effective in producing roughly the same level of consonant intelligibility for normal listeners as hearing loss does for impaired listeners. Although there were individual differences, there were no impaired listeners whose results were clearly and consistently outside the range of masked-normal results. When equated for articulation index, 6% of the data points from impaired listeners fell below the range of data from normal listeners, whereas 7% of the impaired points fell above the normal range. When performance at a constant value of articulation index is plotted as a function of the average hearing loss of the listener, there is no clear dependence. Finally, the consonant confusions exhibited by the impaired were well-simulated with noise masking, a result that has been seen in other studies (Wang, Reed, and Bilger 1978; Fabry and Van Tasell, 1986). Thus, our conclusion based on this sample of non-elderly subjects with mild-to-moderate hearing losses is that the primary limitation in understanding noisy speech, aside from the noise itself, is the limited audibility of the speech signal due to elevated thresholds.

Amplitude Compression

Our work on amplitude compression can be subdivided into four projects: 1) Multiband Amplitude Compression; 2) Principal-Component Amplitude Compression; 3) Adaptive Automatic Volume Control; and 4) Peak-Clipping Amplitude Compression.

Multiband Amplitude Compression

To estimate the optimal range of speech levels to present to an impaired listener, intelligibility was measured with three compression systems that differed parametrically in the amount of speech energy presented above the listener's elevated detection thresholds (DeGennaro, 1982). The three systems provided amplification to place 25, 50, or 90 percent of the short-term amplitude distributions in each of 16 frequency bands within the listener's residual auditory area. With band gains set to achieve these varying degrees of audibility, listeners then selected compression ratios to achieve maximum intelligibility and long-term listening comfort while listening to octave bands of compressed running speech. The reference linear amplification system was constructed by having subjects set octave bands of speech to their most comfortable listening level. The four systems were compared in terms of CVC intelligibility.

The principal results of this study, from three ears (of two subjects) with bilateral flat losses and dynamic ranges of 18-33 dB, were as follows: 1) the subjects generally responded to increases in the range of audible speech, from 25 to 50 to 90 percent, with higher effective compression ratios. Measurements of amplitude level distributions suggest that the subjects selected compression ratios that resulted in 1% peak speech levels being below discomfort thresholds; 2) Speech intelligibility scores with the three reference systems were, at best, equivalent to those of the comparison linear system. Further, the best performance with compression was achieved with moderate compression ratios, even though a higher percentage of speech energy was placed above threshold with high compression ratios; 3) Consonant error patterns indicated that while compression improved distinctions between stops and fricatives relative to linear

amplification, distinctions among stops and among fricatives, which are often considered to be dependent on spectral cues, were degraded. It was concluded that it may be necessary not only to improve audibility but also to preserve and/or enhance spectral distinctions.

Principal-Component Amplitude Compression

Experiments were conducted (Bustamante, 1986) with four sensorineural hearingimpaired listeners to test the effectiveness of principal-component amplitude compression (see also Sec. D-1-a). All subjects had bilateral flat losses, roughly normal discomfort levels, and reduced dynamic ranges of 18-31 dB. Two implementations, involving compression of the first principal component (PC1) or compression of both the first and second principal components (PC1 and PC2), were compared to linear amplification (LA), independent compression of multiple bands (MBC), and wideband compression (WC). The MBC system placed 50 percent of the speech energy in each of 16 frequency bands above the subject's detection threshold. The WC system provided high-frequency emphasis of the speech signal prior to the wideband compression amplifier, similar to the most promising compression system studied by Henrickson (1982). The linear amplification system was constructed by having subjects set octave bands of speech to their most comfortable listening level. Frequency shaping was applied in a similar manner to the post-compression output of the two compression systems and the WC system. Speech tests were conducted at two levels: each listener's most comfortable listening level (MCL) and at 10-15 dB below MCL. The five systems were compared on the basis of intelligibility measures using both CVC nonsense syllables (600 trials per system-level combination) and Harvard sentences (I.E.E.E., 1969; 200 keywords per system-level combination).

The major results of this study were that: 1) compression of short-term overall level with compression of PC1 and WC maintains speech intelligibility equivalent to that with LA at MCL and over a wider range of levels than is possible with LA; 2) compression of spectral tilt (by compressing both PC1 and PC2) degrades speech intelligibility; and 3) independent compression of multiple bands with MBC can provide intelligibility comparable to or better than that with compression of PC1 and WC at MCL, but generally does not maintain the same level of performance over a 10-15 dB range of input levels. Vowel scores were high with all processing schemes while consonant scores were significantly lower, particularly for the two more severely impaired listeners. Both compression of PC1 and WC improved consonant scores for these listeners relative to LA but the gains were not large, indicating that either these compression schemes are not capable of making all speech sounds audible or that making speech sounds audible is not sufficient to compensate for all hearing impairments.

Preliminary Study of Adaptive Automatic Volume Control

Automatic Volume Control (AVC) systems are amplitude compressors designed to maintain a relatively constant output level without affecting short-term level variations, as might benefit listeners with peaked articulation functions or limited tolerance ranges for speech (e.g., Poliakoff, 1950). Since AVC systems tend to amplify background noise during pauses in speech, they are likely to prove distracting in many listening situations. To address this problem we have begun to study adaptive AVC systems which can adjust their characteristics automatically on the basis of estimates of speech and noise levels. Bristol (1983) developed an AVC system that combined a compressor having

fixed characteristics with an expandor (intended to reduce output levels during pauses in speech, e.g., McAulay and Malpass, 1980) having a variable expansion threshold. Two expansion ratios (ERs) and two compression processors were studied: a wideband system, and a multiband system with independent compression in each of 16 critical-bandwidth channels.

The systems were evaluated by a normal-hearing listener using conversational sentences presented in a background of steady flat-spectrum Gaussian noise (S/N = +10dB). Measurements indicated that the expansion processing increased the difference between output levels when speech was present and when speech was absent from 10 dB to 17 dB (ER = 2.5) and 31 dB (ER = 4.5) for both compression systems. However the processing introduced some perceptual distortions and reduced keyword intelligibility scores (without processing: 94% in quiet, 84% in noise; compression alone: 74% multiband, 69% wideband; expansion alone: 79% for ER = 2.5, 70% for ER = 4.5). However, when expansion was combined with multiband compression, there was little additional reduction in scores over that with compression alone (74% for ER = 2.5 and 70% for ER = 4.5). These measurements, which were meant to measure the perceptual distortions introduced by the systems rather than to estimate their potential benefit under conditions of varying speech and noise levels, suggest that the expansion processing does not improve intelligibility by attenuating noise during pauses in speech, but may nevertheless be beneficial if used in conjunction with improved multiband AVC compression.

Peak-Clipping Amplitude Compression

In this project we (Silletto, 1984) have begun assessing infinite clipping as a means of amplitude compression by determining: 1) the compression of the range of speech levels when clipping is followed by filtering (as is presumed to occur when clipped speech is analyzed by the ear); and 2) the spectral distortions due to clipping and how these can be minimized by pre-filtering. We have also done preliminary experiments with a three-band clipping system (Hildebrant, 1982). Clipping followed by filtering compresses the range of third-octave speech-level distributions (between 10% and 90% cumulative levels) to 10-15 dB, compared to input ranges of 30-40 dB. This compression is relatively independent of the characteristics of the filter following the clipper. Despite the radical distortion of the input wave, spectral distortions are not severe. An empirical rule of thumb is that if the input spectral envelope has a global maximum at some frequency f, then there will be a maximum near f in the spectral envelope of the output. While there may be additional local maxima added or changed by clipping, generally the largest peak is preserved.

This rule led to the design of a system that separates the first three speech formant regions prior to infinite clipping (Hildebrant, 1982). The output of each of the three clippers is then filtered over the same range as its respective input filter to remove out-of-band distortion. The three channels are added after this post-filtering to form the signal that is presented to the listener. The system was tested under two conditions with recordings of PB-50 word lists and two normal-hearing listeners. In the first condition multi-talker babble was added to the speech prior to processing. The effect of this processing can be summarized as an effective decrease in signal-to-noise ratio of about 6 dB, relative to unprocessed speech. Our results with this system, which has some similarity to a system described by Thomas and Ravindran (1974), do not corroborate their results indicating intelligibility enhancement of noisy speech by clipping. The

second condition was an attempt to simulate a reduced dynamic range. A white noise was added to processed speech; this noise elevated tone-detection thresholds to be approximately constant across frequency. Discomfort threshold was simulated by a visual peak indicator that was lit when the signal exceeded a threshold set to be 25 dB above detection threshold. The listeners adjusted the level of the processed or unprocessed speech (prior to addition with the threshold noise) so that the indicator lit very infrequently when running speech was presented. The unprocessed speech was passed through a whitening filter to produce a flat long-term speech spectrum. With a 25-dB dynamic range, both subjects scored 4% correct words with whitened speech, while with 3-band clipped speech they scored 33 and 40% correct words. Additional tests using Harvard sentences produced scores of 16 and 18% correct key words with whitened speech and 98% correct for both subjects with 3-band clipped speech. These results demonstrate that it is possible for an amplitude-compression system to yield superior intelligibility, at least for normal listeners, relative to a linear system with properly-chosen frequency-gain characteristic. It is also clear that the benefits of an amplitude compressor will be seen only when the listener's dynamic range is markedly smaller than the normal range of speech amplitudes.

Frequency Lowering

We have conducted work on a vocoder-based system for lowering the frequency content of natural speech (Posen, 1984) as well as on the development of low-frequency artificial codes for speech sounds (Foss, 1983; Power, 1985).

Vocoder-Based Frequency Lowering

The vocoder-based method was modeled after a system described by Lippmann (1980) in which speech levels in high-frequency bands are used to modulate low-frequency bands of noise, which are then added to lowpass-filtered speech. In the real-time processing scheme implemented for our studies, the four high-frequency bands were each 2/3-octave wide with center frequencies from 1 to 5 kHz, while the four low-frequency noise bands were each 1/3-octave wide with center frequencies from 400 to 800 Hz. The level of each low-frequency band of noise was controlled by the level of the corresponding high-frequency band of speech (using the obvious monotonic relationship). The modulated noise bands were added to the unprocessed speech signal such that the 10% cumulative level of each noise band was 12 dB below the 10% cumulative level of speech in the same 1/3-octave band. The combined signal was then lowpass filtered at 800 Hz to simulate a sharply sloping, high-frequency hearing loss.

Performance using this lowering system was evaluated relative to performance on lowpass-filtered speech with a cutoff frequency of 800 Hz. Two normal-hearing listeners were trained and tested on the identification of 24 consonants in CV syllables spoken by two male and two female speakers. Results indicated equivalent overall performance (roughly 57% correct) for the two conditions. If only the stops, fricatives, and affricates are considered, however, an advantage of 4-7 percentage points was obtained with frequency lowering, a result consistent with that of Lippmann (1980) whose testing included only this set of consonants. For the remaining consonants (i.e., the semivowels and nasals), an advantage of 10-13 percentage points was obtained for lowpass filtering. Based on these results, which are similar to those observed in our previous studies of warped, lowered speech (Reed et al., 1983, 1985), the frequency-

lowering system was modified to suppress the processing of sounds dominated by low-frequency energy. The energy in the spectrum above 1400 Hz was compared to that in the spectrum below 1400 Hz, and processing occurred only if the ratio of high to low frequency energy exceeded a threshold value of about 4 dB. Post-training tests with the modified system indicated an increase in overall performance of 7 percentage points over lowpass filtering (and over the original lowering system). Performance on the semivowels and nasals was similar for the modified system and for lowpass filtering, and was 10 percentage points higher than for the original processing scheme. A slight advantage was also observed for the reception of fricatives and stops through the modified system compared to the original system, suggesting that the processing of vowels may have had a masking effect on the weaker noise signals resulting from the lowered consonants. The major difference in confusion patterns between the modified lowering system and lowpass filtering lies in improved identification of the features affrication and duration (both of which are related to the perception of high-frequency consonants) through the lowering system. Transmission of information regarding place of articulation was equally poor for lowering and filtering.

Artificial Low-Frequency Codes

Artificial frequency-lowering codes were developed for 24 consonants (C) and 15 vowels (V) for two values of lowpass cutoff frequency F (300 and 500 Hz). Individual phonemes were coded by a unique, non-varying acoustic signal confined to frequencies less than or equal to F. The consonant codes were created by varying frequency content (both center frequency and bandwidth), amplitude, duration, and intervals of silence to specify various abstract properties (i.e., voicing, manner, and place) that serve to classify the consonants. The vowels were generated by varying the spectral shape of a ten-tone harmonic complex with 50-Hz spacing for F=500 Hz and 30-Hz spacing for F=300 Hz, where the relative amplitudes of the components were derived from measurements of natural speech sounds. The vowels were further coded as "long" (220 msec) or "short" (150 msec). Diphthongs were generated by varying the frequency and amplitude of the individual components over the 300-msec stimulus duration.

Performance on the coded sounds was compared to that obtained on single-token sets of natural speech utterances lowpass filtered at F. Identification of coded Cs and Vs was examined in normal-hearing listeners for F=500 and 300 Hz (Foss, 1983; Power, 1985). Subjects trained to asymptotic performance with each stimulus set (24 Cs or 15 Vs) and type of processing (artificial coding or lowpass filtering). For a set of 24 consonants in C-/a/ context, performance on coded sounds averaged 90% correct for F=500 Hz and 65% for F=300 Hz, compared to 75% and 40% for lowpass filtered speech. For a set of 15 vowels in /b/-V-/t/ context, performance on coded sounds averaged 85% correct for F=500 Hz and 65% for F=300 Hz, compared to 85% and 50% for the lowpass filtered sounds. The overall results thus indicate that it is possible to construct low-frequency codes that provide better performance than lowpass filtered natural sounds with the same cutoff frequency (at least for the case in which each phoneme is represented by a single token). Furthermore, for the specific codes considered, the coding advantage is greater for consonants than vowels.

In conjunction with this work, we have begun to investigate the effect of token variations on the intelligibility of speech. The studies of Foss (1983) and Power (1985) included tests of both one-token and three-token sets of filtered stimuli. For consonant and vowel identification at both values of F, performance on the single-token sets was

substantially better than on the multiple-token sets, with the size of the effect averaging about 20 percentage points. An additional study was conducted to examine further the effect of number of tokens on identification of consonants in lowpass-filtered CV syllables (DuBois, 1984). The number of tokens per consonant (all produced by the same female talker) ranged from one (one utterance of each syllable in C-/a/ context) to three (three utterances of each syllable in C-/a/ context) to nine (three utterances per syllable in each of three contexts--C-/a/, C-/i/, and C-/u/). As the number of tokens increased from one to three to nine, identification scores decreased from 79 to 64 to 57 percent correct. Thus, the size of the effect appears to be substantial for small numbers of tokens.

We have also begun to investigate the ability of subjects to comprehend streams of coded consonants and vowels (Reed et al., 1986). Results have been obtained with F=500 Hz for a CV indentification experiment in which C was chosen at random from a set of 24 Cs and V was chosen at random from a set of 15 Vs. Performance averaged across two subjects indicated an average C identification score of 67% correct and an average V identification score of 71%, scores that are somewhat lower than those observed in the fixed-context experiments described above. The percentage of syllables in which both C and V were identified correctly averaged 50%. It should be noted, however, that the two subjects tested in these experiments showed very different performance: whereas the average recognition score for one subject was 40%, for the other subject it was 90%. Also, the difference in performance between the tests with fixed and variable context was much larger for the subject with the lower scores.

Speaking Clearly

CECES SALEACIA COCOCOCO REGION SECONOS SECONOS

In addition to the publication of our first report on the analysis of acoustic differences between clear and conversational speech (Picheny et al., 1986), work completed on our clear-speech project includes detailed duration measurements, expansion of a phonetically-labeled speech database, development of a software system for time-scale modifications of speech, and perceptual evaluation of time-modified speech.

Uchanski et al. (1985) describe detailed measurements of segment durations in both conversational and clear speech. The data, which were obtained from three speakers, show that a distinctly non-uniform lengthening of duration occurs as a speaker changes from a conversational to a clear speaking style. Semivowels and unvoiced fricatives are lengthened the most (75% or greater increase) while voiced stops and short vowels are lengthened the least (less than 30% increase). Results from ANOVA on the duration data indicate that stress is not a statistically significant factor and that prepausal lengthening is statistically significant for many groups of sound segments. Segment position at a phrase boundary has a significant effect on duration in both speaking modes. The prepausal effect accounts for roughly 30% of the total variance in duration measures. The significance of the prepausal effect implies that grammatical structure is important in the production of both conversational and clear speech.

Measurement of temporal and spectral characteristics of conversational and clear speech requires an adequate database. During this grant period an additional 660 nonsense sentences (Picheny et al., 1985) were digitized from analog tape and phonetically labeled. These 660 sentences comprise recordings from three speakers and both conversational and clear speaking styles. Including the 300 previously labeled and

CECECE CANADAS

digitized sentences (50 sentences spoken conversationally and clearly by three speakers), our database now contains a total of 960 sentences.

A software system was developed to produce non-uniformly time-scaled sentences. The first part of this system matches the phonetic sequences of the same sentences spoken conversationally and spoken clearly. From the label-matching procedure, a time alignment of the conversational and clear sentences is generated. The time alignment information is used to interpolate linearly across short-time magnitude spectra. Finally, a new time-scaled speech signal is created from the modified magnitude spectra.

A perceptual experiment was performed to isolate the effect of segment duration on intelligibility of conversational and clear speech. The time-scaling system just described was used to modify conversational sentences to have segment durations typical of clear sentences and also to modify clear sentences to have segment durations typical of conversational sentences. In all, four hearing-impaired subjects listened to nonsense sentences produced or modified in five ways: 1) unprocessed conversational speech; 2) unprocessed clear speech; 3) unprocessed conversational speech with repetition of the utterance; 4) non-uniformly sped-up clear speech; and 5) non-uniformly slowed-down conversational speech. The intelligibility scores averaged over the four subjects (roughly 550 items per condition per listener) were:

Condition	1	2	3	4	5
Score (%)	77	91	82	71	74

These results confirm the difference in intelligibility between naturally-produced clear and conversational speech. Repetition of a conversational sentence improves intelligibility, but not nearly as much as speaking clearly. (If the repetition had involved distinct utterances, this improvement would undoubtedly have been greater, but we do not know how much greater). Unfortunately, both modified productions, slowed-down conversational and sped-up clear speech, are perceived less well than natural conversational speech. However, the degradation in performance with these modified productions is less than the degradation seen with uniformly time-scaled speech (Picheny et al., 1986). One interpretation of this difference is that time scaling at the segmental level more closely approximates the natural changes from conversational to clear speech.

18.5 Additional Work

PROPERTY SERVICES CONTRACTOR SERVICES SERVICES

MORRED AND MARKET PROPERTY OF THE PROPERTY OF

Simulation of Hearing Impairment

In a preliminary study (Gilbert, 1984), a biased rectifier was used as a detector in a model of a sensorineural hearing loss. The rectifier parameters were varied to reflect different levels of hearing loss. The output of the rectifier was calculated numerically to generate predictions of recruitment, temporal integration at absolute threshold, and tone masking. With appropriate choices of parameters, the model was able to predict

recruitment and temporal integration, but it failed to predict empirically-observed patterns of tone masking in hearing-impaired listeners.

Use of Articulatory Signals in Automatic Speech Recognition

Automatic speech recognition systems generally attempt to determine the spoken message from analysis of the acoustic speech waveform. In this research we evaluated the performance of the IBM Speech Recognition System (Jelinek, 1985) when the input included measurements of selected articulatory actions occurring during speech production. The system achieved significant recognition rates (for isolated words in sentences) when the acoustic signal was disabled and the input was restricted to articulatory signals similar to those sensed by users of the Tadoma method of tactile-speech recognition (Reed et al., 1985b). In other tests the availability of articulatory inputs improved recognition performance when the acoustic signal was sufficiently degraded by additive white noise. Improvements were observed independent of whether the recognition system made use of the likelihood that words would appear in the vicinity of the other words in a given sentence. (Portions of this work were conducted at, and supported by, the I.B.M. T.J. Watson Research Center.)

References

- ¹ P.M. Zurek and L.A. Delhorne, "Consonant Reception in Noise by Listeners with Mild and Moderate Hearing Impairment," (submitted to J. Acoust. Soc. Am. 1986).
- ² S. DeGennaro, "Multi-Channel Syllabic Compression for Severely Impaired Listeners," Ph.D. Thesis, Dept. of Electr. Eng. and Comp. Sci., M.I.T., Cambridge, Mass., 1982.
- ³ D.K. Bustamante and L.D. Braida, "Compression Limiting for the Hearing Impaired," (submitted to J. Rehab. Res. and Dev. 1986).
- ⁴ K.A. Siletto, "Evaluation of Infinite Peak Clippings as a Means of Amplitude Compression," M.S. Thesis, Dept. of Electr. Eng. and Comp. Sci., M.I.T., Cambridge, Mass., 1984.
- ⁵ E.M. Hildebrant, "An Electronic Device to Reduce the Dynamic Range of Speech," S.B. Thesis, Dept. of Electr. Eng. and Comp. Sci., M.I.T., Cambridge, Mass., 1982.
- ⁶ M.P. Posen, "Intelligibility of Frequency Lowered Speech Produced by a Channel Vocoder," S.M. Thesis, Dept. of Electr. Eng. and Comp. Sci., M.I.T., Cambridge, Mass., 1984.
- ⁷ K.K. Foss, "Identification Experimentation on Low-Frequency Artificial Codes as Representation of Speech," S.B. Thesis, Dept. of Electr. Eng. and Comp. Sci., M.I.T., Cambridge, Mass., 1983.
- ⁸ M.H. Power, "Representation of Speech by Low Frequency Artificial Codes," S.B. Thesis, Dept. of Electr. Eng. and Comp. Sci., M.I.T., Cambridge, Mass., 1985.

- ⁹ C.M. Reed, B.L. Hicks, L.D. Braida, and N.I. Durlach, "Discrimination of Speech Processed by Low-Pass Filtering and Pitch-Invariant Frequency Lowering," J. Acoust. Soc. Am. 74, 409 (1983).
- ¹⁰ C.M. Reed, L.D. Braida, N.I. Durlach and K.I. Schultz, "Discrimination and Identification of Frequency-Lowered Speech in Listeners with High-Frequency Hearing Impairment," J. Acoust. Soc. Am. 78, 2139 (1985).
- ¹¹ C.M. Reed, M.H. Power and N.I. Durlach, "Development and Testing of Artificial Low-Frequency Speech Codes," (to be submitted to J. Speech Hear. Res. 1986).
- ¹² M.A. Picheny, N.I. Durlach and L.D. Braida, "Speaking Clearly for the Hard of Hearing. III: an Attempt to Determine the Contribution of Speaking Rate on Differences in Intelligibility between Clear and Conversational Speech," (to be submitted to J. Speech Hear. Res. 1986).
- ¹³ R.M. Uchanski, C.M. Reed, N.I. Durlach and L.D. Braida, "Analysis of Phoneme and Pause Durations in Conversational and Clear Speech," J. Acoust. Soc. Am. 77, Supp. 1 (1985).
- ¹⁴ M.A. Picheny, N.I. Durlach and L.D. Braida, "Speaking Clearlyfor the Hard of Hearing. I: Intelligibility Differences between Clear and Conversational Speech," J. Acoust. Soc. Am. 78, 96 (1985).
- ¹⁵ E.I. Gilbert, "Investigation of Sensorineural Hearing Impairment Using a Center-Clipping Model," S.B. Thesis, Dept. of Electr. Eng. and Comp. Sci., M.I.T., Cambridge, Mass., 1984.

Publications

- Braida, L.D., "Articulation Testing Methods for Evaluating Speech Reception by Impaired Listeners," in *Speech Recognition by the Hearing Impaired*, edited by E. Elkins, ASHA Reports *14*, 26 (1984).
- Braida, L.D., "Speech Processing for the Hearing Impaired," Proceedings of the Second International Conference on Rehabilitation Engineering, Ottawa, Canada, 1984.
- Braida, L.D., M.A. Picheny, J.R. Cohen, W.M. Rabinowitz and J.S. Perkell, "Use of Articulatory Signals in Speech Recognition," (to be submitted to J. Acoust. Soc. Am.).
- Bustamante, D.K. and L.D. Braida, "Principal Component Amplitude Compression of Speech for the Sensorineural Hearing Impaired," Proceeding of the 7thAnnual Conference of the I.E.E.E. Engineering in Medicine and Biology Society, Chicago, Illinois, 1985, p. 1096.
- Bustamante, D.K. and L.D. Braida, "Principal-Component Amplitude Compression for the Hearing Impaired," (submitted to J. Acoust. Soc. Am. 1986).

- Bustamante, D.K., E. Hildebrant, K. Silleto, P.M. Zurek, L.D. Braida and N.I. Durlach, "New Amplitude Compression Techniques," Proceedings of the International Conference on Rehabitation Engineering, Ottawa, Canada, 1984, p. 293.
- DeGennaro, S., L.D. Braida and N.I. Durlach, "Multichannel Syllabic Compression for Severely Impaired Listeners," J. Rehab. Res. and Dev. 23, 17 (1986).
- Milner, P., L.D. Braida, N.I. Durlach and H. Levitt, "Perception of Filtered Speech by Hearing-Impaired Listeners," in *Speech Recognition by the Hearing Impaired*, edited by E. Elkins, ASHA Reports *14*, 30 (1984).
- Picheny, M.A., N.I. Durlach and L.D. Braida, "Speaking Clearly for the Hard of Hearing. II: Acoustic Characteristics of Clear and Conversational Speech," J. Speech Hear. Res. (1986).

Theses

- Bristol, N., "Automatic Volume Control and Noise Suppression for Hearing Aids," S.M. Thesis, Dept. Electr. Eng. and Comp. Sci., M.I.T., Cambridge, Mass., 1983.
- Bustamante, D.K., "Multichannel Syllabic Compression for Severely Impaired Listeners," Ph.D. Diss., Dept. Electr. Eng. and Comp. Sci., M.I.T., Cambridge, Mass., 1986.
- Laves, A.L., "Consonant Intelligibility and Acoustic Analysis in Clear and Conversational Speech," S.B. Thesis, Dept. Electr., Eng. and Comp. Sci., M.I.T., Cambridge, Mass., 1982.

18.6 Multimicrophone Monaural Aids for the Hearing-Impaired

National Institutes of Health (Grant 1 RO1 NS 21322)

H. Steven Colburn, Cathleen R. Corbett, Nathaniel I. Durlach, Patrick M. Peterson, William M. Rabinowitz, Patrick M. Zurek

The goal of this work is the development of systems that sample the acoustic environment at multiple points in space to form a single-channel output providing enhanced speech intelligibility for the hearing-impaired. Work in the past year has included studies of: 1) an adaptive beam-steering algorithm for interference reduction; and 2) coding of multiple messages for monaural presentation.

1) Adaptive processing schemes vary the complex weightings applied to the microphone signals so that the beam pattern tracks changes in the acoustic environment. Our research in this area (Peterson, 1987; Peterson et al., 1987) has focused on the constrained adaptive beamforming method of Griffiths and Jim (1982). Constrained adaptive beamformers are based on the assumptions that the target and interference are uncorrelated and that the target direction is known, and operate to minimize total ouput power under the constraint that signals from the target direction are preserved. Minimization of total output power then implies minimization of interference and

maximization of target-to-interference ratio. Although the Griffiths-Jim method adapts more slowly than some other methods (e.g., Cioffi and Kailath, 1984), it asymptotically bounds the performance that can be achieved by any constrained adaptive beamformer and is relatively simple to realize.

A two-microphone version of a Griffiths-Jim beamformer has been studied in three environments with different degrees of reverberation. Intelligibility tests were performed on normal-hearing subjects using sentences as the target signal and speech babble as the interference. The microphone signals were generated by passing the target and the interference through simulated room transfer functions (Peterson, 1986). It was assumed that the microphones were separated by 20 cm, that the microphones and sound sources were omnidirectional, and that the interference arose from a single source 45 degrees from the straight-ahead target. The simulated rooms were chosen to represent anechoic space (no reverberation), a living room (moderate reverberation) and a conference room (strong reverberation). Intelligibility of processed sentences was compared to that of unprocessed sentences presented binaurally. All system parameters were held fixed except the length of the adaptive filter; preliminary examination suggested that two lengths be tested, 10 ms and 40 ms. Longer filters can potentially remove more interference, but at the cost of more computation and longer adaptation times. In all cases, the intelligibility tests estimated the asymptotic (adapted) performance of the system. Empirical adaptation times, with the given system parameters, were of the order of one second.

The results of these tests indicate that under the conditions of zero-to-moderate reverberation, the interference reduction achieved by the array exceeds that achieved by the binaural auditory system. In the anechoic condition the interference was reduced by 30 dB, while in the living room environment the interference was reduced 9 dB by the 10-ms filter and 14 dB by the 40-ms filter. Furthermore, under the conference room condition, where reverberation was most severe, intelligibilty performance was not degraded by processing. Research designed to determine the generalizability of these results and their implications for a practical hearing aid is now underway.

2) If we assume that directional channels can be built (i.e., that simultaneous spatially-diverse inputs can be resolved into separate signals), then we must determine how to code the multiple simultaneous signals into a monaural signal that facilitates attention to each of the individual messages. We have completed a study of filtering as a means of coding two or four sentence-length messages (Corbett, 1986). In particular, we evaluated the extent to which the presentation of individual messages in separate spectral regions enhances the joint intelligibility of all messages over that obtained when the wideband messages are simply summed. Different transfer functions were assigned to the different channels in such a way that intelligibility scores were roughly independent of which channel was chosen to carry the target message (and which channels carried the interfering messages). Overall performance was measured by the joint intelligibility, i.e., the intelligibility score averaged over talker/channel combinations used for the target. A given filter configuration was judged to be helpful if the joint intelligibility for this configuration was greater than the joint intelligibility for the reference case in which there was no filtering and all voices were summed in a wideband channel.

Although our results are preliminary, they suggest that, at least for the case of four different talkers speaking simultaneously, joint intelligibility can be improved by the use

of differential filtering. For the best filter configuration tested, the joint intelligibility was 39% compared to the wideband reference score of 22%. Some of our results, however, were less positive. For example, tests with two talkers, easy speech materials, and noise masking (to prevent saturation of intelligibility scores) showed no improvement for filtering. Nevertheless, based on all results to date, we believe that judiciously chosen filtering will provide an overall gain in joint intelligibility for many cases likely to be encountered in real environments.

References

TEST PERSONAL PERSONAL ASSESSED ASSESSED ROOMERS ESPERSON PERSONAL ASSESSED PROFESSO PERSONAL PROFESSOR PERSONAL PERSONAL PROFESSOR PERSONAL PERSONAL PROFESSOR PERSONAL PERSONAL PROFESSOR PERSONAL PROFESSOR PERSONAL PERSONAL

- ¹ P.M. Peterson, "Using Linearly-Constrained Adaptive Beamforming to Reduce Interference in Hearing Aids from Competing Talkers in Reverberant Rooms," Proceedings of the International Conference on Acoustic Signal Processing, 1987.
- ² P.M. Peterson, N.I. Durlach, W.M. Rabonowitz and P.M. Zurek, "Multimicrophone Adaptive Beamforming for Interference Reduction in Hearing Aids," J. Rehab. Res. Dev. (1987).
- Griffiths and C.W. Jim, "An Alternative Approach to Linearly Constrained Adaptive Beamforming," I.E.E.E. Trans. Antennas Propag. AP-30, 27 (1982).
- ⁴ J.M. Cioffi and T. Kailath, "Fast, Recursive Least Squares, Transversal Filters for Adaptive Filtering," I.E.E.E. Trans. Acoust. Speech Signal Process. 32, 304 (1984).
- Peterson, "Simulating the Response of Multiple Microphones to a Single Acoustic Source in a Reverberant Room," J. Acoust. Soc. Am. 80, 1527 (1986).
- ⁵ C.R. Corbett, "Filtering Competing Messages to Enhance Mutual Intelligibility," M.S. Thesis, Dept. of Electr. Eng. and Comp. Sci., M.I.T., Cambridge, Mass., 1986.

19.0 Physiology

Academic and Research Staff

Prof. J. Lettvin, G. Geiger

CONTROL DISSESS CONTROL SYSTEM SECTION

2000 - Transport - 2000 - Transport - Tran

Three or four studies have been issued in the past year from the laboratory of nervous physiology. These are diverse and will be treated separately. We report only on that work is now in print or are ready to be published.

19.1 Strategies of Perception

Gad Geiger, Jerome Lettvin

Three years ago we began studies on peripheral vision. Two papers have been issued, announcing some of the results.^{1,2} These papers are explicit and do not much go beyond the data. It is useful to lay forth here a more general account of the underlying ideas and the meaning of our results. These results are presented first in a cursive way.

There is a visual process, called "lateral masking," by which aggregates of forms take on a textural quality. For example, text presented a few degrees away from the center of gaze is clearly text, but not easily read. It is as if the letters in a group interfere with each other, so that the clear perception of any one letter is compromised. This can be shown not to depend on acuity, which is quite high for peripheral vision in the vicinity of the fovea. For perception such an aggregate seems to possess at best a statistics rather than a precise spatial order. There is a distribution of letter like things, and in this distribution the interior members are clear but not distinct. That is easy enough to check by fixing your eye on some letter in the middle of a line and finding that you can't read those words of three or more letters in length, that lie two words away from the point of fixation.

We showed that the information needed to identify an ordinarily masked letter in the near peripheral field, is not lost by some early visual process since the letter can be made to stand out from the texture when its twin is presented at the point of fixation.

In the course of these experiments we noted that a few subjects did not seem to show much lateral masking in the near periphery. They scored remarkably accurately in identifying each of the letters in short strings of letters presented as far as 10 (degrees) away from the point of fixation. These subjects, interviewed after the study was completed, shared a common property, dyslexia.

Accordingly we were led to compare dyslexics with ordinary readers. To put the results succinctly, dyslexics tend to have visual masking in and around the center of gaze, and much less a few degrees away from that center - the reverse of what holds for ordinary readers.

We devised a series of simple tests that distinguished clearly three populations: ordinary readers, residual dyslexics (who had learned to read), and severe dyslexics (who could hardly read). In the severe adult dyslexics we then showed what we had supspected - that they could learn to read using their peripheral vision. When members of this last group learned to read, they began to show increased masking in the further periphery and a relief of the sever masking immediately around the region of foveal vision. (We now have about fifteen such cases but this material is not yet published).

Our view is that masking is a learned process, strongly task-dependent. It is not intrinsic to visual process in the sense that it follows immutably from some anatomical and physiological imperative. Instead it is a convenient learned way of reducing task-irrelevant detail to texture, while preserving task-relevant detail as form. Most important to us, learning the strategy of masking depends strongly on the motor aspects of practice in performing tasks. This much can be inferred by analogy with the studies on hand-eye coordination done by Richard Held, Ivo Kohler and others. We took advantage of this prior work in designing the pedagogy by which we could bring adult dyslexics from 3rd grade level to 10th grade level over about four months.

But we have gone further in our concept of such processing. We feel that most of us have several task-determined strategies between which we switch on the instant, (tantamount to flipping between modes of operation), as the task requires. Again, such switching has been described for more complex forms of perception by Kohler, Held, and others, so it should come as no surprise that he same principle may hold on elementary levels. What is most interesting is that, as with dyslexics, a strategy can become "frozen."

Since we can now show these attributes of vision both psychophysically and clinically, we feel that the ideas have some strength. Clearly a more precise account is needed, and, indeed, we have one, but it is not easily compressed to the sort of sketch appropriate here.

19.2 Image Sharpening in the Photoreceptor Layer of the Eye

Jerome Lettvin and Gill Pratt

KANANA PIKKAKA PARENA P

A century ago, Helmholtz remarked that he would summarily discharge anyone who brought him a human eye as a good optical device. The reason is obvious. Under optimum focus and aperture of the normal eye, a star-point at infinity is given in the image as a more or less Gaussian distribution of light some 5-10 cones in diameter. Yet whoever possesses a normal eye can see distinctly two stars as two light points when they are separated by a cone-width or even less in the visual field. In short, we see better than is accounted by the optical transfer function.

This argues for a sharpening operation in the retina, somewhat akin to that used conventionally nowadays in computer-aided image processing. Conventional opinion holds that such process occurs in the neural components of the retina, e.g., bipolar and horizontal cells, those neurous that receive information from the receptors. But aside from economy, several reasons have inclined us to reject that view and we are about to publish a working model by which the needed image sharpening is provided by the receptor layer itself.

The basic problem with image sharpening taking place after the receptors is that the receptors are interconnected resistively along the image plane. There are, in fact, two levels of this connectivity between photoreceptors, and the connections are well attested physiologically and anatomically. The lateral spread of signal, with the receptors as nodes in a resistive net, would be even more conducive to informational blur than the optics itself. Thus, if image-sharpening is deferred to the post-receptor nervous tissue, the two blurring factors, taken together, optical and electrical, make for a far worse condition than the blur alone.

Accordingly, on the thesis that poor engineering is not preserved in evolution, we reconsidered the problem. There is, of course, an obvious advantage to a resistive net if the nodes, the receptors, are made voltage sensitive current sources. That is, given a transduction of light to signal voltage at each receptor, and an individual production of current in each receptor that clamps that voltage, the receptor acts as a voltage source in the net, and the current used to clamp that voltage measures the Laplacian between the receptor and its surrounding neighbors. Given that the receptors are effectively AC devices, the Laplacian is the preferred sharpening function to be applied to the image.

This is easy enough to show both formally and by a simple two stage (two transitor) model, and it works quite ideally.

Required for the usefulness of the model is that there are at least: 1) an ionic conductance in the outer segment of the photoreceptor, and that it is governed by photon capture; 2) a voltage-sensitive pump (current generator) for the same ionic species in the inner segment; and 3) a lateral resistive connectivity between receptors.

All three features have been established by physiologists so that the model we propose is not without merit. We have prepared a note on this matter. It has rather more technical detail, and we are submitting it for publication.

19.3 Tectal Processing of Visual Information in a Frog

Arthur Grant, Thomas Sciascia, Jerome Lettvin

Optic tectum is the most massive part of the visual brain in the frog. Its fine anatomy is fairly regular, a sheet of processing columns that map the visual field. But there is no firm description yet of the interval connections.

All of the errors that beset the interpretation of electrical records are first order in this structure. For example, in the uncurarized frog, the axons of the tectal neurous are quite active, but the cell-bodies seldom fire so that the easily had cell-body records are most often useless, while the axons are well-nigh unrecordable above noise level. In addition, there are many cells without axons, and many with what Szekely and Lazar thought to be electrically active dendritic parts. However they had no specific evidence for that conjecture. We can now supply it.

One of the puzzles has been to account for the signals that seem to be from the optic nerve fibers themselves. These are the most salient and reliable transients recorded in the tectum, well-matched to the activity of single fibers in the optic nerve. However,

we have found them to be due to the firing of dendritic appendages of tectal neurous so that they do not have a one-to-one relation with the retinal axous. What is more, these appendages are connected among themselves as Szekely and Lazar have shown so that they form nets. This fact has provided a strong tool for parsing some of the tectal processing. It will be submitted for publication soon.

References

- ¹ G. Geiger and J.Y. Lettvin, "Enhancing the Perception of Form in Peripheral Vision," Perception 15, 119 (1987).
- ² G. Geiger and J.Y. Lettvin, "Peripheral Vision in Persons with Dyslexia," New England J. Med *316*, 1238 (1987).

20.0 Molecular Physics

20.1 Molecule Microscopy

Academic and Research Staff

Prof. J.G. King, Prof. R.M. Latanision, Dr. A. Essig, Dr. J.A. Jarrell, Dr. S.J. Rosenthal

F.L. Freidman Chair National Institutes of Health (Grant AM 25535) Whitaker Foundation

We have been working on molecule microscopy (MM) ever since the first ideas were formulated two decades ago. Much has been accomplished towards defining this rich and complex field; but no single sufficiently important scientific or engineering application has emerged with which we could achieve the successful demonstration needed to guarantee adequate support and rapid progress.

MM involves the detection, with spatial and temporal resolution, of neutral molecules emitted from samples. The sample may be rough or smooth, thick or thin and may be metal, semiconductor, plastic, ceramic, natural or man-made biomaterial. Emitted molecules may diffuse through the sample or evaporate from its surface. These molecules may have been part of the sample or previously deposited from a staining molecular beam. They may evaporate spontaneously either uniformly or non uniformly spatially; in either case spatial resolution is obtained by limiting the solid angle in which molecules are detected by scanning with a small detector or aperture, at some distance from the sample or with a micropipette or field ionizing tip in contact with the sample. Molecules may also evaporate as a result of localized stimulation by focussed beams of radiation or particles, in which case spatial resolution is provided by scanning the beam. Sample temperature is usually set to hold general evaporation at the desired level or to preserve sample integrity. Finally, samples may be in UHV, gaseous atmospheres or in liquids as required provided appropriate detectors are used.

It is clear that the MM is not a single instrument but rather a collection of techniques chosen depending on the nature of the sample and the problem to be investigated. In the next paragraphs we describe some of the work that has been done to date.

Our first instrument used a small scanned aperture to provide spatial resolution. Low resolution images from a variety of samples were obtained. Another kind of MM depends on localized thermal desorption and, because we wish to study the distribution of water on biomaterials we have investigated the desorption of water from representative proteins, carbohydrates and liquids applied in monolayer amounts to a heatable platinum surface. We have also investigated by similar methods the desorption of water from cells grown in situ, cholesterol, DPPL, acrylic gels and CuSO₄. Focussed laser light pulsed and scanned, has been used for localized sample heating so as to produce desorption. Yet another MM uses pulsed focussed electron beams to desorb molecules by ESD. We have measured the cross section for these processes under various conditions. This data along with our extensive experience with field desorption and ionization has made it possible to design an instrument capable of detecting small numbers of molecules adsorbed on sample regions of 1 nm extent or less.

This emphasis on water in biomaterials stems from our conviction that knowledge of the distribution of water on biological samples will shed light on the various mechanisms that provide specificity and selectivity in the interaction of various entities, from ions to viruses.

We have constructed two scanning micropipette MM and have used them to study transport of water in surviving tissue immersed in appropriate solutions. We found that contrary to some hypotheses there is negligible water transport through tight junctions between cells. We are currently considering applying these instruments to studies of localized gaseous transport in polymeric materials, as used in such varied applications as drug release systems and electronic device packaging.

We have designed a specialized MM for studies of hydrogen transport along grain boundaries in ferric metals. This hydrogen appears responsible for stress corrosion fracture according to several hypothetical mechanisms. We also prepared a grant proposal, but received no funding.

Lack of funding has plagued the development of these techniques and devices from the start. With hindsight it seems obvious that substantial funds would not be available to develop complex systems in which problems, solutions and applications cannot be known in advance. Nonetheless, we have accumulated a large amount of miscellaneous data, obtained preliminary results, designed apparatus and prepared grant proposals. Progress has been debilitatingly slow, however, since in a project such as this much effort necessarily is expended in developing each part of the system with many false starts and blind alleys.

CHARLES SECRETARION SECRETARION SECRETARION MANAGEMENT

20.2 Electrical Neutrality of Molecules

Academic and Research Staff

Prof. J.G. King, Prof. A.P. French

International Business Machines, Inc. F.L. Friedman Chair

The assumed equality of the electron and proton charges represents a symmetry in nature which corresponds to no known conservation law, but is based directly on a series of sensitive experimental measurements dating from 1925. These measurements have involved four different experimental techniques: 1) the gas-efflux method; 2) the isolated-body method (analogous to the Millikan oil-drop experiment); 3)—the molecular-beam method; and 4) acoustical methods. During the period 1960-1965 we carried out many gas efflux experiments. In these experiments the electric charge carried by a gas can be determined by measuring the change in potential of the electrically insulated container from which it escapes. A reliable upper limit on the net charge per molecule can be inferred provided that suitable precautions are observed. Many procedures, tests and calibrations intended to prevent the appearance of spurious charge or the masking of genuine charge were carried out. The result of 1356 effluxes with seven gases (H₂, D₂, He, N₂, O₂, A, SF₆) under various experimental conditions can be summarized thus: no molecule carries a charge greater in magnitude than 10⁻²⁰ of the magnitude of the elementary charge, e.

Further interpretations arise with various assumptions. Assuming that the sum of the proton and electron charge $Q_n + Q_e = \alpha e$ and that the charge on the neutron $Q_n = \beta e$ the A and N₂ data yield $\alpha \le (0 \pm 0.1) \times 10^{-20}$ and $\beta \le (\pm 0.4) \times 10^{-20}$. Assuming that $Q_p + Q_e = Q_n$ (as suggested by charge conservation, the decay of the free neutron and the neutrality of (anti) neutrinos), that the charges add up in atoms or molecules composed of Z protons and electrons and N neutrons and that matter is not a mixture of constituents with opposite charge differences, the experiments with SF₆ imply $Q_p + Q_e = Q_n \le (0 \pm 3)x10^{-23}e$. Finally, assuming that the charge has a velocity dependence $q = q_0(1 + kv^2/c^2)$ and that protons and electrons in argon have mean square velocities corresponding to their binding energies gives $k \le 5x10^{-20}$. In 1973 we published results of first acoustical neutrality experiment in which an oscillating electric field drives the hypothetically charged gas to produce sound. Later attempts to refine this method ran into difficulties with large second harmonic signals which put impossibly stringent requirements on linearity and waveform purity. Now, however, we feel that the inverse experiment in which an acoustic standing wave results in detectable periodic oscillations of charge density can yield limits six to eight orders of magnitude better than any previous result. The experiment is in effect a periodic version of the gas efflux method with no average transport of gas. Design studies and pilot experiments are now being carried out in order to prepare a proposal.



REGISSION - EXCESSES - REGISSION - REGISSION - PROPERTY - PROPERTY - STATES

21.0 Quantum Optics and Photonics

Academic and Research Staff

Prof. S. Ezekiel, Dr. P.R. Hemmer, J. Kierstead, Dr. H. Lamela-Rivera, B. Bernacki, D. Morris

Graduate Students

L. Hergenroeder, S.H. Jain, V.D. Natoli, C.E. O'Connor III, V. Pevtschin, M.G. Prentiss, M.S. Shahriar, S.P. Smith, F. Zarinetchi

Undergraduate Students

S. Miller, I. Robinson, R.S. Rizk, C. Neils, J. Kuchar

U.S. Air Force - Office of Scientific Research (Contract F49620-82-C-0091)
U.S. Air Force - Rome Air Development Center
Joint Services Electronics Program (Contract DAAG29-83-K-0003)
National Science Foundation Grant (Grant PHY 82-10369)

21.1 Investigation of Error Sources in a Laser Raman Clock

We have continued our precision studies of laser induced stimulated resonance Raman interactions in a sodium atomic beam with emphasis on Ramsey's method of separated oscillatory fields. We observed Raman-Ramsey fringes for a field separation of up to 30 cm, and the data were consistent with theoretical predictions. We have also been investigating the performance of a clock based on this interaction in a sodium atomic beam to determine the feasibility of such a scheme and to demonstrate any possible advantages over conventional microwave excited clocks. Recent performance showed a stability of 1 x 10⁻¹¹ for a 5000 second averaging time. This compares favorably with commercial cesium clocks when difference in atom transit time and transition frequency are taken into consideration.

Currently we are studying potential sources of long term frequency error in the Raman clock. Some of the error sources are similar to those in microwave clocks, such as the effects of path length phase shift, external magnetic fields, background slope, atomic beam misalignment and second order Doppler. The other error sources are unique to the Raman clock and include laser frequency detuning, laser intensity changes, laser beam misalignment, optical atomic recoil, the presence of nearby hyperfine levels, and other smaller effects.

Our present investigations have centered around error sources that are unique to the Raman process. For example, we have found that laser detuning from resonance by 1% of the atomic linewidth can cause a fractional error of 2.4×10^{-11} . Also a 1% change in laser intensity can generate an error of 2.5×10^{-12} . Efforts are underway to find ways of reducing both detuning and intensity errors. In addition, laser misalignment can also be a source of significant error. A laser beam translation of 0.1 mm can cause an error

of 3 x 10^{-11} . The use of fiberoptics is being investigated for the minimization of misalignment error.

Publications

Hemmer, P.H., G.P. Ontai, and S. Ezekiel, "Precision Studies of Stimulated Resonance Raman Interactions in an Atomic Beam," J. Opt. Soc. Am. B (1986).

Hemmer, P.H., V.D. Natoli, M.S. Shahriar, B. Bernacki, H. Lamela-Rivera, S.P. Smith and S. Ezekiel, "Study of Several Error Sources in a Laser Raman Clock," Proceedings of 41st Annual Frequency Control Symposium, Philadelphia, Pennsylvania, 1987.

21.2 Physics of Stimulated Resonance Raman Effect

In conjunction with our experimental studies of the stimulated resonance Raman effect for potential clock applications, we have also performed detailed theoretical studies. Among other things, these theoretical studies have resulted in the development of a classical mechanical model for the quantum mechanical resonance Raman process, namely a set of three classical coupled pendulums.

In this pendulum model, individual pendulum oscillations correspond to atom field composite states and the coupling springs serve to couple the pendulum oscillations in the same way that the laser field couples atom field composite states. Using standard approximations for atom field calculations, it is found that a one to one correspondence exists between the (complex) pendulum oscillation amplitudes and the (complex) composite state amplitudes. Moreover, it is also found that the familiar atom field "dressed" states are analogous to normal modes of the coupled pendulum system.

Thus, the pendulum system provides the means to actually "see" what happens in the resonance Raman interactions. This allows us to give simple physical interpretations to many of our more puzzling experimental observations. For example, in our two zone Raman studies in an atomic beam, we find that the effects of laser detuning becomes smaller at higher laser intensities. Using pendulums, we find that this occurs because the Raman interaction generates a single atom field superposition dressed state at high laser intensities, (single pendulum mode); but laser detuning effects result from the interference of two superposition states in the region between interaction zones.

In addition to the pendulum analogy, we are also performing density matrix calculations of the Raman lineshapes and comparing these to our experimental results.

21.3 Observation of Raman-Ramsey Fringes in a Cesium Atomic Beam Using a Semiconductor Laser

Stimulated resonance Raman interactions have been observed in a cesium atomic beam using a semiconductor laser at 852 nm. The semiconductor laser, which has a linewidth of 30 MHz, was amplitude modulated at about 4.6 GHz and the resulting sidebands were used to excite the Raman transition at 9.212 GHz. Using separated field excitation, Ramsey fringes for a separation of 8 cm have been observed with a linewidth

of approximately 2 kHz. This fringe width is consistent with the theoretically predicted value. Work is under way to use the Raman/Ramsey fringe to stabilize a microwave oscillator in a way similar to our sodium Raman clock employing a dye laser.

The interest in the semiconductor laser excited Raman cesium clock is based on its potential small size, light weight, and low cost, as well as high performance.

21.4 Influence of Atomic Recoil on the Spectrum of Resonance Fluorescence From a Two-Level Atom

The fluorescence spectrum of a two-level atom, which is of fundamental importance to the understanding of atom-field interaction, has received considerable attention during the past few years. Calculations show that for a stationary two-level atom in a monochromatic excitation field, the fluorescence spectrum is composed of three peaks which are symmetric with respect to the excitation-field frequency. A number of experiments have been conducted to measure this spectrum, and such symmetric spectra have indeed been observed. However, under certain conditions, asymmetric spectra were also observed. In particular, we observed a symmetric spectrum for atoms in a uniform field and an asymmetric spectrum in a field gradient.

We have recently investigated the cause of this asymmetry which has been hitherto unexplained and we now feel confident that it is caused by atomic recoil. We have performed a detailed calculation that takes into account atomic recoil, the field gradient and the direction of the observation of the fluorescence and showed that the spectrum of resonance fluorescence becomes asymmetric consistent with observations. Moreover, we also showed that by including the forces on the atoms due to the laser field, asymmetry can also occur in a uniform field.

Publications

Prentiss, M.G. and S. Ezekiel, "Influence of Atomic Recoil on the Spectrum of Resonance Fluorescence From a Two-Level Atom," Phys. Rev. A 35, 922 (1987).

21.5 Studies in a Passive Resonator Gyroscope

A passive resonator rotation sensor or "gyroscope" is a ring resonator in which counter-propagating light beams within the resonator experience a non-reciprocal phase shift due to an applied rotation rate. Because of this phase shift the resonance frequency of the resonator for the counter-propagating directions are not identical. This difference in resonance frequency, Δf , is measured by means external to the resonator, e.g., by locking the frequencies of the external laser beams to corresponding resonances of the cavity.

Our research demonstrated that because of backscattering within the cavity, the difference in resonance frequency Δf cannot be measured as long as the applied rotation is below a certain value determined by the degree of backscattering. This behavior which is called "lock-in" has long been observed in ring laser gyros where a laser amplifier is placed within the resonator. In our passive approach, lock-in occurs if all the

information about backscattering is fed faithfully to the servo loops which hold the external laser frequencies to the cavity resonance.

Lock-in was observed using mechanical rotation and also non-mechanical rotation, e.g., by sweeping the frequency of one of the external lasers. The theory of lock-in relative to our passive set-up was developed and used to understand the observed behavior in the neighborhood of lock-in. Finally, we demonstrated several non-mechanical schemes of eliminating lock-in in passive resonator gyroscope.

The operation of servo loops which lock the external laser frequencies to the cavity resonance requires the generation of discriminants from the resonances of the cavity. These discriminants are produced by modulating the perimeter of the cavity sinusoidally at 30 kHz and demodulating the output intensity of the cavity using a phase sensitive detector (lock-in amplifier). In normal operation of the gyroscope the phase of the lock-in amplifier is adjusted to yield the largest demodulated output. In this case the lock-in amplifier is in phase with respect to the modulation on the perimeter of the cavity. When we set the phase of the lock-in amplifier to be 90 degrees with respect to the modulation on the cavity (i.e., detecting the quadrature signal) we did not get zero across the resonance lineshape. This indicated that the cavity lifetime influenced the discriminant signal. This is a plausible argument since our cavity linewidth of 50 kHz is comparable to the 30 kHz modulation frequency.

The distortions observed in quadrature were in good agreement with our computer generated models for this process, and furthermore, our model predicts a decrease in the amplitude of this distortion as we either increase the cavity linewidth or decrease the modulation frequency. We have experimentally verified this by first modulating at 1 kHz, and then using a cavity with linewidth of 500 kHz. These distortions in the discriminant are important because they can generate errors in the measurement of Δf .

The short term rms noise of the gyroscope with an integration time of 3 sec is 0.05 deg/hr which is close to the shot noise on the light. Currently we are investigating both short term and long term error sources.

Publications

Zarinetchi, F., and S. Ezekiel, "Observation of Lock-In Behavior in Passive Resonator Gyroscope," Optics Lett. 11, 401, (1986).

21.6 Studies of Nonreciprocal Phase Shift in a Fiberoptic Ring Resonator Gyroscope

A nonpolarization maintaining fiber optic ring resonator with a finesse of 80 has been used to investigate error sources in a fiber ring resonator rotation sensor. Detailed observations of the resonant backscatter revealed that Rayleigh backscatter was the primary source of offset drift when a cavity modulation technique was used. Using this common modulation technique a long-term variation of offset of 42°/hr was observed. Short-term noise three times the short noise limit was measured.

By using external acousto-optic modulators to frequency modulate the two counterpropagating beams at different frequencies prior to entering the resonator, the

effect of the backscatter was eliminated. Long-term variation of the offset on the order of 8°/hr was observed. One possible source of this variation is the change in the birefringence of the fiber. The use of polarization, or better, a single polarization resonator would significantly reduce the effect of this birefringence. The short-term noise was approximately 16 times higher than shot noise. This was attributed to the noise added by the acousto-optic frequency modulators.

Preliminary observations of the optical Kerr effect showed an offset of 2°/hr/mwatt input power difference. This is in approximate agreement with the calculated value of the optical Kerr effect and may be eliminated by a simple servo technique.

Publications

Ezekiel, S., "A Brief History of Fiber Gyros and M.I.T.'s Contributions to Fiber Gyro Development," S.P.I.E. 719, 9, (1987).

21.7 Investigation of Noise in a Fiber Interferometer Gyroscope

In a multiturn fiber interferometer gyroscope a broadband light source, e.g., a superluminescent diode (SLD), is used to reduce any undesirable backscatter and also the optical Kerr effect. However, SLDs do not produce a lot of power and their lifetime is limited because they operate at a much higher current density than semiconductor lasers.

We have investigated the use of a chirped frequency semiconductor laser to produce an effectively broad width so as to replace the SLD. The frequency of a semiconductor laser may be chirped by varying the injection current. A number of techniques for chirping the laser have been studied with emphasis on the effect of mode hopping and on any broadband noise created by the chirping.

Using a chirped laser with a width of 28 GHz, we were able to reduce the optical Kerr effect from 50°/hr to a negligible value. At the same time, we achieved a short term noise close to the short noise with the intensity on the detector being one hundred times larger than with a superluminescent diode.

21.8 Sensitive Techniques for Detection of Residual Higher Order Modes in a Quasi-Single-Mode Fiber

Pure single mode propagation in an optical fiber is important in many applications, such as wideband fiberoptic communication and precision interferometric fiberoptic sensors.

Various methods exist for evaluating single mode fibers that are based on cutoff wavelength measurements. For instance, the cutoff wavelength may be determined by observing the near field pattern or by the rise in bending loss. Other methods are based on mode interference. The cutoff wavelength methods are not able to detect a small contribution of higher order modes and the interferometric schemes either are elaborate,

i.e., require an external interferometer setup, or they need special equipment such as tunable sources. Our scheme is also based on mode interference within the fiber but requires neither a special light source nor an elaborate setup.

In our experiment light from a single frequency He-Ne source is focused into an optical fiber, part of which is wrapped around a 2-cm diameter piezo-electric transducer (PZT). By driving the PZT with a sinusoidal signal at f_m, we can generate a modulation of the difference between the propagation constants for the fundamental and a higher order mode. The output of the fiber is detected on a movable small aperture photo diode and passed through an amplifier before phase sensitive demodulation by a lock-in amplifier. Using a multi-mode fiber with core diameter of 5.2 microns we were able to demonstrate the sensitivity of this technique. We measured residual higher order mode amplitudes as low as 10⁻⁴ of the primary mode.

Publications

\$33.6 \$222322 \$332333 353200 \$333000 \$222222##\$\$\$\$\$\$\$ "\$3322004 \$332232 \$2666660 \$6666664 6622622 6

Nakajima, Y., and S. Ezekiel, "Sensitive Determination of the Existence of Higher-Order Modes in a Quasi-Single-Mode Fiber," Opt. Lett. 11, 815, (1986).

21.9 Investigation of Absolute Stability of Water-Vapor-Stabilized Semiconductor Laser

Single-frequency semiconductor lasers are useful in a number of applications, such as fiber optic communication, interferometry, sensors, and high-resolution spectroscopy. In most of these applications the frequency of the laser must be long-term stable. A simple and convenient method of stabilizing the laser frequency is to lock it to a transition in an atomic or molecular vapor, e.g., cesium, rubidium, or water (H₂O) vapor. We have investigated the long term stability of the frequency of a double-heterostructure AlGaAs laser locked to a transition in a simple water vapor cell. We demonstrated that the stability depended on the vapor temperature which influenced the pressure shift in water vapor. Pressure-induced frequency shifts resulting from temperature variations were found to range from 3 MHz/°C at room temperature to 1 MHz/°C at 0°C. We determined that an absolute stability of 1 part in 10¹0 with an averaging time constant of 10 sec could be achieved by controlling the temperature of the water vapor to 0.01°C.

Publications

Pevtschin, V., and S. Ezekiel, "Investigation of Absolute Stability of Water-Vapor-Stabilized Semiconductor Laser," Opt. Lett. 12, 172, (1987).

22.0 Atomic Resonance and Scattering

Academic and Research Staff

Prof. D. Kleppner, Prof. D.E. Pritchard, Dr. S. Vianna, Dr. J. Derouard, Dr. A. Martin, Dr. G.P. Lafyatis, Dr. R. Ahmad-Bitar, Dr. T.W. Ducas

Graduate Students

E. Raab, R. Ahmad-Bitar, V. Bagnato, M.M. Kash, C.H. Iu, G.R. Welch, B. Hughey, T. Gentile, E. Hilfer, R.W. Flanagan, R. Hulet, P.J. Martin, A.H. Miklich, P. Magill, B. Oldaker, R. Stoner, E. Cornell, B. Stewart, S. Paine, R. Weiskoff

22.1 Basic Atomic Physics

22.1.1 Rydberg Atoms in a Magnetic Field

National Science Foundation (Grant PHY 83-06273)

Michael M. Kash, George R. Welch, Chun-Ho lu, Daniel Kleppner

We have produced Rydberg atoms in a lithium atomic beam using cw dye lasers, and developed the technology for detecting these atoms with electric field ionization. These advances have brought us close to the point where we can start carrying out high resolution measurements on highly excited atoms in a strong magnetic field by cw laser spectroscopy.

Understanding the diamagnetic spectrum of an atom with a single valence electron presents a formidable challenge to theory and experiment.¹ The classical and quantum mechanical equations of motion are easily constructed, but in spite of the simplicity of the problem the solutions are elusive and our understanding is far from complete.

Numerical techniques have been applied to both the classical² and quantum³ dynamics, but the results possess features which are difficult to interpret. Construction of an approximate constant of motion is a promising method for predicting the spectrum of a hydrogen atom in a uniform magnetic field.⁴ Our primary task is to measure the level anticrossing sizes and linewidths in the diamagnetic spectrum of atomic lithium, for these can establish the credibility of such an operator.⁵

The excitation of lithium Rydberg atoms is performed with a two-step, three-photon process. The first step is a two-photon transition from the 2s state to the 3s state. This step is detected by observing the cascade fluorescence ($3s \rightarrow 2p$, $2p \rightarrow 2s$) through a fiber optic bundle with a sensitive photomultiplier tube. The transition is excited by 735 nm light from a Coherent ring dye laser. The $2p \rightarrow 2s$ fluorescence as a function of ring laser frequency is shown in Fig. 22.1. The ring laser is stabilized again slow drift by locking to the larger peak's center. The second step is a one-photon transition from the 3s state to the np state. This is observed by counting electrons which are produced in ionizing the excited atoms as they move from the interaction volume into a region of static electric field, 5-10 kV/cm. The electrons are counted with a surface barrier diode.

Standard devices such as electron multiplier tubes, channelrod multipliers, or microchannel plates do not operate in a strong magnetic field greater that 1 Tesla. Figure 22.2 illustrates the electron counting rate versus linear laser frequency, near the $3s \rightarrow 40$ transition. The FWHM linewidth of 28 MHz represents an important advance in Rydberg atom spectroscopy.

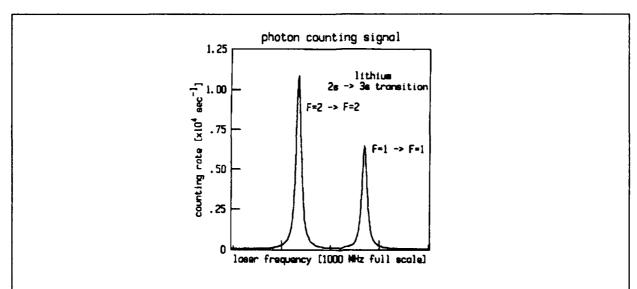
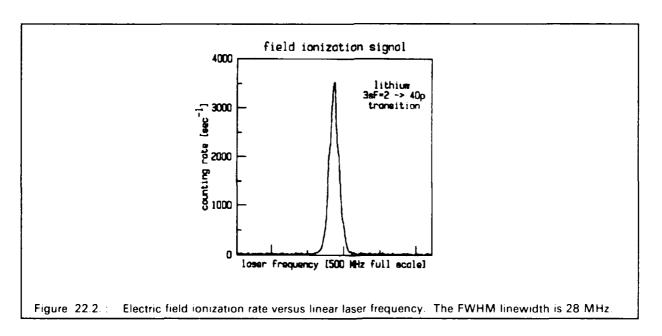


Figure 22.1.: Cascade fluorescence (2p \rightarrow 2s) rate versus ring laser frequency. The two peaks reflect the hyperfine structure of the $3^2S_{1/2}$ and $2^2S_{1/2}$ states of lithium 7.



To minimize the electric field in the atom's rest frame, the atomic beam of lithium is parallel to the axis of a solenoid superconductive magnet. The interaction region consists of an aluminum cylinder whose axis is parallel to the atomic beam. The cylinder also contains prisms to deflect the lasers so that the laser and atom beams intersect at

right angles, to minimize Doppler broadening. The interaction region combines efficient collection of cascade fluorescence with good geometric rejection of scattered laser light.

We expect to energize the magnet in the near future.

References

- ¹ J.C. Gay, "High-Magnetic Field Atomic Physics," in Progress in Atomic Spectroscopy, edited by H.J. Beyer, H. Kleinpoppen, New York: Plenum, 1984.
- ² J. Delos, S.K. Knudson and D.W. Nord, Phys. Rev. A 30, 1208 (1984).
- ³ J.C. Castro, M.L. Zimmerman, R.G. Hulet, D. Kleppner and R.R. Freeman, Phys. Rev. Lett. 45, 1780 (1980).
- ⁴ D.R. Henick, Phys. Rev. A 26, 323 (1982).
- ⁵ M.L. Zimmerman, M.M. Kash and G.R. Welch, J. Phys. Collog. C2, 43, 113 (1982).

22.2 Rydberg Atoms and Radiation

U.S. Navy - Office of Naval Research (Contract N00014-79-C-0183) Joint Services Electronics Program (Contract DAAL03-86-K-0002) National Science Foundation (Grant PHY 84-11483)

Barbara Hughey, Thomas Gentile, E. Hilfer, S. Vianna, R.G. Hulet, Daniel Kleppner

22.2.1 Inhibited Spontaneous Emission

We have achieved our initial goal in the study of basic radioactive processes using Rydberg atoms - the observation of inhibited spontaneous emission. An experiment has been carried out demonstrating that spontaneous emission can be effectively turned off.

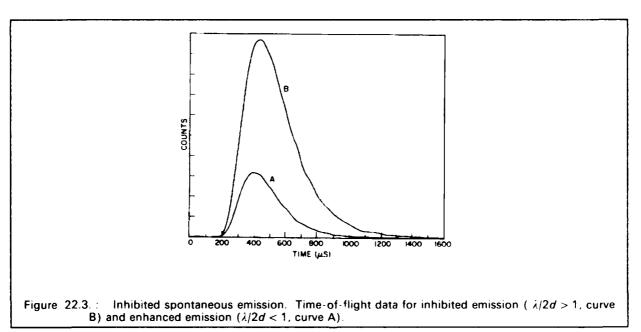
The underlying principle is that spontanous emission results from the radioactive coupling between matter and a continuum of vacuum states. However, the assumptions underlying the conventional calculation of the density of modes in free space are not always valid. In particular, cavities can dramatically effect spontaneous emission. Such effects are difficult to observe in the optical regime because of the problem of making good fundamental mode cavities at short wavelengths. Excellent cavities can be made at microwave wavelengths, but spontaneous emission is enhanced by a factor of n^4 where n is the principle quantum number, allowing such effects to be studied.

The experiment involved measuring the natural lifetime (i.e. the inverse of the spontaneous emission rate) for the transition $n=23 \rightarrow n=22$ in cessium. "Circular" Rydberg states were employed.³ These states have the maximum possible angular momentum m=l=n-1; their value lies in possessing only a single dipole radiation channel. The radiative lifetime was measured by time-of-flight spectroscopy.

Atoms were excited to the Rydberg state by light from pulsed dye lasers and by multiphoton microwave absorption. They then drifted approximately 15 cm to a time-resolved detector which was sensitive only to the n=22 atoms. The drift time was chosen to be close to the free space radiative lifetime. Thus, the time-of-flight spectrum was the product of the probability density for the Maxwell-Boltzmann velocity distribution of the atomic beam and the exponential decay curve for spontaneous emission. To assure accuracy of the method, the free space lifetime was compared to the theoretical result and was found to agree within the experimental resolution, approximately 2%.

Next, the drift space was modified by the introduction of two parallel conducting plates separated by the distance $d=\lambda/2$. The plates behaved effectively as waveguide at cutoff. It can be shown that in this situation the decay rate switches abruptly from zero to a value slightly greater than the free space value as the cutoff separation is exceeded. In the experiment the plate separation was kept fixed and the wavelength was slightly varied by the Stark effect in an applied electric field.

Figure 22.3 shows the experimental time-of-flight curves on either side of cutoff. The area under the curves is proportional to the total number of atoms that reached the detector. The most conspicuous effect of inhibited spontaneous emission is the great increase in area. However, the shape of the curve also contains information about the lifetime. In the inhibited region the lifetime was determined to be at least 20 times larger that the free space value.



Inhibited spontaneous emission offers the possibility of increasing the resolution of spectroscopic measurements beyond the limit set by the natural lifetime. The experiment has also achieved significantly longer time-of-flight times than previously possible with Rydberg atoms, providing a useful technical advance toward high resolution millimeter wave spectroscopy.

SCOOLS CONTRACTOR OFFICE STREET POSSESSE

22.2.2 Rydberg Atoms in Cavities

Thomas Gentile, Barbara Hughey, Daniel Kleppner

We are carrying out a study of single Rydberg atoms radiating into a single mode of the radiation field at a temperature which is effectively zero. Work is in progress on designing the beam and preparing the cavity.

References

- ¹ Kleppner, D., Phys. Rev. Lett. 47, 223 (1981).
- ² Hulet, R.G., E. Hilfer, D. Kleppner, Phys. Rev. Lett. 55, 2137, (1985).
- ³ Hulet, R.G., and D. Kleppner, Phys. Rev. Lett. *51*, 1430 (1983).

22.3 Experimental Study of Momentum Transfer to Atoms by Light

National Science Foundation (Grant PHY 86-05893)

Peter J. Martin, Bruce G. Oldaker, Andrew H. Miklich, Jacques Derouard, David E. Pritchard

We are investigating the radiative forces experienced by a two-level atom interacting with light. These forces provide a new way to study the fundamental interaction between atoms and radiation, and also have important implications in the slowing, cooling and trapping of neutral atoms using light.

By deflecting a highly collimated (0.7 ħ k FWHM resolution), state-selected, and velocity selected 11% FWHM) atomic sodium beam with a well-characterized light wave, we are able to make quantitative measurements of many aspects of momentum transfer to atoms by light. Our apparatus is the only one in the world capable of quantitative comparison with a single photon resolution.

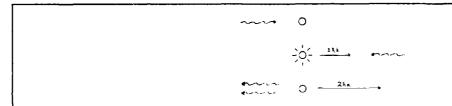
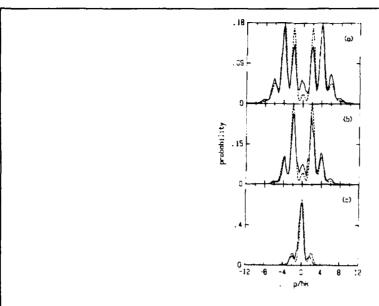


Figure 22.4.: This shows schematically the absorption/simulated emission process. a) Atom at rest absorbs a photon and 1 hk of momentum b) A photon from the counterpropagating travelling wave causes stimulated emission by the excited atom c) Atom in ground state moves with 2 hk of momentum and a photon has been traded from one travelling wave to another.

Emphasis this year has been on momentum transfer by a standing wave. Here the momentum transfer can be viewed in terms of a classical force (the dipole force) which arises from the interaction of the induced electric dipole moment with the gradient of the standing-wave electric field. If the laser is detuned far enough from resonance, spontaneous emission is neglible and the process can be described by a semi-classical Hamiltonian. The momentum transfer can also be described as absorption/stimulated emission of photon pairs from the two counterpropagating traveling waves which make up the standing wave (see Fig. 22.4), a view which predicts momentum transfer in discrete units of 2 hk as we observed. If the standing wave is considered as a diffraction grating, 2 hk is the reciprocal lattice vector in which momentum must be transferred if the grating is not excited.

The latest results concerned the force on a moving atom. If the atom initially has a non-zero velocity component, $\mathbf{v}_{||}$, along the k-vector of the standing wave, then the two counterpropagating waves appear to be Doppler shifted, one by $+k\mathbf{v}_{||}$ and the other by $-k\mathbf{v}_{||}$. This Doppler shift leads to a dephasing of the absorption/stimulated emission process and a predictable reduction in the momentum transfer to the atom. Figure 22.5 shows typical data of the momentum transfer for three different velocities,

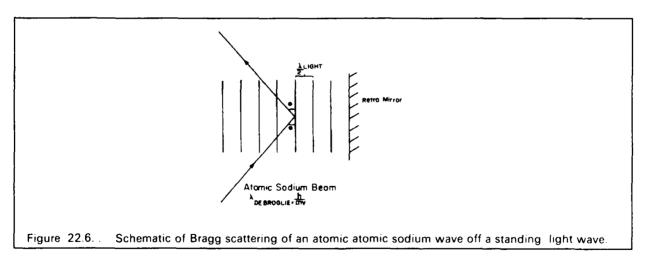
55 (CKKKK) 5555555 (SSSSSSS)



COCCUST ROLLOCAL SESSENCE ASSESSED ASSESSED FOR SESSENCE OF THE COLUMN TO THE COLUMN T

Figure 22.5.: Diffraction patterns of atomic sodium from a standing light wave for different initial velocities of the sodium atom along the k-vector of the standing wave. a) $v_{||} = -1.2$ m/sec b) $v_{||} = -0.77$ m/sec c) $v_{||} = 1.5$ m/sec. Dashed line is theoretical prediction convolved with measured experimental resolution.

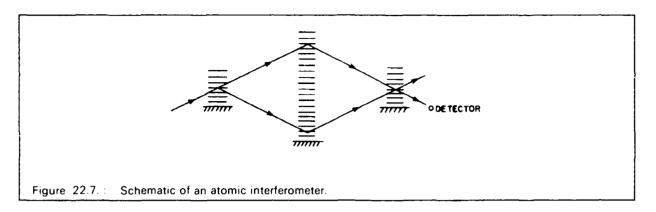
 v_{11}^{-1} The dashed lines are predictions for this case which we obtained from a fully quantum mechanical theory which we derived this year.



Another breakthrough this year has been the observation of Bragg scattering of atomic waves off a standing wave light "crystal." If the atomic beam is viewed as a plane wave and the antinodes of the standing wave define crystal planes, then large resonances for momentum transfer occur for incident angles, θ , satisfying the Bragg law,

$$2d\sin\theta = n\lambda_{DB}$$
, where $d = \frac{\lambda_{hght}}{2}$, $\lambda_{DB} = \frac{h}{mv}$

is the deBroglie wavelength of the atomic wave, and n is an integer (see Fig. 22.6).²



Evidence of this new phenomenon opens up new possibilities for the construction of an "atomic interferometer"; which is basically a device that interferes atomic waves. Figure 22.7 shows schematically such a device. The "atomic beam splitter" uses Bragg scattering to split the atomic beam coherently. The "atomic mirror" again uses Bragg scattering to steer the two beams to the last "atomic beam splitter" which recombines the two beams. If the effective path length of one of the two legs of the interferometer is modulated (for example, by the use of an electric field), there will be a modulation of the relative phases of the two recombined beams and intensity modulation at the detector. Besides the point of showing complete duality of particles and waves, this device can be used to measure the polarizability of the atoms, the phase shift produced by passage through a gas, the light shift, and possibly the Casimir shift. The Casimir shift arises because the lowest order modes of the vacuum fluctations are excluded from the region between two parallel conducting plates due to electromagnetic boundary conditions at the plates. If one of the paths of the interferometer passes through this region, then there will be less of an energy shift of the ground state of the atoms on this path of the interferometer, and hence a phase shift at the detector.

References

¹ P.J. Martin, P.L. Gould, B.G. Oldaker, and A.H. Miklich, accepted for publication in Phys. Rev. A.

² A.F. Bernhardt, and B.W. Shore, Phys. Rev. A. 23, 1290 (1981).

22.4 Atom-Molecule Collisions

National Science Foundation (Grant ECS 84-21392)

Brien Stewart, Peter Magill, Richard Stoner, Jacques Derouard, David E. Pritchard

What happens when an atom collides with a rapidly rotating, vibrating molecule? The answer to this question is emerging in a detailed experimental study of vibrotationally inelastic (VRI) collisions in our laboratory.^{1 2 3 4 5} The subject of our study is the atom-diatom system

$$\operatorname{Li}_{2}^{\bullet}(v_{i},j_{i}) + \operatorname{Ne} \xrightarrow{V_{rel}} \operatorname{Li}_{2}^{\bullet}(v_{i} + \Delta v_{i},j_{i} + \Delta j) + \operatorname{Ne}.$$

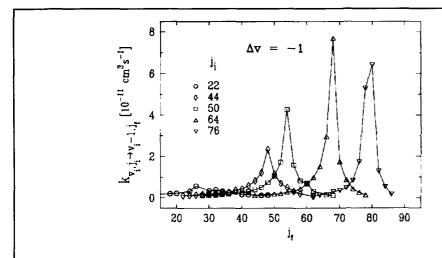
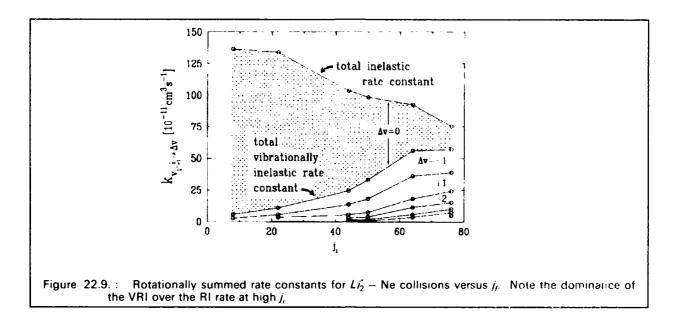


Figure 22.8.: Rate constants for Li_2^2 – Ne collisions for $\Delta v = -1$ versus j_f . Note the large rates and very narrow peaks for high j_f

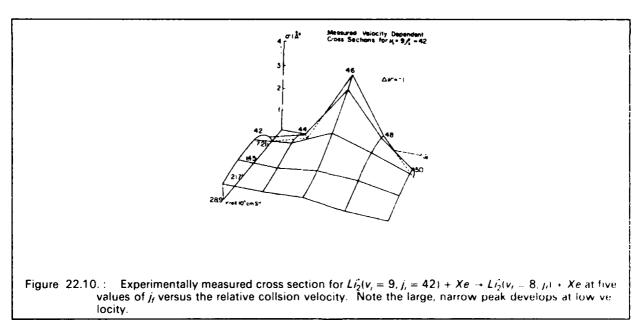
We use single mode tunable dye lasers to select the initial vibrational (v_i) and rotational (j_i) levels of the Li_2 molecule; in addition, we can select the collision velocity via the Doppler shift. Our investigation has uncovered a new type of vibrationally inelastic collision process: at high j_i the VRI cross section becomes very large, but with a very narrow j_i distribution for a given Δv . In addition, the peak of this distribution is correlated with Δv according to the rule $\Delta j = -4\Delta v$.

Figure 22.8 shows experimental rate constants for $\Delta v = -1$ and j_i ranging from 22 to 76. Note the large, sharply peaked rate constants at large j_i ; the largest of these corresponds to a level-to-level cross section of 8\AA^2 . At $j_i = 64$, the width of the j_i distribution is only $3\hbar$. This resonance-like behavior has prompted us to name the phenomenon "quasi-resonant $V \longleftrightarrow R$ transfer," quasi-resonant, because the peak of the j_i distribution is not determined by internal energy conservation, that is, by a simple interconversion of vibrational and rotational energy.

Inelastic rates summed over j_i are shown in Figure 22.9, illustrating that VRI collisions are the dominant inelastic process at high j_i . At the highest j_i measured, the quasi-resonant V \longleftrightarrow R rate accounts for more than 2/3 of the total inelastic rate. This is a complete reversal of what occurs at low j_i , the regime of essentially all previous studies. At low j_i , VRI rates are much smaller than purely rotational inelastic (RI) rates and have broad, unspecific j_i distributions, as can be seen in the j_i = 22 data of Figure 22.8.



At sub-thermal velocities, the quasi-resonant process is strengthed further. Figure 22.10 shows velocity dependent cross sections measured by our VSDS (Velocity Selection via the Doppler Shift) technique. The cross section and final state specificity are increased by lowering the velocity. Again, this behavior is exactly the opposite of what is observed at low j_n where increases in velocity *enhance* vibrational inelasticity.



We have modeled quasi-resonant $V \longleftrightarrow R$ transfer using classical trajectories calculated by a technique that allows us to follow the time dependence of the vibrational action (corresponding to the vibrational quantum number). Examination of many trajectories has enabled us to describe the dynamics of the quasi-resonant process and characterize the conditions under which it occurs. At low j, the force on the vibrator is largely averaged out by the molecular oscillation, which induces much more rapid changes in the intermo-

lecular potential than either the rotation or translation; the result is little change in the vibration. At high j_i , the molecule rotates substantially during a vibrational period, yielding a sudden force on the vibrator that can produce large changes in the vibration. The correlation of Δv and Δj results from a subtle interaction of the vibrational and rotational phases at the instant of maximum force. Finally, at very low velocity, the molecule can collide several times with the atom due to the rapid rotation, resulting in an enhancement in the above effects and a strengthening of $V \longleftrightarrow R$ transfer. Each of these effects can be seen in Figure 22.11, a plot of some of the dyanmical variables versus time through one collision, The top two graphs (of v and j) show that at each step through the collision Δv and Δj are anti-correlated and that each "collisionette" of an end of the molecule with the atom builds on the others, resulting in a large net transfer.

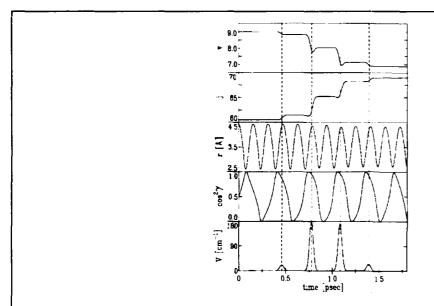


Figure 22.11.: Plot of the vibrational action (v), the rotational action (f), the internuclear separation (f), cosine of the rotational angle (f) and the intermolecular interaction energy (f) as functions of time through a single, simple collision. Note the peaks in V(t) corresponding to "collisionettes."

Because this model has been successful, we can use it to make predictions about as yet unobserved classical effects. A good example of such an effect is the collisional reorientation of the molecular rotation axis. For collisions which are either rotationally inelastic or not, the *direction* of the angular momentum vector \vec{j} can be altered. Utilizing the polarization of the incident and fluorescent light, the reorientation cross section can be measured experimentally. Classical trajectory calculations can readily make predictions about the amount of reorientation and the cross section for it. In addition, trajectories naturally give the velocity dependence of this process which can also be measured experimentally using the Doppler shift.

References

- ¹ K.L. Saenger, N. Smith, S.L. Dexheimer, C. Engelke, and D.E. Pritchard, J. Chem. Phys. 79, 4076 (1983).
- ² T. Scott, Ph.D. Thesis, M.I.T., Cambridge, Mass., 1985.

- ³ P. Magill, T. Scott, B. Stewart, N. Smith, and D.E. Pritchard, to be submitted to J. Chem. Phys.
- ⁴ T. Scott, B. Stewart, P. Magill, N. Smith, and D.E. Pritchard, to be submitted to J. Chem. Phys.
- ⁵ B. Stewart, P. Magill, T.P. Scott, J. Derouad, and D.E. Pritchard, to be submitted to Phys. Rev. Lett.
- ⁶ N. Smith, T. Scott, D.E. Pritchard, J. Chem. Phys. 81, 1229 (1984).
- ⁷ N. Smith, J. Chem. Phys. 85, 1987, (1986).
- ⁸ P. Magill, B. Stewart, D.E. Pritchard, to be submitted to Phys. Rev. Lett.

22.5 Magnetic Trapping of Neutral Atoms

U.S. Navy - Office of Naval Research (Contract N00014-83-K-0695)

Vanderlei Bagnato, Gregory Lafyatis, Alexander Martin, Eric Raab, Riyad Ahmad-Bitar, David E. Pritchard

We are working on a program to slow, trap and cool neutral atoms. Laser light is used to slow and cool atoms and magnetic forces are used to trap them. Ultimately we hope to be able to trap atoms for days and cool them to temperatures on the order of 10^{-6} K In addition to the interesting scientific and technical challenges involved in trapping and cooling atoms, we hope to open several new lines of investigation with these cooled atoms. Cold trapped atoms constitute a good system for studying collective phenomena such as Bose condensation, low energy - Na and Na - Na', and coherent optical effects (the deBroglie wavelength can exceed the optical wavelength). They also offer opportunities for performing ultra-high resolution spectroscopy and are extremely promising candidates for a new generation of frequency standards.

In 1986 we completed construction of our neutral trap apparatus and began doing experiments with it. Our first successful run has advanced the state of the neutral atom slowing and trapping art by several orders of magnitude. We have continuously stopped atoms with laser light, continuously loaded them into our 0.1K deep superconducting magnetic trap, and held them for up to six minutes. Continuous trap loading is an important advance over previous pulsed loading 1 schemes because it permits the accumulation of large numbers of atoms in the trap and, hopefully, enables the study of collective phenomena in the trap. Our trap, though somewhat more complicated in design and construction than the two previously reported atom traps 2 has the advantage of a uniform magnetic field region in its center in which optical pumping and precision spectroscopy of cooled atoms may be undertaken. Fluorescence from trapped atoms has been observed for 10 sec with intense illumination. Finally, we have observed trapping decay times of two minutes -- two orders of magnitude better than the previously reported traps. It is our expectation that we will soon see trapping times of hours, or perhaps days, giving us sufficient time to perform experiments on the trapped atoms. We are now in a position to

move neutral traps from the status of laboratory curiosities to that of powerful tools for new research in physics.

Figure 22.12 is a schematic of our experiment. Superconducting magnets were designed and constructed to provide the necessary field to slow and trap neutral atoms. Na atoms from a 500°C oven are slowed, in two stages, by laser beams propagating counter to the atomic beam. A tapered magnetic field creates a Zeeman shift in the atomic levels and compensate for the changing Doppler shift of the atoms as they slow. The second laser beam is retroflected and cools the atoms to milliKelvin temperatures near the trap's center. We trap atoms in states whose electron spin is parallel to the magnetic field --these atoms experience a force towards regions of weak field (c.f. Stern-Gerlach experiment). The field minimum located at the center of our trapping magnets constitutes a 0.12K deep trap for atoms. Photodiodes located at several places within the apparatus are used to detect fluorescence from the slowing and trapped atoms.

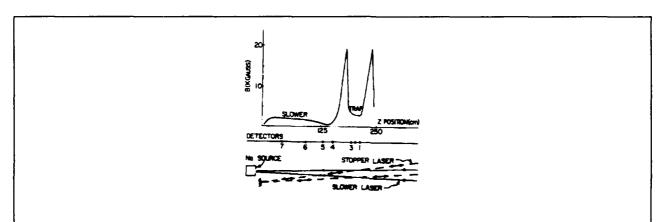


Figure 22.12.: Schematic of the experiment. The upper figure shows the magnetic field profile, below the positions of the detectors are shown, and at the bottom of the atomic source and laser configurations.

Figure 22.13 is a composite of several runs in which the trap lifetime was measured by recording the fluorescence from trapped atoms. The sequence used to make up Figure 22.13 was: lasers on to fill the trap, lasers off for a (variable) period of time, second laser turned back on to probe the remaining atoms. Our diagnostics for those initial measurements were coarse and presently we can only make a lower limit estimate in the number of atoms in the trap: $\approx 10^8$. There may well be two orders of magnitude more trapped atoms which have inadvertently decayed to another hyperfine state which is well out of resonance with the laser light. This inadvertent optical pumping should enable us to perform RF resonance on the trapped atoms. In the future we hope to accumulate more atoms, study Doppler cooling of the trapped atoms (expected to achieve submilliKelvin temperatures), investigate "cyclic" cooling of atoms ³ (projected to achieve temperatures near $1\mu K$) and use RF resonance both to study the trapped atoms and possibly to develop a frequency standard.

References

- ¹ Migdall, A. et. al., Phys. Rev. Lett. 54, 2595 (1985).
- ² Chu, S., J.E. Bjorkholm, A. Ashkin, Cable, Phys. Rev. Lett. 27, 314 (1986).

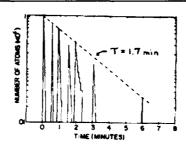


Figure 22.13.: Result of several runs. Each curve is the result of charging the trap, blocking both laser beams, and after the indicated time, turning back on the stopping beam and recording the fluorescence from trapped atoms.

³ Pritchard, D.E., Phys. Rev. Lett. 51, 1336 (1983).

22.6 Precision Mass Spectroscopy of lons

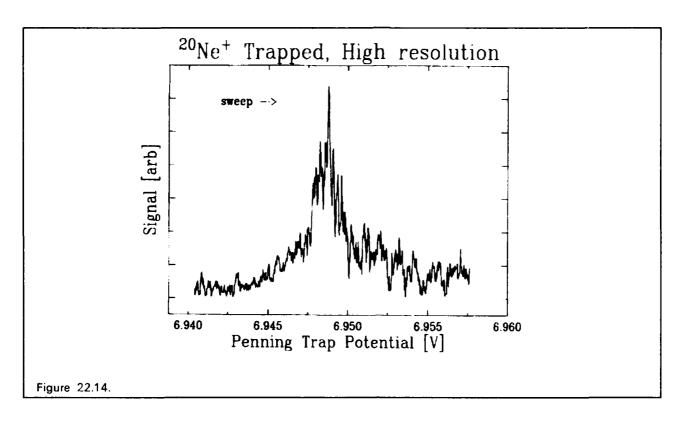
National Science Foundation (Grant CHE 84-21392)

Joint Services Electronics Program (Contract DAALO3-86-K-0002)

Eric Cornell, Robert W. Flanagan, Greg P. Lafyatis, David E. Pritchard, Robert M. Weisskoff

We are developing an experiment to determine the mass of individual atomic and molecular ions at precisions of 10⁻¹¹. This technique will allow us to do a variety of experiments which address issues of both fundamental and applied physics:

- The ³H⁺ ³H_e⁺ mass difference is an important parameter in ongoing experiments to measure the electron neutrino rest mass.
- Excitation and binding energies of typical atomic and molecular ions might be studied by "weighing" the small increase in energy: $\Delta m = E_{bind} / c^2$.
- Experiments that weigh γ -rays can be used in a new method to determine N_A , the Avogadro constant.
- Traditional applications of mass spectroscopy should benefit from the several orders of magnitude improvement in both accuracy and sensitivity our approach offers over conventional techniques.

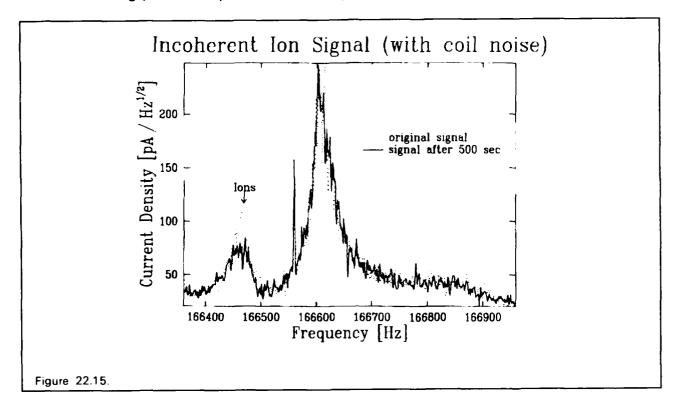


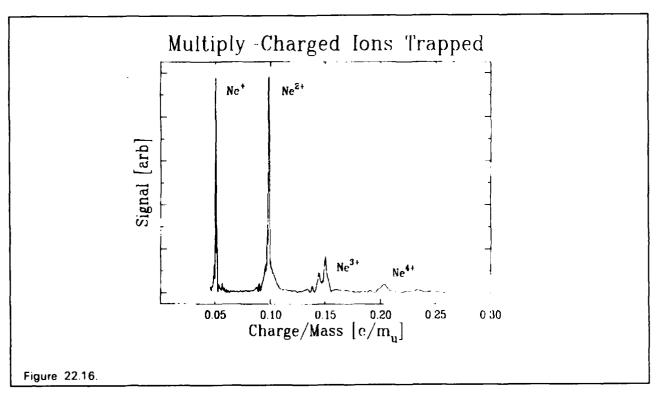
We will measure ratios of cyclotron frequencies, and, therefore, masses of a small number of atomic or molecular ions in a Penning trap at 4.2K. To attain the precision we seek, it will be necessary to work with only one, or at most, two ions in the trap. Space charge from other ions would lead to undesirable frequency shifts. Thus, our mass spectrometer will have the ultimate sensitivity -- a single particle.

We will use ion trapping techniques based on methods developed at the University of Washington, where they have made precision measurements on protons, electrons and positrons at the 10^{-11} level. Trapped ions are detected by the small currents which they induce in the trap electrodes as they move. However, because atomic and molecular ions have larger masses, and thus lower resonant frequencies, they induce much smaller currents than the particles studied at Washington. Consequently, much of our past effort has been to develop a detector using a SQUID (Superconducting QUantum Interference Device) and superconducting electronics to measure these small induced currents, typically $\sim 3 \times 10^{-15} \text{A}$

This year we assembled our apparatus and began making measurements with the short term goal of detecting and manipulating single ions. Although we have detected many species, ²⁰Ne⁺ has proved a convenient species to work with. To date, we have been able to observe clouds of fewer than five ions. Figure 22.14 is a typical observation of an ion cloud, which is driven resonantly by voltages applied to the trap. In Figure 22.15, we turned off the drives and observed the ions oscillating incoherently in the trap, measured with a fourier transform of the endcap currents. We also have made multiply charged species by leaving on the electron gun (below the trap) and further ionizing already trapped ions. Figure 22.15 is a broad scan in which we detected Ne⁺, Ne²⁺, Ne³⁺, and Ne⁴⁺ made in that manner.

In the coming year we hope to observe single ions and begin cyclotron resonance work.





23.0 Plasma Dynamics

Academic and Research Staff

Prof. G. Bekefi, Prof. A. Bers, A. Ram, Prof. B. Coppi

Visiting Scientists

V. Fuchs¹, C. Lashmore-Davies²

Graduate Students

K. Kupfer

23.1 Relativistic Electron Beams

U.S. Air Force - Office of Scientific Research (Grant AFOSR 84-0026) National Science Foundation (Grant ECS 85-14517) U.S. Department of Energy (Contract DE-FG05-84ER 13272) Lawrence Livermore National Laboratory (Subcontract 6264005)

George Bekefi

During the past year we have undertaken four studies: 1) nonlinear characteristics of the free electron laser; 2) measurements of electron temperature on the free electron laser gain; 3) optical guiding measurements; and 4) the design of a new type of helical wiggler.

23.1.1 Nonlinear Characteristics of the Free Electron Laser

We have completed measurements of the nonlinear radiation intensity and of the wave refraction index of our free electron laser. This laser operates in the Raman regime. Power saturation, synchrotron oscillations, and the wave refractive index were studied as a function of beam energy, beam current and the axial position within the wiggler. Very good agreement with computer simulations have been obtained.

23.1.2 Effect of Electron Beam Temperature on FEL Operation

At sufficiently low beam currents, electron beam temperature effects cause the gains of collective (Raman) regime free electron lasers to be lower than the predictions of cold beam theory. This gain degradation has been measured as a function of the beam current, the wiggler magnetic field and the interaction frequency. The measurements are used to estimate the electron beam temperature, and the estimated temperature is close to the temperature predicted by numeric simulations.

Visiting Scientist, I.R.E.Q., Quebec, Canada

² Visiting Scientist, Culham Laboratory, U.K.A.E.A., Abingdon, Oxfordshire, England

23.1.3 Optical Guiding Measurements

Optical guiding is an important phenomenon predicted by theory, but as yet not observed experimentally. This phenomenon would mitigate the effects of diffraction and thereby allow the length of FEL wigglers to exceed the Rayleigh range. We carried out what we believe are the first measurements of optical guiding.

23.1.4 The Design of a New Type of Helical Wiggler

We have come up with a very simple design for a permanent magnet helical wiggler which may be useful for free electron laser and cyclotron maser applications. The wiggler is composed of a cyclindrical array of staggered samarian-cobalt bar magnets.

During the coming year we plan to continue work in all areas described above. In addition, we will undertake an experimental and theoretical study if free electron efficiency enhancement. To this purpose, we have designed a helical wiggler in which the periodicity is tapered to allow the electrons to remain in phase synchronism with the wiggler field.

23.2 Plasma Wave Interactions - RF Heating and Current Generation

National Science Foundation (Grant ECS 82-13430) U.S. Department of Energy (Contract DE-AC02-78-ET-51013)

Abraham Bers, Vladimir Fuchs, Chris Lashmore-Davies, Abhay Ram, Kenneth Kupfer

Our analytical and computational work of the past year is briefly described in the following four subsections. A general theoretical framework was developed for treating mode-conversion and instability in inhomogeneous plasmas (subsection 23.3). This has lead to a new formulation of the transmission coefficient through the mode-conversion region of a fast-Alfven wave with an ion-Bernstein wave (subsection 23.4.1). Analytic description of the ion-Bernstein wave parallel-wavenumber enhancement due to toroidal effects have been obtained (subsection 23.4.2). Studies of lower-hybrid current drive have continued to address and evaluate relativistic effects (subsection 23.5). We have also extended the formulation and identification of absolute instabilities from dispersion relations that are transcendental in the wavenumber (subsection 23.6); this has proven useful in identifying the onset of von-Karman vortices in fluid dynamics as a transition from convective to absolute instability.

23.3 Coupled-Mode Propagation and Instability in Inhomogeneous Plasmas

The free energy of a plasma system is often associated with the distribution of particles in velocity space (e.g., anisotropic temperature, drifts, etc.). Linear theory exhibits this free energy in the form of stable negative-energy waves. These waves are driven unstable when coupled to positive-energy waves, or when positive dissipation extracts free energy from the system. The space-time evolution of such instabilities is well un-

derstood for the case of infinite, homogeneous plasmas; yet in many real systems, which are inherently finite and nonuniform, it is the very presence of the spatial inhomogeneity which allows the unstable coupling to take place. A general theoretical framework has been developed to treat such linear coupled-mode instabilities in weakly nonuniform plasmas. We have developed two independent, yet supporting, formalisms that allow for the extraction of an embedded pairwise coupling event from a general local dispersion relation, and provide an unambiguous partial differential equation, second order in both space and time, describing the space-time evolution of the resulting instability.

The first approach requires the expansion of the local dispersion relation, $D(k_x, \omega; x) = 0$, about special mode boundaries in Fourier-Laplace transform space. This generalizes our earlier work on propagation and mode conversion in stable plasmas.² The mode boundaries isolate the various branches of the local dispersion relation, and allow for analytic continuation of the modes only at the appropriate coupling points, k_{x0} , ω_0 , and x_0 , given by the three (generally complex) conditions:

$$D(k_{x0}, \omega_0; x_0) = 0, (1)$$

$$\frac{\partial D}{\partial k_x} \bigg|_{0} = 0, \tag{2}$$

and

$$\frac{\partial D}{\partial \omega} \bigg|_{0} = 0. \tag{3}$$

In general, such coupling points will be six-dimensional objects, and represent branch points in the complex x-plane, and saddle points in both the complex k_x -plane and the complex ω -plane. This means that for a frequency fixed at the coupling point frequency, ω_0 , two branches of the mapping:

$$D(k_x, \omega_0; x) = 0; x \in C, k_x = f_k(C)$$
 (4)

will meet at k_{x0} , provided that the contour C passes through x_0 . Likewise, for a wavenumber fixed at $k_x = k_{x0}$ two branches of the mapping:

$$D(k_{v0}, \omega; x) = 0; x \in C, \omega = f_{\omega}(C)$$
(5)

will meet at ω_0 provided C passes through x_0 . The modes are coupled both in space and time.

We require a boundary in the complex k_x -plane which confines the separate branches of the mapping in Eq.(4) to mutually exclusive regions of the complex k_x -plane. The branches are only allowed to intersect the mode boundary (and couple to other branches) at the coupling points, defined by Eqs. (1)-(3). At the same time, we require a boundary in the complex ω -plane which confines the different branches of the mapping in Eq.(5), and allows them to couple only at the coupling points. The two

boundaries which satisfy these conditions are found by simultaneously mapping the dependent contours:

$$\frac{\partial D(k_c(x), \, \omega_c(x); \, x)}{\partial k_x} = 0; \, x \in C, \, k_c(x) = g_k(C)$$
 (6)

and

$$\frac{\partial D(k_c(x), \, \omega_c(x); \, x)}{\partial \omega} = 0; \, x \in C, \, omega_c(x) = g_\omega(C)$$
 (7)

With the mode boundaries so defined we are assured that the boundary $k_c = g_k(C)$ and the modes $k = f_k(C)$ have only the coupling wavenumber k_{x0} in common for $\omega = \omega_0$ The inverse mapping of $k_c = g_k(C)$ through the dispersion relation may therefore be interpreted as the appropriate branch cut in the complex x-plane:

$$C_{bk} = f_k^{-1}[g_k(C)].$$
 (8)

Likewise, for $k_x=k_{x0}$, we are assured that the boundary $\omega_c=g_\omega(C)$ and the modes $\omega=f_\omega(C)$ have only the coupling frequency ω_0 in common. The contour $\omega_c=g_\omega(C)$ therefore defines the boundaries of the Riemann sheets of the mapping $\omega=f_\omega(C)$, and the branch cut in the complex x-plane is given by:

$$C_{b\omega} = f_{\omega}^{-1}[g_{\omega}(C)]. \tag{9}$$

A pairwise space-time coupling event may be extracted from a general local dispersion relation by expanding to second order about both the mode boundary in the complex k_x -plane and the mode boundary in the complex ω -plane. If the wave amplitude in the coupling region is written in the form:

$$\Phi(x, t) = \phi(x, t) \exp \int ik_c(x)dx - i\omega_{0t}t, \qquad (10)$$

then the partial differential equation governing the slowly varying amplitude function $\phi(x, t)$ takes the form:

$$A(x) \left[\frac{\partial^2 \phi}{\partial t^2} - 2i(\frac{\partial \phi}{\partial t})s(x) - \phi s^2(x) \right] + \frac{\partial^2 \phi}{\partial x^2}$$
 (11)

$$+B(x)\left[\frac{\partial^2\phi}{\partial x\partial t}-i(\frac{\partial\phi}{\partial x})s(x)\right]+Q(x)\phi=0$$

where:

$$A(x) = \frac{\partial^2 D/\partial \omega^2}{\partial^2 D/\partial k_x^2} \bigg|_{C},$$
(12)

$$B(x) = \frac{-2\partial^2 D/\partial k_x \partial \omega}{\partial^2 D/\partial k_x^2} \bigg|_{C},$$
(13)

$$Q(x) = \frac{-2D}{\partial^2 D/\partial k_x^2} \bigg|_{c'}$$
 (14)

and

$$s(x) = \omega_0 - \omega_c(x). \tag{15}$$

The second technique developed removes the singular behavior from the standard geometric optics hierarchy of equations in the region of a coupling point. This is accomplished through a renormalization and reordering of the hierarchy in a self-consistent manner. The resulting partial differential equation describing the slowly varying envelope function of the instability is given by:

$$A_0 \frac{\partial^2 \phi}{\partial t^2} + \frac{\partial^2 \phi}{\partial x^2} + B_0 \frac{\partial^2 \phi}{\partial x \partial t} + Q(x)\phi(x, t) = 0, \tag{16}$$

where:

$$A_0 = \frac{\partial^2 D_{ii} / \partial \omega^2}{\partial^2 D_{ii} / \partial k_x^2} \bigg|_{0}, \tag{17}$$

$$B_0 = \frac{-2\partial^2 D_{ii}/\partial k_x \partial \omega}{\partial^2 D_{ii}/\partial k_x^2} \bigg|_{0}, \tag{18}$$

and

$$Q(x) = \frac{-2\hat{c}D_{ii}/\hat{c}x}{\hat{c}^2D_{ii}/\hat{c}k_x^2} \left|_{0} (x - x_0). \right|$$
(19)

Here, D_{ii} is the element of the diagonalized dispersion tensor containing the coupling point given by Eqs. (1-3) with D replaces by D_{ii} . Note that in the near vicinity of the coupling point, $x \to x_0$, so that $s(x) \to 0$, the partial differential equation derived using the mode-boundary expansion, Eq.(11), reduces to the simpler form of Eq.(16). Although these two equations are essentially identical very near the coupling point, there are very important differences between the two results. The mode-boundary expansion, Eq.(11), is more global in nature, in the sense that it may be used to describe coupling in the presence of a group of two or more coupling points which are close together in the complex x -plane, so that a WKB description of the modes between the separate coupling points is not valid. The renormalized geometric optics expansion, Eq.(16), on the other hand, is inherently limited to the treatment of a single coupling region, which must be sufficiently separated from its nearest neighbor. By expanding the local dispersion relation along the mode boundaries in the complex k_r -plane and ω -plane, we are assured that the two modes described by our second order partial differential equation are indeed the two modes which couple at x_0 . We are also able to analytically continue our equation along the mode boundaries to the physical domain of the wave propagation, the real x-axis, and are therefore certain that the partial differential equation representation is valid for real x, even though the coupling point occurs off of the real x-axis.

Using these approaches we have solved for the space-time evolution of the relativistic-electromagnetic instability³ in an inhomogeneous magnetic field.

References

- ¹ G. Francis, Ph.D. Diss., Dept. of Physics, M.I.T., Cambridge, Mass., 1987.
- ² V. Fuchs, K. Ko, and A. Bers, Phys. Fluids *24*, 1261, (1981).
- ³ A. Bers, J.K. Hoag, and E.A. Robertson, R.L.E. Quarterly Progress Report No. 77, April 1965, pp. 149-152.

23.4 Propagation, Mode-Conversion and Absorption in lon-Cyclotron Heating

Analysis of energy propagation and absorption in ion-cyclotron heating of tokamak plasmas has relied on numerical solutions of fourth (and sixth) order differential equations for slab models of the plasma (poloidal) cross section. Realistic two-dimensional and fully toroidal geometry analyses would become quite unwieldy. We have undertaken to show that the analysis of the slab model can be simplified considerably. A first-order differential equation is shown to describe the transmission coefficient for the fast wave, and it is solved analytically. A second order differential equation is shown to adequately describe both transmission and reflection. Including toroidal effects in propagation, conditions for electron absorption on the mode-converted ion-Bernstein waves are also described analytically.

23.4.1 Transmission and Reflection of the Fast-Wave

The fast wave transmission coefficient can be obtained analytically using nonresonant (quasimode) perturbation theory¹ in an inhomogeneous plasma.² Away from the mode-conversion region, the fast wave can be described approximately by the Vlasov-Maxwell equations in the limit of $(\kappa_\perp v_7 | \Omega) = 0$, $(v_7 = \kappa T/m)$, $\Omega = eB_0/m$; we designate the corresponding dispersion tensor by \overline{D}_0 . In a large tokamak plasma, the propagation of the fast wave in these regions may be treated by the usual geometric optics formalism;³ assuming the inhomogeneity to be in $x[\overline{B}_0 = \hat{z}B_0(x)]$, let $\overline{E}_0(x) = E_0(x)\overline{e}_0(x)$ be the electric field, $\overline{e}_0(x)$ its polarization vector, and $s_x(x)$ the time-averaged power flow density in x. In the localized region around mode conversion the plasma dynamics must include the effects of finite $(k \perp v_7/\Omega)$ for ions, so that the dispersion tensor becomes $\overline{D}_0 + \overline{X}_1$. As regards the fast wave propagation through this region, we model it as non-resonantly perturbed by these effects to first-order in $(v_7/\Omega)^2$. Thus the perturbed fast wave electric field becomes, in general, $\overline{E} = a(x)\overline{E}_0(x)$, where a(x) is a slowly-varying complex amplitude which is ordered with the nonresonant perturbation current density $\overline{J}_p = -i\omega \varepsilon_0 \overline{X}_1 \cdot \overline{E}$; we then find

$$\frac{da(x)}{dx} = \frac{-\frac{1}{4}\overline{E}_0^*(x)\cdot\overline{J}_p(x,t)}{s_v(x)},$$
(1)

which can be solved for a(x). The power transmission coefficient is thus given by:

$$T = \frac{\left| \overline{E}(x \to -\infty) \right|^2}{\left| \overline{E}(x \to +\infty) \right|^2} = e^{-2\pi\mu}$$
 (2)

For a plasma containing a minority ion species, e.g., hydrogen in a deuterium plasma, we find (subscripts 1 and 2 to stand for, respectively, majority (d) and minority (h) ions):

$$\mu = \frac{1}{\pi} \int_{-\infty}^{+\infty} |N\perp| \operatorname{Im} \left\{ \overline{\varepsilon}_{0}^{\bullet} \cdot (\overline{\overline{D}}_{0}^{\partial} + \overline{\overline{X}}_{1}) \cdot \overline{\varepsilon}_{0} \right\} d\xi = \frac{R_{A}}{8} \frac{N_{\perp 0}^{5}}{(1 + N_{\perp 0}^{2})^{2}} \left[\beta_{1} + \frac{\eta}{N_{\perp 0}^{2}} \right]$$
(3)

where $\overline{D}_0^{\partial}$ is the anti-hermitian part of \overline{D}_0 ; $N_{\text{B},\perp}=k_{\text{B},\perp}c_A/\omega$; c_A the (majority ion) Alfven velocity; $\eta=n_2/n_1$ is the minority to majority concentration ratio; $\beta_1=(v_{t1}/c_A)^2$ is the majority ion plasma beta $R_A=R_0\omega/c_A$; R_0 is the plasma major radius = the scale length of the (toroidal) magnetic field (B_0) variation; $=x\omega/c_A$, and x=0 is the position of the majority ion's second harmonic cyclotron layer; and N_\perp has been approximated by its cold-plasma value at resonance $N_{\perp 0}^2=(1-3N_{\parallel}^2)(1+N_{\parallel}^2)/(1+3N_{\parallel}^2)$. The analytic result for the transmission coefficient given by (3) has been compared with numerical computations of fourth-order differential equations that model the mode conversion region 45 Excellent agreement is obtained as a function of all relevant parameters, i.e., k=n, n_{\perp} and T_{\perp}

A fast wave incident upon a mode conversion region will in general undergo some where tion. Hence a more complete description of the fast wave involves describing both transmission and reflection. This entails finding an appropriate second-order differ-

ential equation in which the coupling to the ion-Bernstein wave (i.e. mode-conversion) and dissipation (in the mode-conversion region) are incorporated in a modified propagation description of the fast wave. To obtain this we first derive an appropriately approximated dispersion relation for the fast wave from the exact hot plasma dispersion relation. Neglecting electron inertia effects and retaining terms only to first-order in $(k_\perp v_7/\Omega)^2$, we obtain the desired approximate fast wave dispersion relation.⁶ Then, letting $N_\perp \to i(d/d\xi)$ we find the appropriate second-order differential equation that describes the fast wave transmission and reflection:

$$\frac{d^2F}{d\xi^2} + Q(\xi)F = 0 \tag{4}$$

where F is proportional to E_{ν} of the fast wave,

$$Q(\xi) = \frac{(1 - 3N_{\parallel}^{2})(1 + N_{\parallel}^{2} - 2\Gamma_{1} - 2\Gamma_{2})}{1 + 3N_{\parallel}^{2} - 3\Gamma_{1} - 3\Gamma_{2}};$$

$$\Gamma_{1} = \frac{N_{\perp 0}^{2}\sqrt{\beta_{1}}}{4N_{\parallel}} Z(a_{1}\xi);$$

$$\Gamma_{2} = \frac{\eta}{4N_{\parallel}\sqrt{\beta_{1}}} V Z(a_{2}\xi)$$
(5)

 $V=v_{t2}/v_{t1}$ and $v_t^2=2\kappa T/m$; $Z(a\xi)$ is the plasma dispersion function; $a_1=1/N_{\parallel}\sqrt{\beta_1}\,R_A$; and $a_2=a_1/V$. The power transmission and power reflection coefficients for the fast wave can be readily obtained from numerical solutions of (4). These have been compared with results from numerical computations of fourth-order differential equations .^{4.5} Excellent agreement is found for both second-harmonic and ion-ion hybrid scenarios, and as a function of k_{\parallel} and η .

References

- ¹ A. Bers, In *Plasmas Physics Les Houches 1972*, edited by C. DeWitt and J. Peyraud, New York: Gordon and Breach Science Publishers, 1975.
- ² G. Francis, Ph.D. Thesis, Dept. of Physics., M.I.T., Cambridge, Mass., 1987.
- ³ H.L. Berk and D.L. Book, Phys. Fluids 12, 649 (1969).
- ⁴ P.L. Colestock and R.J. Kashuba, Nucl. Fusion 23, 763 (1983).
- ⁵ H. Romero and J. Scharer, Nucl. Fusion 27, 363 (1987).
- ⁶ C.N. Lashmore-Davies, G. Francis, A.K. Ram, A. Bers, and V. Fuchs, Bull. Amer. Phys. Soc. 31, 1420 (1986).

23.4.2 Electron Absorption on the Mode-Converted Ion-Bernstein Wave

The fast wave, as discussed in sub-section 23.3.1, undergoes mode-conversion to an ion-Bernstein wave (IBW) near the second harmonic resonance layer (for a single ion-species plasma) or near the hybrid resonance layer (for a two ion-species plasma). This conversion process is efficient for small k_{\parallel} 's which carry substantial power from a single loop antenna. We have developed a numerical code which solves for the propagation of the IBW in three-dimensional torroidal geometry. 1.2 The local dispersion function, D, used for the rays is that for a hot Maxwellian plasma and includes all the nine elements of the dielectric tensor. The spatial profiles of the magnetic field, density and temperature are explicitly included in D. The toroidal ray equations have been set up for an axisymmetric tokamak with concentric flux surfaces but can be generalized to other flux surfaces. The numerical analysis shows that the IBW with small initial k_{\parallel} propagates radially (immediately after mode conversion) away from the modeconversion region. Along this path the poloidal mode number increases substantially. Consequently, k_{\parallel} also increases to the point where the IBW can effectively damp on the electrons. Results show that there is a large enough increase in k_{\parallel} for short distances (compared to the minor radius) of radial propagation that the IBW will damp its energy onto the electrons. This could help explain the experimentally observed electron heating in the ICRF heating of tokamak plasmas, as, for example, on JET.

A simple analytical model has also been developed to go along with the detailed numerical analysis. This model incorporates the essential physics of the IBW and is simple enough to provide substantial information on the propagation of IBW. Furthermore, the results from this model are in excellent agreement with the numerical results. One consequence of the model is an expression which relates the increase in the poloidal mode number, m, to the radial distance of propagation of the IBW.

$$\Delta m \approx \frac{2}{3} \frac{\omega_{cd}^2}{k_r v_{td}^2} \left(2 + 11 \frac{v_{td}^2}{c^2} \frac{\omega_{pd}^2}{\omega_{cd}^2}\right) \frac{r sin\theta}{R + r cos\theta} \Delta r \tag{1}$$

This result is for a deuterium plasma with a hydrogen minority. ω_{cd} , ω_{pd} and v_{td} are the deuterium cyclotron frequency, plasma frequency and thermal velocity respectively, at the radial position r (determined from the toroidal axis) where the IBW is assumed to start propagating, c is the speed of light, θ is the poloidal angle, R is the major radius and k, is the radial wave number at the position r. The connection between k_{\parallel} and m is given by:

$$k_{\parallel} = \frac{1}{|B|} \left[\left(\frac{m}{r} \right) B_{\theta} + \left(\frac{n}{R + r \cos \theta} \right) B_{\phi}^{\prime} \right] \tag{2}$$

where n is the toroidal mode number, B_{θ} and B_{ϕ} are the poloidal and toroidal components, respectively, of the total magnetic field, |B|. Since we assume that there are no variations along the toroidal direction, n is a conserved quantity along the IBW. Consequently, an increase in k_{\parallel} is directly connected to an increase in m. Furthermore, if

we ignore B_{θ} there would be no change in k_{\parallel} . Thus, the enhancement of k_{\parallel} depends upon the presence of a poloidal magnetic field and its variation due toroidicity.

References

¹ A.K. Ram and A. Bers, Book of Abstracts, 1986 Sherwood Controlled Fusion Theory Conference, New York, Apirl 14-16, 1986.

² A.K. Ram and A. Bers, Bull. Am. Phys. Soc. 31, 1420 (1986)

23.5 Relativistic Treatment of Lower Hybrid Current Drive with Wide Spectra

In hot plasmas ($T_{bulk}>1keV$) electrons resonant with lower hybrid spectra of interest to current drive have relativistic energies, and are therefore appropriately described by the relativistic Fokker-Planck equation (in momentum rather than velocity space). Previous discussions^{1,2,3} of relativistic current drive have limited themselves to point or narrow-band spectra and give the corresponding figure of merit J/P_d . We have initiated a numerical and analytic study of the effect of wide-band spectra in (p_{\parallel} , p_{-}) momentum space.⁴ Results in terms of J and P_d are given for a number of situations of interest but also more detailed momentum-space behavior is discussed. Of particular interest for wide spectra is the problem of perpendicular broadening of the distribution. An analytic estimate of T_{\perp} is found, and this permits the formulation of a theory based upon an averaged Fokker-Planck equation.

Suprathermal electrons populating the quasilinear plateau on the distribution function produced during lower hybrid current drive in hot plasmas (i.e., for bulk plasma temperatures exceeding about 1 keV) are very energetic (typically having energies up to about 1 MeV), and must be described by the relativistic Fokker-Planck equation in momentum space:

$$\frac{\partial f}{\partial t} + div(\vec{S}_{coll} + \vec{S}_{rf}) = 0$$
 (1)

The collisional flux vector \vec{S}_{coll} is approximated to describe test electrons colliding with Maxwellian background ions and electrons. Its appropriate relativistic form is derived in Refs. 2, 3, and 5. The quaslinear flux due to RF fields \vec{S}_{rl} , which for lower-hybrid waves is in the parallel (to the external magnetic field) direction, is

$$\vec{S}_{rf} = \hat{\rho}_{\parallel} D_{QL} \frac{\partial f}{\partial \rho_{\parallel}} \tag{2}$$

The wave-spectrum is represented by the quasilinear diffusion coefficient D_{QL} , which was modelled by the function:

$$D_{QL} = const > 0; \quad v_1 \le v_1 \le v_2 \tag{3}$$

$D_{OL} = 0$ elsewhere

The F.-P. equation (1) was solved numerically using the finite-element boundary-value-problem solver TWODEPEP supplied by IMSL. We developed appropriate pre-processor and diagnostics packages to adapt TWODEPEP for the Fokker-Planck problem. The code is currently installed on an IBM 3084, which allows the use of only up to 6 Mbytes of in-core memory. This limits our calculations to electron tails not exceeding about 800 keV, which is insufficient for bulk plasmas hotter than 1 keV, with lower-hybrid spectra whose range exceeds $v_{\parallel} = 16v_{th}$. Nevertheless, even with these restrictions, relativistic calculations produced major differences from a non-relativistic treatment as is demonstrated in Table I.

Our focus was to carefully analyze the effect of spectrum width on the current J, and power dissipated P_d . The calculations revealed a very important effect of perpendicular broadening of the distribution function. Unlike in the nonrelativistic case, an enhanced T_{\perp} , here also enhances the quasilinear plateau length in p_{\parallel} and hence the current. This important effect then led us to develop an analytic theory of T_{\perp} , so we could predict the perpendicular broadening, and this in turn enabled us to perform perpendicular averaging of the two-dimensional Fokker-Planck equation (1).

The principal problems we are now facing in the development of an appropriate one-dimensional relativistic F.-P. equation which accounts for two-dimensional dynamics are:

- relativistic coupling of p_{\perp} and p_{\parallel} in an ansatz for $f(p_{\perp},p_{\parallel})$.
- matching of the quasilinear plateau to the bulk of the distribution function.

The one-dimensional representation, together with two-dimensional techniques extended to include highly relativistic electrons, will enable us to study a number of questions related to LH current drive in hot plasmas.

References

SS KARAGO WARRED ACCESSOR CONTRACTOR

- ¹ N.J. Fisch, Phys. Rev. A 24, 3245 (1981).
- ² K. Hizanidis and A. Bers, Phys. Fluids 27, 2671 (1984).
- ³ C.F.F. Karney and N.J. Fisch, Phys. Fluids 28, 116 (1985).
- ⁴ V. Fuchs, M.M. Shoucri, C.N. Lashmore-Davies and A. Bers, Bull. Am. Phys. Soc. 31, 1423 (1986).
- ⁵ J.D. Mosher, Phys. Fluids *18*, 846 (1975).

Table 1 2-D Relativistic Code Results

$$T_{bulk} = 1keV; v_1 = 4v_7; D_{QL} = 3(mv_7)^2 v_o, v_o = 4\pi (\frac{e^2}{4\pi\varepsilon_o})^2 - \frac{\ln \Lambda n_e}{m_e^2 v_T^3}, v_T^2 = kT/m_e$$

Nonrelativistic

Relativistic

V ₂	Z _i	10 ² J	10⁴p _d	J/P _d	10 ² J	10⁴r	o _d J/P _c	P _{max}
8	1	0.7	2.4	29	.79	2.48	32	40
12	1	2.3	4.3	53	3.2	5.3	60	40
16	1	4.8	6.3	77	14.5	12.3	118	60
16	4	7.3	13.4	55	28.3	32	88	60
16	9	9.2	27	34	44.0	74	60	60

J in units of (nev_T)

 P_d in units of $(mn\nu_0 v_{T}^{-2})$

Note: P_{max} is the upper limit of integration in momentum, in units of (mv_T)

23.6 Absolute Instabilities from Cusp-Maps in the Complex Frequency Plane

The distinction between absolute and convective instabilities for a spatially homogeneous medium can be made by studying the dispersion relation $D(\omega,k)=0$ of the medium, where ω is the complex frequency, and k the complex wavenumber. Let G(x,t) be the response of the medium at a location x and time t to an impulsive excitation applied at the origin. The response G(x,t) is expressed by the Fourier-Laplace integral:

$$G(x,t) = \frac{1}{(2\pi)^2} \int_{\mathcal{L}} d\omega \int_{\mathcal{F}} dk \, \frac{e^{i(kx-\omega t)}}{D(\omega,k)} \tag{1}$$

where L and F are appropriate integration contours in the complex ω and k planes, respectively. For most physical problems, the double integral in (1) cannot be easily evaluated for all t. In order to distinguish between absolute and convective instabilities, however, we only need to know the asymptotic behaviour of G(x,t) for large times. This can be determined using a well-known method of analytic continuation, in which the Laplace contour L is deformed towards the lower half of the complex ω -plane. If L can be deformed below the real ω -axis, the instability is convective. Otherwise, $G(x,t\to\infty)$ is dominated by the "pinch-point" singularity having the largest temporal growth rate; this is the case of an absolute instability.

The procedure described above, requires obtaining from the dispersion relation the wavenumber k as a function of the frequency ω . However, in many physical problems it is easier to determine ω as a function of k, than the other way around. For such cases, we have developed a procedure which locates pinch-points without having to map from the ω -plane into the k-plane.²³ This new procedure is implemented by deforming the F-contour off the real k-axis in such a way that its image in the ω -plane progresses downward from the highest branch of the map of the real k-axis (Figure 23.1). Double roots of the dispersion relation (ω_o, k_o) , are easily detected by the local angle-doubling property of the map: $(\omega-\omega_0)\sim (k-k_o)^2$. In the simplest cases, absolute instabilities occur when the deformed F -contour maps into the complex ω -plane as shown in Figure 1, where the point ω_a is found to lie in the upper-half ω -plane, beneath a single unstable branch of the image of the real k-axis. The point ω_{ac} connecting two Riemann sheets of the multi-sheeted ω -plane, is only covered by the image of the real k-axis on one of these two sheets. Thus, if the L-contour, deformed to pass through ω_o , is mapped in to the k-plane, its image will pinch the deformed F-contour at k_0 Consideration of this simple topology was useful in stability analysis of flow in the wake of a circular cylinder, where vortex formation was found to correspond with the absolute versus convective properties of the instability.4 The procedure for cases leading to mappings of higher topological complexity can be found in reference [3].

References

- ¹ A. Bers, In *Handbook of Plasma Physics*, Vol. 1, edited by M. N.Rosenbluth and R. Z. Sagdeev, North Holland, 1983, Chapter 3.2.
- ² K. Kupfer, A. Bers, A.K. Ram, Bull. Am. Phys. Soc. 31, 1402 (1986).

- ³ K. Kupfer, A. Bers, and A.K. Ram, M.I.T. Report PFC/JA-87-13 (1987); to appear in Phys. Fluids 1987.
- ⁴ G.S. Triantafyllou, M.S. Triantafyllou, C. Chryssostomidis, J. Fluid Mech. *170*, 461 (1986).

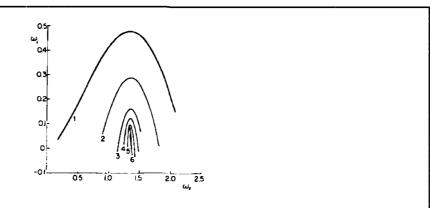


Figure 23.1.: Curve 1 image of the real k-axis in the ω plane; curves 2 through 6: images of lines parallel to the real-k axis. The pinch point is located at the cusp of curve 6.

23.7 Physics of Thermonuclear Plasmas

U.S. Department of Energy (Contract DE-AC02-78ET-51013)

Bruno Coppi

The main theme of this program is the theoretical study of plasmas in thermonuclear regimes. Topics include, but are not limited to, study of basic plasma properties (stability, transport, ...), simulation of present day and future experiments on magnetically confined plasmas, and design of machines for fusion burn experiments and advanced fuels. Theoretical guidance for and participation in the Alcator experimental program are an important part of our effort.

We are particularly interested in the physics of high density plasmas that has been pioneered by the Alcator program in view of its outstanding confinement as demonstrated by the record values of the parameter, $n\tau_{\text{E}}$, and the degree of plasma purity 1/($Z_{\text{eff}}\text{-}1)$ achieved. An analysis that we presented to the Department of Energy about six years ago indicated that shorter than expected confinement times in Alcator C plasmas should have been attributed not to a degradation of electron energy confined but instead to an increase of the ion thermal conductivity. This analysis led to the well known pellet injection experiments in Alcator C that result in the record $n\tau_{\text{E}}$. The circumstantial evidence for our analysis was an observation that density profiles formed as a result of neutral gas injection in Alcator C were "flatter" than those of other experiments. In particular, the parameter:

$$\eta_i = \frac{dlnT_i}{dr} / \frac{dlnn}{dr}$$

had values, even in the central part of the plasma column, that were above the threshold for the onset of "ion mixing modes" that can produce a strong effective ion thermal conductivity. Therefore, it was natural to suggest that the "cure" was to be found in producing density profiles that were peaked to the extent that η_i could be close to unity and the relevant experiments appear to have confirmed our expectation. In fact, the idea of "profile consistency" that was being formulated at that time implied that it would have been difficult to alter the canonical shape of the electron temperature profile, compared to the relative ease with which density profiles were modified. The concomitant prediction that the impurity transport had to be influenced by the change in η_i been also verified by the observations. These circumstances and the need to have a firmer basis, than presently available, on which to predict the ion thermal energy losses in future ignition experiments, have led us to intensify our efforts and those of our colleagues at the Princeton Plasma Physics Laboratory on developing further the linear and the nonlinear theory of ion mixing modes. At the same time, we have started an effective collaborative effort with our colleagues of the (Princeton) TFTR team who have carried out the latest pellet injection experiments. These experiments, performed for the purpose of providing (if possible) a detailed interpretation of energy losses, have achieved new record values of the confinement parameter $n\tau_{\text{F}}$.

The line of compact experiments that we have proposed first in 1975, as a follow up to the Alcator and Frascati Torus programs, and developed through a series of design studies in later years was adopted as the next major undertaking of the U.S. fusion program in 1985; three major centers (Lawrence Livermore National Laboratory, M.I.T., and Princeton) are now committed to this line of investigation. In addition, following the agreements to pursue collaboration in fusion research with the U.S.S.R. concluded at the Geneva Summit meeting, a compact ignition experiment has been considered as the first step to be taken in a more general frame for the development of fusion research through the end of this century. Meanwhile, the Ignitor effort that was initiated in Europe about 10 years ago has been stepped up and a set of tests on the most critical machine component is being planned.

The Alcator C-Mod machine that is now under construction at M.I.T. is based on a magnetic confinement configuration adopted already in the Ignitor design and that we had studied in the early seventies under the name of Megator. Those studies proposed experiment that, like Alcator C-Mod, combine high magnetic field and compact geometry with tight aspect ratio and elongated plasma cross section. Such designs were intended to produce plasma currents exceeding 1 Mega Amperes while maintaining current densities in the same range as those expected, at that time, in the Alcator experiments.

In the next subsections we present several major topics of theoretical investigation: the principle of profile consistency, fishbone oscillations in beam injected as well as ignited tokamaks, transport simulations in current and planned experiments, and an analysis of the pathways to ignition.

23.7.1 Profile Consistency

Among the general criteria that we have tried to formulate a few years ago in order to describe the "anomalous" transport characteristics (that are not explained by clas-

sical transport theories that include the effects of discrete particle collisions only) of magnetically confined plasmas is the so-called "Principle of Profile Consistency." ¹ The main implication of this principle is that the transport coefficients that conform to it depend on the global properties of the plasma column. Another implication is that there are two kinds of physical processes involved: one that reconstructs the canonical electron temperature profile after it is severely disrupted, such as when a massive pellet is injected in the plasma column, and one that determines the rate of electron energy transport under nearly steady state conditions. Thus a variety of transport equations that can describe both processes have been considered, including one that involves the presence of an inward flow term that is difficult to justify on the basis of the properties of known microinstabilities and is not suitable to represent the wider range of experimental information now available. Instead it is more appropriate to introduce an effective thermal conductivity that has a nonlinear dependence on the electron temperature gradient, such as

$$\kappa_{\text{eff}} = \left\lceil \kappa_s^2 + \kappa_f^2 \left(\frac{a^2}{T_e \dot{\alpha}} - \frac{\partial T_e}{\partial r^2} + 1 \right)^2 \right\rceil^{1/2},$$

where the canonical electron temperature profile is represented by $T_e^c(r) = T_{eo} \exp(-\alpha)$, $\alpha \equiv \alpha(r^2/a^2)$, a is the plasma minor radius, κ_s is the thermal conductivity that persists when T_e is completely relaxed on the $T_e^c(r)$ profile, and κ_F the coefficient corresponding to the fast process that rearranges $T_e(r)$ when it is forced to depart from $T_e^c(r)$. Considering $\kappa_F^2 > \kappa_s^2$ and steady state conditions, the peak value T_{eo} is determined by the "minimum departure condition," namely that

$$\mathsf{F}(\mathsf{T}_{\mathsf{eo}}) = \int_0^{\alpha_{\mathsf{b}}} \ \frac{\mathsf{d}\alpha}{\kappa_{\mathsf{f}}} \left[\left(\frac{\overline{\mathsf{S}}_{\mathsf{e}} \mathsf{a}^2}{4 \dot{\alpha} \; \mathsf{T}_{\mathsf{e}}^{\mathsf{c}}} \right)^2 \; - \kappa_{\mathsf{s}}^2 \right]^{1/2}$$

be a minimum; α_b denotes the value of α at the edge of α the plasma column where $\overline{S}_e(r) \equiv (2/r^2) \int r' S_e(r') dr'$, $S_e(r)$ is the electron energy source and $\alpha_b \equiv \alpha(r=a)$. Therefore κ_s need not be function of the profile of $S_e(r)$ in order to enforce profile consistency and can be used directly as derived from a nonlinear theory of the type of microinstability deemed to be responsible for it. One that is considered of special interest for this is the so-called ubiquitous mode² that is driven by the electron temperature gradient and produces thermal energy transport without corresponding particle transport. In the case where only ohmic heating is present, the adopted diffusion coefficient $D_{th}^e = \kappa_s/n$ is

$$D_{th}^{e}{\simeq}2.4\times10^{18}(a/r)B_{\theta}/(nT_{e})(Z./A_{i})^{1/4}(q_{s}R)^{-1/2}cm^{2}/\;sec$$

where T_e is in keV, B_θ in kG, n in cm⁻³, R in cm, $Z \cdot /A_i \equiv v_s^2/(T_e/m_p)$, m_p the proton mass and v_s the ion sound velocity of the considered plasma. When injected heating is dominant

$$8\pi/(B_{\theta}r)^2\int_{0}^{r}dr^2 d(nT_e)/d\ell nr$$

becomes the limiting factor and D_{th}^{e} acquires the scaling $D_{th}^{e} \propto 1/B_{\theta}$. The existence of two processes, fast and slow, on the temperature evolution has been confirmed by the Alcator pellet injection experiments.³ Observations made by electron cyclotron emission have shown that, within a time of the order of 200 μ sec-300 μ sec after the central

electron temperature has dropped due to the injection of the pellet, the electron temperature profile recovers its typical Gaussian shape. This time scale is shorter by as much as two orders of magnitude than the electron energy transport time scale controlled by $\kappa_{\rm s}$ The propagation of sawtooth heat pulses is also indicative of the existence of two transport time scales.

23.7.2 Fishbones

The most striking of all collective processes that have been so far observed in magnetically confined, neutral beam-injected plasmas is the so-called "fishbone instability," named after the characteristic skeletal signatures of the plasma temperature and poloidal magnetic field fluctuations. Fishbone bursts are correlated with losses of energetic beam particles, reducing the beam heating efficiency and thus limiting the maximum achievable β (=kinetic pressure/magnetic pressure). The mode structure is typically dominated by the m° = 1, n° = 1 poloidal and toroidal harmonics, with a frequency of oscillation in the 10-20 kHz range. This frequency is of the same order and sign⁹ as that of both the core-ion diamagnetic frequency $\omega_{\rm di}$ and the magnetic drift frequency $\omega_{\rm Dh}$ of energetic beam particles that are trapped in magnetic wells along the equilibrium field lines. The appearance of fishbone activity coincides roughly with the threshold for the onset of pressure-driven m° = 1 internal kink modes in a toroidal confinement configuration.

We have proposed 10,11 a theoretical model of the linear instability process based on the following: 1) the excited mode has a frequency of oscillation nearly equal to the ion diamagnetic frequency and is one of the two m° = 1 modes that are found under the conditions for ideal MHD instability, but are rendered marginally stable by finite ion Larmor radius effects of the core-plasma; 2) the mode excitation energy is related to the plasma pressure gradient; and 3) the presence of a "viscous" dissipative process, e.g., produced by a mode-particle resonance, is required for this instability to develop. In the case of perpendicular netural beam injection, the relevant mode particle resonance is $\omega = \omega_{\rm Dh}^{\rm (c)}(\epsilon,\mu)$, where $\omega_{\rm Dh}^{\rm (c)}$ is the average-along-the-orbit magnetic drift frequency of energetic ions having energy $\varepsilon = (1/2) \rm m_h v^2$ and magnetic moment $\mu = (1/2 \rm B) \rm m_h v_\perp^2$. In fact, $\omega_{\rm di}/\omega_{\rm Dh}^{\rm (c)} \sim (T_i/T_h)(R/r_n) \times (1+\eta_i) \sim 1$ for typical beam parameters, where $T_{\rm i(h)}$ is the core-ion (hot-ion) temperature, $r_n = |d\ell_n \rm n_i/dr|^{-1}$ and $\eta_i = d\ell_n \rm T_i/d\ell_n n_i$.

As a consequence of the excited mode, resonant beam ions can be transported out of the plasma column.^{12,13} In Ref. 10 we have constructed a simple nonlinear model for the instability cycle based on the resistive damping of the fishbone mode once the number of resonating particles has dropped sufficiently. Another possibility is that the saturated mode may be damped in a process connected to the spatial phase mixing of an Alfven wave packet, as was first proposed in Ref. 14.

These considerations lead to the following picture for the interplay between fishbone bursts and sawtooth oscillations. The instabilities of the fishbone mode and the resistive internal kink mode involve different threshold values of the poloidal beta, $\beta_p = [8\pi/B_\theta^2(r_o)][\overline{p}(r_o) - p(r_o)], \text{ where } \overline{p}(r_o) = r_0^{-2} \int_{-r_o}^{r_o} p(r) dr^2 \text{ and } r_o \text{ is the radius of the mode rational surface where the inverse rotational transform q=1. For the resistive kink, <math display="inline">\beta_{p,crit}^{rk}$ is determined by the combined effects of ion viscosity and ion diamagnetic frequency. Since the resistive kink mode has a frequency much lower than ω_{di} it does not interact efficiently with the beam and thus depends on resistivity for the dissipation. The threshold

value for the fishbone mode is lower, $\beta_{p,crit}^{fm} < \beta_{p,crit}^{rk}$. The value of β_p increases along the sawtooth ramp, as the pressure profile steepens. When, $\beta_{p,crit}^{fm} < \beta_p < \beta_{p,crit}^{rk}$, only the fishbone mode is unstable, but it saturates and decays quickly on a fast (a few msec) time scale, resulting in expulsion of energetic particles while leaving the macroscopic central plasma region essentially unaffected. As soon as β_p exceeds $\beta_{p,crit}^{rk}$, the resistive internal kink mode is excited and it determines the "crash" of the sawtooth.

We emphasize that this physical picture relies on the assumption of relatively large values of the core-ion diamagnetic frequency. When diamagnetic frequency effects are neglected, a recent analysis, ¹⁶ valid for arbitrary values of the ideal MHD energy functional, has determined that ion viscosity brings about a reduction in the growth rate of the m° = 1 mode, but by itself is insufficient to completely stabilize it. When the core-ion diamagnetic frequency is large, on the other hand, ion viscosity stablization is easily achieved. ¹⁵

These results have several consequences for the prediction of sawtooth oscillations in compact ignition experiments, 17 to the extent that the plasma can be driven near (or past) the ideal MHD marginal stability threshold of $m^{\circ}=1$ modes. First, sawtooth crashes may occur only when the minimum value of δW exceeds a (possibly negative) threshold value during the temperature ramp, as the pressure profile steepens. Second, sawteeth may be suppressed even though q<1 in part of the plasma. Third, in toroidal plasmas where the "poloidal beta" parameter is relatively high and the $m^{\circ}=1$ instability is driven primarily by the pressure gradient, disruptions may relax the pressure profile only, leaving the q-profile unchanged.

23.7.3 Transport Simulation

ed Docesterral Perserveri Erretzeek Debester - Personer - Cecester - Cestester - Cestester - Cestester - Cestester

The investigation of the radial energy balance and thermal transport in large size Ohmic plasmas carried out in collaboration with Princeton Plasma Physics Laboratory has reached a major milestone, where a one dimensional, numerical transport model with sawtooth oscillations has been shown^{18,19} to reproduce Ohmic TFTR plasmas run from 1983-86. Some 40 representative discharges were simulated, including current, density, and toroidal magnetic field scans from different operating periods. The numerical model can be used to characterize a "standard" TFTR Ohmic discharge (without anomalous ion thermal conductivity). It provides a sensitive check on Z_{eff} and, to a lesser extent, plasma composition measurements beyond that available from a standard analysis code. Points of discrepancy between simulation and experiment have been analyzed and accounted for.

Analysis of the simulated discharges shows the inherent limitations on the accuracy to which a transport model can be determined from experiment under fairly ideal conditions (well-diagnosed plasma, similar types of discharges). The extent to which a different driving mechanism can be supported by experiment has been investigated by considering ranges of parameters, including varying size plasmas. Assuming the fundamental nature of profile consistency (for either the electron temperature T_e or the toroidal current density J_{ϕ}), the major effect of a different driving mechanism is to change the dependences of voltages, peak temperatures, and energy confinement times on the plasma parameters. Rather than model different diffusion coefficients, the original transport results were analyzed for trends in the discrepancy between simulation

and experiment. Results suggest a stronger inverse dependence of the diffusion coefficient on the major radius R, indicative of gradient-driven or drift wave type transport. However, the results are not conclusive because of the accumulated differences due to the experimental uncertainties and to the systematic variations between different types of discharges, which have not been quantified before. Trials with different diffusion coefficients also show that the dependence on the plasma parameters is difficult to distinguish, as long as a reasonable temperature profile shape is produced. The likely thermal transport mechanisms are thus difficult to distinguish on the basis of Ohmic data alone. Auxiliary heating adds other uncertainties, as well as changing the underlying plasma instabilities when it is strong.

Sawtooth oscillations, in the model used, were shown to have relatively little (\sim 10%) effect on the volume integrated energy balance, despite large changes in the electron temperature (30% in T_{eo}), toroidal current density, and Ohmic heating radial profiles.²⁰ The effect was studied by disabling the trigger for the sawtooth crash, while retaining the best fit input parameters and thus shows the effect of the numerical model. Flattening the temperatures and particle densities during an instantaneous crash, and redistributing the current according to helical flux conservation adequately accounts for the roughly linear variation of $T_{eo}/< T_e>$ (central/volume average) with the safety factor q_a at the plasma edge. Experimental profiles (ECE) indicate an additional narrowing of the T_e profile with increasing q_a noticeable at higher $q_a \ge 4$.

In the past year we have added alongside the relatively simple, fast one dimensional transport code a more complex 1 1/2 D version (BALDUR, modified by Glenn Bateman of Princeton Plasma Physics Laboratory). Thus we have been able to self-consistently take into account effects important for compact ignition experiments, such as the paramagnetic increase in the magnetic field at low β_p , the distribution of plasma current with a realistic geometry, the time dependent evolution of the plasma configuration due to the initial ramping of current and magnetic field.²¹ Using similar transport models, results from this code generally confirm our earlier predictions of the behavior of the ignition process.^{17,22} As expected, some vary, for instance, the sawtooth size increases in 1 1/2 D with a helical flux conservation model.

We are using the 1 1/2 D code in collaboration with our other research efforts to model new Ignitor parameters, test the effects of different forms for anomalous electron thermal transport, and investigate the consequences for ignition of the possible presence of anomalous ion heat transport due to η_i modes.²³ Since the latter transport increases strongly with T_i its effects can be quite deleterious if it extends over a significant portion of the plasma column.

An extension to DD and D³He fusion regimes has been under way for the 1D code and is planned for the 1 1/2 one as well. It incorporates the set of fusion reactions between D, T, He³ and their fusion products in a self-consistent manner, keeping track of fusion "ash" as well as energetic particles. The macroscopic effects of synchrotron radiation will be included. The ignition scenario envisions DT ignition with auxiliary heating in a modified compact ignition device, then addition of D and He³. Initial studies have been done of the device parameters with DT alone.

23.7.4 Density Limit and Path to Ignition

In order to reach ignition, it is desirable to maintain the highest possible value of the confinement parameter $n\tau_e$, implying operation at relatively high densities where collisional (neoclassical) ion thermal losses and electron-ion bremsstrahlung become significant in the global energy balance. These losses are equal to the energy per unit time deposited by the fusion reaction products at the "minimum ignition temperature." Near and above this temperature, the presence of anomalous ion thermal conductivity due to collective modes can strongly affect the optimal value of the density that yields the fastest approach to the attainment of ignition for a given amount of external power. We have considered in particular the so-called η_i modes²³ with perpendicular wavelengths considerably greater than the ion gyroradius, which produce an ion thermal conductivity proportional to $nT_i^{3/2}$. In collaboration with W. Tang of Princeton Plasma Physics Laboratory, we have constructed an approximate model equation for the steady state energy balance in the central region of the plasma column and have obtained multi-valued solutions for the density as a function of temperature, ion thermal anomaly strength, and external heating power.²⁴

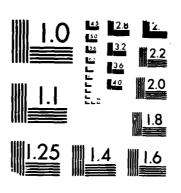
For the case of no ion anomaly, there is a maximum density allowed for the plasma to reach the minimum ignition temperature T_m , while beyond T_m all densities are allowed. In the presence of an anomaly, a critical external power must be supplied to provide a channel between allowed density regions as the temperature increases beyond T_m . For a realistic temperature dependence of the fusion reaction cross section, the density must be progressively adjusted above a minimal value in order to heat the plasma to temperatures considerably larger than T_m .

We have verified the analytical properties of the model equation with 1 1/2 D numerical simulations, 17,25 applied to the parameters of the Ignitor compact ignition experiment.

References

- ¹ B. Coppi, Comments Plasma Phys. Controlled Fusion 5, 261 (1980).
- ² B. Coppi and G. Rewoldt, Phys. Rev. Lett. 33, 1320 (1974).
- ³ C.C. Gomez, Ph.D. Diss., M.I.T., Cambridge, Mass., Report PFC/RR-86-8, 1986.
- ⁴ K. McGuire et al., Phys. Rev. Lett. 50, 891 (1983).
- ⁵ D. Johnson et al., In *Plasma Physics and Controlled Fusion Research*, Vienna: I.A.E.A., 1983, Vol. 1, p. 9.
- ⁶ J.D. Strachan et al., Nuclear Fusion 25, 863 (1985).
- ⁷ D.O. Overskei et al., In *Heating in Toroidal Plasmas*, Rome: E.N.E.A., 1984, Vol. 1, p. 29.
- ⁸ W.W. Heidbrink et al., Phys. Rev. Lett. 57, 835 (1986).

RLE (RESEARCH LABORATORY OF ELECTRONICS) PROGRESS
REPORT NUMBER 129(U) MASSACHUSETTS INST OF TECH
CAMBRIDGE RESEARCH LAB OF ELECTRON. J ALLEN ET AL.
JAN 87 ARO-23223. 43-EL DAAL03-86-K-8002 F/G 14/2 MD-R193 799 3/4 UNCLASSIFIED NL



MICROCOPY RESOLUTION TEST CHART

IREAL: STANDARDS 1963 A

- ⁹ B. Coppi, contribution presented at the Varenna Workshop on Plasma Transport, Varenna, Italy, 1982, and at the PPPL Workshop on Bean-Shaped and High- β Tokamaks, Princeton, New Jersey, 1983.
- ¹⁰ B. Coppi and F. Porcelli, Phys. Rev. Lett. *57*, 2272 (1986).
- ¹¹ B. Coppi, S. Migliuolo, and F. Porcelli, submitted to Phys. Fluids (1987).
- ¹² B. Coppi and A. Taroni, Plasma Phys. 26, 2958 (1983).
- ¹³ R.B. White et al., Phys. Fluids 26, 2958 (1983).
- ¹⁴ V.W. Gribkov, B.B. Kadomtsev and O.P. Pogutse, JETP Lett. 38, 15 (1983).
- ¹⁵ F. Porcelli and S. Migliuolo, Phys. Fluids 29, 1741 (1986).
- ¹⁶ F. Porcelli, Phys. of Fluids 30, 1736 (1987).
- ¹⁷ B. Coppi, R. Englade, S. Migliuolo, F. Porcelli, and L. Sugiyama, in *Plasma Physics and Controlled Nuclear Fusion Research*, Kyoto, Japan (to be published by I.A.E.A., Vienna, 1987).
- ¹⁸ J. Martinell, Ph.D. Thesis, Dept. of Physics, M.I.T., Cambridge, Mass., 1986.
- ¹⁹ L. Sugiyama, J. Martinell, and P. C. Efthimion, "Predictive Transport Simulation of TFTR Ohmic Discharges," M.I.T., R.L.E. Report PTP-87/1, submitted to Nucl. Fusion.
- ²⁰ L. Sugiyama, "R and a Dependence of Electron Anomalous Thermal Transport," M.I.T., R.L.E. Report PTP-86/8, August 1986.
- ²¹ R. Englade and L. Sugiyama, Sherwood Theory Conference, New York, 1986.
- ²² L. Sugiyama, M.I.T., R.L.E. Report PTP-84/2, 1984.
- ²³ T. M. Antonsen, Jr., B. Coppi and R.C. Englade, Nuclear Fusion 19, 641 (1979).
- ²⁴ B. Coppi and W. Tang, Princeton Plasma Physics Laboratory Report PPPL-2343, 1986, submitted to Phys. Fluids.
- ²⁵ R. Englade, Bull. Am. Phys. Soc. *31*, 1565 (1986).



24.0 Digital Signal Processing

Academic and Research Staff

Prof. A.V. Oppenheim, Prof. J.S. Lim, Prof. B.R. Musicus, Prof. A.B. Baggeroer, G. Aliberti

Graduate Students

J. Bondaryk, D. Cobra, M. Covell, W.P. Dove, M. Feder, D. Griffin, D. Harasty, J. Hardwick, D. Izraelevitz, J. Jachner, T. Joo, D. Martinez, E. Milios, C. Myers, T. Pappas, J. Rodriguez, A. Silva, P. van Hove, M. Wengrovitz, A. Zakhor

Support Staff

toppostate variables sociation economic economic economics

25.25.25

P. Eiro, D. Gage

Part-time Assistants/Special Projects

S. Corteselli, A. Donato, M. Dove

Introduction

The Digital Signal Processing Group is carrying out research in the general area of signal processing. In addition to specific projects handled on campus, there is close interaction with Lincoln Laboratory and the Woods Hole Oceanographic Institution. While a major part of our activities focus on the development of new algorithms, there is a strong conviction that theoretical developments must be closely tied to applications. We are involved with the application areas of speech, image, video, and geophysical signal processing. We also believe that algorithm development should be closely tied to issues of implementation because the efficiency of an algorithm depends not only on how many operations it requires, but also on how suitable it is for the computer architecture it runs on. Also strongly affecting our research directions is the sense that while, historically, signal processing has principally emphasized numerical techniques, it will increasingly exploit a combination of numerical and symbolic processing, a direction that we refer to as knowledge-based signal processing.

In the area of knowledge-based signal processing, there are currently two research projects. One involves the concept of symbolic correlation, which is concerned with the problem of signal matching using multiple levels of description. This idea is being investigated in the context of vector coding of speech signals. Symbolic correlation will entail the use of both symbolic and numeric information to efficiently match a speech signal with stored code vectors. The second project in this area deals with the representation and manipulation of knowledge and expressions in the context of signal processing. This work examines issues such as the representation of knowledge, derivation of new knowledge from that which is given, and strategies for controlling the use of this knowledge.

In the area of speech processing, we have, over the past several years, worked on the development of systems for bandwidth compression of speech, parametric speech modeling, time-scale modification of speech and enhancement of degraded speech. Recently, a new model-based speech analysis/synthesis system has been developed. This system has been shown to be capable of high quality speech production, and it is currently being used in several mid-rate speech coding systems. Future work is aimed at using the speech model at lower bit rates through efficient coding techniques. Research is also continuing on adaptive noise cancellation techniques in a multiple microphone environment.

In image processing, we are pursuing a number of projects on restoration and enhancement. One project involves the estimation of coronary artery boundaries in angiograms. This research has produced a more robust model of the coronary angiograms, which consequently, improves the estimates of the arterial dimensions. A second image processing project is studying the removal of ghosts from television signals. This form of degradation is caused by multi-path channels and can be removed by the use of an appropriate inverse filter. The stable filter which results in general non-causal and, therefore, some form of time reversal must be used to implement the filter.

In the area of geophysical signal processing, current research is focused on the transformation of side scan sonar data. In practice, this data is corrupted by a number of factors related to the underwater environment. In this project, the goal is to explore digital signal processing techniques for extracting the topographic information from the actual sonographs. Concepts under study include the removal of distortions caused by towfish instability and reconstruction based on multiple sonographs taken from different angles.

There are also a number of projects directed toward the development of new algorithms with broad potential applications. For some time we have had considerable interest in the broad question of signal reconstruction from partial information, such as Fourier transform phase or magnitude. We have shown theoretically how, under very mild conditions, signals can be reconstructed from Fourier transform phase information alone. This work has also been extended to the reconstruction of multi-dimensional signals from one bit of phase, and, exploiting duality, zero-crossing and threshold crossing information. Current research in this area is aimed at reconstruction from distorted zero-crossings. In addition, the reconstruction from multiple threshold crossings is being studied. This problem has been shown to be better conditioned than recon-We are also examining the problem of struction using only a single crossing. narrowband signal detection in wideband noise. This project looks to compare several different techniques under a number of computational constraints. Research also continues on relationships between information theory and stochastic estimation. We are exploring applications to statistical problems, iterative signal reconstruction, short-time analysis/synthesis, and parameter estimation.

With the advent of VLSI technology, it is now possible to build customized computer systems of astonishing complexity for very low cost. Exploiting this capability, however, requires designing algorithms which not only use few operations, but also have a high degree of regularity and parallelism, or can be easily pipelined. The directions we are exploring include systematic methods for designing multi-processor arrays for signal processing, isolating signal processing primitives for hardware implementation, and

searching for algorithms for multi-dimensional processing that exhibit a high degree of parallelism. We are also investigating highly parallel computer architectures for signal understanding, in which a mixture of intensive computation and symbolic reasoning must be executed in an integrated environment.

24.1 Reconstruction of Two-Dimensional Signals From Distorted Zero Crossings

National Science Foundation (Grant ECS 84-07285)
U.S. Navy - Office of Naval Research (Contract N00014-81-K-0742)

Alan V. Oppenheim, Joseph E. Bondaryk

It has been shown in theory that most two-dimensional, periodic, bandlimited signals are uniquely specified by their zero crossings or threshold crossings. It has also been proven that such two-dimensional images can in practice be reconstructed from threshold crossing information only.

It is the aim of this research to show that such an image, that has been affected by a non-linear, perhaps non-monotonic, distortion, can be reconstructed from the distorted signal's threshold crossing information. The threshold crossings will describe a set of linear equations, which can be solved to find the Fourier coefficients of the original image. An inverse DFT is then used to recover this image. The distortion may then be characterized by comparison of the original and distorted images. This research will attempt to identify the factors which most affect the reconstructability of the signal.

24.2 Digital Processing of Side Scan Sonar Data

National Science Foundation (Grant ECS 84-07285)
U.S. Navy - Office of Naval Research (Contract N00014-81-K-0742)

Alan V. Oppenheim, Daniel T. Cobra

Since its introduction in the early sixties, side scan sonar has proved to be a very important tool for underwater exploration, and in particular for marine geology. Several of its applications include surveying the sea floor, the search and location of objects on the bottom of the sea, and the prospection of mineral deposits.

The information contained in reflected sound waves is used by side scan sonar to produce a graphic record, called a sonograph, which constitutes a composite representation of the topographic features and the relative reflectivity of the various materials of the seabed. Due to several factors, however, sonographs do not provide a precise depiction of the topology. Geometric distortions can be caused by motion instability of the towfish on which the transducers are mounted, which can be caused by variable ship speeds and sea currents. The record can also suffer from interferences such as those caused by dense particle suspension in the water, shoals of fish, or by ultrasonic waves generated by passing ships. As a result, the extraction of topographic information from sonographs requires extensive practice and is often a tedious and time-consuming task.

Our general goal is to explore the application of digital signal processing techniques to side scan sonar data. At present, two specific problems are being contemplated. One is the estimation and correction of the distortions caused by towfish instability. The other is to determine the topography of the sea bed from the stereoscopic information contained in two or more sonographs of the same area made from different angles. The research is being conducted under M.I.T.'s joint program with the Woods Hole Oceanographic Institution, with the cooperation of the U.S. Geological Survey.

24.3 Representation and Manipulation of Signal Processing Knowledge and Expressions

National Science Foundation Fellowship National Science Foundation (Grant ECS 84-07285) U.S. Navy - Office of Naval Research (Contract N00014-81-K-0742)

Alan V. Oppenheim, Michele Covell

poposoon someone appropriate appropriate contracts

The phrase "signal processing" is used to refer to both "symbolic" and "numeric" manipulation of signals. "Symbolic" signal processing manipulates the signal description as opposed to the signal values with which "numeric" signal processing is primarily concerned. Efforts have been made to create computer environments for both types of signal processing.^{1,2} Some issues that arise as a result of this work concern uniform representation of knowledge, derivation of new knowledge from that which is given, and strategies for controlling the use of this knowledge. This research will be concerned with these areas and how they apply to digital signal processing.

Representations that have been used in symbolic signal processing^{1,2,3} have been largely distinct from those used in numeric signal processing.^{1,4} The types of representations used are further separated by the control structures that the numeric and symbolic information commonly assume, the distinction essentially being the same as the distinction between Algol-like languages and logic programming languages. This dichotomy results from the differing amounts of available knowledge about the appropriate approaches to the problems being addressed. By separating the control structure from application knowledge, this dichotomy can be avoided.

Strategies for controlling when knowledge about a signal is used should be provided and new strategies should be definable, since these control structures provide additional information about the problem space, namely approaches that are expected to be profitable. Control strategies can also be used to outline new approaches to a problem, approaches that would not be considered by simple trigger-activated reasoning.

Finally, the ability to derive new knowledge from that which is given is desirable. This ability would allow the amount of information initially provided by the user to be minimized. The environment could increase its data base with new conclusions and their sufficient preconditions. Two immediate advantages of providing the environment with this ability are the reduction in the programming requirements and the possible "personalization" of the data-base. A reduction in programming requirements is available since information that is derivable from given information need not be explicity encoded. Commonly, this type of information is provided to improve the performance of the derivation process. Secondly, since the environment would add information to

the data set according to conclusions prompted by the user's queries, the data set would expand those areas which the user had actively explored.

References

STATES STATES ASSESSED FROM THE STATES CONTRACT DESIGNATION OF CONTRACT OF CON

- ¹ Dove, W.P., "Knowledge-Based Pitch Detection," Ph.D. Diss., M.I.T., Cambridge, Mass., 1986.
- ² Kopec, G., "The Representation of Discrete-Time Signals and Systems in Programs," Ph.D. Diss., M.I.T., Cambridge, Mass., 1980.
- ³ Milios, E., "Signal Processing and Interpretation using Multilevel Signal Abstractions," Ph.D. Diss., M.I.T., Cambridge, Mass., 1986.
- ⁴ Myers, C., "Signal Representation for Symbolic and Numerical Processing," Ph.D. Diss., M.I.T., Cambridge, Mass., 1986.

24.4 Iterative Algorithms for Parameter Estimation with Applications to Array Processing

National Science Foundation (Grant ECS 84-07285)
U.S. Navy - Office of Naval Research (Contract N00014-81-K-0742)

Alan V. Oppenheim, Meir Feder, Ehud Weinstein³

Many signal processing problems may be posed as statistical parameter estimation problems. A desired solution for the statistical problem is obtained by maximizing the Likelihood (ML), the A-Posteriori probability (MAP) or some other criterion, depending on the a-priori knowledge. However, in many practical situations, the original signal processing problem may generate a complicated optimization problem, e.g., when the observed signals are noisy and "incomplete."

An iterative framework for maximizing the likelihood, the EM algorithm, is widely used in statistics. In the EM algorithm, the observations are considered "incomplete" and the algorithm iterates between estimating the sufficient statistics of the "complete data" given the observations and a current estimate of the parameters (the E step), and maximizing the likelihood of the complete data, using the estimated sufficienct statistics (the M step). When this algorithm is applied to signal processing problems, it yields, in many cases, an intuitive appealing processing scheme.

In the first part of this research, we investigate and extend the EM framework. By changing the "complete data" in each step of the algorithm, we can achieve algorithms with better convergence properties. In addition, we suggest EM type algorithms to optimize other (non ML criteria). We also develop sequential and adaptive versions of the EM algorithm.

³ Woods Hole Oceanographic Institution

In the second part of this research, we examine some applications of this extended framework of algorithms. In particular, we consider:

- Parameter estimation of composite signals, i.e., signals that can be represented as a decomposition of simpler signals. Examples include:
 - 1) multiple source location (or bearing) estimation and
 - 2) multipath or multi-echo time delay estimation.
- Noise cancellation in a multiple microphone environment (speech enhancement)
- Signal reconstruction from partial information (e.g., Fourier transform magnitude).

The EM-type algorithms suggested for solving the above "real" problems provide new and promising procedures, and they thus establish the EM framework as an important tool to be used by a signal processing algorithm designer.

24.5 A New Mixed-Excitation Speech Model and Its Application to Bit-Rate Reduction

National Science Foundation (Grant ECS 84-07285)
Sanders Associates, Inc.
U.S. Air Force - Office of Scientific Research (Contract F19628-85-K-0028)
U.S. Navy - Office of Naval Research (Contract N00014-81-K-0742)

Jae S. Lim, Daniel W. Griffin

THE POLICE OF THE PROPERTY OF

One approach to speech coding involves estimating and encoding the parameters associated with some underlying speech model (vocoders). The encoded speech model parameters are then transmitted and the receiver decodes them, employing the speech model to synthesize speech. Examples of vocoders include linear prediction vocoders, homomorphic vocoders, and channel vocoders. In these vocoders, speech is modeled on a short-time basis as the response of a linear system excited by a periodic impulse train for voiced sounds or random noise for unvoiced sounds. For this class of vocoders, speech is analyzed by first segmenting speech using a window such as the Hamming window. Then, for each segment of speech, the excitation parameters and system parameters are determined. The excitation parameters consist of the voiced/unvoiced decision and the pitch period. The system parameters are used to synthesize an excitation signal consisting of a periodic impulse train in voiced regions and random noise in unvoiced regions. This excitation signal is then filtered using the estimated system parameters.

Even though vocoders based on this underlying speech model have been quite successful in synthesizing intelligible speech, they have not been successful in synthesizing high quality speech. As a consequence, they have not been widely used in mid-rate coding applications requiring high quality speech reproduction. The poor quality of the synthesized speech is due to fundamental limitations in the speech models, inaccurate estimation of the speech model parameters, and distortion caused by the parameter coding.

The goal of this research is to develop an improved speech model, together with methods to estimate the speech model parameters robustly and accurately, and apply the resulting speech analysis/synthesis system to the problem of bit-rate reduction. In this model, the short-time spectrum of speech is modeled as the product of an excitation spectrum and a spectral envelope. The spectral envelope is some smoothed version of the speech spectrum. The excitation spectrum is represented by a fundamental frequency, a voiced/unvoiced (U/UV) decision for each harmonic of the fundamental, and the phase of each harmonic declared voiced. In speech analysis, the model parameters are estimated by explicit comparison between the original speech spectrum and the synthetic speech spectrum. Current work is concentrated on efficient coding of these speech model parameters. Preliminary results indicate that very good quality reproduction can be obtained with this speech coding system for both clean and noisy speech without the "buzziness" and severe degradation (in the presence of noise) typically associated with vocoder speech rate at a rate of 9.6 kbps.

24.6 Mixed Causuality IIR Filtering for Nonminimum Phase Channel Compensation

National Science Foundation (Grant ECS 84-07285)
U.S. Navy - Office of Naval Research (Contract N00014-81-K-0742)

Alan V. Oppenheim, Daniel J. Harasty

A feedforward (or multipath) channel models the physical situation which gives rise to television ghosts. Digital compensation for these artifacts can be achieved by designing a filter which is the inverse of the ghosting filter. This filter, however, is stable and causal only if the ghosting filter is minimum phase, that is, all of its singularities lie inside the unit circle. If the ghoster is nonminimum phase, the stable inverse filter has an infinite impulse response which extends backwards in time. Such an impulse response can be achieved if the data can be run backwards through a regular IIR filter. Since the prospect of having the entire video signal in storage to do the filtering is unlikely, investigation of a method of piece-wise time reversal is necessary.

Basically, the MCIIR system is approximated by separating the deghosting system into two cascadable systems: the first has a strictly causal impulse response corresponding to the poles inside the unit circle, and the second has a strictly anticausal impulse response corresponding to the poles outside the unit circle. The ghosted signal is fed normally through the causal system, and then broken into blocks to be time flipped, fed through the time-reversed implementation of the anticausal portion, and flipped again upon output. Unfortunately, the anticausal portion is not in the correct state when a new block is introduced, and so a portion of the outputed block (of a length equal to the effective length of the anticausal filter) must be disregarded as corrupted by the transient response of the filter. Consequently, overlapping blocks must be used to obtain valid values for all output samples.

24.7 A 4.8 Kbps High Quality Speech Coding System

National Science Foundation (Grant ECS 84-07285)
U.S. Navy-Office of Naval Research (Contract N00014-81-K-0742)

Jae S. Lim, John C. Hardwick

Recently completed research has led to the development of a new speech model. This model has been shown to be capable of producing speech without the artifacts common to model based speech systems.¹ This ability makes the model particularly applicable to speech coding systems requiring high quality reproduction at a low bit rate. A 9.6 kbps based on this model is documented.² In addition, slight modifications of this system have been made which extend it to 8 kbps. Both of these systems have been shown to be capable of high quality output.

The purpose of this research is to explore methods of using the new speech model in a 4.8 kbps speech coding system. Results indicate that a substantial amount of redundancy exists between the model parameters. Current research efforts are aimed at methods of exploiting this redundancy in correspondence with more efficient quantization of the model parameters. Preliminary experiments verify that these techniques will permit a substantial bit reduction without major degradations in speech quality.

References

CONTRACT CON

- ¹ Griffin, D.W., and J.S. Lim, "A New Model-Based Speech Analysis/Synthesis System," I.E.E.E. International Conference on Acoustics, Speech and Signal Processing, Tampa, Florida, 1985, pp. 513-516.
- ² Griffin, D.W., and J.S. Lim, "A High Quality 9.6 kbps Speech Coding System," I.E.E.E. International Conference on Acoustics, Speech and Signal Processing, Tokyo, Japan, 1986.

24.8 Multi-Representational Signal Matching

Canada, Bell Northern Research Scholarship
Canada, Fonds pour la Formation de Chercheurs et l'Aide a la Recherche
Postgraduate Fellowship
National Science Foundation (Grant ECS 84-07285)
Canada, Natural Science and Engineering Research Council
Postgraduate Fellowship
U.S. Navy - Office of Naval Research (Contract N00014-81-K-0742)

Alan V. Oppenheim, Jacek Jachner

This work investigates the idea of performing signal matching by integrating different signal representations in the matching procedure. In as much as the signal representations can be numeric or symbolic, multi-representational matching is an approach to signal matching in the case when the signals are described by a mix of numeric and symbolic representations.

As a framework in which to study signal matching, current work is focusing on the vector coding of speech signals. Recent progress in speech waveform coders has demonstrated the feasibility of high quality speech at very low bit rates (less than 8

kb/s) using an adaptive predictive coder strategy with block quantization of the prediction residual. The computations required to select an optimum vector codeword, even for moderately sized codebooks, are prohibitively long. Using an implementation of such a coder in the KBSP package on LISP machines, our current focus is to efficiently match a given sequence of speech data with a stored codebook of vectors by using multiple signal representations.

24.9 Detection of Narrowband Signals in Wideband Noise

National Science Foundation (Grant ECS 84-07285)
Sanders Associates, Inc.
U.S. Navy - Office of Naval Research (Contract N00014-81-K-0472)

Alan V. Oppenheim, Tae H. Joo

SEESSEE DESPENDED DIVINISE DESPENDED FORESSEES BELLEVILLE NOVELLA DESPENDED DE CONTROL DE L'ARCONNELLE DE L'AR

The search for radio signals transmitted by extraterrestrials is a complex, multidimensional search problem because little is known about the transmitted signal. Current searches for extraterrestrial intelligence (SETI) collect data from a predetermined range of signals. These data are then processed to detect all synthetic components. (Synthetic components of signals are those which do not originate naturally. This assumes that the synthetic component is generated by extraterrestrials.) The assumption that the transmitted signal is a continuous wave (CW) at certain frequencies is commonly used in determining the range. Existing SETI systems use a frequency of 1450 MHz, atomic hydrogen line.

Due to uncertainties in the transmitter locations, the relative velocities and the receiver antenna beamwidth, the frequency of the CW signal is unknown but is within 200 KHz of 1420 MHz. The propagation experiences multi-path which spreads the CW signal to a bandwidth of about 0.05 Hz. Therefore, SETI systems must search a wide frequency band (approximately 400 KHz) to detect a very narrowband (0.05 Hz) signal in poor signal-to-noise ratio (SNR) conditions.

Current SETI systems use FFT's to compute the spectrum. Each spectrum is then compared to a threshold to detect a peak. Because the SNR is low, the frequency bin size of the FFT is matched to the bandwidth of the narrowband signal. Therefore a 2²³, or approximately 400 KHz/0.05 Hz, length FFT is required. In an existing system known as mega-channel extraterrestial array (META)¹, this FFT is computed in two steps. First, the signal is filtered by 128 band-pass filters. Second, each band-pass filtered signal is transformed by a 64K length FFT. These computations are made using fixed point arithmetic. There are alternative implementations of this DFT-based method. The performance of different implementations, within constraints of the finite register length and other computational limitations, will be examined.

If the received signal is modelled as a sinusoid in white noise, modern spectrum estimators (e.g., the maximum entropy method) or frequency estimators (e.g., Pisarenko's method) can be employed. The performance and applicability of these algorithms, within constraints of computational limitations will be examined.

Reference

¹ Horowitz, P., J. Forster and I. Linscott, "The 3-Million Channel Narrowband Analyzer," in *The Search for Extraterrestrial Life: Recent Developments*, edited by M.D. Papagiannis. Hingham, Mass.: Kluwer Academic Publishers, 1985, pp. 361-371.

24.10 Estimation of Coronary Artery Boundaries in Angiograms

National Science Foundation (Grant ECS 84-07285)
U.S. Navy - Office of Naval Research (Contract N00014-81-K-0742)

Jae S. Lim, Thrasyvoulos N. Pappas

The precise and objective measurment of the severity of coronary obstructions from coronary angiograms is important in the treatment of patients with ischemic heart disease. An angiogram is an x-ray picture of the coronary arteries in which a contrast agent has been injected via a catheter.

Coronary artery imaging presents special problems because of the arteries' location on the beating heart and their shape and size. As a result, many techniques that have been used quite successfully for stenosis determination of other arteries, like the femoral and carotid, do not have satisfactory performance when applied to coronary arteries. These algorithms are quite heuristic and find the boundaries of the artery as the inflection points of a series of densitometric profiles perpendicular to the vessel image. Even though this approach is computationally simple, there is no theoretical justification for it.

We consider a different approach which more fully exploits the detailed characteristics of the signals involved. Specifically, we develop a model of the film density of the coronary angiograms and use it to estimate the diameter and cross-sectional area at each point along the vessel. Our model accounts for the structure of the vessel and background, as well as the distortions introduced by the imaging system (blurring and noise). We have developed both a one-dimensional model of the density profiles perpendicular to the vessel image, and a two-dimensional model of rectangular sections of the image. The parameters of the model include the vessel center-point locations and the radius at each point. The spatial continuity of the vessel is incorporated into the model and contributes to the accuracy of the estimation procedure. The algorithms are tested on synthetic data, on x-rays of contrast-medium-filled cylindrical phantoms obtained over a wide range of radiographic conditions, and on real coronary angiograms. Our results indicate that the 1-D algorithms have better performance than current methods, and preliminary results indicate that the 2-D algorithms have better performance than 1-D algorithms.

24.11 Reconstruction of Multidimensional Signals from Multilevel Threshold Crossings

Fanny and John Hertz Foundation Fellowship National Science Foundation (Grant ECS 84-07285) U.S. Navy - Office of Naval Research (Contract N00014-81-K-0742)

Alan V. Oppenheim, Avideh Zakhor

It has been shown theoretically that under mild conditions multidimensional signals can be recovered from one bit of phase. Exploiting duality, they can also be recovered from zero crossings or one-level crossings. In practice, recovery from zero crossings, which is essentially an implicit sampling strategy, is highly ill-considered. That is, the number of position bits of zero crossings required for reconstruction is rather large. One way to improve robustness is to reconstruct from multilevel threshold crossings as opposed to one level.

In this research, we extend some of the well-known results in interpolation theory in order to define a new implicit sampling strategy which can ultimately be used to find the sufficient condition for recovery from multilevel threshold crossings. We then use algebraic geometry ideas to find conditions under which a signal is almost always reconstructable from its multilevel threshold crossings. As it turns out, the set of signals which do not satisfy this latter condition are of measure zero among the set of all bandlimited, periodic two-dimensional signals.

Simulations are used to verify the above ideas experimentally. It is shown that the reconstruction becomes more robust as the number of threshold levels are increased. Furthermore, the robustness is improved if more points are used for reconstruction. At the extreme case, where all the points corresponding to each threshold are used, the theory of projections of convex sets can be used to derive an iterative algorithm for reconstruction.

Finally, the ideas developed for recovery from level crossings will be applied to the problem of reconstruction of continuous images from half-tone ones.

24.12 Knowledge-Based Pitch Detection

National Science Foundation (Grant ECS 84-07285) Sanders Associates, Inc. U.S. Navy - Office of Naval Research (Contract N00014-81-K-0742)

Alan V. Oppenheim, Webster P. Dove, Randall Davis

Knowledge-based signal processing (KBSP) is the application of the numerical algorithms of signal processing and the symbolic inference techniques of expert systems on problems where both numerical and symbolic information are present. One class of problems in this area includes those for which both numeric and symbolic input information is available. The Knowledge-Based Pitch Detection (KBPD) project prepared a system to describe the excitation of a sentence of speech (voicing and

periodicity) given a recorded waveform and a phonetic transcript of the sentence. Through this project we learned more about the general problem of integrating numeric and symbolic processing.

This problem is interesting because pitch detection is an old problem with no completely successful solution (for high quality resynthesis). Existing programs attack the problem with a single unified algorithm based on the detection of periodicity. Typically, this will work some places and not others. For example, it is common for voiced sections at the ends of sentences to be irregular and not periodic. Algorithms based on periodicity cannot conclude voicing in such regions and therefore they make voiced-to-unvoiced errors there.

With more information available to it, the KBPD system can avoid such problems. Since it has a transcript, KBPD starts with strong information about the voicing of the sentence in the middle of the phonemes of the transcript. However, aligning the transcript precisely with the sentence so that the boundaries of the phonemes are correct require interaction between the transcript representation and numerical measurements of the waveform. Also, the actual rendition of a given phoneme may vary enough between speakers and sentences that a normally voiced phoneme is not actually voiced. So the system must verify the transcript against the observed properties of the sentence to avoid mistakes.

By combining the results of several different methods of analysis rather than relying on a single algorithm, KBPD spreads the risk of errors. To the extent that these different methods both cooperate effectively and span the phenomena of the problem, one can expect the system to be more robust than a single algorithm approach. The key to this cooperation is the explicit representation of credibility in the results of each component.

Expert systems have capitalized on the representation of credibility for performing symbolic inference when both knowledge and problem information are uncertain. KBPD moves these techniques to the domain of numeric processing with the explicit representation in the program of both certainty and accuracy for numeric results. The extra information (beyond the basic result values) allows the system to merge results from different components without specific information about the nature of the components. This in turn allows the integration of new components into the system without major rewriting of existing code, and allows the final results to be based on the components that rated themselves most credible. While there is some question as to how reliably a given algorithm can be expected to rate its own performance, clearly this is an improvement over the conventional program assumptions that the algorithm's result "are the answer," and it has the virtue of presenting to the operator some information about the overall credibility of results.

This project also developed a program called the Pitch Detector's Assistant (PDA). It serves as both an assistant in the pitch detection process, and a workbench to evaluate numeric and symbolic processing techniques in pitch detection programming.

As an end product, it might be used to generate excitation information for off-line speech storage applications (like talking appliances) or for speech research into the

properties of pitch as an information carrying medium. It is clearly not for real-time applications like vocoding, though it might be used for vocoding experiments.

As a workbench for pitch detection programming, the PDA allows us to assess what kind of symbolic information is useful in the pitch detection problem by experimenting with ways of using it.

As a KBSP catalyst, it has prompted the development of new data structures (for representing temporal estimates and pitch estimates). Furthermore, it has motivated the development of a signal processing environment (called KBSP) that dramatically reduces the time to implement signal processing algorithms. This software environment is also capable of embedding symbolic processing functions (like the generation of symbolic assertions) within numerical algorithms. That capacity, together with a rule-based system capable of invoking signal processing functions, permits a flexible, two-way communication between the numeric and symbolic parts of the system. Finally, this project has led to the clarification of some of the features of symbolic inference in the context of numeric information. Specifically, we have found that recognition of equivalent assertions is more difficult in a numeric context, and that there are more ways of combining numeric assertions than symbolic ones.

This project was completed in June 1986.

24.13 Reconstruction of a Two-Dimensional Signal from the Fourier Transform Magnitude

National Science Foundation (Grant ECS 84-07285)
U.S. Navy - Office of Naval Research (Contract N00014-81-K-0742)

Jae S. Lim, David Izraelevitz

In the case of an arbitrary multidimensional discrete signal, the phase and magnitude of the Fourier transform are independent functions of frequency. However, in many situations there is additional information regarding the signal which provides a very strong connection between the phase and magnitude. Specifically, it has been shown that almost all multidimensional signals which are non-zero only over a specified domain are uniquely specified, in a sense, by knowledge of the Fourier transform magnitude alone. Several algorithms have been developed for reconstructing such a signal from its Fourier transform magnitude; however, they all fall into either of two categories: they are heuristic algorithms which sometimes do not converge to the true reconstruction, or they are computationally too expensive for even moderate size signals.

In this research, we present a new algorithm for reconstruction from Fourier transform magnitude which is a closed form solution to the problem and which has been used to reliably construct signals of extent up to 20 by 20 pixels. The algorithm is based on posing the problem of Fourier transform magnitude reconstruction as requiring the explicit factorization of the z-transform of the autocorrelation sequence of the unknown function. This z-transform is easily computed from knowledge of the Fourier transform magnitude. A new procedure is developed for factoring large

bivariate polynomials and this algorithm is applied to the needed factorization of the autocorrelation z-transform.

This project involves studying the data noise sensitivity of the algorithm and of the problem of reconstruction from Fourier transform magnitude in general, as well as developing a detailed comparison of the behavior of the present algorithm with previously proposed algorithms.

This project was completed in May 1986.

24.14 Model-Based Motion Estimation and its Application to Restoration and Interpolation of Motion Pictures

Center for Advanced Television Studies
National Science Foundation (Grant ECS 84-07285)
U.S. Navy - Office of Naval Research (Contract N00014-81-K-0742)

Jae S. Lim, Dennis M. Martinez

Motion pictures can be manipulated in a variety of ways of compensating for motion within the image sequence. An important component of all motion-compensated image processing systems is motion estimation. Previous approaches to motion estimation have encountered two primary problems, computational complexity and estimation accuracy. This work is concerned with the development and analysis of computationally efficient motion estimation algorithms which can determine motion trajectories very accurately.

A model-based motion estimation algorithm has been developed. This algorithm requires significantly less computation than traditional approaches. In addition, it can determine velocity fields more accurately than commonly used region matching methods. The algorithm is based on a local three-dimensional signal model and a local translational velocity model. It is possible to estimate complex velocity fields encountered in real-life television images with the algorithm.

We applied this algorithm to several problems in motion picture restoration and interpolation. Image restoration algorithms which operate on a single frame at a time usually remove noise at the expense of picture sharpness. However, we demonstrated that motion-compensated restoration systems can remove noise with little or no loss in picture sharpness.

The algorithm has also been used successfully for frame interpolation. A motion-compensated frame interpolation system was developed which permits computing frames at arbitrary times. This system can be used in a variety of applications involving frame rate modification. A number of experiments have shown that this motion-compensated interpolation system produces motion pictures with better motion rendition than traditional frame repetition systems.

This project was completed in September 1986.

24.15 Signal Processing and Interpretation using Multilevel Signal Abstractions

National Science Foundation (Grant ECS 84-07285)
Sanders Associates, Inc.
U.S. Navy - Office of Naval Research (Contract N00014-81-K-0742)

Alan V. Oppenheim, Evangelos E. Milios

A signal processing system which integrates signal and symbol processing was developed for acoustic waveform processing and interpretation. The design of the system was derived from the systematic observation (protocol collection) and subsequent analysis of human signal processing activity. The resulting system consists of: 1) a harmonic-set formation subsystem, which produces harmonic sets present in acoustic spectra and their symbolic description; and 2) a geometrical hypothesis formation and testing subsystem, which forms hypotheses about the acoustic source motion based on the data, and then performs detailed testing against the data. The system is being built using a hybrid methodology combining both procedural and declarative programming and accommodates both algorithmic and heuristic techniques in signal processing. Modules perform spectral peak analysis using rules that stem from human perceptual considerations. The rule-based approach is enhanced to allow thresholds to be set from examples through the same rules used for classification. In comparison to previous signal/symbol processing systems, which relied mostly on symbol processing, this system is based on the concept that a tight interaction of signal processing and interpretation can save a lot of symbol processing.

This work was done in collaboration with the Machine Intelligence Technology Group at the M.I.T. Lincoln Laboratory. This project was completed in June 1986.

24.16 Signal Representation for Symbolic and Numerical Processing

Amoco Foundation Fellowship National Science Foundation (Grant ECS 84-07285) Sanders Associates, Inc. U.S. Navy - Office of Naval Research (Contract N00014-81-K-0742)

Alan V. Oppenheim, Cory S. Myers

One important aspect of our work on Knowledge-Based Signal Processing (KBSP) is the development of a suitable environment for carrying out the research and for exploring mechanisms for integrating numerical and symbolic processing. As part of our KBSP work, we have developed the KBSP software package, an innovative software package for signal processing on the LISP Machine. The KBSP software package provides a uniform signal processing package that is integrated into an interactive, symbolic processing environment, the LISP Machine. The package provides computational speed, ease of development, and a close correspondence between abstract signal processing concepts and programming implementation.

As an outgrowth of the KBSP package, this research is devoted to the incorporation of symbolic manipulation facilities into the numerical KBSP spackage. Symbolic manipulation of signals involve the manipulation of signal representations rather than signal values. One example of this symbolic manipulation is the symbolic generation of Fourier transforms. The system understands many primitive signals, their Fourier transforms, and rules for the manipulation of Fourier transforms with respect to other signal processing operations, such as addition, multiplication, and convolution. For many signals, the system is able to parse the signal's representation and generate its Fourier transform without any reference to the numerical values of the signal.

One area in which the symbolic manipulation of signal representation is a natural one is the area of varying the signal processing according to "context". Context can include properties of the signals under consideration, properties of the hardware, or properties of the world. For example, different FFTs can be used when the signal is real-valued or when it is complex-valued, different filtering algorithms can be used to achieve different trade-offs among multipliers, adds, and memory references, and different spectral modeling techniques can be used for different speech sounds. The goal of this research is to automate the decision process used in algorithm selection.

As an initial step in automating the algorithm decision process, we have developed a system for the LPC analysis of a speech signal given a time-aligned phonetic transcript of the speech signal and a symbolic description of the recording environment. In this system, the parameters of the LPC analysis -- the number of poles, the window size, and the frame rate -- are varied according to the information present in the phonetic transcript. For example, a long window and a low frame rate are used in the steady-state portion of vowels and a short window and a high frame rate are used in the area of stop releases.

We are currently working on more general techniques that will allow many different sources of information to be used in choosing a signal processing algorithm. One aspect of this problem is the specification of properties of both signals and systems. We are trying to develop a symbolic signal processing language in which standard signal processing properties such as finite-durationness, symmetry, linearity, shift-variance, etc., are easily represented and manipulated by the system.

We are also studying methods for the manipulation of signal representations so that the system can determine equivalent forms for algorithm implementation. For example, the system will be able to implement a filter in either the time-domain or the frequency-domain. This capability will be used to automatically choose different algorithms to implement the same signal processing operation for different input signals and for different trade-offs among the different factors that affect computational cost.

This project was completed in August 1986.

24.17 Reconstruction of Undersampled Periodic Signals

National Science Foundation (Grant ECS 84-07285)
U.S. Navy - Office of Naval Research (Contract N00014-81-K-0742)

Alan V. Oppenheim, Anthony J. Silva

Under certain circumstances, it may be impossible to sample a signal at a rate greater than twice the highest spectral component present. In particular, the sampling rate might be limited by the A/D converter and associated hardware used. However, for certain classes of undersampled signals, complete recovery is still possible (at least theoretically), in spite of the well-known Nyquist criterion.

Periodic signals form one such class. Consider undersampling a periodic signal whose harmonic frequencies are mutually prime to the sampling rate. The harmonics have zero bandwidth⁴ and though aliased into the baseband (-Fsamp/2 to + Fsamp/2 Hz), they do not overlap. The Nyquist criterion is stated generally for low-pass waveforms with energy presumably spread smooth across their spectra. Because of this, it discounts the possibility of recovery after the non-destructive aliasing above.

In what follows, we assume the sampling rate is stable and known to a modest degree of accuracy. When the signal period is known, recovery is trivial. The time sample x[n] are sorted by interpreting the index "n" modulo the normalized signal period⁵ then placing each sample in the appropriate place in a "composite" period. No samples will overlap if the mutual primality requirement above is met.

A far more interesting problem exists when the signal period is known. Rader¹ has presented an iterative recovery technique in which a multiplicity of trial signal periods is used as moduli in the sorting process above. The trial period yielding the best reconstruction is retained as the estimate of the true signal period. Results from number theory (Farey sequences, modular or congruential arithmetic, etc.) are exploited to make the approach practicable.²

We searched for ways to accelerate the Rader algorithm. An analogous frequency domain algorithm, also employing number theory, was developed. It consisted of determining the frequencies and amplitudes of the aliased harmonics, sorting them, and inverse transforming. Performance of all algorithms and their variants in the presence of noise, slightly wavering signal frequency and amplitude, and other undesirable conditions, were examined.

This project was completed in January 1986.

References

- ¹ C.M. Rader, "Recovery of Undersampled Periodic Waveforms," I.E.E.E. Trans. Acoust., Speech, Signal Process., *ASSP-25*, 3, 1977.
- ² G.H. Hardy and E.M. Wright, *An Introduction to the Theory of Numbers*, Oxford University Press, 1956.

⁴ Of course, the signal would have to be known and sampled for all time to yield truly zero-bandwidth harmonics.

⁵ The ratio of the signal and sampling periods.

24.18 Silhouette-Slice Theorems

National Science Foundation (Grant ECS 84-07285) U.S. Navy - Office of Naval Research (Contract N00014-81-K-0742)

Jae S. Lim, Patrick van Hove

This research addresses the relationships between an object and the boundaries of its silhouettes, which are referred to as contours, corresponding to various threedimensional (3-D) orientations of the line of sight. For this purpose, special models of objects and silhouettes are considered. The property sphere of an object is defined on a unit sphere which is related to the object by a 3-D Gaussian mapping. Similarly, the property circle is related to the contour it represents by a 2-D Gaussian mapping. In earlier computer vision work, property spheres and circles have been used independently, and their applications have been limited to the representation of scalar fields of object properties.

In a first stage, we have shown how the concepts of property spheres and circles can be usefully combined to relate the properties of an object and those of its contours. Specifically, it is proved that a slice through the property sphere of an object leads to the property circle of the contour corresponding to the line of sight perpendicular to that slice.

In a second stage, a new concept of object modeling has been introduced, where the property sphere is used as a domain for vector and tensor fields of object properties. In particular, a new representation of 3-D objects and 2-D silhouettes, referred to as the Curvature Transform (CT), maps the inverse of the curvature tensor field of the surface of an object on its property sphere, and the radius of curvature of the contour of a silhouette on its property circle. The key advantage of this representation is that a slice through the CT of an object followed by projection of the tensor field produces the CT of the contour corresponding to the line of sight perpendicular to the slice.

The study progressed with attempts to use these new concepts in the reconstruction of object shape from silhouette information. Surface reconstruction procedures have been proposed in the field of machine vision, in the contexts of shape from photometric stereo, shading, texture, and motion. These procedures reconstruct a viewer-dependent 2 1/2-D sketch of the surfaces. The surface reconstruction procedure which is attempted here would provide a full 3-D sketch of the objects.

This work was done in collaboration with the Distributed Sensor Systems group at the M.I.T. Lincoln Laboratory. This project was completed in September 1986.

The Hilbert-Hankel Transform and Its Application 24.19 to Shallow Water Ocean Acoustics

Fanny and John Hertz Foundation Fellowship National Science Foundation (Grant ECS 84-07285) U.S. Navy - Office of Naval Research (Contract N00014-81-K-0742)

TOTAL TOTAL CONTROL OF THE PROPERTY AND THE PROPERTY AND THE PROPERTY OF THE P

Alan V. Oppenheim, George V. Frisk, Michael S. Wengrovitz⁶

The problem of continuous-wave acoustic field propagation in shallow water is being investigated. In this environment, components of the field alternately reflect off both the ocean surface and the ocean bottom. In effect, the water can be considered as an acoustic waveguide, bounded by the ocean surface and the underlying ocean bottom. Several aspects of this waveguide propagation problem are being studied. The first concerns the development of an accurate numerical model to predict the magnitude and phase of the acoustic field as a function of range from the source, given the geoacoustic parameters of the water and the bottom. A technique has been developed which computes the field based on its decomposition into trapped (resonant) and continuum (non-resonant) components.

A second aspect being studied is the application of the Hilbert-Hankel transform to both the synthesis and inversion of these fields. This transform has a number of interesting and useful properties and forms the basis for a reconstruction method in which the real (imaginary) part of the complex-valued field is obtained from the imaginary (real) part.

Finally, the inherent sensitivity of extracting the bottom plane-wave reflection coefficient from measurements in the reverberant waveguide environment was researched. Results indicate that there are several invariant waveguide parameters which do not depend on the properties of the underlying media. By exploiting the invariance of these parameters, it is possible to design an actual ocean experiment from which an improved reflection coefficient estimate results.

This project was completed in January 1986.

24.20 Speech Enhancement Using Adaptive Noise Cancellation

National Science Foundation Fellowship National Science Foundation (Grant ECS 84-07285) U.S. Air Force - Office of Scientific Research (Contract F19628-85-K-0028) U.S. Navy - Office of Naval Research (Contract N00014-81-K-0742)

Jae S. Lim, Jeffrey J. Rodriguez

In many military environments, such as fighter jet cockpits, the increasing use of digital communication systems has created a need for robust vocoders and speech recognition systems. However, the high level of acoustic noise makes the vocoders less intelligible and makes reliable speech recognition more difficult. Therefore, we are using Widrow's Adaptive Noise Cancelling (ANC) algorithm to enhance the noise-corrupted speech.¹

ANC is a noise-reduction method that uses multiple inputs. In the fighter jet application, we use two microphones: a primary and a reference. The primary microphone

⁶ Woods Hole Oceanographic Institution

is located inside the pilot's oxygen face mask, and the reference microphone is attached to the exterior of the face mask. In this configuration, the primary microphone records the noise-corrupted speech, while the reference microphone ideally records only the noise. When these two inputs are processed, the reference noise is filtered and subtracted from the primary signal. Hopefully, the resulting signal will contain the undegraded speech signal with very little noise.

This project was completed in January 1986.

Reference

¹ B. Widrow, et al., "Adaptive Noise Cancelling: Principles and Applications," Proc. I.E.E.E., 63, 12, (1975).

25.0 Cognitive Information Processing

Academic and Research Staff

Prof. W.F. Schreiber, Prof. R.-S. Gong⁷, Prof. J. Lang, Prof. J. Lim, Dr. C.W. Lynn, Dr. L. Picard, Prof. D.H. Staelin, Prof. D.E. Troxel, Mr. J. Ward.

Graduate Students

G. Bartlett, K. Christian, A. Garcia, M. Heytens, S. Hsu, S.-L. Huang M.A. Isnardi, R. Jayavant, E. Krause, D. Kuo, C. Lee, H.S. Malvar, S. Marshall, D. Martinez, J. Ono, D. Pan, D. Pian, J. Piot, J. Preisig, J.-P. Schott, J. Shapiro, L. Singer, B. Szabo, A. Tom, T. Tsakiris, R. Vinciguerra, J. Wang, G. Wornell.

25.1 Advanced Television Research Program

Members of the Center for Advanced Television Studies, an industry group consisting of American Broadcasting Company, Ampex Corporation, Columbia Broadcasting Systems (until 5/86), Harris Corporation (until 5/86), Home Box Office, Kodak (from 1/87), Public Broadcasting Service, National Broadcasting Company, RCA Corporation, Tektronix, Zenith (from 5/86), and 3M Company (until 5/86).

William F. Schreiber

25.1.1 Goals

The purpose of this program is to conduct research relevant to the improvement of broadcast television systems. Some of the work is carried out in RLE and some in other parts of MIT, including the Media Laboratory by Prof. Andrew Lippman, Prof. Stephen Benton, and Adjunct Prof. Arun Netravali. Audience research is carried out by Prof. W. R. Neuman in the Political Science Department. Reporting is by means of theses and published papers.

25.1.2 Background

The Japan Broadcasting Company (NHK) has demonstrated a high definition television system of 1125 lines, 30 frames, 60 fields, 25 MHz bandwidth, with image quality comparable to 35-mm motion pictures. Substantial improvements in image quality over that of the existing NTSC and PAL systems have been demonstrated by laboratories in Europe, Japan, and the United States which require only signal processing and the use of special electronic components, such as frame stores, at the receiver. These systems do not require increasing the present 6-MHz bandwidth. Still other systems have been demonstrated that achieve nearly NHK quality by adding a second channel to the present broadcast signal. In view of all these developments and of the economic im-

⁷ Visiting Scientist

portance of the US television industry, it was deemed appropriate by the sponsors to fund a research program at an American university.

25.1.3 Research Activities

In this contract year, we have completed the assembly of our image-processing system, based on a VAX 11/785, including a high-speed disk subsystem. The latter, which became operational in 1987, permits simulation of full moving high-definition TV sequences. The Audience Research Facility in Danvers, Mass. was also completed, and both of these facilities were used to carry out a variety of studies.

Studies have been carried out on motion estimation and perception, optimum filtering, TV system modeling, visual psychophysics, and audience reaction to degraded images and sound. Extensive work has been done in motion estimation, and this has been applied to frame-rate conversion (e.g., 24-fps film to 60-fps TV) and to noise reduction without blurring. Elimination of defects in the US standard (NTSC) TV system by signal processing has also been demonstrated, and some proposed improved TV systems have been simulated.

Publications

- Bartlett, G., "Observations of the Spatial and Temporal Response of Human Color Vision," M.S. Thesis, Dept. Electr. Eng. and Comp. Sci., Cambridge, Mass., 1986.
- Christian, K., "The Design of an Integrated-Circuit 3D Gaussian Interpolator," M.S. Thesis, Dept. Electr. Eng. and Comp. Sci., M.I.T., Cambridge, Mass., 1985.
- Hsu, S.C., "The Kell Factor: Past and Present," S.M.P.T.E. 95, 2 (1985).
- Isnardi, M.A., "Modeling the Television Process," Ph.D. diss., Dept. Electr. Eng. and Comp. Sci., M.I.T., Cambridge, Mass., 1986.
- Krause, E.A., "Motion Estimation for Frame-Rate Conversion," Ph.D. diss., Dept. Electr. Eng. and Comp. Sci., M.I.T., Cambridge, Mass., 1985.
- Kuo, D.D., "Design of Dual Frame Rate Image Coding Systems," M.S. Thesis, Dept. Electr. Eng. and Comp. Sci., M.I.T., Cambridge, Mass., 1987.
- Malvar, H.S., "Optimal Pre- and Post-Filtering in Noisy Sampled Data Systems," Ph.D. diss., Dept. Electr. Eng. and Comp. Sci., Cambridge, Mass., 1986.
- Martinez, D.M., "Model-Based Motion Estimation and its Application to Motion Pictures," Ph.D. diss., Dept. Electr. Eng. and Comp. Sci., M.I.T., Cambridge, Mass., 1986.
- Pan, D.Y., "Adaptive Filtering for Sampled Images," Ph.D. diss., Dept. of Electr. Eng. and Comp. Sci., 1986.
- Schreiber, W.F., "Improved Television Systems: NTSC and Beyond," to be published in S.M.P.T.E. in 1987.

- Tom, A., "Prediction of FIR Pre and Post-Filter Performance Based Upon a Visual Model," M.S. Thesis, Dept. Electr. Eng. and Comp. Sci., Cambridge, Mass., 1986.
- Wang, J.S., "Real-Time Multi-Dimensional Interpolation," M.S. Thesis, Dept. Electr. Eng. and Comp. Sci., M.I.T., Cambridge, Mass., 1986.

25.2 Computer Graphics

Donald E. Troxel, Charles W. Lynn, Len Picard, Armando Garcia, Shiao-Li Huang, Joanne Ono, Todd Tsakiris, Ralph Vinciguerra

25.2.1 Display Architecture for Interactive Graphics Programmable Frame Buffer Systems

International Business Machines, Inc.

Our research during the past four years has focused on the architecture of interactive graphics work stations, the user interface, the manipulation of sub-images, and algorithms for shading, texture mapping, and anti-aliasing. We have developed novel shading algorithms suitable for realistic image synthesis on graphics work stations. Hierarchical object modeling and ray tracing techniques are combined with efficient hidden surface algorithms to produce images that approximate the quality of pictures now produced by conventional ray tracing algorithms, but at considerable reduction in computation time. We continue to investigate the problem of producing anti-aliased color displays.

25.2.2 Programmable Frame Buffer Systems

International Business Machines, Inc.

Our research during the past four years has focused on the architecture of interactive graphics work stations, the user interface, the manipulation of sub-images, algorithms for shading, texture mapping, and anti-aliasing, and the raster display itself. This past year we acquired a second IBM PC/XT equipped with a YODA display. One PC/XT is also equipped with a 370 board and appropriate software so that it is possible to compile microcode for the YODA display.

We continue to investigate the problem of producing anti-aliased displays in conjunction with our investigation of shading algorithms. There has been considerable literature and increasing use of anti-aliasing in order to generate more pleasing displays for a given spatial sampling grid. This, of course, impacts architectural considerations as the size of the required image refresh memory can be reduced, thus altering the trade-offs. An interesting question concerns the trade-off between the spatial and gray scale resolution; i.e., how should available memory be allocated to optimize quality.

The issue of color adds an additional dimension to the problem. Present practice is to apply anti-aliasing algorithms separately to the red, green, and blue separations. This

has the unfortunate effect of producing color fringes on anti-aliased lines. This does not appear to be optimum; however, it is not obvious what color space should be used when calculating anti-aliasing in order to maintain both a pleasing display and true colors. Another way to look at this problem is to ask what trajectory in color space should one use in performing the anti-aliasing computation.

The distinction between image processing and graphic systems has been blurred as their hardware architectures have evolved toward each other. We are interested in providing tools and functional capabilities to simplify the task of the applications implementors and also to provide guidance to future hardware architects as to the trade-offs of the parameters of frame buffer systems. These parameters include the number of bit planes in the visible frame buffer, the size and number of bit planes in invisible frame buffers, the number of entries in a video color look up table, the number of bits in each video color look up table entry, and the manner in which the addresses of the video color look up table entries are generated.

The basic functional capabilities desired include transparency and anti-aliasing, clipping, zooming (other than by pel replication), and window management (i.e., dynamic overlays, animation, and palindromic sequences for depth cueing).

A recently completed PhD thesis by Armando Garcia developed novel shading algorithms suitable for realistic image synthesis on graphics work stations. Hierarchical object modeling and ray tracing techniques are combined with efficient hidden surface algorithms to produce images that approximate the quality of pictures now produced by conventional ray tracing algorithms, but at considerable reduction in computation time. These new algorithms implement rendering, reflection, and shadowing and have been programmed to run on both a DEC VAX-11/750 with an IRIS graphics terminal, and an IBM-PC/XT with the YODA attachment. For the most part, the algorithms are device independent, and simply make use of the IRIS/YODA hardware for drawing polygons and single pixels.

25.3 Computer Aided Fabrication System Structure

Defense Advanced Research Agency (Contract N00014-85-K-0213)

Donald E. Troxel, Rajeev Jayavant, Michael Heytens

The Computer Aided Fabrication (CAF) system structure carried out within RLE is part of a larger project within MTL. The overall goal of the CAF project is to integrate computers into the control, data collection, modeling, and scheduling of the integrated circuit fabrication process.

Previously, an initial, rudimentary CAF system was implemented. This included a personal notebook and data structures. During this period we have completed installation of the primary CAF computer, terminal concentrators, wiring of the facility with RS232 ports, and installation of terminals in the fabrication laboratory.

We have interfaced to the MIT physical plant computer which monitors a large number of sensing points such as resistance of DI water, etc., in our facility. We capture all alarms printed, maintain a log of active alarms, and have provided a mechanism for remote query of the status of the monitored points.

We have interfaced to some processing and measuring equipment. The Dektak profilometer has been interfaced with the CAF computer and software has been developed for transmitting screen plots and for printing these plots on either a laser printer or terminal. The Nanospec has been interfaced and data collection software installed. We have also provided a connection to the BTU furnace controller both for the creating and downloading of furnace recipes.

We have decided to use INGRES as a relational data base and have initiated an active project to define a scheme. We have initiated the development of a process flow language. This language will have a lisp-like form, although this need not be apparent of process design engineers.

The meaning of our process flow language will be provided by several interpreters - fabrication, simulation, production scheduling, and a "walk-through" interpreter. The walk-through interpreter will, we think, prove useful in the design of a process, the communication of the process to others, and in its approval by lab management.

reservation in the contract of the contract of



26.0 Electromagnetic Wave Theory and Applications

Academic and Research Staff

Prof. J.A. Kong, Prof. I.V. Lindell, Prof. C.H. Chen, Dr. M.C. Lee, Dr. T.M. Habashy, Dr. R.T. Shin, Q. Gu, A. Sihvola, Z. Li, N. Lu

Graduate Students

K. Adler, R. Basch, M. Borgeaud, D. Gaylor, K. Groves, H.C. Han, J.F. Kiang, R. Kim, C.F. Lee, F.C. Lin, S.V. Nghiem, S.Y. Poh, D. Rennie, S. Rogers, A. Schwartz, L. Sichan, M.J. Tsuk, A. Tulintseff, T.E. Yang, N. Yamashita, H.A. Yueh,

26.1 Electromagnetic Waves in Multilayer Media

Joint Services Electronics Program (Contract DAAL03-86-K-0002)

Jin A. Kong, Ann Tulintseff, Ying E. Yang, Herng A. Yueh

We have generalized the transient analysis method for the time-domain bi-directional coupling of a pair of nonuniformly couple dispersionless transmission lines. The transmission line equations are decoupled using the method of characteristics and the equations are solved iteratively. A new set of variables is introduced so that the transformed equations are simpler and both the codirectional and contradirectional coupling can be easily calculated. By virtue of the formulation, causuality is preserved and each higher order term in the perturbational series can be interpreted as a partial reflection along the lines due to nonuniform coupling. Since, in practice, the terminations for interconnecting lines in integrated circuits can be linear or nonlinear, we shall investigate both cases. Solutions accurate to the first order in spatial derivatives of the coupling coefficients, which is analytically managable, are presented. In the cases with linear loads the unit-step response can be obtained in closed-form to the first order, and arbitrary excitations can be handled by convolution. Numerical integration for the cases with nonlinear loads is also shown to be more efficient than integration based on the original coupled partial differential equations.

Vias in multilayered integrated circuits are treated like transmission lines with loadings where they encounter holes in ground planes separating different layers. We have modeled a ground plane with a hole and a circular conductor at the center of the hole as a radial waveguide, which in turn is connected to the via, another section of transmission line. Thus, by computing the characteristic impedance of the former, we have derived the equivalent load impedance of the via hole. The load impedance is one important parameter in calculating the transient propagation along vias.

We have investigated reliable models for many integrated circuits which contain strip lines at different heights that run parallel or perpendicular to each other. First the capacitances associated with the two offset parallel strips at different heights between ground planes are computed using the conformal mapping approach. As an extension, a simplifield circuit of parallel-plate lines with transverse ridges is introduced to model two parallel strips with perpendicularly crossing strips on top. We treated it as a distributed circuit consisting of transmission lines segments with periodical capacitive loading. In order to calculate the coupling between two lines, we reduced this structure to two equivalent single line circuits, viz. the even mode and the odd mode circuits. The Laplace transform approach can be easily applied to find out the transient response. The numerical computation carried out for various environments shows that the crossing strips will cause serious trouble for signals with a rise time of less than 50 ps to propagate along distances of 2 cm or longer.

26.2 Remote Sensing with Electromagnetic Waves

National Science Foundation (Grant ECS 85-04381)

Jin A. Kong, Robert T. Shin, Freeman C. Lin

The study of electromagnetic field intensity propagation in a continuous random medium has been of great interest in the areas of microwave remote sensing of earth terrain media. We have included both multiple scattering and spatial coherence effects in solving the problem of the field intensity propagation in an anistropic random medium layer. The modified radiative transfer (MRT) equations which describe propagation and scattering of the electromagnetic field intensity in a layered anistropic random medium are derived from the Bethe-Salpeter equation with the ladder approximation and the Dyson equations with the nonlinear approximation. The Dyson equation and the Bethe-Salpeter equation are the exact integrodifferential equations that the first and second moments of the field propagating in a continuous random medium must satisfy, respectively. Backscattering enhancement is observed due to the spatial coherence effects between upward and downward propagating waves. It also occurs for the half-space case because of coupling between ordinary and extraordinary waves in an anisotropic random medium layer. The depolarization effect is predicted in the first-order renomalization approximation to the MRT equations.

In the study of discrimination and classification of earth terrain utilizing polarimetric scattering properties, we use a two-layer anisotropic random medium model to characterize earth terrain media such as vegetation, forest, snow and ice which exhibit stron volume scattering effects and anisotropic behavior. The random medium has a background permittivity and its randomness is characterized by a three-dimensional correlation function with variance and correlation lengths. The polarimetric properties of the backscattering coefficients are found to include depolarization effects in the single-scattering approximation in contrast with the isotropic random medium which does not exhibit cross-polarization terms in the first order backscattering. The Mueller matrix can be transformed to a covariance matrix which is also useful in characterizing the polarimetric scattering properties. Physical interpretations will be given for the properties of the covariance matrix elements.

A general mixing formula is derived for discrete scatterers immersed in a host medium. The inclusion particles are assumed to be ellipsoidal. The electric field inside the scatterers is determined by quasistatic analysis, assuming the diameter of the inclusion particles to be much smaller than the wavelength. The results are applicable to general

multiphase mixtures, and the scattering ellipsoids of the different phases can have different sizes and arbitrary ellipticity distribution and axis orientation, i.e., the mixture may be isotropic or anisotropic. The resulting mixing formula is nonlinear and implicit for the effective complex dielectric constant, because the approach in calculating the internal field of scatterers is self-consistent. Still, the form is especially suitable for iterative solution. The formula contains a quantity called the apparent permittivity, and with different choices of this quantity the result leads to the generalized Lorenz-Lorenz formula, the generalized Polder-van Santen formula, and the generalized coherent potential-quasicrystalline approximation formula. Finally, the results are applied to calculating the complex effective permittivity of snow and sea ice.

The combined rough surface and volume scattering effects have been studies with the radiative transfer theory. The rough surface scattering effect has been observed to be important for both the active and the passive remote sensing of earth terrain. This is particularly important in the remote sensing of vegetation and soil moisture because most crop fields have uneven surfaces which are quasiperiodic in nature. The scattering of electomagnetic waves from a periodic dielectric interface will be studied by using the extended boundary condition approach and the Rayleigh method. We propose to first solve for the scattering field amplitudes and obtain the emissivity by using the principles of reciprocity and energy conservation. Because of the exact nature of the theory, reciprocity relations and energy conservation will be shown to be satisfied exactly, and the unambiguous emissivity of a periodic dielectric rough surface will be obtained.

Surface-based radiometer data, helicopter-born data, and satellite data taken from either a controlled field, the Arctic region or the Antarctic region have indicated that the sea ice signatures are modified by snow cover due to the volume scattering effects. In order to realistically model the snow-cover sea ice, the three-layer random medium has been developed where the snow layer is modeled by an isotropic random medium and the ice layer by an anisotropic random medium. In snow, the fluctuation of the permittivity and the physical sizes of the granular ice particles are characterized by a variance and two correlation lengths. In ice, the anisotropic effect is attributed to the elongated structures and the preferred alignment of the air bubbles, brine inclusions and other inhomogeneities. Two variances are required to characterize the fluctuations of the permittivities along or perpendicular to the tilted optical axis. The physical sizes of those scattering elements are also described by two correlation lengths. All theoretical results match favorably well with the experimental data for thick first-year and multi-year sea ice with and without the cover of dry and wet snow.

Polarimetric radar backscattering from anisotropic earth terrain such as snow-covered ice fields and vegetation fields with row structures provides a challenging modeling program from the electromagnetic point of view. Snow, ice and vegetation all exhibit volume scattering effects. For snow, the scattering is caused by granular ice particles; for ice, the air bubbles and brine inclusions; and for vegetation, the leaves, the trunks and other inhomogeneities. We model earth terrain covers as random media characterized by brine inclusions and vegetation with row structures, the random medium is assumed to be anisotropic. A three-layer model is used to simulate a vegetation field or a snow-covered ice field with the top layer being ice or trunks, and the bottom layer being sea water or ground.

In order to take into account the polarimetric information, we related the backscattered Stokes vector to the incident Stokes vector by the Mueller matrix, which com-

pletely describes the scattering (in amplitude, phase, frequency, and polarization) from the three-layer anisotropic random medium. The Mueller matrix properties, as well as the covariance matrix issues, relevant to the radar backscattering are examined. It is shown that for an isotropic medium, eight of the 16 elements of the Mueller matrix are identically zero. However, the tilted anisotropic permittivity of the middle layer (sea ice or trunks) generates a full non zero Mueller matrix.

26.3 Remote Sensing of Earth Terrain

National Aeronautics and Space Administration/Goddard Space Flight Center (Contract NAG5-270)

Min C. Lee, Freeman C. Lin

26.4 Remote Sensing of Upper Atmosphere

National Aeronautics and Space Administration Goddard Space Flight Center (Contract NAG5-270)

Min C. Lee, Jin A. Kong, S.V. Nghiem, K.M. Groves, H.C. Han

26.5 Microwave Emission and Scattering

National Aeronautics and Space Administration Goddard Space Flight Center (Contract NAG5-725)

Min C. Lee, Freeman C. Lin

We have developed a fully polarimetric radar model for the purpose of evaluating the radar backscatter from several types of earth terrain such as vegetation, tree canopy and The Mueller matrix and polarization covariance matrix are described for polarimetric radar systems. The evaluation of full polarimetric backscattering coefficients is useful in the design and analysis of optimal radar detection and classification schemes and in creating randomly generated radar returns for Monte-Carlo simulations. For many types of earth terrain (such as vegetation), the scattering effects due to medium inhomogeneities play an important role in determination of radar backscattering coefficients. The volume scattering properties of a medium can be modeled in two ways: random fluctuation of permittivity (random medium approach), and discrete particles imbedded in a homogeneous medium (discrete scatter approach). We have used the two-layer random medium model to characterize the earth terrain and calculate the Mueller and covariance matrices in the backscattering direction. The earth terrain is modelled by a layer of random permittivity, described by a three-dimensional correlation function, with variance, and horizontal and vertical correlation lengths. model is applied, using the wave theory with Born approximations carried to the second order that accounts for depolarization effects, to find the backscattering elements of the polarimetric matrices. It is found that eight of 16 elements of the Mueller matrix are identically zero, corresponding to a covariance matrix with four zero elements. Mueller and covariance matrices are illustrated by comparing with experimental data.

The strong fluctuation theory with the distorted Born approximation has been applied to the solution of the radar backscattering coefficients for three-layer configurations such as vegetation canopies and snow-covered ice fields. The top layer is considered to be isotropic (snow or leaves) with a spherical correlation function, the middle layer is assumed to be anisotropic (ice or trunks) with an exponentially decaying correlation function, and the bottom layer is a homogeneous medium (sea water or ground). Furthermore, the permittivity of the middle layer is first described as "discrete", constituted by a background permittivity being either isotropic or anisotropic and a scatterer permittivity being isotropic. Associated with the discrete model, a fractional volume density represents the amount of scatterers. The discrete random medium model is then mapped onto a continuous random medium to obtain a permittivity function depending upon position. In order to take into account the polarimetric information, we related the backscattered Stokes vector to the incident Stokes vector by the Mueller matrix, which completely describes the scattering (in amplitude, phase, frequency and polarization) from the three-layer random medium. The Mueller matrix properties, as well as the covariance matrix issues, relevant to the radar backscattering is examined. It is shown that for an isotropic medium, eight of the 16 elements of the Mueller matrix are identically zero. However, the tilted anisotropic permittivity of the middle layer (sea or trunks) generates a full nonzero Mueller matrix.

Several mechanisms have been investigated to explain the observed spectral broadening of injected VLF waves. They can be generally grouped into two categories: 1) nonlinear scattering of VLF signals by ionospheric density fluctuations; and 2) excitation of electrostatic waves by the injected VLF waves. In the first category, the nonlinear mode conversion of VLF waves into lower hybrid waves occurs when the VLF signals are scattered off the ionospheric density fluctuations. An elliptically polarized wave mode with a large wave number results from this process. The spectral broadening of VLF waves may, therefore, be attributed to the Doppler effect sensed by the airborne detector. The second category involves a different mechanism exciting electrostatic waves (lower hybrid waves, low frequency quasi-modes, etc.) by the injected VLF waves. This process tends to produce a spectrally broadened transmitted pulse with peaks at a discrete set of frequencies on both sides of the nominal carrier frequency.

Continued effort has been made on the studies of non linear EM wave interactions with the upper atmosphere. Three problems have been examined: 1) parametric excitation of whistler waves by an HF heater; 2) the resonant ionospheric heating at the electron gyrofrequency; and 3) enhanced ionspheric modifications by the combined operation of HF and VLF heaters. We studied the parametric excitation of whistler waves as the possible mechanism of VLF wave generation by an HF heater. It is found that the threshold of the instability is lower than the peak amplitude of the electric field 3 v/m available with the Tromso heating facility if the effect of swelling on the field amplitude is taken into account. The thermal filimentation instability of heater waves that generates the high frequency sideband modes and the zero-frequency modes (associated with magnetic and density fluctuations) can also occur during the resonant ionospheric heating at the electron gyrofrequency. The instability threshold is mainly imposed by the electron cyclotron damping, while that is determined by the offresonance (i.e, the detuning) effect if the heater wave frequency is not very close to the electron gyrofrequency. Enhanced ionospheric modifications by the combined operation of HF and VLF heaters have been analyzed. Intense airglow and height distribution of plasma lines can be expected.

Three natural processes occurring in the upper atmosphere have been theorectically 1) aura electrojet-induced ionospheric irregularities; 2) analyzed. They are: geomagnetic field perturbation due to the stimulated scattering of lower hybrid wave modes; and 3) spectral characteristics of geomagnetic VLF pulsations. The modification of the electron-neutral collision frequency due to the electron temperature perturbation in the electrojet can lead to a thermal instability causing the filamentation of auroral electrojet current and giving rise to purely growing magnetic field-aligned density irregularities in the E-region of the high-latitude ionosphere. Our preliminary analysis has shown that geomagnetic fluctuations can be caused by the stimulated scattering instability of lower hybrid waves that can be produced by particle precipitation and whistler waves. The energy spectrum of magnetospheric cavity modes is theoretically calculated showing sharp peaks at discrete frequencies in agreement with observations. Our theoretical model shows that only the discrete set of magnetospheric cavity eigenmodes can efficiently couple the perturbations excited on the boundary of the magnetosphere to the field-line resonant mode excited inside the inner turning point of the cavity eigenmodes.

We are studying a four-wave interaction process exciting ionospheric density fluctuation and geomagnetic fluctuation via the stimulated scattering of whistler waveinduced or particle precipitation-triggered lower hybrid waves. A low-frequency quasi-mode which is about half the wave length of the pump lower hybrid wave. We are currently comparing the theoretical predictions with some in-situ measurements made by orbiting satellites in the topside atmosphere.

The scattering and emission effects of earth terrain media are studied by the multilayer random medium model for the active and passive microwave remote sensing. The snow-covered ice fields and forest are studied with a three-layer random medium model. The dyadic Green's functions are derived in the far field. With the Born approximation, the backscattering cross sections for copolarization and cross-polarization are calculated for active microwave remote sensing. For passive microwave remote sensing, the bistatic scattering coefficients are computed. Then, the principles of reciprocity and energy conservation are invoked to calculate emissivities.

Active and Passive Remote Sensing of Ice **26.6**

U.S. Navy Office of Naval Research (Contract N00014-83-K-0258)

Jin A. Kong, Robert T. Shin, Freeman C. Lin, Maurice Borgeaud

Geophysical media encountered in nature are generally mixtures of materials that exhibit different dielectric characteristics. In remote sensing applications, it is desirable to treat the microscopically complicated mixture as macroscopically homogeneous and characterize it by an effective permittivity. Many natural heteorgeneous media have been widely studied from this point of view. Examples are snow, lake ice, sea ice, soil, vegetation canopy, rocks and forests. One of the constituents in these mixtures is often water, which makes the dielectric properties sensitive to small variations in fractional component volumes, because the permittivity of water normally greatly differs from that of other components. This fact makes dry and wet snow dielectrically different, and also partly distinguishes the permittivity of one-year and multi-year sea ice to a great extent.

2000

The dielectric mixtures have been analyzed by starting with the study of a two-phase mixture, where dielectric spheres of permittivity are embedded in a host material of permittivity, the analysis is extended to ellipsoids of arbitrary orientation and multiphase mixtures. The materials may be lossy, in which case their dielectric constants are complex numbers. This leads also to a complex effective permittivity for the mixture where the imaginary part stands for the absorption losses of the mixture. However, the scattering losses are not incorporated in the effective permittivity because the analysis is confined within the limits of the quasistatic approach taken. The result is, therefore, a low-frequency solution, its validity range being determined by the size of the constituent particles of the mixture and the wavelength of the operating frequency. Self-consistency is built through the so called "apparent permittivity" and the resulting formula for the effective permittivity is shown to reduce to previously obtained mixing formulas.

The correlation function for sea ice with brine inclusions is extracted from the photograph of the sea ice sample. The effective permittivity is derived by the strong fluctuation theory and bilocal approximation. The backscattering coefficients for active remote sensing and the brightness temperatures for passive remote sensing are calculated. The strong fluctuation theory will be further developed to arrive at the modified radiative transfer equations and to take into account the anisotropic effects. The strong fluctuation random medium theory will then be applied to the modelling of various earth media such as snow-ice and vegetation canopy.

The polarimetric radar model has been applied to study the ice fields. We have used the two-layer random medium model to characterize the ice fields and calculate the Mueller and covariance matrices in the backscattering direction. The ice layer has a background permittivity and its randomness is characterized by a three-dimensional correlation function with variance and correlation lengths. The radar backscattering coefficients are obtained by applying the first order Born approximation, which accounts for single scattering effects. The analytic expressions for backscattering coefficients are found to include depolarization effects in the single-scattering approximation, in contrast with the isotropic random medium which does not exhibit cross-polarization terms in the first order backscattering. We have transformed the Mueller matrix to a covariance matrix which is also useful in characterizing the polarimetric scattering properties. The Mueller and covariance matrices are illustrated by comparing with experimental data.

Experimental data taken from either a controlled field, the Arctic region, or the Antarctic region have indicated that the sea ice signatures are modified by snow cover due to the volume scattering effects. In the active and passive microwave remote sensing of snow-covered ice fields, the volume scattering effects are studied with a three-layer model as derived in the far field. With the Born approximation, the back-scattering cross sections for copolarization and cross-polarization are calculated for active microwave remote sensing. The autocorrelation and cross-correlation functions are assumed to have a Gaussian and exponential form in the lateral and vertical direction, respectively. For passive microwave remote sensing, the bistatic scattering coefficients are computed. Then, the principles of reciprocity and energy conservation are invoked to calculate emissivities. Theoretical results are illustrated by matching the experimental data taken from dry and wet snow-covered sea ice.

The snow-covered sea ice is studied with a three-layer random medium model. The snow layer is modeled by an isotropic random medium to account for the volume scattering effect which is due to randomly distributed granular ice particles. The ice layer is modeled by an anisotropic random medium to account for the volume scattering which is due to brine inclusions, air bubbles, and other inhomogeneities. The dyadic Green's function for this three-layer model is derived in the far field. With the Born approximation the backscattering cross sections for copolarization with cross-polariztion are calculated for active microwave remote sensing. The autocorrelation with cross-correlation functions are assumed to have Gaussian and exponential form in the lateral and vertical directions, respectively. For passive microwave remote sensing, the bistatic scattering coefficients are computed. Then the principles of reciprocity and energy conservation are invoked to calculate emissivities. Theoretical results are illustrated by matching the experimental data taken from dry and wet snow-covered ice.

The three-layer random medium model for the snow-covered sea ice has been studied under the assumption of week fluctuations of the permittivities. However, there is a large contrast between the permittivities of air, ice, brine and water. Therefore, we have generalized the three-layer random medium model with the strong fluctuation theory to account for the large permittivity fluctuations in the snow-covered sea ice. The random permittivity fluctuation in the sea ice caused by the brine inclusions are characterized by a correlation function which can be extracted from the digitized photographs of a sea ice sample. The strong fluctuation theory and the bilocal approximation are used to derive the effective permittivities for snow and sea ice. The singularity of the dyadic Green's function is properly considered. The distorted Born approximation is then used to calculate the bistatic scattering coefficients. Theorectical results are illustrated by comparing with the experimental data for thick first-year sea ice covered by dry snow.

26.7 Time Domain Wave Propoagation in Circuits

U.S. Navy - Office of Naval Research (Contract N00014-86-K-0533)

Jin A. Kong, Ann Tulintseff, Michael J. Tsuk, Soon Y. Poh

26.8 Time Domain Electromagnetic Waves

U.S. Army - Research Office Durham (Contract DAAG29-85-K-0079)

Jin A. Kong, Ying E. Yang, Ann Tulintseff, Michael J. Tsuk

26.9 Wave Transmission and Coupling in Multilayered Media

International Business Machines, Inc.

Jin A. Kong, Soon Y. Poh, Qizheng Gu, Jean-Fu Kiang, Ying-Ching E. Yang

sociation concern intercone

On the analysis of transient behavior of pulse propagation along conducting strips in multilayer dielectric media, we have: 1) modeled and calulated the impedance parameters and propagation characteristics for simple structures; 2) analyzed the transient response of signal transmission on strip lines with perpendicularly crossing strips geometry; 3) with periodical meshed ground plane; 4) generalized the method of characteristics for signal propagation on nonuniformly coupled transmission lines; and 5) studied the transient response of point and line sources excitation on two-layer media. We have also applied the technique of wave transmission matrices in periodic structures to examine transmission and reflection properties in striplines with meshed ground planes. A numerical Fourier inversion can then be done to obtain the time-domain response. Preliminary results support the previous conclusion.

In applying the method of moments to solving the EM scattering problems, it is necessary to solve a large matrix when the dimension for the scatterer is larger than several wavelengths. Tremendous amount of computer CPU time will be spent on solving the matrix equation. When only the far field properties such as scattering cross section is of interest, we can use the sparce matrix technique to reduce the amount of computation. Some algorithms are compared to solve the sparce matrix. The Gaussian elimination algorithm, Cholesky decomposition algorithm, several versions of conjugate gradient methods are used. the number of multiplications and divisions (flops) are counted for comparing the efficiency of these algorithms. The effect of the nonzero element positions to the efficiency is also studied by defining the clustering index.

Another way of incorporating the effect of complicated geometry is to use continuous line model while considering the coupling between parallel lines in multilayered integrated circuits to be uniform. In addition to the scheme that combines the method of characteristics and perturbational series to simplify the computation of the transient response from the coupled transmission line equations, new transformation for decoupling enables us to generalize this formulation to calculate the near-end and far-end crosstalks to very high accuracy, given arbitrary positional dependence for both capacitive and inductive coupling coeefficients.

A general method of analyzing the time-domain bi-directional coupling of a pair of nonuniformly coupled dispersionless transmission lines has been derived. The transmission line equations are decoupled using the method of characteristics and the equations are solved iteratively. In the cases with linear loads, the unit-step response can be obtained in closed-form to the first order approximation, and arbitrary excitations can be handled by convolution. General approximate solutions to the transient response on two identical, nonuniformly coupled transmission lines terminated with linear or nonlinear loads have been obtained through an iterative scheme. The iterative method is very useful when the coupling coefficients are slowly varying with position since the zeroth order or first order approximation would be sufficiently accurate yet much easier to calculate. Furthermore, with the help of newly devised special transformations, we have shown that both the codirectional coupling and contradirectional coupling of the problem with unit-step excitation and linear loads have closed form expressions up to the first order approximation. Arbitrary excitation can then be taken into account by convolution. This method is hence more efficient. As for nonlinear terminations, numerical integrations are performed along the characteristics. Examples have been given for both cases to illustrate the use of this method. Extension to problems in which the phase velocities of coupled lines are not equal, or where more than two coupled lines are involved is also under consideration.

26.10 Radar Scene Generation for Tactical Decision Aids

National Aeronautics and Space Administration/Goddard Space Flight Center (Contract NAG5-269)

Jin A. Kong, A. Swartz, Freeman C. Lin, Robert T. Shin

26.11 MMW Clutter Simulation Baseline Model

Simulation Technologies

recessors conserved acceptant

Jin A. Kong, A. Swartz, Freeman C. Lin, Robert T. Shin

For millimeter wave (MMW) clutter simulation we have developed a multi-layer random medium model to study the volume scattering effects. The vegetation fields such as corn, alfalfa, soybeans, meadow, etc., are modeled by the two-layer isotropic random medium. The vegetation fields with row structures are modeled by the two-layer anisotropic random medium. The snow-covered ice fields and forests are modeled by a three-layer random medium in which an isotropic random medium is used to simulated the snow layer and the leaves and an anisotropic random medium to simulate the ice layer and the trunks. The dyadic Green's functions for these multi-layer models are derived in the far field. With the Born or distorted Born approximations, the backscattering cross sections for copolarization and cross-polarization are calculated for active microwave remote sensing.

For radar image simulation, a set of "efficient" and "user-friendly" FORTRAN programs has been generated to calculate the normalized, co-polarized and cross-polarized backscattering cross sections for the scattering geometry. The numerical results of these FORTRAN codes cover all polarizations within the frequency range of 1 GHz to 100 GHz for all angles of incidence and all angles of scattering.

The radiative transfer (RT) equations for a general layered structure have been implemented in our VAX 11/750 computers. Both the random medium model and the discrete scattering model have been used in the radiative transfer theoretical developments. Due to the wide applications of the radiative transfer theory, it is important to determine the limitation of such a theory, and, moreover, to determine the conditions under which the RT equations might follow from a general wave formalism. Under the assumption of far field interaction and incoherence among waves in different directions, RT equations have been derived from wave theory for an unbounded medium. The MRT theory that incorporates partial coherent effects has been developed by applying the nonlinear approximation to Dyson's equation together with the ladder approximation to the Bethe-Salpeter equation.

We have used the two-layer anisotropic medium model to characterize the clutter and calculate the Mueller and covariance matrices in the backscattering direction. The random medium has a background permittivity and its randomness is characterized by a three-dimensional correlation function with variance and correlation lengths. The polarimetric properties of the backscattering coefficients are studied by calculating the full Mueller matrix. The radar backscattering coefficients of a two-layer anisotropic random medium are obtained by applying the first order Borm approximation, which

accounts for single scattering effects. The analytical expressions for backscattering coefficients are found to include depolarization effects in the single scattering approximation, in contrast with the isotropic random medium which does not exhibit cross-polarization terms in the first order backscattering. We have transformed the Mueller matrix to a covariance matrix which is also useful in characterizing the polarimetric scattering properties. Physical interpretations will be given for the properties of the covariance matrix elements.

Along with the development of theoretical models tailored for the active and passive remote sensing of earth terrain, we have made use of the theoretical results to match the available data collected with radars and radiometers from satellites, aircraft and truck-mounted platforms. The distinctive characteristics as identified by the theoretical results are useful in explaining trends in data curves. Consistent measurement features as displayed in experimental data sets will prompt the development of more complete and useful theories, and the refinement of the theoretical models along with the improvement of interpretation will prompt the suggestion of new experiments. This effort will be continued throughout our research program. The most sensitive parameters for each model will be identified in their order of importance to facilitate the application of the theoretical models to data interpretation, which will lead to a reliable scheme for radar scene generation in its application to the Tactical Decision Aids (TDA) for the Air Land Battlefield Environment (ALBE) Thrust Program.

26.12 Acoustic and Electromagnetic Wave Studies.

Schlumberger-Doll Research

Jin A. Kong, Tarek M. Habashy, Soon Y. Poh

A scalar and a vector Mathieu transform pair are developed, which facilitate the analysis of mixed boundary-value problems that are governed by the scalar and vector Helmholtz wave equations in the elliptic cylinder coordinate system. The properties of the transform kernels have been studied and their orthogonality relationships have been derived both in the spatial and spectral domains. Also the corresponding Parseval's theorems have been deduced. These transforms are very useful in formulating the scattering of electromagnetic waves from elliptical disks which has applications in modeling microstrip antennas. Also, these transforms can be used in formulating the reflection and transmission from open-ended elliptical waveguides.

The transient electromagnetic radiation by a vertical electric dipole on a two-layer medium is analyzed using the double deformation technique, which is a model technique based on identification of singularities in the complex frequency and wavenumber planes. We have shown that the existence of a pole locus on the negative imaginary frequency axis, which dominates the early time response, proves crucial in obtaining the solution for all times. A variety of combinations of parameters are used to illustrate the double deformation technique, and results are compared with those obtained via explicit inversion, and a single deformation method.

Publications

- Borgeaud, M., J.A. Kong and R.T. Shin, "Polarimetric Microwave Remote Sensing of Anisotropic Earth Terrain with Stron Fluctuation Theory." IGARSS '87 and URSI Meeting, University of Michigan, Ann Arbor, Michigan, 1987.
- Borgeaud, M., R.T. Shin and J.A. Kong, "Theoretical Models for Polarimetric Radar Clutter," J. Electromagnetic Waves Appl., 1, 73 (1987).
- Borgeaud, M., J.A. Kong and F.C. Lin, "Microwave Remote Sensing of Snow-Covered Sea Ice," 1986 International Geoscience And Remote Sensing Symposium, Zurich, Switzerland, September 1986, p. 8.
- Borgeaud, M., J.A. Kong and R.T. Shin, "Polarimetric Radar Clutter Modeling with a Two-Layered Anisotropic Random Medium," International Union of Radio Science, Commission F Open Symposium, University of New Hampshire, Durham, New Hampshire, July 28-August 1, 1986.
- Borgeaud, M., R.T. Shin and J.A. Kong, "Theoretical Modeling of Polarimetric Radar Clutter," National Radio Science Meeting, Philadelphia, Pennsylvania, June 9-13, 1986.
- Chen, C.F., and G. Freeman, "A New Formula for Partial Fraction Expansion of a Transfer Matrix," Comp. and Maths. with Appls., 12A, 9 963 (1986).
- Gaylor, D., T.M. Habashy and J.A. Kong, "Fields Due to a Dipole Antenna Mounted on Top of a Conducting Pad of Finite Extent in a Layered Stratified Medium," National Radio Science Meeting, Philadelphia, Pennsylvania, June 9-13.
- Gu, Q., and J.A. Kong, "Transient Analysis of Single and Coupled Lines with Capacitively-Loaded Junctions," I.E.E.E. Trans. Microwave Theory Tech., MTT-34, 9, 952 (1986).
- Gu, Q., J.A. Kong and Y.E. Yang, "Time Domain Analysis of Nonuniformly Coupled Lines," J. Electromagnetic Waves Appl. 1, 2, 111 (1987).
- Habashy, T.M., J.A. Kong, and W.C. Chew, "Scalar and Vector Mathieu Transform Pairs," J. Appl. Phys. 60, 10, 3395 (1986).
- Habashy, T.M., J.A. Kong and W.C. Chew, "Resonance and Radiation of the Elliptic Disk Microstrip Structure. Part I: Formulation." I.E.E.E. Trans. Antennas and Propag., to be published in 1987.
- Kiang, J.F., J.A. Kong and D.A. Shnidman, "Comparison of Algorithms to Solve Sparce Matrix in EM Scattering Problem," National Radio Science Meeting, Philadelphia, Pennsylvania, June 9-13, 1986.
- Kong, J.A., *Electromagnetic Wave Theory.* New York: Wiley-Interscience, 1986. 696 pp.

- Kuo, S.P., and M.C. Lee, "Parametric Excitation of Whistler Waves by HF Heater," Proceedings of the International Symposium on Modification of the Ionosphere by Powerful Radio Waves, Suzdal/Moscow, U.S.S.R., September 9-12, 1986, p. 109.
- Kuo, S.P., and M.C. Lee, "Stimulated Backscattering of Lower Hybrid Waves," Phys. Fluids 29, 4, 1024 (1986).
- Lee, C., and R.T. Shin, "Radar Cross Section Prediction Using a Hybrid Method," National Radio Science Meeting, Philadelphia, Pennsylvania, June 9-13, 1986.
- Lee, J.K. and J.A. Kong, "Modified Radiative Transfer Theory for a Two-Layer Anisotropic Random Medium," National Radio Science Meeting, Philadelphia, Pennsylvania, June 9-13, 1986.
- Lee, M.C., J.A. Kong and S.P. Kuo, "On the Resonant Ionospheric Heating at the Electron Gyrofrequency," Proceedings of the International Symposium on Modification of the Ionosphere by Powerful Radio Waves, Suzdal/Moscow, U.S.S.R., September 9-12, 1986, p. 111.
- Lee, M.C., J.A. Kong and S.P. Kuo, "Enhanced Ionospheric Modifications by the Combined Operation of HF and VLF heaters," Proceedings of the International Symposium on Modification of the Ionosphere by Powerful Radio Waves, Suzdal/Moscow, U.S.S.R., September 9-12, 1986, p. 146.

DINDON BUILDING DINGER SEEDING KEEKEE

- Lee, M.C., and S.P. Kuo, "Resonant Electron Diffusion as a Saturation Process of the Synchrotron Maser Instability," J. Plasma Phys. 35, 1, 177 (1986).
- Lin, F.C., J.A. Kong and R.T. Shin, "Theoretical Models for Active and Passive Microwave Remote Sensing of Snow-covered Sea Ice," IGARSS 87 and URSI Meeting, University of Michigan, Ann Arbor, Michigan, 1987.
- Lin, F.C., and J.A. Kong, "Remote Sensing of Snow-Covered Sea Ice," International Union of Radio Science, Commission F Open Symposium, University of New Hampshire, July 28-August 1, 1986.
- Lin, F.C., J.A. Kong, R.T. Shin and Y.E. Yang, "Backscattering and Propagation of Radar Pulses in Earth Terrain Mrdia," I.E.E.E. IMTC/86 Meeting, Boulder, Colorado, March 24-27, 1986.
- Nghiem, S., M.C. Lee and J.A. Kong, "Nonlinear EM Wave Interactions with the Neutral Atmosphere," International Union of Radio Science Commission F, Open Symposium, University of New Hampshire, Durham, New Hampshire, July 28-August 1, 1986.
- Poh, S.Y., and J.A. Kong, "Transient Response of a Vertical Electric Dipole on a Two-Layer Medium," J. Electromagnetic Waves Appl. 1, 1, 135 (1987).
- Poh, S.Y., J.A. Kong and M. Tsuk, "Transient Response of Dipole Antennas on Two-Layer Media," National Radio Science Meeting, Philadelphia, Pennsylvania, June 9-13, 1986.

- Rogers, S.W., and R.T. Shin, "Radar Cross Section Prediction for Coated Perfect Conductors with Arbitrary Geometries," National Radio Science Meeting, Philadelphia, Pennsylvania, June 9-13, 1986.
- Sihvola, A., and J.A. Kong, "Effective Permittivity of Dilectric Mixtures," International Union of Radio Science Commission F Open Symposium, University of New Hampshire, Durham, July 28-August 1, 1986.

27.0 Microwave and Quantum Magnetics

Academic and Research Staff

Prof. F.R. Morgenthaler

Graduate Student

C.M. Rappaport

27.1 Microwave Hyperthermia

National Institutes of Health (Grant 5 PO1 CA31303)

Frederic R. Morgenthaler, Carey M. Rappaport

Our understanding of both physics and physiology is challenged in trying to optimize techniques for heat production and for the thermometry associated with Hyperthermia modalities used in connection with cancer therapy. Fundamental considerations are based on designing proper microwave applicators which must be able to handle the microwave power required to raise the temperature of the tumor. They must also minimize the amounts of microwave power being delivered to the healthy tissue or being radiated into free space.

The Ph.D. thesis research of Carey Rappaport is nearing completion. The paper, "Localized Hyperthermia with Electromagnetic Arrays and the Leaky-Wave Troughguide Applicator," was published last year in the IEEE Transactions on Microwave Theory and Techniques, MTT-39, 5 (May 1986), pp. 636-643. Another paper entitled "Optimal Source Distribution for Maximum Power Dissipation at the Center of a Lossy Sphere" has been accepted for presentation in the 1987 IEEE Microwave Theory and Techniques Society International Symposium in Las Vegas. The entire digest summary is reproduced below.

27.2 Optimal Source Distribution for Maximum Power Dissipation at the Center of a Lossy Sphere

Carey M. Rappaport and Frederic R. Morgenthaler

27.2.1 Abstract

The ideal penetration limits for localized, non-invasive heating of tumors at the center of a volume of muscle tissue are determined. Using both an integral formulation and a modal approach, the optimum surface phase and amplitude source distributions which prevent excessive heating of healthy, intervening tissue are derived.

27.2.2 Introduction

In non-invasive microwave hyperthermia cancer therapy it is important to know the penetration depth limits of radiation which produces local power maxima. For treatment which provides heat at depth at the site of a localized tumor, overheating intervening tissue must be avoided. Two questions are vital to understanding the possibilities and limitations of this type of treatment: "What is the maximum radius of a sphere of biological tissue for which an optimally distributed source will generate as much power as its center as at its surface?" and "What is this optimum source distribution?"

27.2.3 Lossy Sphere Field Solutions

A spherical geometry allows the greatest exposure of a focal target point to sources on the surface for a given minimum depth of lossy medium. Thus the sphere represents the best possible non-invasive hyperthermia configuration. Although medical applications of heating spherical volumes are limited to only head and whole body, the knowledge gained from studying this best-case heating geometry will aid in the design of more practical hyperthermia systems.

The development of the optimal solution uses both the surface-current integration formula and the spherical harmonic solutions to the wave equation.

The greatest constructive interference at the center of a sphere results when the polarizations of all the surface sources are parallel: pointing in, say, the z-direction, as shown in Figure 27.1. Any additional symmetrical radial component (or, correspondingly,

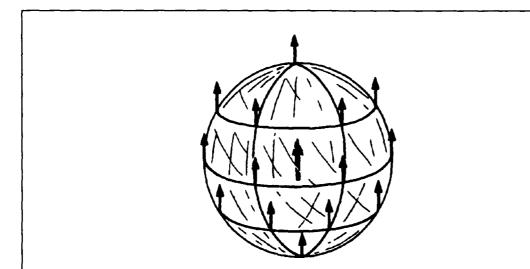


Figure 27.1.: Currents polarized in the z-direction on the surface of a sphere, and the resulting maximum constructive interference of electrical field at the center.

polar-angle component) ends up cancelling itself in the center, and any unsymmetrical components perpendicular to z obviously do not contribute to the z-component.

Integrating these parallel currents on a spherical surface of radius R is straightforward for a uniform distribution $J(r') = \delta(r - R)\hat{z}$. Without loss of generality, choose observation points along the z-axis, which lie a distance r from the sphere's center. Using the law of cosines for the source to observer distance in the Green's function integral yields:

$$E = -jw(\bar{l} + \frac{1}{k^2} \nabla \nabla) \cdot \int_0^{\pi} d\theta' \int_0^{2\pi} d\phi' R^2 \sin \theta' \mu \frac{e^{-jk\sqrt{R^2 - r^2 - 2rR\cos\theta'}}}{4\pi\sqrt{R^2 + r^2 - 2rR\cos\theta'}} \hat{z}$$
 (1)

The resulting power in a sphere of muscle tissue, normalized to that at the center, is plotted as a function of radius at $\theta=\pi/2$ in Figure 27.2 for some of the important hyperthermia frequencies. For these plots, $\kappa=\beta-j\alpha$, and the values of and were obtained for the various frequencies using experimentally derived values of dielectric constant and conductivity. It is the intersections with unity that determine the maximum allowable radius of tissue that can be heated without overheating the surface.

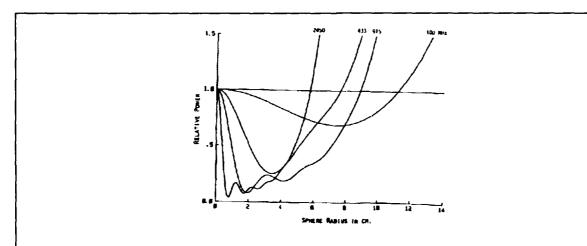


Figure 27.2.: Dissipated power in a sphere of muscle tissue as a function of radius for four standard hyperthermia frequencies: uniform current distribution.

27.2.4 Modal Analysis

Although the unform surface current distribution intuitively seems optimal, additional improvement becomes apparent from a model viewpoint. The harmonics of a sphere produce electric field as represented by:

$$E = \hat{r}A_n \frac{n(n+1)}{kr} j_n(kr)P_n(\cos\theta) + \hat{\theta}A_n[j_{n-1}(kr) - \frac{n}{kr} j_n(kr)]$$
 (2)

$$[n\cos\theta P_n(\cos\theta) - nP_{n-1}(\cos\theta)](\frac{1}{\sin\theta})$$

The key feature in this equation is that since the spherical Bessel functions, j_n vary as $(kr)^n$, the only mode which contributes to field in the center, r=0, is the n=1 mode. The Legendre polynomials $P_0(x)$ and $P_1(x)$ evaluate to 1 and x respectively, and so it becomes evident that the first mode corresponds to the uniform surface current case. However, since the higher order modes approach 0 in the center, they can be used to counteract the large, undesirable values of field elsewhere. Specifically, a distribution can be synthesized from modes with appropriate chosen phase and amplitude to partially cancel the field at the surface and thereby increase the maximum allowable sphere size.

The distribution of power on the surface of a large, lossy sphere for uniform current varies as $\sin^2\theta$, as seen from equation (1) with n=1 and by recalling $j_1(kR) < j_0(kR)$ for kR >> 1. Reducing the surface peak at $\pi/2$ is accomplished by adding the n=2 and the n=3 modes, which contain $\sin(3\theta)$ and $\sin(5\theta)$ terms, such that the surface power (rather than current) is more nearly a uniform function of θ . With the object of minimizing the maximum surface value of the sum of modes, the coefficients B_1 and B_2 of the function $\sin(\theta) + B_1 \sin(3\theta) + B_2 \sin(5\theta)$ of the function which produce three equal peaks are sought. An iterative method is used to find the solutions to this transcendental equation, which results in $B_1 = .2355$, $B_2 = .0640$. Additional, higher order terms could be used, but the reduction in power would only be in the order of .005, not warranting the added computational complexity.

Combining the first three modes using equation (2) with the A_{π} chosen to normal the Bessel function values at R, to combine the nth order Legendre polynomial values, and to normalize the power at the center, results in the surface power distribution shown in Figure 27.3. Plotted as a function of, it is observed that there is a sizable reduction of peak power and that the power is more evenly spread across the surface. Also, it is clear that the fifth order ripple is very close to ideal. The normalized maximum surface power is lowered by a factor of 0.78. Figure 27.4 plots the power as a function of radius at $\theta = \pi/2$ for the sum of three modes, for the same frequencies as in Figure 2. Comparing these two figures shows maximum radius increases of 1.72, 0.84, 0.57, and 0.32 cm for frequencies of 100, 433, 915, and 2450 MHz., respectively.

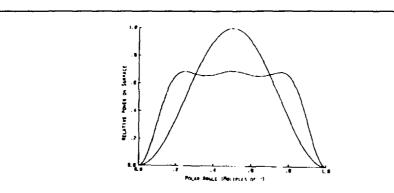
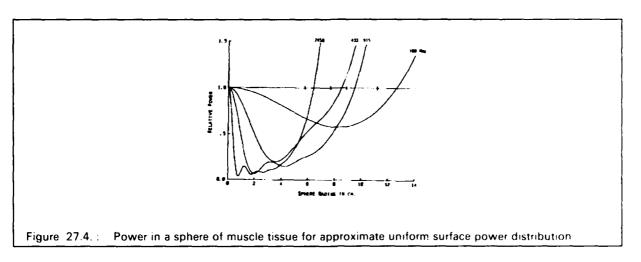


Figure 27.3.: Surface power as a function of θ for single mode (uniform current), and three mode (approximate uniform power) distributions.



27.2.5 Conclusion

The dimensions of the largest convex volume of muscle tissues which can be heated non-invasively, without overheating the surface, has been determined for the standard electromagnetic hyperthermia frequencies. These limits are the theoretical best cases (within 0.5) is not possible to improve on them by altering the surface phase or amplitude distribution. For other tissue geometries, the maximum penetration depth will, of course, be lower.

Although penetration depth increases with decreasing frequency below 433 MHz., the resolution of the focal spot at the center decreases. However, due to the non-linear dependence of complex dielectric constant on frequency, increasing the frequency does yield an increase in penetration depth for a limited range, as shown by the plot of 915 MHz. power curves. For 433 MHz. $\alpha/\beta=0.396$, whereas for 915 MHz. it is 0.231. There is a small advantage to using a more uniform power surface distribution than the uniform current distribution. The improvements are more pronounced for the lower frequencies, since wavelengths are longer, and the slopes of the power curves are shallower.

References

- ¹ Kong, J.A., Electromagnetic Wave Theory, New York: Wiley, 1986, p. 229.
- ² Guy, A.W., "Analyses of Electromagnetic Fields Induced in Biological Tissue by Thermographic Studies on Equivalent Phantom Models," I.E.E.E. Trans. Microwave Theory Tech. MTT-19, no. 2, 1971, p. 205.
- ³ Stratton, J.A., *Electromagnetic Theory*, New York: McGraw-Hill, 1941, p. 416.



28.0 Radio Astronomy

Academic and Research Staff

Prof. B.F. Burke, Prof. J.W. Dreher, Prof. D.H. Staelin, Dr. M. Shao, J.W. Barrett, Dr. P.W. Rosenkranz, Dr. G. de Jager

Graduate Students

L.D. Clark, Jr., R.W. Holm, M.J. Kelly, B.E. Hines, A.C. Briancon, T.A. Arias, J.D. Moores, R.V. Hammerschlag, P.M. Cassereau, H.S. Malvar, P.G. Bonanni, A.J. Gasiewski, G.J. Bartlett, J.C. Preisig, J.M. Shapiro, G.W. Wornell, B.I. Szabo, C. Carilli, J. Hewitt, G. Langston, M. Heflin, S. Conner

28.1 Galactic and Extragalactic Research

National Science Foundation (Grant AST 86-17172)

John Dreher, Bernard F. Burke, C. Carilli, J. Hewitt, G. Langston, Michael Heflin, Samuel Connor, Vivek Dhawan

We have discovered a "counter-jet" in the radio galaxy Cygnus A. This follows the earlier achievement, with Perley of the National Radio Astronomy Observatory (NRAO), of the discovery of the relativistic jet that emanates from the active galactic nucleus (a discovery that was made through their new methods of image processing at the the Very Large Array (VLA) at NRAO). A related project, a detailed polarization map of the radio galaxy, has also been completed. A new observing project, one of the largest programs ever undertaken at the VLA, has been begun to extend these methods to a larger selection of radio galaxies.

We have also been searching for new gravitationally-lensed quasars in collaboration with colleagues at Princeton and CalTech. One prime example, Q0023+171, has been discovered and six promising new candidate objects are being studied in greater detail. About 4000 radio maps, taken with the VLA, are being processed as part of their program. A successful series of VLBI experiments has been conducted at 7 mm wavelength, with the intention of establishing that band for standard VLBI operations. A synthesized map at 7 mm of the active galaxy 3C84 (Perseus A) has been prepared and represents the most highly detailed map ever made of that unusual object, with a resolution of 140 micro-arc-seconds. Prof. Burke is also continuing as U.S. principal investigator for the QUASAT satellite, a joint U.S.-European project to establish a VLBI station in space to get higher angular resolution than can be achieved with earth-based VLBI stations alone.

28.2 Long-Baseline Astrometric Interferometers

U.S. Navy - Office of Naval Research (Contracts N00014-84-C-2082 and N00014-86-C-2114)

David H. Staelin, Michael Shao, John W. Barrett, Lloyd D. Clark, Jr., R. Walter Holm, Matthew J. Kelly, Braden E. Hines

During 1986 construction of the Mark III optical astrometric interferometer continued at the Mount Wilson Observatory. Initial measurements were made of stellar positions using the inner pair of pedestals in the North-South direction; these are separated by 12 meters. These initial crude measurements, performed without the benefit of laser measurements of pedestal position, yielded relative stellar positions over wide angles with sub-arcsecond accuracy. These have further demonstrated the ability of the two-color technique to yield instantaneous stellar positions with a precision more than five times superior to that of the single-color technique.

Three significant subsystems were developed for the Mark III interferometer: an optical delay line, a siderostat control system, and a photon camera star tracker. To adjust the path length of the delay to provide coherence between the two beams, a movable retroreflector was mounted on rails inside a vacuum chamber. Three actuators are used to control the optical path length: a stepper motor, a voice coil, and a piezoelectric transducer. A heterodyne laser interferometer with a resolution of 5 nanometers and a maximum slew rate of 0.6 meters per second monitors the optical path length through the delay line. The rms servo tracking error was approximately 8, 11, and 18 nanometers for delay line velocities of 0, 63, and 790 microns per second, respectively.¹

The Mark III siderostat subsystems employed open-loop pointing, for which the accuracy was \sim 4 arc minutes. For automatic operation of the Mark III interferometer pointing accuracies of \sim 5-10 arc seconds were sought. An 8-parameter geometric model was developed to describe the siderostat. A single siderostat was tested at Mount Wilson Observatory, and yielded accuracies better that 10 arc seconds with some restrictions.² A multi-beam laser assembly to monitor the position of each siderostat mirror relative to a local invar plate was designed. Work on this system is continuing.

A photon camera star tracker was designed, analyzed and tested. Laboratory testing of the tracker indicated that the rms tracking error in one axis was about 0.1 arc second with a detected photon rate of 13,500 photons per second, and about 0.2 arc seconds for 2500 photons per second.³

References

- ¹ R.W. Holm, "A High-Speed, High-Resolution Optical Delay Line for Stellar Interferometry Applications," S.M. Thesis, Dept. of Electr. Eng. and Comp. Sci., M.I.T., Cambridge, Mass., 1986.
- ² M.J. Kelly, "A Siderostat Control System," S.M. Thesis, Dept. of Electr. Eng. and Comp. Sci., M.I.T., Cambridge, Mass., 1986.
- ³ L.D. Clark, Jr., "A Photon Camera Star Tracker for Stellar Interferometry," S.M. Thesis, Dept. of Electr. Eng. and Comp. Sci., M.I.T., Cambridge, Mass., 1986.

28.3 Tiros-N Satellite Microwave Sounder

National Oceanic and Atmospheric Administration (Contract NA84AA-D-00001) SM Systems and Research, Inc.

Philip W. Rosenkranz, David H. Staelin, Alain C. Briancon

The National Oceanic and Atmospheric Administration (NOAA) operates polar-orbiting weather satellites which now carry four-channel passive microwave spectrometers (MSU) that map the three-dimensional temperature field of the atmosphere at 6- or 12-hour intervals. This instrument will be superseded at the end of this decade by the Advanced Microwave sounding Unit (AMSU), which has 15 channels that image the earth with 50-km resolution every 12 hours at frequencies distributed from 23 to 90 GHz.

A study of multi-dimensional temperature profile retrieval techniques for use with MSU and AMSU was completed.¹ Both adaptive and non-adaptive retrieval techniques were studied, and under certain circumstances useful improvements could be obtained.

Additional studies of methods for estimating surface emissivity and for theoretically predicting atmospheric transmittances were continued.

References

¹ A.C. Braincon, "Estimation and Modeling of Multidimensional Non-Stationary Stochastic Processes: Application to the Remote Sensing of Atmospheric Temperature Fields," Ph.D. Diss., Dept. of Electr. Eng. and Comp. Sci., M.I.T., Cambridge, Mass., 1986.

28.4 High-Resolution Passive Microwave Imaging of Atmospheric Structure

National Aeronatics and Space Administration/Goddard Space Flight Center (Grant NAG 5-10)

David H. Staelin, Philip W. Rosenkranz, John W. Barrett, Pierino G. Bonanni, Albin J. Gasiewski

During 1986 a new imaging Millimeter-wave Temperature Sounder (MTS) was flown for the first time from the NASA ER-2 aircraft near 65,000 feet. The MTS includes a double-sideband receiver with eight channels, each ~ 200 MHz wide, covering the spectral region from 118.75 \pm 0.45 to 118.75 ± 2.1 GHZ. These channels sampled atmospheric temperature throughout the atmosphere beneath the aircraft. The cross-track scan sampled the atmosphere at 14 spots covering the region \pm 45° from nadir with a 7.5° spot beamwidth. An integration time of \sim 0.1 sec per spot yielded \sim 0.5 K brightness temperature resolution. The MTS also carried a nadir-looking 53.6-GHz radiome ter and a wide-angle television camera. The MTS was successfully flown during the experiments GALE (February 1986) and COHMEX (June-July 1986). Strip map images of atmospheric millimeter-wave radiance revealed the zone of precipitation,

the altitudes of the cell tops, the concentration of frozen precipitation aloft, and the temperature structure around the cell. Those data reveal what may be the first direct observation of small thermal waves (less than \sim 1K) in the vicinity of fronts. A data reduction and display system was developed and has yielded excellent images (1024 X 1024 pels, 8-bit color) of these data.

A statistical model for error growth in numerical weather prediction models was developed and found to yield results similar to those of Lorenz and Leith, but with the added advantages that 10σ levels and the primitive equations were employed. The results predict, for example, that AMSU (50-km resolution) should significantly improve mesoscale forecasts relative to other systems with resolution of a few hundred kilometers. A simple equation predicts limits to the predictability of atmospheric dynamics as a function of the spectral regions of interest and for which data is available.

28.5 Video Image Processing

Center for Advanced Television Studies Brazil, Conselho Nacional de Desenvolvimento Cientifico e Tecnologico

David H. Staelin, Gerhard de Jager, Henrique S. Malvar, Gregory J. Bartlett, Jerome S. Shapiro, Bernard I. Szabo,

Optimal pre- and post-filtering in noisy sampled-data systems was studied in the context of video and audio communications for storage systems, with optimality considered in a weighted mean-square error sense. The system model included additive noise in the input signal and in the channel. Optimal pre- and post-filters were derived for three basic classes of systems, characterized by Infinite Impulse Response (IIR), Finite Impulse Response (FIR), and block filters. Also studied were filters with nearly optimal performance that can be implemented using various fast transforms. An analytic form and a fast version were derived for a previously introduced class of pre- and post-filters for block processing with overlapping basic functions, namely, "Lapped Orthogonal Transforms (LOT's)." In all of these classes, for typical image processes and coding applications, improvements over traditional systems were obtained in the weighted error spectrum on the order of 1-6 dB.1

Experiments were performed to characterize the spatial and temporal response of human color vision. It was found that peak luminance sensitivity occurred for test gratings at a spatial frequency near 2 cycles per degree, and for temporal variations near 4 Hz. The corresponding peak sensitivities for chrominance signals were near 1 cycle per degree and 2 Hz for I, and 0.6 cycles per degree and 7 Hz for Q. The surprising result was that the temporal sensitivity for the I component of chrominance is sufficiently low that this fact could be used to reduce the bandwidth required for communicating color television signals.²

A quantitative measure that performs well at predicting the absolute and comparative subjective picture quality of two-dimensional decimated and interpolated still images was studied. Subjective testing of 24 subjects determined viewers' preferences for degraded images. The error measure which performed best as a predictor of subject preferences suggested that these images were judged on the basis of mean-square error in the worst portion or portions of the image, using an area which is approximately 0.5%

CONTRACTOR OF THE PROPERTY OF

of the whole; an exception was blur, for which subjects tended to evaluate the entire image.3

By exploiting the relationship between the Discrete Cosine Transform (DCT) and the Discrete Hartley Transform (DHT), a new fast and numerically stable algorithm for computing the DCT was developed.⁴ This technique is notable for its utilization of a minimum number of multiplications, although somewhat more additions are required.

References

- ¹ H.S. Malvar, "Optimal Pre- and Post-Filtering in Noisy Sampled-Data Systems," Ph.D. Diss., Dept. of Electr. Eng. and Comp. Sci., M.I.T., Cambridge, Mass., 1986.
- ² G.J. Bartlett, "Observations of the Spatial and Temporal Response of Human Color Vision," S.M. Thesis, Dept. of Electr. Eng. and Comp. Sci., M.I.T., Cambridge, Mass., 1986.
- ³ A.S. Tom, "Prediction of FIR Pre- and Post-Filter Performance Based upon a Visual Model," S.M. Thesis, Dept. of Electr. Eng. and Comp. Sci., M.I.T., Cambridge, Mass., 1986.
- ⁴ H.S. Malvar, "Fast Computation of Discrete Cosine Transform through Fast Hartley Transform," Electronics Lett. 22, 352 (1986).

28.6 Nonthermal Radio Emission from the Jovian Planets

National Aeronautics and Space Administration/Goddard Space Flight Center (Grant NAG 5-537)

David H. Staelin, Tomas A. Arias, Roeland V. Hammerschlag, John D. Moores

The Planetary Radio Astronomy (PRA) experiment on the Voyager 1 and 2 spacecraft observed radio emission from Earth, Jupiter, Saturn and Uranus in 198 channels distributed over the band from 1.2 kHz to 40.5 MHz. During 1986 we continued to study the Jovian modulated spectral activity in the band below ~1.3 MHz. Efforts to explain these data theoretically have been unsuccessful to date. However, the characteristics of this emission have been studied quantitatively.¹

During 1986 Voyager 2 encountered Uranus, disclosing the existence of high magnetic fields and strong emissions radiated principally away from the sun. These observations also yielded the most accurate rotation period yet obtained for the planet, 17.24 +.01 hours.²

Theoretical studies of the Io-generated Alvren waves were initiated. Preliminary results suggest that the currents observed by the Voyager magnetometer experiment can be explained, and also perhaps the observed \sim 3- kev particle energies deduced earlier.³

References

- ¹ T.A. Arias, "Modulated Spectral Activity in the Inner Jovian Magnetosphere, "S.B. Thesis, Dept. of Phys., M.I.T., Cambridge, Mass., 1986.
- ² J.W. Warwick, et al., "Voyager 2 Radio Observations of Uranus," Science, 233 *102* (1986).
- ³ D.H. Staelin and P.W. Rosenkranz, "Formation of Jovian Decametric S Bursts by Modulated Electron Streams," J. Geophys. Res. 87, 10 (1982).

28.7 Video Bandwidth Compression Techniques

U.S. Army (Contract MDA 903-84-K-0297)

David H. Staelin, Gerhard de Jager, Henrique S. Malvar, James C. Preisig, Gregory W. Wornell

Successful full-motion codina of video sequences characteristic videoconferencing can be performed at data rates of 56 kbps and lower only when adaptive coding techniques are employed. Adaptive block transform coding, with and without motion compensation, has been studied using both the Discrete Cosine Transform (DCT) and a new class of transforms, designated Lapped Orthogonal Transforms (LOT), which have basis functions that overlap the basis functions in adjacent blocks while retaining orthogonality. These two techniques were compared using interframecoded full-motion head-and-shoulders sequences at 28 and 56 kbps. quality assessment experiments revealed the superiority of LOT over the DCT with low data rates when no motion compensation was used. The improvement was no longer significant at 56 kbps with full motion compensation.¹

Reference

THE TRANSPORT OF THE PROPERTY OF THE PROPERTY

¹ P.M. Cassereau, D.H. Staelin, and G. de Jager, "Encoding of Impages Based on a Lapped Orthogonal Transform," submitted to I.E.E.E. Trans. Commun., 1987.

29.0 Publications and Meetings

29.1 Meeting Papers Presented

The following is a list of papers presented at conferences and meetings by R.L.E. faculty, staff and students during 1986. Publication information is included for items published in conference proceedings and journals.

January 1986

SEESTAL MEESTAGE CONTRACTION OF SECTION OF S

167th Meeting American Astronomical Society, Houston, Texas, January 5-9, 1986

Abstracts in Am. Astron. Soc. 17, 4 (1985):

Hewitt, J.N., E.L. Turner, C.R. Lawrence, D.P. Schneider, J.E. Gunn, M. Schmidt, J.H. Mahoney, G.I. Langston, and B.F. Burke, "The Multiple Source 0023 + 171: a Dark Gravitational Lens," p. 907.

Plasma Physics Colloqium, California Institute of Technology, Pasadena, California, January 16, 1986

Coppi, B., "Plasma Physics in Space and Laboratory."

Symposium on Space Plasma, M.I.T., Cambridge, Massachusetts, January 20-24, 1986

Coppi, B., "Plasma Physics in Space and Laboratory."

Age of the Photon: Symposium on the Uses and Possibilities of Light, M.I.T., Cambridge, Massachusetts, January 22-23, 1986

Ezekiel, S., "Overview of Photon Sources and Applications."

Fujimoto, J.G., "Short Pulse Lasers."

Haus, H.A., "Elements of Optical Computing."

Kleppner, D., "Lasers and Atomic Physics."

Symposium on Recent Advances VLSI, Santa Clara, California, January 30, 1986 (Sponsored by the Industrial Liaison Office, M.I.T., Cambridge, Massachusetts)

Allen, J., "Designing High-Performance Integrated Circuits for Digital Signal Processing."

Smith, H.I., "Submicron Structures and Quantum-Effect Devices."

Hughes Research Laboratory Seminar, Malibu, California, January 31, 1986

Smith, H.I., "Submicron Structures and Quantum-Effect Devices." (invited paper)

February 1986

- Seminar on Plasma Physics, Columbia University, New York, February 21, 1986
 - Luckhardt, S.C., "Current Drive and Instability Phenomena."
- Topical Meeting on Integrated and Guided-Wave Optics, Atlanta, Georgia, February 26-28, 1986
 - Summaries in *Technical Digest*:
 - Abbas, G.L., V.W.S. Chan, and J.G. Fujimoto, "Far-Field and Spectral Control of Laser Diode Arrays Using Injection Locking," p. 40.
 - Gabriel, M.C., H.A. Haus, and E.P. Ippen, "Thermal Index Changes by Optical Absorption in Group III-V Semiconductor Waveguides," p. 30.

March 1986

population and property property and passes and property

- I.E.E. Instrumentation and Measurement Technology Conference, University of Colorado, Boulder, Colorado, March 25-27, 1986
 - Papers in Conference Record:
 - Lin, F.C., J.A. Kong, R.T. Shin, and Y.E. Yang, "Backscattering and Propagation of Radar Pulse in Earth Terrain Media," p. 270.
- 1986 March Meeting, American Physical Society, Las Vegas, Nevada, March 31 April 4. 1986
 - Abstracts in Bull. Am. Phys. Soc. 31, 3 (1986):
 - Berker, A.N., and S.R. McKay, "Modified Hyperscaling Relation for Phase Transitions Under Random Fields," p. 683.
 - Fujimoto, J.G., "Studies of Nonequilibrium Conditions in Metals Using Femtosecond Laser Pulses," p. 663.
 - Isaacs, E.D., D. Heiman, J.J. Zayowski, R.N. Bicknell, and J.F. Schetzina, "Magnetically-Tunable (Cd, Mn)Te Quantum Laser," p. 605.
 - Kleppner, D., "Rydberg Atoms and the Limits of Measurement," p. 218. (invited paper)
 - Kortan, A.R., R.J. Birgeneau, and M.S. Dresselhaus, "A New Commensurate-Incommensurate Transition of Stage-4 Bromine Intercalated Graphite," p. 597.
 - Mochrie, S.G.J., R.J. Birgeneau, A.R. Kortan, and P.M. Horn, "Melting Transition in High Stage Bromine-Intercalated Graphite," p. 597.
 - Youngdale, E.R., D.M. Larsen, and R.L. Aggarwal, "Observation of Stress-Tuned, Magnetic-Field-Induced Anti-Crossing Between 1s(T2) States of Opposite Spin in Ge(As)," p. 695.

April 1986

- Topical Meeting on Signal Recovery and Synthesis II, Optical Society of America, Honolulu, Hawaii, April 2-4, 1986
 - Papers in Technical Digest:
 - Curtis, S.R., and A.V. Oppenheim, "Reconstruction of Multidimensional Signals from Zero Crossings," p. 126.
 - Izraelevitz, D., and J.S. Lim, "A New Algorithm for Closed Form Image Reconstruction from Fourier Transform Magnitude," pp. 54-57.
 - van Hove, P., "Reconstruction of Axisymmetric Objects from One Silhouette," pp. 87-90.
 - Wengrovitz, M.S., A.V. Oppenheim, and G.V. Frisk, "Reconstruction of a Complex-Valued Field Using the Hilbert-Hankel Transform," pp. 140-143.
- Collegium Workshop on Thin Film Processing, Materials Processing Center, M.I.T., Cambridge, Massachusetts, April 7, 1986
 - Smith, H.I., "The Use of Submicron Patterning in Controlling Crystalline Films on Amorphous Substrates."
- I.E.E. International Conference on Acoustics, Speech and Signal Processing, Tokyo, Japan, April 7-11, 1986
 - Papers in ICASSP '86:
 - Chen, F.R., and V.W. Zue, "Lexical Access and Verification in a Broad Phonetic Approach to Continuous Digit Recognition," pp. 1089-1092.
 - Espy-Wilson, C., "A Phonetically Based Semivowel Recognition System," pp. 2775-2778.
 - Ghitza, O., "Speech Analysis/Synthesis Based on Matching the Synthesized and Original Representations in the Auditory Nerve Level," pp. 1995-1998.
 - Glass, J.R., and V.W. Zue, "Detection and Recognition of Nasal Consonants in American English," pp. 2767-2770.
 - Goldor, R., "A Model of Peripheral Auditory Transduction Using a Phase Vocoder with Modified Channel Signals," pp. 1955-1958.
 - Griffin, D.W., and J.S. Lim, "A High Quality 9.6 KBPS Speech/Analysis Synthesis," pp. 125-128.
 - Huang, C.B., "The Effect of Formant Trajectory and Spectral Shape on the Tense/Lax Distinction in American Vowels," pp. 893-896.
 - Huttenlocher, D.P., "A Broad Phonetic Classifier," pp. 2259-2262.
 - Leung, H.C., and V.W. Zue, "Visual Characterization of Speech Spectrograms," pp. 2751-2754.
 - Musicus, B.R., and A.M. Kabel, "Maximum Entropy Pole-Zero Estimation," pp. 1389-1392.

- Myers, C., "On the Use of Linear Programming for Spectral Estimation," pp. 189-192.
- Nawab, H., V. Lesser, and E. Milios, "Conceptual Diagnosis of Signal Processing Systems," pp. 2911-2914.
- Pardo, J.M., "On the Determination of Speech Boundaries: A Tool for Providing Anchor Time Points in Speech Recognition," pp. 2267-2270.
- Pitrelli, J.F., "Recognition of Word Final Unstressed Syllables," pp. 2771-2774.
- Seneff, S., "A Computational Model for the Peripheral Auditory System: Application to Speech Recognition Research," pp. 1983-1986.
- Wengrovitz, M.S., A.V. Oppenheim, and G.V. Frisk, "Reconstruction and Propagating Complex Wave Field Using the Hilbert-Hankel Transform," pp. 2875-2878.
- Zue, V.W., D.S. Cyphers, R.A. Kassel, D.H. Kaufman, H.C. Leung, M. Randolph, S. Seneff, J.E. Unverferth, III, and T. Wilson, "The Development of the M.I.T. LISP-Machine Based Speech Research Workstation," pp. 329-332.
- Zue, V.W., and L.F. Lamel, "An Expert Spectrogram Reader: A Knowledge-Based Approach to Speech Recognition," pp. 1197-1200.
- Plasma Physics Colloquium, Purdue University, West Lafavette, Indiana, April 8, 1986
 - Coppi, B., "Advances in Fusion Research."
- 1986 Sherwood Theory Conference, New York, April 14-16, 1986

Abstracts in Proceedings:

- Bonoli, P.T., M. Mayberry, and M. Porkolab, "Theoretical Studies of Lower Hybrid Current Drive in the Versator II Tokamak," paper 1C-9.
- Coppi, B., "Physics and Design Issues for Ignition Experiments," paper 1B-6.
- Coppi, B., and F. Pegoraro, "Possible Candidate Microinstability for Anomalous Electron Transport," paper 3E-1.
- Coppi, B., and F. Porcelli, "Theoretical Model of Fishbone Oscillations." paper 3E-2.
- Englade, R.C., and L.E. Sugiyama, "Current Ramp and Ignition in a High Field Tokamak," paper 1C-28.
- Francis, G., and A. Bers, "A Model for Minority Absorption in Ion Cyclotron Heating," paper 3C-15.
- Fuchs, V., M. Shoucri, J. Teichmann, and A. Bers, "Runaway Electron Distributions and Their Stability with Respect to the Anomalous Doppler Resonance," paper 3C-30.
- Kesner, J., M. Gerver, B. Lane, Y.T. Lau, and R.S. Post, "Magnetic Divertor Stabilized Confinement Devices," paper 2D-1.
- Lau, J.T., and M.J. Gerver, "Axial Eigenmodes of Ion Loss-Cone Instabilities in the TARA Plug and Anchor," paper 3D-6.

STREET STREET, MERSELLE NEWSSIES COLORGE STREET

- Luckhardt, S.C., A. Bers, V. Fuchs, and M. Shoucri, "The Anomalous Doppler Instability During Lower-Hybrid Current Drive," paper 1C-33.
- Migliuolo, S., "Temperature Anisotropy Driven Low Frequency Instabilities in Homogeneous Plasmas," paper 3C-2.
- Porcelli, F., and S. Migliuolo, "Ion Viscosity Stabilization of Resistive Internal Kinks," paper 3C-29.
- Pu, Y.K., R. Englade, and S. Migliuolo, "Trapped Electron Effects on Anomalous Ion Heat Transport," paper 1C-25.
- Ram, A., and A. Bers, "Enhancement of the Parallel Wavenumbers on the Mode-Converted Ion-Bernstein ICRF Waves," paper 2D-38.
- Ramos, J.J., "Vertical Stability of Shaped Tokomaks," paper 3C-14.
- Shoucri, M., V. Fuchs, and A. Bers, "Relativistic 2-D Fokker-Planck Code for Lower-Hybrid Current Drive," paper 2C-3.
- Sugiyama, L.E., and J. Martinelli, "A Model for TFTR Ohmic Discharges," paper 2C-4.
- Tang, W.M., and B. Coppi, "Influence of Anomalous Thermal Losses on Ignition Conditions," paper 3D-21.
- Seminar at the Sohio Research Center, Cleveland, Ohio, April 16, 1986
 - Atwater, H.A., "Device Quality Crystalline Films on Amorphous Substrates by Zone-Melting Recrystallization and Grain Growth Processes."
- Workshop at the University of Maryland, College Park, Maryland, April 17-18, 1986
 - Coppi, B., "Anomalous Transport and Profile Consistency."
 - Sugiyama, L.E., "Review of the Theory of Anomalous Transport and Profile Consistency."
- Hitachi Central Research Laboratory Seminar, Kokubunii, Japan, April 18, 1986
 - Melngailis, J., "Focused Ion Beam Fabrication." (invited paper)
- Electronic Materials and Devices Seminar, Princeton University, Princeton, New Jersey, April 21, 1986
 - Fujimoto, J.G., "Generation and Applications of Femtosecond Laser Pulses."
- Osaka University Seminar, Osaka, Japan, April 21, 1986
 - Melngailis, J., "Focused Ion Beam Technology and Submicron Devices." (invited paper)
- Institute of Acoustics Seminar, Academy of Sciences, Beijing, China, April 26, 1986
 - Melngailis, J., "Focused Ion Beam Technology and Applications." (invited paper)

SPEECH TECH '86, New York, New York, April 28-30, 1986

Papers in *Proceedings*:

Klatt, D.H., "Text to Speech: Present and Future," pp. 221-226.

Annual Spring Meeting of the Association for Research in Vision and Ophthalmology, Sarasota, Florida, April 28 - May 2, 1986

Abstracts in ARVO '86:

Birngruber, R., C.A. Puliafito, A. Gawande, W-Z. Lin, R.W. Schoenlein, and J.G. Fujimoto, "Femtosecond Retinal Injury Damage Studies," p. 314.

Changsha Research Seminar, Changsha Research Institute of Equipment for Semiconductor Technologies, Changsha, Hunan, China, April 30, 1986

Melngailis, J., "Focused Ion Beam Technology." (invited paper)

May 1986

I.E.E. International Symposium on Circuits and Systems, San Jose, California, May 5-7, 1986

Papers in ISCAS '88:

Glasser, L., and J.L. Wyatt, Jr., "Fundamental Tradeoff Between Noise Margin Gain and Delay in a Simple MOS Inverter."

O'Brien, P.R., and J.L. Wyatt, Jr., "Signal Delay in ECL Interconnect," pp. 755-758.

Workshop on Technologies and Ultrasmall Electronic Devices, Clemson University, Clemson, South Carolina, May 6-7, 1986

Melngailis, J., "Focused Ion Beam Fabrication." (invited paper)

Department of Biological Science and Engineering Colloquium, Tsinghua University, Beijing, China, May 11, 1986

Chen, S.-H., "Microemulsions."

I.E.E.E. Custom Integrated Circuits Conference, Rochester, New York, May 12-14, 1986

Musil, C.R., J.L. Bartlet, and J. Melngailis, "Focused Ion Beam Microsurgery for Integrated Circuit-Repair or Customization."

111th Meeting, Acoustical Society of America, Cleveland, Ohio, May 12-16, 1986

Abstracts in J. Acoust. Soc. Am. 79, Suppl. 1 (1986):

Bickley, C., "Formant Estimation of High Fundamental Frequency Speech," p. \$38.

- DiBenedetto, M-G., "Influence of Fundamental Frequency in the Perception of Vowel Height," p. S8.
- Klatt, D.H., "History of Text-to-Speech Conversion for English," p. S24.
- Koehnke, J., and H.S. Colburn, "Binaural Detection and Discrimination: Impaired Listeners," p. S22.
- Passaro, C., J. Koehnke, and H.S. Colburn, "Binaural Detection and Discrimination: Normal Listeners," p. S21.
- Randolph, M.A., and V.W. Zue, "On Finding the Relationship Between Phonetic Categories and Spectral Shape."
- Stevens, K.N., "Turbulence Noise Sources in the Vocal Tract," p. S82.
- Zurek, P.M., and L.A. Delhorne, "Speech Reception in Noise by Hearing-Impaired Listeners," p. S23.
- Custom Integrated Circuits Conference, Rochester, New York, May 13, 1986
 - Allen, J., "DSP Alternatives: Custom versus Standard Components."
- University of Sydney, Department of Chemistry Colloquium, Sydney, Australia, May 17, 1986
 - Chen, S.-H., "Structure in Strongly Interacting Ionic Micellae Solutions."
- 1986 Spring Meeting, American Geophysical Union, Baltimore, Maryland, May 19-22, 1986
 - Abstracts in EOS 67, Nos. 1-25 (1986):
 - Kuo, S.P., M.C. Lee, and A. Wolfe, "Dominance of Discrete Magnetospheric Cavity Modes on the Generation of Field-Line Resonances," p. 348.
 - Lee, M.C., J.F. Kiang, and S.P. Kuo, "On the Cause of Spectral Broadening of Injected VLF Waves," p. 317.
 - Migliuolo, S., "Temperature Anisotropy Driven Low Frequency Instatilities in Homogeneous Plasmas," p. 348.
- Plasma Astrophysics Meeting, Sukhumi, U.S.S.R., May 19-28, 1986
 - Coppi, B., "Plasma Physics in Uranus Encounter." (invited paper)
 - Coppi, B., "Theoretical and Experimental Advices in the Physics of Fusion Plasmas." (invited paper)
- Applied Mathematics Department Colloquium, Australian National University, Canberra, Australia, May 20, 1986
 - Chen, S.-H., "SANS Studies of Small Angle Neutron Scattering Microemulsions."
- ICRF Workshop, University of Wisconsin, Madison, Wisconsin, May 20-21, 1986

- Francis, G., A. Bers, and A.K. Ram, "Minority Absorption and Parallel Wavenumber Enhancement on the Mode Converted Bernstein Wave."
- NSF Workshop on Optical Nonlinearities, Fast Phenomena and Signal Processing, University of Arizona, Tucson, Arizona, May 22-23, 1986
 - Papers in Proceedings:
 - Haus, H.A., and N.A. Whitaker, "Extension of Picosecond Sampling Device," pp. 159-167.
 - Lin, W.Z., J.G. Fujimoto, and E.P. Ippen, "Femtosecond Processes in Semiconductors," pp. 272-280.
- Faculty of Applied Science Colloquium, Royal Institute of Technology, Melbourne, Australia, May 23, 1986
 - Chen, S-H., "Structure and Dynamics of Glass-like Microemulsions."
- Department of Physical Chemistry Colloquium, University of Melbourne, Melbourne, Australia, May 24, 1986
 - Chen, S-H., "Structure in Strongly Interacting Ionic Micellae Solutions."
- KEK National Laboratory for High Energy Physics, Tsukuba, Japan, May 26, 1986
 - Chen, S-H., "Small Angle Neutron Scattering Studies of Strongly Interacting Ionic Micellae Systems."
- M.I.T. Tokyo Office of the Industrial Liaison Program Seminar, Tokyo, Japan, May 27, 1986
 - Chen, S-H., "Small Angle Neutron Scattering Studies of Solubilization of Proteins in Microemulsions."
- 30th International Symposium on Electron, Ion, and Photon Beams, Boston, Massachusetts, May 27-30, 1986
 - Chou, S.Y., H.I. Smith, and D.A. Antoniadis, "Drain Current Oscillations in Sub-100-nm Channel Si MOSFET's Fabricated Using X-Ray Lithography."
 - Melngailis, J., D.J. Ehrlich, S.W. Pang, and J. Randall, "Cermet as an Inhorganic Resist for Ion Litography."
- Mitsubishi Kasei Institute for Life Sciences Colloquium, Tokyo, Japan, May 28, 1986
 - Chen, S.-H., "The Structure and Frontal Dimension of Protein-Detergent Complexes."

SAI DECEMBER O PRINCIPARIO SERVICIO DE PATRICIO A CONTRA CONTRACA DISTINIO DE SAINON D

June 1986

- S.P.I.E. 1986 Quebec International Symposium on Optical and Optoelectronic Applied Sciences and Engineering, Quebec City, Canada, June 2-6, 1986
 - Papers in S.P.I.E. 663 (1986):
 - Shapiro, J.H., R.W. Reinhold, and D. Park, "Performance Analyses for Peak-Detecting Laser Radars," pp. 38-56.
- Conference on Academic Research: National and International Perspectives, University of Pavia, Pavia, Italy, June 4-6, 1986
 - Coppi, B., "Academic Research in the International Context."
- 1986 National Radio Science Meeting, International Union of Radio Science, Philadelphia, Pennsylvania, June 8-13, 1986
 - Abstracts in Program, and Abstracts:
 - Borgeaud, M., R.T. Shin, and J.A. Kong, "Theoretical Modeling of Polarimetric Radar Clutter," p. 50.
 - Gaylor, D., T.M. Habashy, and J.A. Kong, "Fields Due to a Dipole Antenna Mounted on Top of a Conducting Pad of Finite Extent in a Layered Stratified Medium," p. 38.
 - Lee, C.F., and R.T. Shin, "Radar Cross Section Prediction Using a Hybrid Method," p. 194.
 - Lee, J.K., and J.A. Kong, "Modified Radiative Transfer Theory for Two-Layer Anisotropic Random Medium," p. 47.
 - Poh, S.Y., J.A. Kong, and M.J. Tsuk, "Transient Response of Dipole Antennas on Two-Layer Media," p. 272.
 - Rogers, S.W., and R.T. Shin, "Radar Cross Section Prediction for Coated Perfect Conductors with Arbitrary Geometries," p. 191.
- Speech Research Symposium, Trenton, New Jersey, June 9-11, 1986
 - Griffin, D.W., and J.S. Lim, "A High Quality 8KBPS Speech Analysis/Synthesis System."
- 14th International Conference on Quantum Electronics, San Francisco, California, June 9-13, 1986
 - Papers in Technical Digest:
 - Gould, P.L., G.A. Ruffo, P.J. Martin, J.L. Picque, R.E. Stouer, and D.E. Pritchard, "Experimental Study of Light Forces on Atoms: Diffraction and Diffusion," p. 224. (invited paper)
 - Ho, S.-T., P. Kumar, and J.H. Shapiro, "Quantum Theory of Nondegenerate Multiwave Mixing."

- Kleppner, D., "Cavity Quantum Electrodynamics," p. 114. (invited paper)
- Lin, W.Z., J.G. Fujimoto, E.P. Ippen, and R.A. Logan, "Femtosecond Studies of Absorption Saturation Dynamics in GaAs," p. 50. (invited paper)
- Maeda, M.W., P. Kumar, and J.H. Shapiro, "Observation of Squeezed Noise Produced by Forward Four-Wave Mixing in Sodium Vapor."
- Shapiro, J.H., M.C. Teich, B.E.A. Saleh, P. Kumar, and G. Saplakoglu, "Theory of Light Detection in the Presence of Feedback."
- Conference on Laser and Electro-Optics, Laser Institute of America, San Francisco, California, June 9-13, 1986
 - Papers in Proceedings:
 - Birngruber, R., C.A. Puliafito, A. Gawande, W.Z. Lin, R.W. Schoenlein and J.G. Fujimoto, "Femtosecond Retinal Injury Study," p. 152. (invited paper)
 - Fujimoto, J.G., "Short Course on Femtosecond Pulse Generation and Measurement." (invited paper)
 - Nakazawa, M., and E.P. Ippen, "Theory of the Synchronously Pumped Fiber Raman Laser," pp. 54-55.
 - Stix, M.S., M.P. Kesler, E.P. Ippen, and P.S. Cross, "Experimental Observations of Subpicosecond Dynamics in GaAlAs Laser Diodes," pp. 264-265.
 - Swanson, E.A., G.L. Abbas, V.W.S. Chan, F.G. Walther, and J.G. Fujimoto, "Fast Electronic Beam Steering of the Output Beams of Laser Diode Arrays," pp.78-80.
- 5th Topical Meeting, Optical Society of America, Snowmass, Colorado, June 16-19, 1986
 - Papers in *Ultrafast Phenomena V*, edited by G.R. Fleming and A.E. Siegman. New York: Springer-Verlag, 1986:
 - Farrar, M.R., R.L. Williams, Y.-X. Yan, L-T. Cheng and K.A. Nelson, "Impulsive Stimulated Rayleigh Brillouin and Raman Scattering: Experiments and Theory of Light Scattering Spectroscopy in the Time Domain," pp. 532-535.
 - Lin, W.Z., J.G. Fujimoto, E.P. Ippen, and R.A. Logan, "Ultrafast Carrier Dynamics in GaAs and Al_xga_{1-x}As," pp. 193-196.
 - Schoenlin, R.W., W.Z. Lin, J.G. Fujimoto, and G.L. Eesley, "Femtosecond Studies of Nonequilibrium Electronic Processes in Metals," pp. 261-263.
 - Stix, M.S., R.L. Williams, Y-X.Yan, L-T. Cheng, and K.A. Nelson, "Ultrafast Dynamics in GaAlAs Diodoe Laser Amplifiers," pp. 213-217.
- Workshop on Localized States in Petrohydrolic Bonded Amorphous Solids, Bloomfield Hills, Michigan, June 18-20, 1986
 - Joannopoulos, J.D., and Y. Bar-Yam, "Structure and Electronic States in Disordered Systems."

SECTION OF SECRETARIES OF SECURITY SECTION SECRETARIES SECRETARIES SECURITY SECRETARIES SECRETARIES SECTION SE

168th Meeting, American Astronomical Society, Ames, Iowa, June 22-26, 1986

Abstracts in Bull. Am. Astron. Soc. 18, 2 (1986):

Burke, B.F., J.E. Gunn, J.N. Hewitt, G.I. Langston, C.R. Lawrence, M. Schmidt, D.P. Schneider, and E.L. Turner, "An Apparent Gravitational Lens with 157 Image Separation," p. 674.

Dreher, J.W., and W.J. Welch, "Implosive Star Formation in W51?," p. 684.

Symposium on The Role of Alpha Particles in Magnetically Confined Fusion Plasmas, Aspenasgarden, Goteborg, Sweden, June 24-27, 1986

Coppi, B., "Physics of Compact Ignition Experiments."

ACM/I.E.E.E. Design Automation Conference, Las Vegas, Nevada, June 29-July 2, 1986

Lin, S.L., and J. Allen, "MINPLEX - A Compactor that Minimizes the Bounding Rectangle and the Individual Rectangles in a Layout."

Laser Cooling and Trapping Seminar, Research Institute for Theoretical Physics, Helsinki, Finland, June 30 - July 7, 1986

Pritchard, D.E., and V. Bagnato, "Trapping of Neutral Atoms."

Pritchard, D.E., and P. Martin, "Momentum Transfer from Light."

Pritchard, D.E., and E. Raab, "Trapping of Neutral Atoms."

16th COSPAR '86 Meeting, Toulouse, France, June 30 - July 12, 1986

Rosenkranz, P.W., "Impact of Initial Errors on Numerical Weather."

July 1986

NATO Advanced Scientific Institute Meeting, L'Aquila, Italy, July 7, 1986

Allen, J., "Module Generators for VLSI Design." In Logic Synthesis and Silicon Compilation for VLSI Design, edited by P. Antognetti, G. de Micheli, and A. Sangiovanni. Dordrecht, The Netherlands: Martinus Nijhoff Publishers, 1986.

Gordon Conference on Lasers in Biology and Medicine, Meriden, New Hampshire, July 7-11, 1986

Fujimoto, J.G., "Time Resolved Spectroscopy Techniques and Applications." Puliafito, C., "Ophtalmologic Applications."

30th International Congress of the International Union of Physiological Sciences, San Francisco, California, July 8-11, 1986

Abstracts in Proceedings:

- Freeman, D.M., and T.F. Weiss, "Hydrodynamics Study of Stereociliary Tuft Motion," p. 19.
- Naval Research Laboratory, Washington, D.C., July 16, 1986
 - Smith, H.I., "Submicron Structures Research at M.I.T."
- 12th International Congress on Acoustics, Symposium on Units and Their Representation in Speech Recognition, Montreal, Canada, July 21-22, 1986

Papers in *Proceedings*:

AND DESCRIPTION OF THE PROPERTY OF THE PROPERT

- Huttenlocher, D., and M. Withgott, "On Acoustic Versus Abstract Units of Representation," pp. 61-62.
- Klatt, D.H., "Representation of the First Formant in Speech Recognition and in Models of the Auditory Periphery," pp. 5-7.
- Klatt, D.H., "Models of Phonetic Recognition I: Issues that Arise in Attempting to Specify a Feature-Based Strategy for Speech Recognition," pp. 63-66.
- Seneff, S., "Characterizing Formants Through Straight-Line Approximation without Explicit Formant Tracing," pp. 75-76.
- Stevens, K.N., "Models of Phonetic Recognition II: An Approach to Feature-Based Recognition," pp. 67-68.
- Zue, V.W., "Models of Phonetic Recognition III: The Role of Analysis by Synthesis in Phonetic Recognition," pp. 69-70.
- VLSI CAD Tools and Applications Summer School, Beatenberg, Switzerland, July 21 August 1, 1986
 - Allen, J., "Introduction to VLSI Design."
- 12th International Congress on Acoustics, Toronto, Canada, July 24-31, 1986

Papers in *Proceedings*:

- Bickley, C., B. Lindblom, and L. Roug, "Acoustic Measures of Rhythm in Infants' Babbling or 'All God's Children Got Rhythm'," paper A6-4.
- Cohen, M.H., and J.S. Perkell, "Palatographic and Acoustic Measurements of the Fricative Consonat Pair /s/ and /s/," paper A3-5.
- Holmberg, E.B., R.E. Hillman, and J.S. Perkell, "Relationship Among Parameters of the Glottal Waveform and Intensity Variation for Male and Female Speakers," paper A3-10.
- Perkell, J.S., "Anticipatory Coarticulation of Lip Rounding."
- Perkell, J.S., and C-M. Chiang, "Preliminary Support for a Hybrid Model of Anticipatory Coarticulation," paper A3-6.
- Symposium on Wave Propagation: Remote Sensing and Communications, International Union of Radio Science, Durham, New Hampshire, July 28-August 1, 1986

Papers in *Proceedings*:

- Borgeaud, M., J.A. Kong, and R.T. Shin, "Polarimetric Radar Clutter Modeling with a Two-Layer Anisotropic Random Medium," paper 4.4.1 4.4.4.
- Lin, F.C., and J.A. Kong, "Remote Sensing of Snow-Covered Ice," paper 4.5.1 4.5.4.
- Nghiem, S., M.C. Lee, and J.A. Kong, "Nonlinear Electromagnetic Wave Interactions with the Neutral Atmosphere," paper 2.7.1 2.7.4.
- Sihvola, A., and J.A. Kong, "Effective Permittivity of Dielectric Mixtures," paper 4.6.1 4.6.4.

August 1986

- 16th IUPAP International Conference on Thermodynamics and Statistical Mechanics, Boston, Massachusetts, August 11-15, 1986
 - McKay, S.R., and A.N. Berker, "Phase Diagram, Specific Heat, and Magnetization of the d=3 Random-Field Ising Model."
- SIAM Conference on Linear Algebra in Signals, Systems and Control, Boston, Massachusetts, August 12-14, 1986

Abstract in Final Program:

- Wyatt, J.L., C.A. Zukowski, and P. Penfield, Jr., "Step Response Bounds for a Large-Scale Linear Systems Described by M-Matrices, with VLSI Application," p. A35.
- 1986 International Conference on Solid State Devices and Materials, Tokyo, Japan, August 19-23, 1986

Paper in Proceedings:

Smith, H.I., "A Statistical Analysis of Microlithography," pp. 13-16. (invited paper)

Oji International Seminar on Highly Excited States of Atoms and Molecules, Fuji-Yoshida, Japan, August 20, 1986

Papers in Proceedings:

Kleppner, D., "An Introduction to Cavity Quantum Electrodynamics," pp. 53-59.

September 1986

- 8th International Free Electron Laser Conference, Glasgow, Great Britain, September 1-5, 1986
 - Bekefi, G., J.S. Wurtele, and I.H. Deutsch, "Free Electron Laser Radiation Induced by a Periodic Dielectric Medium."

- Fajans, J., J.S. Wurtele, and G. Bekefi, "Measurements of Amplification, Nonlinear Power Saturation, and Phase Shift (Wave Refractive Index) in a Raman Free-Electron Laser."
- Hartemann, F., and G. Bekefi, "Cerenkov Electrooptical Shutter A New Subnanosecond Relativistic Electron Beam Diagnostic for FEL Applications."
- Second Neil Brice Memorial Symposium on Magnetospheres of the Outer Planets, Iowa City, Iowa, September 1-5, 1986
 - Coppi, B., and P.S. Coppi, "Theoretical Model of Uranus' Bow-Shock."
 - McNutt, R.L. Jr., J.W. Belcher, H.S. Bridge, B. Coppi, A.J. Lazarus, S. Olbert, J.D. Richardson, M.R. Sands, R.S. Selesnick, J. D.Sullivan, R.E. Hartle, K.W. Ogilvie, E.C. Sittler, Jr., F. Bagenal, R.S. Wolff, V.M. Vasyliunas, G.L. Siscoe, C.K. Goertz, and A. Eviatar, "Plasma Observations in the Magnetosphere of Uranus."
- I.E.E. International Symposium on Geoscience and Remote Sensing, Zurich, Switzerland, September 8-11, 1986

Papers in IGARSS '86:

- Borgeaud, M., J.A. Kong, and F.C. Lin, "Microwave Remote Sensing of Snow-Covered Sea Ice," pp. 133-138.
- International Symposium on Modification of the Ionosphere by Powerful Radio Waves, Suzdal, U.S.S.R., September 8-12, 1986

Papers in Proceedings:

- Kuo, S.P., and M.C. Lee, "Parametric Excitation of Whistler Waves by HF Heater," pp. 109-110.
- Lee, M.C., J.A. Kong, and S.P. Kuo, "On the Resonant Ionospheric Heating at the Electron Gyrofrequency," pp. 111-112.
- Lee, M.C., J.A. Kong, and S.P. Kuo, "Enhanced Ionospheric Modifications by the Combined Operation of HF and VLF Heaters," pp. 146-147.
- SEMICON/EAST 1986, Boston, Massachusetts, September 16-18, 1986. (Sponsored by Semiconductor Equipment and Material Institute of California)

Papers in Technical Proceedings:

- Melngailis, J., G.J. Dunn, and W.B. Thompson, "Focused Ion Beam Induced Deposition," pp. 53-61.
- S.P.I.E. Conference on Fiber Optoelectronics and Laser Applications in Science and Engineering, Cambridge, Massachusetts, September 21-26, 1986

Papers in Proceedings:

Covell, M., and J. Lim, "Low Data - Rate Video Conferencing," S.P.I.E. 707, 75 (1986).

- Ezekiel, S., "A Brief History of Fiber Gyros and M.I.T.'s Contributions to Fiber Gyro Development," *S.P.I.E.* 719, 9 (1986).
- International Conference on Microlithography and Related Microelectronic Technologies, Interlaken, Switzerland, September 23-25, 1986
 - Plotnik, I., M. Porter, M. Toth, S. Akhtar, and H.I. Smith, "Ion-Implant Compensation of Tensile Stress in Tungsten Absorbed for Low Distortion X-Ray Masks."
- 13th International Symposium on Gallium Arsenide and Related Compounds, Las Vegas, Nevada, September 28 October 1, 1986

Abstract in Proceedings:

Chou, Y., C. Lam, D.A. Antoniadis, H.I. Smith, and C.G. Fonstad, "Characterization of Modulation-Doped FET's Using the Shubnikov-de Haas Oscillations," pp. 40-41.

October 1986

1986 Conference on Quantum Optics, European Physical Society, Florence, Italy, October 3, 1986

Coppi, B., "Advances in the Physics of Thermonuclear Plasmas."

Materials Week '86, Lake Buena Vista, Florida, October 4-9, 1986

Abstracts in Final Program:

Melngailis, J., "Focused Ion Beam Fabrication," p. 30.

1986 International Symposium on Information Theory, University of Michigan, Ann Arbor, Michigan, October 6-9, 1986

In Abstracts of Papers:

Shapiro, J.H., "Squeezed State Photodetection." (invited paper)

- 1986 I.E.E.E. International Conference on Computer Design, Port Chester, New York, October 6-9, 1986
 - Chu, T-A., and L.A. Glasser, "Synthesis of Self-timed Control Circuits from Graphs: an Example."
- 1986 U.S. Workshop on the Physics and Chemistry of Mercury Cadmium Tellurite, Dallas, Texas, October 7-9, 1986
 - Yuen, S.Y., P.A. Wolff, P. Becla, and D. Nelson, "Free Carrier Spin-Induced Faraday Rotation in HgCdTe and HgMnTe."

- Plasma Physics Colloquium, University of Maryland, College Park, Maryland, October 13. 1986
 - Coppi, B., "Physics of Ignition Experiments."
- 1986 Annual Meeting, Optical Society of America, Seattle, Washington, October 19-24, 1986
 - Abstracts in Technical Digest:

projection respected interpretary interpretary analysistes

- Fujimoto, J.G., "Short Course on Femtosecond Pulses, Generation and Measurement.'
- Maeda, M.W., P. Kumar, and J.H. Shapiro, "Squeezed States Experiments in Sodium Vapor," p. 55.
- Pritchard, D.E., C.E. Wieman, E.L. Raab, R.N. Watts, V. Bagnato, and R. Stoner, "Light Trapps Using Spontaneous Forces."
- Shao, M., M.M. Colavita, D. Staelin, and K. Johnston, "Initial Operating Characteristics of the Mark III Stellar Interferometer," p. 36.
- Wong, N.C., and J.L. Hall, "High Performance Laser Frequency Stabilization Using an External Electrooptic Phase Shifter," p. 138.
- Digital Signal Processing Workshop, Chatham, Massachusetts, October 19-22, 1986
 - Griffin, D.W., and J.S. Lim, "A High Quality 8 KBPS Speech Coding System."
 - Mook, D.R., S. Lang, T. Joo, W.P. Dove, and J. Smith, "A KBSP Approach to Sensor Fusion and Situation Assessment."
 - Myers, C.S. and W.P. Dove, "Signal Representation and Manipulation in Computers."
 - Seneff, S., "Line-Formants: a 2 1/2 D Sketch of a Synchrony Spectrogram."
 - Silva, J.A., and A.V. Oppenheim, "Reconstruction of Undersampled Periodic Signals."
- 33rd National Symposium of the American Vacuum Society, Baltimore, Maryland, October 27-31, 1986
 - Coppi, B., "Physics of Compact Ignition Experiments." (invited paper)
 - Coppi, B., "Advance Ignition Experiment and Plasma Interaction."
- M.I.T. Physics/Industry Forum on Physics in One and Two Dimensions, Cambridge, Massachusetts, October 29-30, 1986
 - Smith, H.I., "Fabrication and Physics of Very Short, Very Narrow and Planar Superlattice MOSFET's."
- 40th Anniversary Symposium, Research Laboratory of Electronics, M.I.T., Cambridge, Massachusetts, October 31, 1986

- Burke, B.F., "Radio Astronomy: Fourier Transforming the Universe."
- Coppi, B. "Plasmas in Heaven and on Earth: Space Physics and Fusion Research."
- Gomory, R.E., "Perspective on University Research and How It Relates to Industry."
- Ippen, E.P., "High-Speed Optics."
- Kleppner, D., "Atomic Physics and the Frontiers of High Precision."
- Lee, P., "Quantum Transport and Fluctuations in Small Devices."
- Oppenheim, A.V., "Signal Processing and Representation."
- Packard, D., "Remarks by David Packard at the 40th Anniversary Symposium."
- Smith, H.I., "Submicron Structures Technology and Future Electronics."
- Stevens, K.N., "Understanding the Links Between Language, Speech and Hearing: Problems and Progress."

November 1986

- Laser '86, Ninth International Conference on Lasers and Applications, Orlando, Florida, November 3-7, 1986
 - Lin, W.Z., J.G. Fujimoto, E.P. Ippen, and R.A. Logan, "Femtosecond Carrier Dynamics in GaAs and Al_x Ga_{1-x} s." (invited paper)
 - Nelson, K.A., M.R. Farrar, R.L. Williams, and Y.X. Yan, "Impulsive Stimulated Scattering: Real-Time Observations of Coherent Vibrational Motion and Vibrationally-Induced Rearrangements."
- 1986 Fall Meeting of the Division of Plasma Physics, American Physical Society, Baltimore, Maryland, November 3-7, 1986
 - Abstracts in Bull. Am. Phys. Soc. 31, 9 (1986):
 - Bekefi, G., J.S. Wurtele, and I.H. Deutsch, "Free Electron Laser Radiation Induced by a Periodic Dielectric Medium," p. 1481.
 - Benjamin, R.A., C.L. Fiore, J.L. Terry, S.M. Wolfe, S. McDermott, J.Moody, M. Porkolab, T. Shepard, Y. Takase, and H.W. Moos, "Ion Temperature Profile Measurements in Alcator C Plasmas," p. 1587.
 - Berkman, V.J., M.P. J. Gaudreau, M.S. Shuster, R.P. Torti, and S. F. Horne, "The Tara Neutral Beam Fault Detection and Control System," p. 1425.
 - Bonoli, P.T., and M. Porkolab, "Modelling of Lower Hybrid Current Drive in the Presence of Fusion Generated Alpha-Particles," p. 1521.
 - Brau, K., S. Golovato, J. Irby, B. Lane, J. Kesner, R.S. Post, D.K. Smith, and E. Sevillano, "Hot Electron Anchor Stabilization Studies," p. 1423.
 - Casey, J.A., B. Lane, J. Kesner, and R.S. Post, "The Tara Divertor as a Halo Generator," p. 1424.

- Chen, K-I., S.C. Luckhardt, S.M. Bentivegna, J.P. Berrettini, M. Porkolab, and J.N.S. Villasenor, "Particle Transport Study During Versator II LHCD Experiments," p. 1614.
- Chen, X., D.L. Smatlak, B. Lane, R.S. Post, R.C. Garner, S. Hokin, and D.L. Goodman, "Hollow Baseball-Seam Hot-Electron Plasma Equilibrium in the Constance B Mirror Experiment," p. 1426.
- Cohen, B.I., and M. Porkolab, "Parametric Instabilities Associated with Intense Pulsed ECRH," p. 1516.
- Colborn, J.A., R.R. Parker, K-I. Chen, S.C. Luckhardt, and M. Porkolab, "A Slotted-Waveguide Fast-Wave Coupler on Versator II," p. 1614.
- Coleman, J.W., J.D. Sullivan, R.F. Vieira, D.A. Moe, J.J. Zielinski, G.A. Hallock, and N.A. Zaidi, "The Tara Heavy Ion Beam Probe: Calibration and Initial Operations," p. 1425.
- Coppi, B., "Compact Ignition Experiments: State of the Art," p. 1504.
- Coppi, P.S., and B. Coppi, "Theoretical Model of Uranus' Bow-Shock," p. 1532.
- Daley, K.F., E.S. Marmar, J.L. Terry, R. Walling, and B. Whitten, "X-ray and VUV Observations of Neon-like Krypton from the Alcator C Tokamak," p. 1588.
- Detregiache, P., B. Coppi, and F. Pegoraro, "Reconnection in High Temperature Plasmas," p. 1436.
- Englade, R., "1 1/2 D Simulation of an Ignitor Device," p. 1565.
- Fajans, J., G. Bekefi, and B. Lax, "Experimental Study of the Collective (Raman) Free Electron Laser," p. 1555.
- Fajans, J., J.S. Wurtele, G. Bekefi, D.S. Knowles, and K. Xu, "Measurements of Amplification, Nonlinear Power Saturation, and Phase Shift (Wave Refrective Index) in Raman Free-Electron Laser Amplifier," p. 1481.
- Farish, T.J., and R.S. Post, "A Magnesium Vapor Jet Neutralizer," p. 1425.
- Fiore, C.L., F.S. McDermott, J.D. Moody, T.D. Shepard, and M. Porkolab, "Results of Fast Neutral and Neutron Measurements on Alcator C ICRF Injected Discharges," p. 1587.
- Francis, G., and A. Bers, "Coupled Mode Instabilities in Inhomogeneous Plasmas," p. 1605.
- Fuchs, V., M.M. Shoucri, C.N. Lashmore-Davis, and A. Bers, "Relativistic Treatment of Lower Hybrid Current Drive with Wide Spectra," p. 1423.
- Gaudreau, M.P.J., J. Tarrh, R.S. Post, D.K. Smith, P. Thomas, V. Berkman, K. George, and W. Stein, "The Tara Device and Operation," p. 1425)
- Gerver, M.J., K. Brau, J. Kesner, B. Lane, Y.T. Lau, and G. Shuy, "Drakon Equilibrium and Transport Studies," p. 1391.
- Golovato, S.N., D.K. Smith, K. Brau, J. Casey, W. Guss, S. Horne, J. Irby, K. Kesner, B. Lane, R. Meyer, R.S. Post, E. Sevillano, J. Sullivan and R. Torti, "ICRF Effects in the Tara Tandem Mirror," p. 1423.
- Gomez, C.C., M. Greenwald, S.M. Wolfe, and I.H. Hutchinson, "Transient Electron Temperature Relaxation During Pellet Injection in Alcator C," p. 1588.

- Goodman, D.L., R.S. Post, D.L. Smatlak, and D.K. Smith, "Ion Heating and Transport in the Constance B Mirror Experiment," p. 1426.
- Goodrich, R.T., and G.W. Shuy, "Neutral Transport in the Tara Center Cell with a Magnetic Divertor," p. 1424.
- Greenwald, M., M. Foord, C. Gomez, T. Petrasso, J. Terry, and S. Wolfe, "A Regime of Improved Particle and Energy Confinement Following Pellet Injection in the Alcator C Tokamak," p. 1588.

CONTRACTOR OF THE PARTY OF THE

- Guss, W.C., S.Golovato, S.F. Horne, J.H. Irby, J. Kesner, R.S. Post, E. Sevillano, D.K. Smith, R.P. Torti, X.Z. Yao, and M.E. Mauel, "Reduced End Losses During ECRH on Tara," p. 1423.
- Gwinn, D., P. Bonoli, M. Greenwald, I. Hutchinson, B. Lipschultz, E. Marmar, D.B. Montgomery, R. Parker, R. Pillsbury, M. Porkolab, J. Ramos, J. Schultz, D. Sigmar, R. Thome, and S. Wolfe, "Alcator C-MOD: A Compact High Performance Tokamak," p. 1589.
- Hartemann, F., and G. Bekefi, "Cerenkov-Electrooptic Shutter A Subnanosecond Intense, Relativistic Electron Beam Diagnostic," p. 1431.
- Hartemann, F., G.L. Johnston, G. Bekefi, and R.C. Davidson, "Two-Dimensional Fluid Model of the Cross-Field Free Electron Laser for Resonance Operation," p. 1540.
- Hayes, M.A., K-I. Chen, S.C. Luckhardt, P.T. Bonoli, M. Porkolab, and D. Sibelius, "RF Prober Measurements of Lower-Hybrid Waves in the Edge Region of the Versator II Tokamak and Comparison with Theory," p. 1614.
- Hokin, S.A., R.S. Post, and D.L. Smatlak, "Velocity-Space Diffusion of Super-Adiabatic Electrons," p. 1426.
- Horne, S.F., R.P. Torti, K. Brau, J.A. Kasey, J. Coleman, M. Gaudreau, S.N. Golovato, W.C. Guss, J. Irby, J. Kesner, B. Lane, L. Pocs, R.S. Post, E. Sevillano, D.K. Smith, J.D. Sullivan, and X.Z. Yao, "Tara Neutral Beam Injection Results," p. 1423.
- Humphreys, D.A., and I.H. Hutchinson, "Analysis of Vertical Stability in Alcator C-MOD," p. 1590.
- Hutchinson, I.H., "Ohmic Ignition What is Required?," p. 1565.
- Irby, J., K. Brau, J. Casey, S.N. Golovato, W. Guss, S. Horne, J. Kesner, B. Lane, R. Myer, R.S. Post, E. Sevillano, J. Sullivan, an R. Torti, "M-1 Fluctuations in the Tara Tandem Mirror Experiment," p. 1423.
- Kato, C., and I.H. Hutchinson, "Measurements of Polarized Electron Cyclotron Emission from Alcator C," p. 1589.
- Kirkpatrick, D.A., F. Hartemann, G. Bekefi, and A. Berg, "Time Resolved Emittance Measurements from a Field Emission Electron Gun," p. 1431.
- Knowlton, S., M. Porkolab, J. Squire, Y. Takase, S. Texter, P. Bonoli, and S. McDermott, "Radial Diffusion of Energetic Electron Generated by Lower Hybrid Waves in Alcator C," p. 1587.
- Kupfer, K., A. Bers, and A.K. Ram, "The Cups Map in the Complex-Frequency Plane for Absolute Instabilities," p. 1402.

- LaBombard, B., and B. Lipschultz, "Scaling of Scrapeoff Layer Paramenters in the Alcator-C Tokamak," p. 1589.
- Lane, B., J. Kesner, R.S. Post, and J.A. Casey, "Stabilization of Interchange Fluctuations by the Tara Magnetic Divertor," p. 1424.
- Lashmore-Davies, C.N., G. Francis, A.K. Ram, A. Bers, and V. Fuchs, "Analytic Model for Minority Heating in ICRF," p. 1420.
- Lee, M.C., and S.P. Kuo, "Magnetic Field Generation Through the Stimulated Scattering Instability of Lower Hybrid Waves," p. 1402.
- Luckhardt, S.C., K-I. Chen, R.D. Kaplan, M. Porkolab, and J.S. Squire, "Initial Electron Cyclotron Heating Experiments on the Versator II Tokamak," p. 1614.
- Machuzak, J.S., P. Woskoboinikow, W.J. Muiligan, D.R. Cohn, M. Gerver, W.C. Guss, R.S. Post, J.D. Sullivan, and R.J. Temkin, "137 GHz Gyrotron Plasma Fluctuation Scattering and Electron Cyclotron Emission Diagnostics in the Tara Plug," p. 1425.
- Manning, H.L., J.L. Terry, C.L. Fiore, E.S. Marmar, S. McDermott, J.E. Rice, S.M. Wolfe, R.D. Benjamin, J. Moody, M. Porkolab, T. Shepard, and Y. Takase, "Observations of Increases in Global Particle and Central Impurity Confinement Time with Ion Bernstein Wave Injection in Alcator C Plasmas," p. 1587.
- Marmar, E.S., M. Greenwald, and J.L. Terry, "A Novel Technique for Current Density Profile Measurement in Tokamaks: Polarization Angle of Zeeman Components from Neon-Doped Deuterium Pellets," p. 1588.
- Migliuolo, S., "Finite- β Ion Temperature Gradient Instability in Sheared Magnetic Fields," p. 1606.
- Moody, J.D., C. Fiore, F.S. McDermott, M. Porkolab, Y. Takase, and the Alcator Group, "Ion Bernstein Wave Heating Experiments on the Alcator C Tokamak," p. 1586.
- Moran, T.G., and J. Irby, "Atomic and Molecular Hydrogen Emission in the Tara Tandem Mirror Experiment," p. 1424.
- Myer, R.C., S. Golovato, and D.K. Smith, "Kinetic Effects in Tandem Mirror ICRH Experiments," p. 1425.
- Parker, R.R., I. H. Hutchinson, S. Knowlton, B. Lipschultz, and S. McDermott. "Simultaneous Plasma Current and Toroidal Field Ramp-Up Experiments on Alcator C," p. 1589.
- Pegoraro, F., B. Coppi, and Y.K. Pu, "Possible Candidate Microinstability for Anomalous Electron Transport," p. 1495.
- Petrasso, R.D., J. Hopf, K.W. Wenzel, D.J. Sigmar, J.L. Terry, and M. Greenwald, "Evidence for a Sign Change in the Convective Velocity," p. 1588.
- Porcelli, F., B. Coppi, and S. Migliuolo, "Excitation of m° = 1 Modes by Circulating Energetic Particles," p. 1620.
- Porcelli, F., and L.E. Sugiyama, "Non-monotonic Current Density Profiles and mo = 1 Modes," p. 1436.
- Pribyl, P.A., "Variation of Magnetic Energy During Sawteeth," p. 1589.
- Ram, A.K., and A. Bers, "Intense Electron Heating by ICRF Waves," p. 1420.

- Rice, J.E., and E.S. Marmar, "Observation of Poloidally Asymmetric Brightness Profiles of Argon Satellites from the Alcator C Tokamak," p. 1589.
- Shepard, T.D., C.L. Fiore, S.F. Knowlton, F.S. McDermott, R.R. Parker, M. Porkolab, and Y. Takase, "Fast Wave ICRF Heating Experiments on the Alcator C Tokamak," p. 1586.
- Shuy, G.W., J. Kesner, C.W. Lee, and B. Boghasian, "Tandem Mirror End Cell Physics Model," p. 1427.
- Squire, J., P. Bonoli, S. Knowlton, M. Porkolab, Y. Takase, and S. Texter, "Modelling of Suprathermal Electron Energy Transport During Lower Hybrid Current Drive in Alcator C," p. 1588.
- Sugiyama, L., and J. Martinelli, "SawteethTransport and Energy Confinement in Ohmic Plasmas," p. 1450.
- Sullivan, J.D., W.C. Guss, S.N. Golovato, J.H. Irby, R.S. Post, E. Sevillano, D.K. Smith, J.S. Machuzak, P.Woskoboinikow, S. Hiroe, F. H. Seguin, and R.J. Schneider, "Electron Parameters in the Plug and Barrier of Tara," p. 1424.
- Takase, Y., C. Fiore, S. McDermott, J. Moody, M. Porkolab, and J. Squire, "CO₂ Scattering from Ion Bernstein Waves in Alcator C," p. 1587.
- Terry, J.L., E.S. Marmar, J.E. Rice, B.L. Whitten, and R. Walling, "Intensities of the 3p to 3s Transitions in Ne-like Fe," p. 1588.
- Tetreault, D., "Turbulent Relaxation in Tokamaks and RFP's," p. 1604.
- Torti, R.P., S.F. Horne, L.Pocs, K. Brau, J.A. Casey, J. Coleman, M. Gaudreau, S.N. Golovato, W.C. Guss, J. Irby, J. Kesner, B. Lane, R.S. Post, E. Sevillano, D.K. Smith, J. Sullivan, and X.Z. Yao, "Gas Effects on Tara Axicell Operation," p. 1424.
- Villasenor, J.N., M. Porkolab, K-I. Chen, and S.C. Luckhardt, "A Comparison of Parametric Decay Spectra During 800 MHz and 2.45 GHz Current Drive in the Versator II Tokamak," p. 1613.
- Wan, A.S., B. Lipschultz, S. McDermott, T.D. Shepard, J.L. Terry, H.L. Manning, R.R. Parker, M. Porkolab, and T.F. Yang, "The Eff e ct of ICRF on the Alcator C Scrape-off Layer Plasma," p. 1587.
- Wolfe, S.M., C. Fiore, J. Terry, S. Knowlton, S. McDermott, J. Moody, M. Porkolab, and Y. Takasa, "Transport Analysis of Alcator C Discharges with Ion Bernstein Wave Injection," p. 1587.
- Yao, X.Z., J.A. Casey, S. Golovato, W.C. Guss, J.H. Irby, J.S. Machuzak, R.C. Myer, J.D. Sullivan, E. Sevillano, and M.E. Mauel, "Tara Axicell Electron Power Balance," p. 1423.
- Zielinski, J.J., G.A. Hallock, N.A. Zaidi, J.W. Coleman, J.D. Sullivan, D.A. Moe, and R.F. Vieira, "Space Potential Measurements on Tara Using a Heavy Ion Beam Probe," p. 1425.
- I.E.E. 1986 Workshop on VLSI Signal Processing, University of Southern California, Los Angeles, California, November 5-7, 1986

- Allen, J., "Plenary Address: the Design of High-Performance Digital Signal Processing Systems."
- 1986 Asilomar Conference on Signal Systems and Computers, Pacific Grove, California, November 9-12, 1986
 - Oppenheim, A.V., "Numerical and Symbolic Representation."
- I.E.E.E. International Conference on Computer-Aided Design, Santa Clara, California, November 11-13, 1986
 - Papers in ICCAD-86:
 - Hohol, T., and L.A. Glasser, "RELIC: A Reliability Simulator for Integrated Circuits," pp. 517-520.
- 11th International Conference on Plasma Physics and Controlled Nuclear Fusion Research, Kyoto, Japan, November 13-20, 1986
 - Coppi, B., A. Airoldi, A. Angelini, G. Bonizzoni, G. Cenacchi, A. DeLuca, C. Ferro, S. Francesio, A. Koch, L. Lanzavecchia, J. Rauch, G. Rubinacci, D. Scovenna, P. H. Titus, and G. Volta, "Advances in the Design of Compact Ignition Experiments."
 - Coppi, B., R. Englade, S. Migliuolo, and L.E. Sugiyama, "Ignition Physics Processes Compact Experiments."
- Seminar on the Horizons of Neurobiology, State University of New York, Buffalo, New York, November 25, 1986
 - Weiss, T.F., "Origins of Mechanical Frequency Selectivity in the Ear." (invited paper)
- First Australian Conference on Speech, Science and Technology, Australian National University, Canberra, Australia, November 25-26, 1986
 - Papers in *Proceedings*:
 - Glass, J.R., and V.W. Zue, "Signal Representation for Acoustic Segmentation," pp. 124-129.
- Invited Presentation, University of Kushu, Fukuoka, Japan, November 28, 1986
 - Coppi, B., "Physics and Technology of Compact Ignition Experiments."

December 1986

Material Research Society Meeting, Symposium A, Boston, Massachusetts, December 1-6, 1986

Papers in Proceedings:

Atwater, H.A., "Ion Beam Enhanced Grain Growth in Thin Films."

International Electron Device Meeting, Los Angeles, California, December 7-10, 1986

Papers in IEDM '86:

Towe E., and C.G. Fonstad, "Mixed-Mode Plane-Locked Quantum Well Laser Array," pp. 626-629.

112th Meeting of the Acoustical Society of America, Anaheim, California, December 8-12, 1986

Abstracts in J. Acoust. Soc. Am. 80, Suppl. 1 (1986):

Braida, L.D., M.A. Picheny, J.R. Cohen, W.M. Rabinowitz, and J.S. Perkell, "Use of Articulatory Signals in Automatic Speech Recognition," p. S18.

Bustamante, D.K., and L.D. Braida, "Wideband Compression and Spectral Sharpening for Hearing-Impaired Listeners," p. S12.

Corbett, R., P.M. Zurek, N.I. Durlach, and W.M. Rabinowitz, "Filtering Competing Messages to Enhance Mutual Intelligibility," p. S77.

Delgutte, B., "Intensity Discriminationa: Relation of Auditory-Nerve Activity to Psychophysical Performance," p. S48.

Goldberg, R., N.A. MacMillan, and L.D. Braida, "Basic Sensitivity and Context Memory on Two-Consonant Continua," p. S124.

Hawkins, S., and K.N. Stevens, "Perceptual Basis for the Compact-Diffuse Distinction for Consonants," p. S124.

Klatt, D.H., "Detailed Spectral Analysis of a Female Voice," p. S79.

Payton, K.L., "Comparison of Simulated Peripheral Auditory Responses to Vowels in Noise with Neural Data," p. S75.

Peterson, P.M., "Using Multiple Microphones and LMS Adaptive Beamforming to Reduce Interference in Hearing Aids from Competing Talkers in Reverberant Rooms," p. S31.

Peterson, P.M., and J.A. Frisbie, "ISPUD an Interactive Environment for Signal Processing on a VAX Computer," p. S31

Randolph, M.A., and V.W. Zue, "The Influence of Phonetic Context on the Acoustical Properties of Stops," p. S95

Uchanski, R.M., L.D. Braida, N.I. Durlach, and C.M. Reed, "The Perception of Temporally-Modified Conversational and Clear Speech by Hearing-Impaired Listeners," p. S78.

Fusion Day, University of Turin, Turin, Italy, December 13, 1986

Coppi, B., "Nuclear Fusion: Scientific and Technological Incentives."

29.2 Journal Papers Published

- Bagnato, V., D.E. Pritchard, and D. Kleppner, "Bose-Einstein Condensation in an External Potential," Phys. Rev. A 35, 10, 4354 (1987).
- Bain, I.L., and L.A. Glasser, "Methodology Verification of Hierarchically Described VLSI Circuits," I.E.E.E. Trans. *CAD-6* 1, 111 (1987).
- Bekefi, G., R.E. Shefer, and W.W. Destler, "Millimeter Wave Radiation from a Rotating Electron Ring Subjected to an Azimuthally Periodic Wiggler Magnetic Field," Nucl. Instrum. Meth. Phys. Res. A250 352 (1986).
- Bekefi, G., R.E. Shefer, and S.C. Tasker, "Beam Brightness from a Relativistic Field-Emission Diode with a Velvet Covered Cathode," Nucl. Instrum. Meth. Phys. Res. A250, 91 (1986).
- Bekefi, G., J.S. Wurtele, and I.H. Deutsch, "Free Electron Laser Radiation Induced by a Periodic Dielectric Medium," Phys. Rev. B 34, 2, 1228 (1986).
- Bell, D.A., H.F. Hess, G.P. Kochanski, S. Buchman, L. Pollack, Y.M. Xiao, D. Kleppner, and T.J. Greytack, "Relaxation and Recombination in Spin-Polarized Atomic Hydrogen," Phys. Rev. B *34*, 11, 7670 (1986).
- Bennett, C.L., C.R. Lawrence, B.F. Burke, J.N. Hewitt, and J. Mahoney, "The M.I.T. Green Bank (MG) 5 GHz Survey," Astrophys. J. Suppl. 61, 1 (1986).
- Berman, R.H., T.H. Dupree, and D.J. Tetreault, "Growth of Nonlinear Intermittent Fluctuations in Linearly Stable and Unstable Simulation Plasma," Phys. Fluids 29, 9, 2860 (1986).
- Bickley, C.A., and K.N. Stevens, "Effects of a Vocal-Tract Constriction on the Glottal Source: Experimental and Modelling Studies," J. Phonetics 14, 373 (1986).
- Birgeneau, R.J., and P.M. Horn, "Two Dimensional Rare Gas Solids," Science 232, 329 (1986).
- Borgeaud, M., R.T. Shin, and J.A. Kong, "Theoretical Models for Polarimetric Radar Clutter," J. Electromag. Waves Appl. 1, 1, 73 (1987).
- Bridge, H.S., J.W. Belcher, B. Coppi, A.J. Lazarus, R.L. McNutt, S. Olbert, J.D. Richardson, M.R. Sands, R.S. Selesnick, J.D. Sullivan, R.E. Hartle, K.W. Ogilvie, E.C. Sittler, Jr., F. Bagenal, R.S. Wolff, V.M. Vasyliunas, G.L. Siscoe, C.K. Goertz, and A. Eviatar, "Plasma Observations Near Uranus: Initial Results from Voyager 2," Science 233, 89 (1986).
- Brou, P., T.R. Sciascia, L. Linden, and J.Y. Lettvin, "The Colors of Things," Sci. Am. 254, 9, 84 (1986).
- Burke, B.F., "Detection of Planetary Systems and the Search for Evidence of Life," Nature 322, 6077, 340 (1986).
- Caflish, R.G., and D. Blankschtein, "Phase Diagrams of Cubic Systems Under Uniaxial Quadratic Symmetry-Breaking Fields," Phys. Rev. B 34, 1, 250 (1986).

- Chomsky, C., "Analytic Study of the Tadoma Method: Language Abilities of Three Deaf-Blind Subjects," J. Speech Hear. Res. 29, 332 (1986).
- Chou, S.Y., and D.A. Antoniadis, "Relationship Between Measured and Intrinsic Transconductances of FET's," I.E.E.E. Trans. *ED-34*, 2, 448 (1987).
- Coppi, B., S. Cowley, R. Kulsrud, P. Detregiache, and F. Pegoraro, "High-Energy Components and Collective Modes in Thermonuclear Plasmas," Phys. Fluids 29, 12, 4060 (1986).
- Coppi, B., and L. Sugiyama, "Spatial Inhomogeneity and Time-Dependent Processes in Ignition Experiments," Comments on Plas. Phys. Contr. Fusion 10, 1, 43 (1986).
- Curtis, S.R., and A.V. Oppenheim, "Reconstruction of Multidimensional Signals from Zero Crossings," J. Opt. Soc. Am. (Special Issue) 4, 1, 221 (1987).
- Curtis, S.R., S. Shitz, and A.V. Oppenheim, "Reconstruction of Nonperiodic Two-Dimensional Signals from Zero Crossings," I.E.E.E. Trans. *ASSP-35*, 6, 890 (1987).
- DeGennaro, S., L.D. Braida, and N.I. Durlach, "Multichannel Syllabic Compression for Several Impaired Listeners," J. Rehab. Res. Devel. 23, 1, 17 (1986).
- Dupree, T.H., "Growth of Phase Space Holes Near Linear Instability," Phys. Fluids 26, 6, 1813 (1986).
- Dupree, T.H., "Large Amplitude Ion Holes," Phys. Fluids 29, 6, 1820 (1986).
- Durlach, N.I., L.D. Braida, and Y. Ito, "Towards a Model for Discrimination of Broadband Signals," J. Acoust. Soc. Am. 80, 1, 63 (1986).
- Durlach, N.I., and X.D. Pang, "Interaural Magnification," J. Acoust. Soc. Am. 80, 6, 1849 (1986).
- Fajans, J., and G. Bekefi, "Measurements of Amplification and Phase Shift (Wave-Refractive Index) in a Free-Electron Laser," Phys. Fluids 29, 10, 3461 (1986).
- Farrar, C.L., C.M. Reed, Y.Ito, N. I. Durlach, L.A. Delhorne, P.M. Zurek, and L.D. Braida, "Spectral Shape Discrimination. I. Results from Normal-Hearing Listeners for Stationary Broadband Noises," J. Acoust. Soc. Am. 81, 4, 1085 (1987).
- Fujimoto, J.G., and T.K. Yee, "Diagrammatic Density Matrix Theory of Transient Four-Wave Mixing and the Measurement of Transient Phenomena," I.E.E.E. J. QE-22, 8, 1215 (1986).
- Gabriel, M.C., H.A. Haus, and E.P. Ippen, "Thermal Index Changes by Optical Absorption in Group III-V Semiconductor Waveguide," I.E.E.E. J. LT-4, 10, 1482 (1986).
- Garrison, S.M., R.C. Cammarata, C.V. Thompson, and Smith, H.I., "Surface-Energy-Driven Grain Growth During Rapid Thermal Annealing (< 10_s) of Thin Silicon Films." J. Appl. Phys. *61*, 4, 1652 (1987).
- Geiger, G., and J. Lettvin, "Enhancing the Perception of Form in Peripheral Vision," Perception 15, 119 (1986).
- Geiger, G., and J. Lettvin, "Peripheral Vision in Persons with Dyslexia," New England J. Med. 316, 1238 (1987).
- Geis, M.W., H.I. Smith, and C.K. Chen, "Characterization and Entrainment of Subboundaries and Defect Trails in Zone-Melting-Recrystallization Si Films," J. Appl. Phys. 60, 3, 1152 (1986).

- Gu, Q., and J.A. Kong, "Transient Analysis of Single and Coupled Lines with Capacitively-Loaded Junctions," I.E.E.E. Trans. MTT-34, 9, 952, (1986).
- Haus, H.A., "On the Radiation from Point Charges," Am. J. Phys. 54, 12, 1126 (1986).
- Haus, H.A., W.P. Huang, S. Kawakami, and N.A. Whitaker, "Coupled-Mode Theory of Optical Waveguides," I.E.E.E. Trans. *LT-5*, 1, 16 (1987).
- Haus, H.A., and M. Nakazawa, "Theory of the Fiber Raman Soliton Laser," J. Opt. Soc. Am. B 4, 5, 652 (1987).
- Haus, H.A., and Y. Yamamoto, "Theory of Feedback-Generated Squeezed States," Phys. Rev. A 34, 1, 270 (1986).
- Haus, H.A., and Y. Yamamoto, "Quantum Circuit Theory of Phase Sensitive Linear Systems," I.E.E.E. J. *QE-23*, 2, 212 (1987).
- Hizanidis, K., A. Bers, V. Fuchs, and R.A. Cairns, "Analytical Model for the Perpendicular Temperature Enhancement in Lower-Hybrid Current Drive," Phys. Fluids 29, 4, 1331 (1986).
- Ho, S-T., S. Ezekiel, R. Haavisto, and J.J. Danko, "Optical Feedback Phase-Stabilization of a Semiconductor Laser," I.E.E.E. J. LT-4, 3, 312 (1986).
- Ho, S-T., P. Kumar, and J.H. Shapiro, "Vector Field Quantum Model of Degenerate Four-Wave Mixing," Phys. Rev. A 34, 1, 293 (1986).
- Hofmann, W.D., and D.E. Troxel, "Making Progressive Transmission Adaptive," I.E.E.E. Trans. *COM-34*, 8, 806 (1986).
- Houtsma, A.J.M., N.I. Durlach, and D.M. Horowitz, "Comparative Learning of Pitch and Loudness Identification," J. Acoust. Soc. Am. 81, 1, 129 (1987).
- Kleppner, D., "Research in Small Groups," Physics Today, p. 79 (March 1985).
- Kleppner, D., "Atomic Stabilization Through Electronic and Nuclear Polarization," Ann. Phy. Fr. 10, 6, 877 (1985).
- Kleppner, D., "Progress in Applying Stable Atomic Hydrogen Methods to Polarized Proton Sources and Jets," J. Physique Colloque 46, C2-665 (1985).
- Kleppner, D., "Is U.S. Science Slipping from First Place?," Technol. Rev. p. 24 (May/June 1986).
- Kleppner, D., "Manipulating Atoms with Light," Helvetica Physica Acta 59, 717 (1986).
- Koehnke, J., and M.F. Cohen, "Masking Effects in Binaural Detection Interaural Time Discrimination," J. Acoust. Soc. Am. 81, 3, 724 (1987).
- Koehnke, J., H.S. Colburn, and N.I. Durlach, "Performance in Several Binaural-Interaction: Experiments," J. Acoust. Soc. Am. 79, 5, 1558 (1986).
- Kuo, S.P., S.C. Kuo, B.R. Cheo, and M.C. Lee, "Analysis of the Harmonic Gyrotron Traveling Wave Amplifier," Int. J. Infrared Millimeter Waves 7, 4, 635 (1986).
- Kuo, S.P., and M.C. Lee, "Saturation of Cyclotron Maser Instability Driven by an Electron Loss-Cone Distribution," Int. J. Infrared Millimeter Waves 7, 4, 629 (1986).
- Kuznetsov, M., "Coupled Wave Analysis of Multiple Waveguide Systems: The Discrete Harmonic Oscillator," I.E.E.E. J. QE-21, 12, 1893 (1985).

WHITE THE PROPERTY SHOWS SHOWS AND WINDS

- Lawrence, C.R., C.L. Bennett, J.N. Hewitt, G.I. Langston, S.E. Klotz, B.F. Burke, and K.C. Turner, "5 GHBz Radio Structure and Optical Identifications of Sources from the MG Survey. II. Maps and Finding Charts," Astrophys. J. Suppl. 61, 105 (1986).
- Lee, M.C., and S.P. Kuo, "Resonant Electron Diffusion as a Saturation Process of the Synchrotron Maser Instability," J. Plasma Phys. 35, 1, 177 (1986).
- Leong, K.W., and J.H. Shapiro, "Phase and Amplitude Uncertainties in Multimode Heterodyning," Optics Commun. 58, 2, 73 (1986).
- Luckhardt, S.C., K-I. Chen, M.J. Mayberry, M. Porkolab, Y. Terumichi, G. Bekefi, F.S. McDermott, and R. Rohatgi, "Particle Confinement and the Anomalous Doppler Instability During Combined Inductive and Lower-Hybrid Current Drive," Phys. Fluids 29, 6, 1986 (1986).
- Matson, M.D., and L.A. Glasser, "Macromodeling and Optimization of Digital MOS VLSI Circuits," I.E.E.E. Trans. *CAD-5*, 4, 659 (1986).
- Melngailis, J., "Focused Ion Beam Technology and Applications," J. Vac. Sci. Technol. B 5, 2, 469 (1987).
- Migliuolo, S., "The Field Swelling and Mirror Modes: Connection of the Two Instabilities," J. Geophys. Res. 91, A7, 7981 (1986).
- Migliuolo, S., "Finite- β Ion Mixing Mode in Sheared Magnetic Geometry," Phys. Fluids 30, 3, 922 (1987).
- Musicus, B.R., and R.W. Johnson, "Multichannel Relative-Entropy Spectrum Analysis," I.E.E.E. Trans. ASSP-34, 3, 554 (1986).
- Ocko, B.M., R.J. Birgeneau, and J.D. Litster, "Crossover to Tricritical Behavior at the Nematic to Smectic A Transition: an X-Ray Scattering Study," Condensed Matter 62, 487 (1986).
- Perkell, J.S., "Coarticulation Strategies: Preliminary Implications of a Detailed Analysis of Lower Lip Protrusion Movements," Speech Commun. 5, 47 (1986).
- Peterson, P.M., "Simulating the Response of Multiple Microphones to a Single Acoustic Source in a Reverberant Room," J. Acoust. Soc. Am. 80, 5, 1527 (1986).
- Picheny, M.A., N.I. Durlach, and L.D. Braida, "Speaking Clearly for the Hard of Hearing. II. Acoustic Characteristics of Clear and Conversational Speech," J. Speech Hear. Res. 29, 434 (1986).
- Porcelli, F., and S. Migliuolo, "Ion Viscosity Stabilization of Resistive Internal Kink Modes," Phys. Fluids 29, 5, 1741 (1986).
- Prentiss, M.G., and S. Ezekiel, "Influence of Atomic Recoil on the Spectrum of Resonance Fluorescence from a Two-Level Atom," Phys. Rev. A 35, 2, 922 (1987).
- Rappaport, C.M., and F.R. Morgenthaler, "Localized Hyperthermia with Electromagnetic Arrays and the Leaky-Wave Troughguide Applicator," I.E.E.E. Trans. *MTT-34*, 5, 636 (1986)
- Schneider, D.P., J.E. Gunn, E.L. Turner, C.R. Lawrence, J.N. Hewitt, M. Schmidt, and B.F. Burke, "The Third Image, the Redshift of the Lens, and New Components of the Gravitational Lens 2016 + 112," Astron. J. 91, 5, 9917 (1986).
- Smith, H.I., "A Review of Submicron Lithography," Superlatt. Microstruc. 2, 2, 129 (1986).

- Smith, N., "On the Use of Action-Angle Variables for Direct Solution of Classical Non-Reactive 3D (Di) Atom-Diatom Scattering Problems," J. Chem. Phys. 85, 4, 1987 (1986).
- Song, W.S., and L.A. Glasser, "Power Distribution Techniques for VLSI Circuits," I.E.E.E. J. SC-21, 1, 150 (1986).
- Warwick, J.W., D.R. Evans, J.H. Romig, C.B. Sawyer, M.D. Desch, M. L. Kaiser, J.K. Alexander, T.D. Carr, D.H. Staelin, S. Gulkis, R.L. Poynterv, M. Aubier, A. Boischot, Y. Leblanc, A. Lecacheux, B.M. Pedersen, and P. Zarka, "Voyager 2 Radio Observations of Uranus," Science 233, 102 (1986).
- Wengrovitz, M.S., A.V. Oppenheim, and G.V. Frisk, "Reconstruction of Complex-Valued Propagating Wave Field Using the Hilbert-Hankel Transform," J. Opt. Soc. Am. A 4. 1, 247 (1987).
- Wolff, P.A., S.Y. Yuen, and G.A. Thomas, "Nonlinear Optics Near the Metal Insulator Transition," Solid State Commun. 60, 8, 645 (1986).
- Yamamoto, Y., and H.A. Haus, "Preparation, Measurement and Information Capacity of Optical Quantum States," Rev. Mod. Phys. 58, 4, 1001 (1986).
- Zakhor, A., and D. Izraelevitz, "A Note on the Sampling of Zero Crossings of Two-Dirnensional Signals," Proc. I.E.E.E. 74, 9, 1285 (1986).
- Zurek, P.M., "Consequences of Conductive Auditory Impairment for Binaural Hearing," J. Acoust. Soc. Am. 80, 2, 466 (1986).
- Zurek, P.M., and N.I. Durlach, "Masker-Bandwidth Dependence in Homophasic and Antiphasic Tone Detection," J. Acoust. Soc. Am. 81, 2, 459 (1987).

29.3 **Journal Papers Accepted for Publication**

- Bekefi, G., F. Hartemann, and D.A. Kirkpatrick, "Temporal Evolution of Beam Emittance from a Field Emission Electron Gun," J. Appl. Phys.
- Bustamante, D.K., and L.D. Braida, "Principal-Component Amplitude Compression for the Hearing Impaired," J. Acoust. Soc. Am.
- Carilli, C.L., and J.H. van Gorkom, "Discovery of Low Redshift, Neutral Hydrogen Absorption in the Radio Spectrum of PKS 2020-370," Astrophys. J.
- Coppi, B., L. Lanzavecchia, and the Ignitor Design Group, "Compact Ignition Experiments: Physics and Design Issues," Comments on Plas. Phys. Contr. Fusion.
- Dreher, J.W., C.L. Carilli, and R.A. Perley, "The Faraday Rotation of Cygnus A: Magnetic Fields in Cluster Gas," Astrophys J.
- Dubner, A.D., G.M. Shedd, H. Lezec, and J. Melngailis, "Ion Beam Induced Deposition of Gold by Focused and Broad Beam Sources," J. Vac. Sci. Technol. B.
- Fajans, J., and G. Bekefi, "Effect of Electron Beam Temperature on the Gain of a Collective Free Electron Laser," I.E.E.E. J. QE.
- Gould, P.L., G.A. Ruff, P.J. Martin, and D.E. Pritchard, "Preparation of a Single-State Atomic Beam by Optical Pumping and Radiative Deflection," Phys. Rev. A.
- Gu, Q., J.A. Kong, and Y.E. Yang, "Time Domain Analysis of Nonuniformly Coupled Line Systems," J. Electromag. Wave Appl.

- Hewitt, J.N., E.L. Turner, C.R. Lawrence, D.P. Schneider, J.E. Gunn, C.L. Bennett, B.F. Burke, J.H. Mahoney, G.I. Langston, M. Schmidt, J.B. Oke, and J.G. Hoessel, "The Triple Radio Source 0023+171: A Candidate for a Dark Gravitational Lens," Astrophys. J.
- Kaxiras, E., Y. Bar-Yam, J.D. Joannopoulos, and K.C. Pandey, "Ab Initio Theory of Polar Semiconductor Surfaces: I. Methodology and the (2x2) Reconstructions of GaAs(111)," Phys. Rev. B.
- Kaxiras, E., Y. Bar-Yam, J.D. Joannopoulos, and K.C. Pandey, "Ab Initio Theory of Polar Semiconductor Surfaces: II. (2x2) Reconstruction and Related Phase Transitions of GaAs(111)," Phys. Rev. B.
- Klatt, D.H.H., "Review of Text-to-Speech Conversion for English," J. Acoust. Soc. Am.
- Maeda, M.W., P. Kumar, and J.H. Shapiro, "Squeezing Experiments in Sodium Vapor," J. Opt. Soc. Am.
- Palmer, J.E., C.V. Thompson, and H.I. Smith, "Grain Growth and Grain Size Distributions in Thin Germanium Films," J. Appl. Phys.
- Poh, S.Y., and J.A. Kong, "Transient Response of a Vertical Electric Dipole (VED) on a Two-Layer Medium," J. Electromag. Wave Appl.
- Rabe, K.M., and J.D. Joannopoulos, "Structural Properties of GeTe at T=0," Phys. Rev. B.
- Rosenkranz, P.W., "Pressure Broadening of Rotational Bands. II. Water Vapor from 300 to 1100 cm +(-1)," J. Chem. Phys.
- Vlannes, N.P., "Experimental Study of Microwave Magnetostatic Waves in Thin Film LPE-YIG with a New Magnetic Induction Probe," J. Appl. Phys.
- Vlannes, N.P., "Optical Probing of Magnetostatic Forward Volume Waves in Thin Film Yttrium-Iron-Garnett," J. Appl. Phys.
- Wintner, E., D.P. Chen, J. Melngailis, and E.P. Ippen, "Optical Generation and Phase-Sensitive Detection of Surface Acoustic Waves in InP," I.E.E.E. Trans. (Ultrasonics).
- Yin, Y-Z., R-J. Ying, and G. Bekefi, "Generation of Electromagnetic Radiation from a Drifting and Rotating Electron Ring in a Rippled Magnetic Field," I.E.E.E. Trans. (QE).
- Yuen, S.Y., P.A. Wolff, P. Becla, and D. Nelson, "Free Carrier Spin Induced Faraday Rotation in HgCeTe and HgMnTe," J. Vac. Sci. Technol. A.
- Zurek, P.M., and L.A. Delhorne, "Consonant Reception in Noise by Listeners with Mild and Moderate Sensorineural Hearing Impairment," J. Acoust. Soc. Am.

29.4 Letters to the Editor Published

- Brook, J.D., R.J. Birgeneau, K.W. Evans-Lutterodt, J.D. Litster, P.M. Horn, G.B. Stephenson, and A.R. Tajbakhsh, "Orientational and Positional Order in a Tilted Hexatic Liquid Crystal Phase," Phys. Rev. Lett. 57, 1, 98 (1986).
- Burke, B.F., "Detecting Earth-like Planets," Nature 324, 518 (1986).

- Chou, S.Y., D.A. Antoniadis, and H.I. Smith, "Observation of Electron Velocity Overshoot in Sub 100-nm-Channel MOSFETS in Silicon," I.E.E.E. Trans. *EDL-6*, 12, 665 (1985).
- Chou, S.Y., D.A. Antoniadis, H.I. Smith, and M.A. Kastner, "Conductance Fluctuations in Ultra-Short-Channel Si MOSFET's," Solid State Commun. 61, 9, 571 (1987).
- Coppi, B., and F. Porcelli, "Theoretical Model of Fishbone Oscillations in Magnetically Confined Plasmas," Phys. Rev. Lett. 57, 18, 2272 (1986).
- Dagli, N., and C.G. Fonstad, "Microwave Equivalent Circuit Representation of Rectangular Dielectric Waveguides," Appl. Phys. Lett. 49, 6, 308 (1986).
- DeSilvestri, S., J.G. Fujimoto, E.P. Ippen, E.B. Gamble, Jr., L.R. Williams, and K.A. Nelson, "Femtosecond Time-Resolved Measurements of Optic Phonon Dephasing by Impulsive Stimulated Raman Scattering in α -Perylene Crystals from 20 to 300 K," Chem. Phys. Lett. *116*, 2, 1462 (1985).
- Fajans, J., J.S. Wurtele, G. Bekefi, D.S. Knowles, and K. Xu, "Nonlinear Power Saturation and Phase (Wave Refractive Index) in the Collective Free Electron Laser," Phys. Rev. Lett. 57, 3, 579 (1986).
- Feder, M., "Maximum Entropy as a Special Case of the Minimum Description Length Criterion," I.E.E.E. Trans. 17-32, 6, 847 (1986).
- Hartemann, F., and G. Bekefi, "Time Resolved Studies of Intense, Relativistic Electron Beams with a Subnanosecond Cerenkov-Electro-Optic Shutter," Appl. Phys. Lett. 49, 25, 1680 (1986).
- Hess, H.F., G.P. Kochanski, J.M. Doyle, T.J. Greytak, and D. Kleppner, "Spin-Polarized Hydrogen Maser," Phys. Rev. A (Rapid Commun.) 34, 2, 1602 (1986).
- Ho, S-T., P. Kumar, and J.H. Shapiro, "Quantum Theory of Nondegenerate Multiwave Mixing," Phys. Rev. A (Rapid Commun.) 35, 9, 3982 (1987).
- Kaxiras, E., K.C. Pandey, Y. Bar-Yam, and J.D. Joannopoulos, "Role of Chemical Potentials in Surface Reconstruction: A New Model and Phase Transition on GaAs(111)2x2," Phys. Rev. Lett. 56, 26, 2819 (1986).
- Kaxiras, E., Y. Bar-Yam, J.D. Joannopoulos, and K.C. Pandey, "Variable Stoichiometry Surface Reconstructions: New Models for GaAs (111) (2x2) and ($\sqrt{19} \times \sqrt{19}$)," Phys. Rev. Lett. 57, 106 (1986).
- Kim, H-J., and C.V. Thompson, "Compensation of Grain Growth Enhancement in Doped Silicon Films," Appl. Phys. Lett. 48, 6, 399 (1986).
- Lin, W.Z., J.G. Fujimoto, E.P. Ippen, and R.A. Logan, "Femtosecond Carrier Dynamics in GaAs," Appl. Phys. Lett. 50, 3, 124 (1987).
- Maeda, M.W., P. Kumar, and J.H. Shapiro, "Observation of Squeezed Noise Produced via Forward Four-Wave Mixing in Sodium Vapor," Optics Lett. 12, 3, 161 (1987).
- Malvar, H., "Fast Computation of Discrete Cosine Transform Through Fast Hartley Transform," Electron. Lett. 22, 7, 352 (1986).
- Mochrie, S.G.J., A.R. Kortan, P.M. Horn, and R.J. Birgeneau, "Novel Melting Transition in a Two-Dimensional Stripe-Domain System," Phys. Rev. Lett. 58, 7, 690 (1987).
- Musicus, B.R., "Comment on 'Dice, Entropy, and Likelihood' by B. Roy Frieden," Proc. I.E.E.E. 74, 5, 762 (1986).

AND PROPERTY OF SECRECAL SOCIETY OF SECRECAL PROPERTY DESCRIPTION OF SECRECAL PROPERTY OF SECRECAL SEC

- Nakajima, Y., and S. Ezekiel, "Sensitive Determination of the Existence of Higher Order Modes in a Single-Mode Fiber," Optics Lett. 11, 12, 815 (1986).
- Payne, M.C., J.D. Joannopoulos, D.C. Allan, M.P. Teter, and D.H. Vanderbilt, "Molecular Dynamics and *ab initio* Total Energy Calculations," Phys. Rev. Lett. *56*, 4, 2656 (1986).
- Payne, M.C., P.D. Bristowe, and J.D. Joannopoulos, "Ab Initio Determination of the Structure of a Grain Boundary by Simulated Quenching," Phys. Rev. Lett. 58, 13, 1348 (1987).
- Pevtschin, V., and S. Ezekiel, "Investigation of Absolute Stability of Water Vapor Stabilized Semiconductor Laser," Optics Lett. 12, 3, 1724 (1987).
- Schoenlein, R.W., W.Z. Lin, J.G. Fujimoto, and G.L. Eesley, "Femtosecond Studies of Nonequilibrium Electronic Processes in Metals," Phys. Rev. Lett. *58*, 16, 1680 (1987).
- Shedd, G.M., H. Lezec, A.D. Dubner, and J. Melngailis, "Focused Ion Beam Induced Deposition of Gold," Appl. Phys. Lett. 49, 23, 1584 (1986).
- Stix, M.S., M.P. Kesler, and E.P. Ippen, "Observations of Subpicosecond Dynamics in GaAlAs Laser Diodes," Phys. Rev. Lett. 48, 25, 1722 (1986).
- Turner, E.L., D.P. Schneider, B.F. Burke, J.N. Hewitt, G.I. Langston, J.E. Gunn, C.R. Lawrence, and M. Schmidt, "An Apparent Gravitational Lens with an Image Separation of 2.6 arc min," Nature 321, 142 (1986).
- Warren, A.C., D.A. Antoniadis, and H.I. Smith, "Quasi One-Dimensional Conduction in Multiple, Parallel Inversion Lines," Phys. Rev. Lett. 56, 17, 1858 (1986).
- Zarinetchi, F., and S. Ezekiel, "Observation of Lock-in Behavior in a Passive Resonator Gyroscope," Optics Lett. 11, 6, 401 (1986).

29.5 Letters to the Editor Accepted for Publication

- Bagnato, V.S., G.P. Lafyatis, A.G. Martin, E.L. Raab, and D.E. Pritchard, "Continuous Stopping and Trapping of Neutral Atoms," Phys. Rev. Lett.
- Lin, W.Z., J.G. Fujmoto, E.P. Ippen, and R.A. Logan, "Femtosecond Dynamics of Highly Excited Carriers in Al_x Ga_{1-x}As," Appl. Phys. Lett.
- Needels, M., M.C. Payne, and J.D. Joannopoulos, "Ab Initio Molecular Dynamics on the Ge(100) Surface," Phys. Rev. Lett.

29.6 Special Publications

- Berman, R.H., D.J. Tetreault, and T.H. Dupree, "Double Layers in Linearly Stable Plasmas Geophysical Monograph 38," In *Ion Acceleration in the Magnetosphere and Ionosphere*, edited by T. Chang. Washington, D.C.: American Geophysical Union, 1986, pp. 328-333.
- Freeman, D.M., and T.F. Weiss, "On the Role of Fluid Inertia and Viscosity in Stereociliary Tuft Motion: Analysis of Isolated Bodies of Regular Geometry," In *Peripheral Auditory Mechanisms. Lecture Notes in Biomathematics 64*, edited by J.B.

- Allen, J.L. Hall, A. Hubbard, S.T. Neely and A. Tubis. New York: Springer-Verlag, 1986, pp. 147-154.
- Klatt. D.H., "The Problem of Variability in Speech Recognition and in Models of Speech Perception (Chapter 14)." In Variability and Invariance in Speech Processes, edited by J. Perkell and D.H. Klatt. Hillsdale, New Jersey: Lawrence Erlbaum Assoc., 1986, pp. 300-319.
- Pritchard, D.E., "Trapping and Cooling Neutral Atoms," In *Electronic and Atomic Collisions*, edited by D.C. Lorents, W.E. Meyerhof, and J.R. Peterson. Elsevier Science Publishers, 1986, pp. 593-604.
- Pang, X.D., and W.T. Peake, "How Do Contractions of the Stapedius Muscle Alter the Acoustic Properties of the Ear?" In *Peripheral Auditory Mechanisms. Lecture Notes in Biomathematics 64*, edited by J.B. Allen, J.L. Hall, A. Hubbard, S.T. Neely, and A. Tubis. New York: Springer-Verlag, 1986, pp. 36-43.
- Rosenkranz, P.W., K.S. Nathan, and D.H. Staelin, "Use of Two-and Three-Dimensional Spatial Filtering for Inversion of Radiometric Measurements." In *Advances in Remote Sensing Retrieval Methods*, edited by A. Deepak, H.E. Fleming, and M.T. Chahine. Hampton, Virginia: A. Deepak Publishing, 1985, pp. 373-383.
- Rosowski, J.J., L.H. Carney, T.J. Lynch III, and W.T. Peake, "The Effectiveness of External and Middle Ears in Coupling Acoustic Power into the Cochlea." In *Peripheral Auditory Mechanisms. Lecture Notes in Biomathematics 64*, edited by J.B. Allen, J.L. Hall, A. Hubbard, S.T. Neely, and A. Tubis. New York: Springer-Verlag, 1986, pp. 3-12.
- Stevens, K.N., "Speech Production and Acoustic Goals (Chapter 7)." In *The Planning and Production of Speech Monograph*, edited by J.L. Lante r. ASHA Report No. 15. Rockville, Maryland: American Speech-Language-Hearing Association, 1986, pp. 38-42.
- Stevens, K.N., S.J. Keyser, and H. Kawasaki, "Toward a Phonetic and Phonological Theory of Redundant Features (Chapter 20)," In *Invariance and Variability in Speech Processes*, edited by J.S. Perkell and D.H. Klatt. Hillsdale, New Jersey: Lawrence Erlbaum Assoc., 1986, pp. 426-449.

29.7 Reports Published

PRODUCES CONTROL SERVICES CONTROL CONT

These reports may be obtained from the Document Room, 36-412, Research Laboratory of Electronics, Massachusetts Institute of Technology, Cambridge, Massachusetts 02139 at the cost listed. Please include a check made out to M.I.T. R.L.E., and allow six to eight weeks for delivery.

- Allen, J., and R. Birgeneau, eds., R.L.E. Progress Report No. 128. Cambridge, Mass.: M.I.T., 1986. Free.
- Dove, W.P., Knowledge-Based Pitch Detection. RLE TR-518. Cambridge, Mass.: M.I.T., 1986. \$12.00.
- Isnardi, M.A., *Modeling the Television Process*. RLE TR-515. Cambridge, Mass.: M.I.T., 1986. \$15.00.
- Izraelevitz, D., Reconstruction of Two-Dimensional Signals from the Fourier Transform Magnitude. RLE TR-517. Cambridge, Mass.: M.I.T., 1986. \$11.00.

- Malvar, H.S., Optimal Pre-and Post-Filtering in Noisy Sampled-Data Systems. RLE TR-519. Cambridge, Mass., M.I.T., 1986. \$12.00.
- Milios, E.E., Signal Processing and Interpretation Using Multilevel Signal Abstractions. RLE TR-516. Cambridge, Mass.: M.I.T., 1986. \$12.00.
- Myers, C.S., Signal Representation for Symbolic and Numerical Processing. RLE TR-521. Cambridge, Mass., M.I.T., 1986. \$13.00.
- Silva, A.J., Reconstruction of Unsampled Periodic Signals. RLE TR-514. Cambridge, Mass., M.I.T., 1986. \$10.00.
- Ulichney, R.A., *Digital Halftoning and the Physical Reconstruction Function*. RLE TR-520. Cambridge, Mass.: M.I.T., 1986. \$24.00.
- van Hove, P.L., Silhouette-Slice Theorems. RLE TR-522. Cambridge, Mass., M.I.T., 1986. \$14.00.
- Wengrovitz, M.S., The Hilbert-Hankel Transform and Its Application to Shallow Water Ocean Acoustics. RLE TR-513. Cambridge, Mass., M.I.T., 1986. \$25.00.



30.0 Current RLE Personnel

Jonathan Allen, Director Daniel Kleppner, Associate Director

Professors

Jonathan Allen
Dimitri A. Antoniadis
Arthur B. Baggeroer
George Bekefi
Abraham Bers
Robert J. Birgeneau
Amar G. Bose
Louis D. Braida
Bernard E. Burke
Sow-Hsin Chen
Bruno Coppi
Thomas H. Dupree
Shaoul Ezekiel
Clifton G. Fonstad
Lawrence S. Frishkopf

Hermann A. Haus
Erich P. Ippen
John D. Joannopoulos
Marc A. Kastner
Nelson Y.-S. Kiang
John G. King
Daniel Kleppner
Jin Au Kong
Francis F. Lee
Patrick A. Lee
Jerome Y. Lettvin
J. David Litster
Frederic R. Morgenthaler
Alan V. Oppenheim

William T. Peake
Miklos Porkolab
David E. Pritchard
William F. Schreiber
Campbell L. Searle
Jeffrey H. Shapiro
William M. Siebert
Henry I. Smith
David H. Staelin
Kenneth N. Stevens
Donald E. Troxel
Thomas F. Weiss
Peter A. Wolff
Henry J. Zimmermann *

Associate Professors

A. Nihat Berker John W. Dreher Lance A. Glasser

SKI KKISSKI DIDINI MANINE MANINE MANINEN BURKKI DIDINIK PIKIKKO PRIBLES DISINIMA PERKENA PE

Peter L. Hagelstein Jae S. Lim

Jacob K. White John L. Wyatt, Jr.

Assistant Professors

Sylvia T. Ceyer James G. Fujimoto Jeffrey H. Lang Bruce R. Musicus Keith A. Nelson Carl V. Thompson II

Senior Research Scientists

Nathaniel I. Durlach Louis A. Kamentsky Dennis H. Klatt Robert H. Rediker

^{*}Emeritus

Principal Research Scientists and Associates

H. Steven Colburn John J. Guinan, Jr. Stanley C. Luckhardt John Melngailis

Joseph S. Perkell Victor W. Zue

Postdoctoral Associates

Alexander Martin Francesco Porcelli

Elias Towe Beat Zysset

Postdoctoral Fellows

Joseph Ashkenazy Robin Davis Carol Espy-Wilson Kenneth W. Grant

Sharon Manuel Karen Payton

Research Staff

Giovanni Aliberti John W. Barrett James M. Carter Marc Cohen Bertrand Delgutte Lorraine A. Delhorne Donald K. Eddington Ronald C. Englade Edward W. Fitzgerald Dennis M. Freeman

THE PARTIES OF THE PA

David H. Kaufman Min-Chang Lee Ivan Mastovsky Stefano Migliuolo Harry Norris Michael Phillips William M. Rabinowitz Charlotte M. Reed Philip W. Rosenkranz John J. Rosowski Stephanie Seneff Stefanie Shattuck-Hufnagel Linda E. Sugiyama Sue S. Syu Ngai Chuen Wong John Wroclawski Sunny Y.C. Yuen Patrick M. Zurek

Visiting Scientists

Giuseppe Bertin Fielding Brown Manuel V. Cerrillo Stefano Coda Paolo Detragiache Theodore W. Ducas Gad Geiger Rong-shu Gong Keikichi Hirose Janet D. Koehnke
Jack Kotik
Chris Lashmore-Davies
Chaim Leibovitch
Zhuzhen Li
John Makhoul
Paul Mataloni
Shigeru Oho
Alain Priou

Stanley J. Rosenthal Thomas Savarino Bruce Schneider Thomas R. Sciascia Randa Seif Elias Snitzer Wen-ke Wang Kongyi Xu Xiuzhen Yu

Research Affiliates

John S. Barlow Bruce Bernacki Ian S. Boardman Robert M. Brown Mark L. Curby Richard S. Goldhor Philip Hemmer Robert E. Hillman

Eva B. Holmberg Joseph A. Jarrell Haruko Kawasaki John D. Kierstead Harlan Lane Leah S. Larkey John L. Locke Leonard Picard Irving Plotnick Soon Yun Poh Ramdas Ram-Mohan Michael Shao Robert T. Shin Frank J. Stefanov-Wagner David A. Steffens Noriko Suzuki Robert A. Ulichney Akhileswar G. Vaidyanathan Kenneth Wacks Jane Webster

Research Assistants

Gary A. Allen Andrew Alston Erik H. Anderson Kristin K. Anderson Robert C. Armstrong Donald G. Baltus Cyrus S. Bamji Pierino Bonnani Maurice Borgeaud Donald E. Bossi Kevin Boyce Stuart D. Brorson Chrisopher Carilli So Kuen Chan Pin-P. Chang Samuel Conner Christopher Corcoran Michelle M. Covell Vivek Dhawan Andrew D. Dubner Susan Dubois Paul Duchnowski Scott B.C. Dynes Jerrold A. Floro **Gregory Francis** Albin J. Gasiewski **Thomas Gentile** David J. Gladstone James R. Glass Arthur C. Grant Daniel W. Griffin **Keith Groves** Katherine Hall Hsiu Chi Han Stephen M. Hannon **Daniel Harasty** John C. Hardwick Michael Heflin Kristian Helmerson **Douglas Henderson**

Michael L. Heytens

Braden E. Hines Seng-Tiong Ho Andrew W. Howitt Long Hsu Thomas T. Huang Weiping Huang William Huang Barbara J. Hughey Chun-Ho lu Rajeev Jayavant Hong Jeong Roy John Michael Kash Robert Kassel Morris P. Kesler Kelsev M. Key Jean-Fu Kiang **Edward Kim** Richard Kim Douglas A. Kirkpatrick Yao-Ching Ku Charlene Kuo Kenneth Kupfer Michael J. LaGasse Lori F. Lamel Suzanne Lau Check Fu Lee Kin Wai Leong Hong Chung Leung Chungpin Liao Chen-Shi Lin Freeman Lin Fu-Chin Liu Ling-Yi Liu Hai Longworth Michael Machado Peter D. Magill Adam Malamy Peter Martin Steven P. McCormick

Michael McCue

Marianne McGonigal Lynne A. Molter-Orr Son Van Nghiem Scott Paine Jovce Palmer Lily Y. Pang Dongwook Park Patrick Peterson Julien Piot John Pitrelli **Matthew Power** G.N. Srinivasa Prasanna Gill Pratt Jason Puchalla Yikang Pu Hui Meng Quek Eric Raab Mark Reichelt Jaesang Ro Jon C. Sandberg Robert W. Schoenlein Hugh Secker-Walker Ghavam Shahidi Mohammed Shahriar Jerome M. Shapiro Richard Singer Stephen P. Smith **David Standley** Deborah Stephan **Brian Stewart** Richard Stoner Ke-Xun Sun Bernard I. Szabo **Eugene Tarnow** Barry L. Thompson Ann Tulintseff Rosalie Uchanski Jesus N. Villasenor James C. Vlcek David B. Walrod Robert Webster

Su-Min Wei Robert Weisskoff George R. Welch Dilys K. Wong Rosalind Wright Ying-Ching Eric Yang Peter T. Yu Herng-Aung Yueh Avideh Zakhor Farhad Zarinetchi Hong Zhang

Teaching Assistants

Harold H. Lim Dan Wang Michael L. Zerkle

Graduate Students

Robert Barat Ricardo Betti Bradley T. Binder Kirk H. Chao Jeffrey A. Colburn Manuel E. Conde Anthony DiRienzo Arthur C. Grant Scott Isabelle Lars U. Jaenchen Marsha Jeung Michael J. Komichak Laura MacGinitie Jeffrey N. Marcus John Moores Bruce G. Oldaker Elizabeth Olson Maurice J. Ostrov Susan L. Phillips Timothy G. Reese Gurhan Saplakoglu Scott Shephard Barbara Shinn Albert Swartz Michael J. Tsuk Xinglong Yan Jenny Yu

Undergraduate Students

Robert G. Atkins Talal Bahrani Leon Balents Susmitha K. Bellam Amy Bertin Jason Bochinski Joseph E. Bondaryk Ike Chang Judy Chen Suephy Chen Sunkyung Choi Cynthia F. Chuang David Duseau Stephen Eikenberry Marcelo F. Fogaca Jaime Garza William Greenberg Mark Hausman Timothy Hawkeye Brian T. Hou Sue-Hane Hsu Tsen-Yu Hung Charles Jankowski

Hemantha Jayawardena Robert Kassel Illy King Weng-Yew Ko Debbie Kulik Joseph C. Landry Ruby Li **Brian Luschwitz** Joyce Ma Mark H. Mabry Sanjay Manandhar Edward L. Markowitz Roderick K. Mason Michael Matter Muriel Medard Leslie M. Melcer Andrew W. Miklich Hirak Mitra Christopher M. Neils **Eugene Opsasnick** Erik Ordentlich Christine Pao

Parag Patil Rebecca Perry Mark Randolph Leonardo Renna Christopher Roller Peter H. Schmidt Andrew Shaw Richard W. Singerman **Prashant Singh Howard Stuart** Javier G. Tam Tali J. Tamir A. Dushvanthi Thurairatnam Rajeev Tewari Sean Tierney Keith A. Tuson **Timothy Wilson** Amy Wong Victor Wong Chan A. Yoon **Gregory Zancewicz** Lori L. Ziernan

Administrative Staff

Donald F. Duffy David W. Foss Virginia R. Lauricella Barbara J. Passero John S. Peck Joseph Sincuck, Jr. Anita T. Sloan Vicky-Lynn Taylor Donna Maria Ticchi

Support and Technical Personnel

Robert W. Aelerud
Janice L. Balzer
Margery Brothers
Mary Ellen Butts
Manuel Cabral, Jr.
Kathleen E. Cairns
Donald A. Clements
John F. Cook
Alfredo D. Donato
Francis Doughty
Phyllis M. Eiro
Dorothy A. Fleischer
Ann Forestell
Deborah Gage
Donna L. Gale

Thalia Garalis
Andrea L. Gelinas
Kyra M. Hall
Venetia Kaloyanides
Barbara King
Cynthia Y. Kopf
Edward R. Lavalle
George H. Leach
Anh Lieu
Catherine Lorusso
Eleanora M. Luongo
John Mandile
Timothy McClure
Rita C. McKinnon
Christine T. Mendelsohn

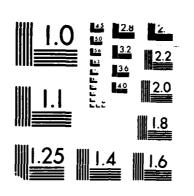
Joseph E. Mitchell Katherine S. Nash Susan E. Nelson John C. Nickerson Donald K. North Veronica Romansky Maxine P. Samuels Clare F. Smith Henry Stram David M. Taylor Mary Tighe Eric P. Watson John Weigel Arlene Wint

31.0 Research Support Index

Amoco Foundation Fellowship	197
Brazil, Counselho Nacional de Desenvolvimento Cientifico e Tecnologica	232
Canada, Bell Northern Research Scholarship	190
Canada, Fonds pour la Formation de Chercheurs et L'Aide a la Recherche, Postgraduate Fellowship	190
Canada, Natural Science and Engineering Research Council, Postgraduate Fellowship	190
Center for Advanced Television Studies	196, 203, 232
Defense Advanced Research Projects Agency (DARPA) Contract MDA-903-85-C-0215 Contract N00014-83-K-0454 Contract N00014-85-K-0213	21 51 206
Draper (Charles Stark) Laboratory, Inc. Contract DL-H-261827	18, 22
Dreyfus (Camille and Henry) Foundation	25
EXXON Foundation	8
Friedman (F.L.) Chair	135, 137
Hertz (Fanny and John) Foundation	193, 200
Hitachi Central Research Laboratory	23
International Business Machines, Inc.	14, 15, 137, 205, 216
Thomas J. Watson Research Center	16
Joint Services Electronics Program (JSEP) Contract DAAL03-86-K-0002	1-3, 5, 6, 16 25-27, 29-31 34, 35, 39, 55 57, 67, 71, 147 158, 209
Contract DAAG29-83-K-0003	3, 63, 69, 139

KMS Fusion, Inc.	9
LeBel (C.J.) Chair	85
Livermore (Lawrence) National Laboratory Subcontract 6264005	161
Subcontract 9459005	1, 8
Maryland Procurement Office	
Contract MDA 904-84-C-6037	45
M.I.T. Energy Laboratory, Synthetic Fuels Center	25
National Aeronautics and Space Administration (NASA)	
Grant NGL22-009-683	8
National Aeronautics and Space Administration (NASA) Goddard Space Flight Center	
Contract NAG5-10	231
Contract NAG5-269	218
Contract NAG5-270 Contract NAG5-537	212 233
Contract NAG5-337 Contract NAG5-725	212
National Institutes of Health	
Grant AM 25535	135
Grant 1 R01 NS21322	128
Grant 5 P01 CA31303	223
Grant 5 P01 NS13126 Grant 5 R01 GM35459	109 40
Grant 5 R01 NS04332	85
Grant 5 R01 NS18682	109
Grant 5 R01 NS20322	109
Grant 5 R01 NS20269	109
Grant 5 T32 NS07040	85
Grant 5 T32 NS07047	109
Grant 6 R01 NS12846	118
National Oceanic and Atmospheric Administration (NOAA)	
Contract NA 84AA-D-00001	231
National Science Foundation	
Fellowship	186, 281
Grant AST 86-17172	229
Grant BNS 83-19874	116
Grant BNS 83-19887	116 158
Grant CHE 84-21392 Grant CHE 85-08734	158 25, 27

RLE (RESEARCH LABORATORY OF ELECTRONICS) PROGRESS
REPORT NUMBER 129(U) MASSACHUSETTS INST OF TECH
CAMBRIDGE RESEARCH LAB OF ELECTRON. J ALLEN ET AL.
JAN 87 ARO-23223. 43-EL DAAL83-86-K-8082 MD-8193 799 UNCLASSIFIED



MICROCOPY RESOLUTION TEST CHART HIREAU - STANDARDS 1963 A

Grant DMR 81-19295	25, 27
Grant DMR 84-18718	15, 73
Grant DMR 85-06030	17
Grant ECS 82-11650	31
Grant ECS 82-13430	162
Grant ECS 83-05448	29
Grant ECS 83-10718	29-31
Grant ECS 83-10941	83
Grant ECS 84-07285	185-203
Grant ECS 84-13178	33, 34
Grant ECS 84-15580	45
Grant ECS 84-21392	147
Grant ECS 85-03443	3
Grant ECS 85-04381	210
Grant ECS 85-06565	1, 6, 7, 14
Grant ECS 85-09143	43
Grant ECS 85-14517	161
Grant ECS 85-52701	35, 37, 39
Grant 1ST 80-17599	85
Grant PHY 82-10369	139
Grant PHY 83-06273	145
Grant PHY 84-11483	147
Grant PHY 84-21392	152
Grant PHY 86-05893	148
Nippon Telegraph and Telephone, Inc.	18, 22
Research Corporation	25
Sanders Associates, Inc.	188, 191, 193
	197
Schlumberger-Doll Research	219
Semiconductor Research Corporation	
Contract 86-05-080	2
Contract 80-03-080	13, 16, 17
Contract 67-31-000	10, 10, 17
Simulation Technologies	218
SM Systems and Research, Inc.	231
Sony International Business Machines, Inc.	14
Symbion, Inc.	109
U.S. Air Force - Office of Scientific Research	
Contract AFOSR-84-0026	161
Contract AFOSR-85-0154	7, 8, 13, 14
Contract AFOSR-85-0213	37, 39

Contract AFOSR-85-0269 Contract AFOSR-85-0376 Contract AFOSR-86-0164 Contract F19628-85-K-0028 Contract F49620-82-C-0091	51 -53 3, 4 77 188, 201 139
U.S. Air Force - Rome Air Development Center	139
U.S. Army	
Contract MDA-903-84-K-0297	234
U.S. Army Research Office - Durham	
Contract DAAG29-84-K-0095	46
Contract DAAG29-85-K-0079	216
U.S. Department of Energy	
Contract DE-AC02-78ET 51013	162, 174
Contract DE-FG05-84ER 13272	161
U.S. Navy - Naval Electronic Systems Command	
Contract N00039-85-C-0254	85
Contract N00039-85-C-0290	85
Contract N00039-85-C-0341	85
U.S. Navy - Office of Naval Research	
Contract N00014-79-C-0183	147
Contract N00014-80-C-0622	83
Contract N00014-80-C-0941 Contract N00014-81-K-0742	47 185-203
Contract N00014-81-K-0742 Contract N00014-83-K-0258	214
Contract N00014-83-K-0695	156
Contract N00014-84-C-2082	229
Contract N00014-84-K-0073	22
Contract N00014-86-C-2114	225
Contract N00014-86-K-0117	40
Contract N00014-86-K-0533	216
Wan-Yuan Company, Peoples Republic of China	74
Whitaker Foundation	135

32.0 Research Project Staff Index

A

Aggarwal, R.L. 53
Ahmad-Bitar, R. 156
Ajuria, S. 6, 13, 14
Akhtar, S. 2
Allen, J. 77
Anderson, E.H. 1, 8, 9
Anderson, K.K. 31, 47
Antoniadis, D.A. 3, 4, 5, 6, 21
Arias, T.A. 233
Armstrong, R. 77
Atwater, H.A. 6, 7, 13, 14

В

Bagnato, V. 156 Bagwell, P. 3, 5 Baltus, D. 77 Bamji, C. 77 Barrett, J.W. 230, 231 Barret, J.L. 22 Bartlett, G.J. 232 Beckerle, J.D. 25, 27 Becla, P. 51 Berker, A.N. 55 Bers, A. 162 Binder, B.T. 43 Birgeneau, R.J. 57 Bonanni, P.G. 231 Bondaryk 185 Borgeaud, M. 214 Bossi, D.E. 46 Bounds, J.K. 43 Braida, L.D. 116, 118 Briancon, A.C. 231 Brocco, L. 77 Brown, M.C. 111 Burke, B.F. 229 Bustamante, D.K. 118

C

Cammarata, R.C. 16 Canizares, C.R. 9 Carilli, C. 229 Carter, J. 1 Carvahlo, B. 73 Ceyer, S.T. 25, 26, 27 Chen, S.-H. 73, 74 Chou, S.Y. 6 Cho, J. 16 Chu, W. 1, 3, 4 Clark, L.D., Jr. 230 Clevenger, L. 16 Cobra, D.T. 185 Colburn, H.S. 128 Connor, S. 229 Coppi, B. 174 Corbett, C.R. 128 Corcoran, C.J. 47 Cornell, E. 158 Covell, M. 186

D

Dagli, G. 33
Davis, R. 193
de Jager, G. 232, 234
Delgutee, B. 110
Delhorne, L.A. 118
Deroo, J. 82
Derouard, J. 150, 152
Dhawan, V. 229
Dove, W.P. 193
Dreher, J. 229
Dubner, A.D. 18, 22
Durlach, N.I. 116, 118, 128

Ε

Eatock, R.A. 110 Eddington, D.K. 114 Enders, R.H. 46

F

Feder, M. 187
Field, S. 3
Flanagan, R.W. 158
Floro, J. 6, 7, 13, 14
Fonstad, C.G., Jr. 33, 34
Fraley, A. 82
Francis, R. 71
Freeman, D.M. 110
Frishkopt, L.S. 110
Frisk, G.V. 201
Fuchs, V. 162
Fujimoto, J.G. 35, 37, 39, 40

G

Garrison, S.M. 6, 13, 14
Gasiewski, A.J. 231
Geiger, G. 131
Gentile, T. 147, 149
Girzon, G. 114
Gladstone, D.J. 26
Glasser, L.A. 80, 83
Grant, Arthur 133
Griffin, D.W. 188
Groves, K.M. 212
Guinan, J.J., Jr. 112, 113
Gu, Q. 216

Н

Habashy, T.M. 219 Hammerschlag, R.V. 233 Hannon, S.M. 46 Han, H.C. 212 Harasty, D.J. 189 Hardwick, J.C. 190 Hauck, C. 77 Haus, H.A. 29, 31, 33 Heflin, M. 229 Hewitt, J. 229 Heytens, M. 206 Hilfer, E. 147 Hines, B.E. 230 Holm, R.W. 230

Ho, S.-T. 45 Huang, W.P. 31 Hughey, B. 147, 149 Hui, K. 55 Hulet, R.G. 147

ı

Im, J.S. 14, 15 Ippen, E.P. 35, 37, 39, 40 Ismail, K. 3, 4 Iu, C.H. 145 Izraelevitz, D. 195

J

Jachner, J. 190 Jacobs, J.B. 21 Jayavant, R. 206 Jeong, H. 80, 82 Jiran, E. 15 Joannopoulos, J.D. 63 Johnson, A.D. 26, 27 John, R.K. 45 Joo, T.H. 191

K

Kahn, H. 17 Kamatsu, K. 1 Kash, M.M. 145 Kastner, M.A. 3, 4, 5 Kelly, M.J. 230 Ketten, D.R. 109 Kiang, J.F. 216 Kidd, R.C. 110 Kim, H.-J. 13, 15 Kirkpatrick, D. 83 Kleppner, D. 145, 147, 149 Kobler, J.B. 112 Kong, J.A. 209, 210, 212, 214, 216, 218, 219 Kumar, P. 45 Kupfer, K. 162 Ku, Y.C. 2

L

Lafyatis, G. 156 Lafyatis, G.P. Lane, D.R. 43 Langston, G. 229 Lashmore, C. 162 Lee, M.B. 25, 26 212 Lee. M.C. Lee, P.A. 69 Leong, K.-W. 45 Lettvin, J. 131, 132, 133 21, 22 Lezec, H. Licini, J.C. 3 47 Liew, S.K. 195 Lim, J.S Lim, J.S. 188, 190, 192, 196, 200, 201 Lin, F.C. 210, 212, 214, 218 Lin, S. 77 Litster, J.D. 71 Liu, L.Y. 31 Longworth, H. 16 Lowther, R.E. 21

M

CONTROL OF THE PROPERTY OF THE

MacMillan, N.A. 116 Maeda, M.W. 45 Magill, P. 152 Mahoney, L. 21 Maiorino, C.D. 16 Malvar, H.S. 232, 234 Mark, M.B. 46 Martinez, D.B. 196 Martin, A. 156 Martin, P.J. 150 McClain, B. 71 McCormick, S. 77 McCue, M.P. 112 McGonigal, M. 26 McKay, S.R. 55 Meirav, U. 3 Melngailis, J. 18, 21, 22, 23 Miklich, A.H. 150 Milios, E.E. 197 Molter-Orr, L. 31 Moores, J.D. 233 Morgenthaler, F.R. 223 Musicus, B.R. 80, 81, 82

Musil, C.R. 21, 22 Myers, C.S. 197

N

Nabors, K. 83 Nghiem, S.V. 212

0

O'Brien, P. 83 O'Connor, K. 82 Oho, S. 29 Oldaker, B.G. 150 Oppenheim, A.V. 185, 186, 187, 189, 190, 191, 193, 197, 198, 201 Orlando, T. 3, 4, 5 Oslick, M. 82

P

Palmer, J. 14 Palmer, J.E. 6, 8, 13, 14 Pang, X.-D. 109, 112 Pappas, T.N. 192 Park, D. 46 Park, S.L. 3 Peake, W.T. 109 Penfield, P. Jr. 83 Peterson, P.M. 128 Phillips, M. 31 Phillips, S.L. 109 Plotnik, I. 1, 2 Poh, S.Y. 216, 219 Porter, M. 2 Power, M.H. 118 Prasana, S. 82 Pratt, G. 132 Preisig, J.C. 232, 234 Pritchard, D.E. 150, 152, 156, 158

Q

Quek, H.M. 1, 6, 13, 14

R

Raab, E. 156
Rabinowitz, W.M. 128
Ram, A. 162
Rappaport, C.M. 223
Rediker, R.H. 47
Reed, C. 118
Ricci, M.A. 73
Rodriguez, J.J. 201
Rosenkranz, P.W. 231
Rosowski, J.J. 109
Ro. J. 18

S

Saplakoglu, G. 45 Schattenburg, M.L. 1, 8, 9 Schembor, E. 82 Schreiber, W.F. 203 Schulberg, M. 26 Sciascia, T. 133 Scott-Thomas, J. 3 Seif, R. 29 Shahidi, G. 5 Shao, M. 230 Shapiro, J.H. 43, 45, 46 Shapiro, J.S. 232 Shedd, G.M. 22 Sheu, E.Y. 73 Shin, R.T. 210, 214, 218 Shirasaki, M. 29 Shu, R.K. 45 Silman, N.E. 46 Silva, A.J. 198 Simonson, R.J. 27 Smith, D.A. 15 Smith, H.I. 1, 2, 3, 4, 5, 6, 7, 8, 9, 13, 14 Song, B. 81 Staelin, D.H. 230, 231, 232, 233, 234 Standley, D. 83 Stephens, L. 116 Stewart, B. 152 Stoner, R. 152

Szabo, B.I. 232

T

Tang, S.L. 25
Thompson, C.V. 6, 7, 8, 13, 14, 15, 16, 17, 18, 22
Thompson, W.B. 23
Tomita, H. 14
Toth, M. 2
Towe, E. 34
Troxel, D.E. 206
Tsuk, M.J. 216
Tulintseff, A. 209, 216
Tu, K.-N. 16

U

Uchanski, R.M. 118

V

van Hove, P. 200 Vianna, S. 147

W

Wang, J.R. 27 Wang, X.Y. 74 Weinstein, E. 187 Weisskopf, R.M. 158 Weiss, T.F. 110 Wei, X.B. 74 Welch, G.R. 145 Wengrovitz, M. 201 Whitaker, N.A. Wolff, P.A. 51, 52 Wong, C.C. 6, 14 Wong, D.L. 29 Wong, N.C. 45 Wong, S. 51 232, 234 Wornell, G.W. Wright, R. 80 Wu, C.F. 73 Wyatt, J.L. Jr. 83

Swartz, A. 218

Y

Yang, Q. 26, 27 Yang, Y.E. 209, 216 Yen, A. 1, 3, 5 Youngdale, E.R. 53 Yueh, H.A. 209 Yuen, S.Y.C. 51, 52 Yu, T.Y. 43

Z

Zakhor, A. 193 Zue, V.W. 118 Zurek, P.M. 118, 128

DATE F/LMED